INFORMATION TO USERS

This manuscript has been reproduced from the microfilm master. UMI films the text directly from the original or copy submitted. Thus, some thesis and dissertation copies are in typewriter face, while others may be from any type of computer printer.

The quality of this reproduction is dependent upon the quality of the copy submitted. Broken or indistinct print, colored or poor quality illustrations and photographs, print bleedthrough, substandard margins, and improper alignment can adversely affect reproduction.

In the unlikely event that the author did not send UMI a complete manuscript and there are missing pages, these will be noted. Also, if unauthorized copyright material had to be removed, a note will indicate the deletion.

Oversize materials (e.g., maps, drawings, charts) are reproduced by sectioning the original, beginning at the upper left-hand corner and continuing from left to right in equal sections with small overlaps. Each original is also photographed in one exposure and is included in reduced form at the back of the book.

Photographs included in the original manuscript have been reproduced xerographically in this copy. Higher quality 6" x 9" black and white photographic prints are available for any photographs or illustrations appearing in this copy for an additional charge. Contact UMI directly to order.

UMI

A Bell & Howell Information Company
300 North Zeeb Road, Ann Arbor MI 48106-1346 USA
313/761-4700 800/521-0600

CREW-CUT AGGREGATES OF POLYSTYRENE-*b*-POLY(ACRYLIC ACID) DIBLOCK COPOLYMERS IN SOLUTIONS

By

Lifeng Zhang

A thesis
submitted to the Faculty of Graduate Studies and Research
in partial fulfillment of the requirements for the degree of

Doctor of Philosophy

Department of Chemistry
McGill University
Montreal, Quebec
Canada
H3A 2K6

October 1996

0-612-30429-9

Abstract

The morphological characteristics of crew-cut micelle-like aggregates of highly asymmetric polystyrene-*b*-poly(acrylic acid) copolymers PS-*b*-PAA, was studied by transmission electron microscopy and light scattering. The insoluble PS block contents in the copolymers ranged from 80 to 98 wt. %. The aggregates were formed by the water addition to the copolymer solution in N,N-dimethylformamide, and then were isolated in aqueous solutions.

Spherical micelles were formed when the PAA content in the copolymers was relatively higher. The PS core radii scaled as $R_{core} \sim N_{PS}^{\ 0.4} N_{PAA}^{-0.15}$, where N_{PS} and N_{PAA} are the lengths of the PS and PAA blocks, respectively. The PAA corona shell dimensions were also studied. As the PAA content in block copolymers decreased, the morphology of the aggregate changed progressively from spheres to cylinders, to vesicles and lamellae, and eventually to compound micelles. The effects of the initial copolymer concentration and the addition of homopolystyrene on the aggregate morphology were also examined. The aggregate morphology appears to be controlled by a force balance mainly involving three aspects, i.e. the stretching of the PS chains in the core, the surface tension between the PS core and the solvent, and the inter-corona chain interactions.

The aggregate morphology can be controlled by adding ions in micro-molar (HCl, NaOH, $CaCl_2$ or $Ca(Ac)_2$) or milli-molar (NaCl) concentrations. In addition to the various morphologies obtained by changing the copolymer composition, large compound vesicles, a new morphology, can be obtained from a single block copolymer. The morphogenic effect of different added ions on the crew-cut aggregates can be ascribed to the changed inter-corona chain repulsive interactions, due to neutralization, protonation, ion-binding, and screened electrostatic field, etc. The range of morphologies obtained in this study is believed to be unprecedented for a block copolymer self-assembly system in low molecular weight solvents.

Résumé

La morphologie et d'autres caractéristiques des aggrégats, sous forme de "crew-cut micelles" (littéralement micelles coupées en brosse), du copolymère hautement asymétrique Polystyrène-b-Poly(acide acrylique) (PS-b-PAA) ont été étudiées par microscopie électronique par transmission et par diffusion de lumière. La portion du bloc de PS insoluble dans le copolymère était de 80 à 98% en poids. Les aggrégats ont été formés par addition d'eau au copolymère en solution dans du N,N-diméthylformamide, puis ont été isolés dans l'eau.

Les micelles étaient sphériques lorsque la proportion de PAA dans le copolymère était relativement élevée. Les rayons du coeur de PS obéissaient à la loi suivante : $R_{core} \sim N_{PS}^{0.4} N_{PAA}^{-0.15}$, où N_{PS} et N_{PAA} sont respectivement les longueurs des blocs de PS et de PAA. Une étude a aussi été menée sur les dimensions de l'enveloppe de PAA. La morphologie des aggrégats passait progressivement de sphère, à cylindre, à vésicule, à lamelle et finalement à des micelles complexées au fur et à mesure que la proportion de PAA dans le copolymère diminuait. Les effets de la concentration initiale en copolymère et de l'addition d'homopolystyrène sur la morphologie des aggrégats a aussi été examinée. Cette morphologie semble être contrôlée par l'équilibre des forces mettant principalement en jeu l'extension des chaînes de PS dans le coeur, la tension de surface entre le polystyrène du coeur et le solvent, ainsi que les interactions entre les chaînes de la couronne.

La morphologie des aggrégats peut être contrôlée par l'ajout d'ions à des concentrations micro-molaires (HCl, NaOH, $CaCl_2$ ou $Ca(Ac)_2$) ou bien milli-molaire (NaCl). Les mêmes morphologies que celles décrites ci-dessus ont été obtenues à partir d'un copolymère mono-bloc grâce à cette technique. Une nouvelle morphologie, de grandes vésicules complexées, a été obtenue. L'effet morphogène de l'ajout d'ions aux aggrégats coupés en brosse peut être attribué aux changements intervenus dans les interactions répulsives entre les chaînes de la couronne. Ces changements ont pour cause la neutralisation, la protonation, les liaisons ioniques, le pouvoir d'écran des champs electrostatiques, etc. Le nombre de morphologies obtenues dans cette étude doit être à ce jour sans précédent en ce qui concerne l'auto-assemblage de systèmes de copolymères en blocs dans des solvents de faible poids moléculaire.

FOREWORD

In accordance with Thesis Specifications of the "Guidelines for Thesis Preparation" (Faculty of Graduate Studies and Research), the following text is cited:

> "Candidates have the option of including, as part of the thesis, the text of one or more papers submitted or be submitted for publication, or the clearly-duplicated text of one or more published papers. These texts must be bound as an integral part of the thesis.
>
> If this option is chosen, **connecting texts that provide logical bridges between the different papers are mandatory**. The thesis must be written in such a way that it is more than a mere collection of manuscripts; in other words, results of a series od papers must be integrated.
>
> The thesis must still conform to all other requirements of the "Guidelines for Thesis Preparation". **The thesis must include**: A table of Contents, an abstract in English and French, an introduction which clearly states the rationale and objectives of the study, a review of the literature, a final conclusion and summary, and a thorough bibliography or reference list.
>
> Additional material must be provided where appropriate (e.g. in appendices) and in sufficient detail to allow a clear and precise judgement to be made of the importance and originality of the research reported in the thesis.
>
> In the case of manuscripts co-authored by the candidate and others, **the candidate is required to make an explicit statement in the thesis as to who contributed to such work and to what extent.** Supervisors must attest to the accuracy of such statements at the doctoral oral defense. Since the task of the examiners is made more difficult in these cases, it is in the candidate's interest to make perfectly clear the responsibilities of all the authors of the co-authored papers."

Foreword

This dissertation is written in the form of seven papers. The papers each comprise one chapter, with a introduction of this work in a first chapter and general conclusions contained in a ninth chapter. Following normal procedure, the papers have been either published or submitted for publication in scientific journals. A list of the papers is given below:

Chapter 2: *Macromolecular Chemistry and Physics* (accepted)
Chapter 3: *Macromolecules* **1995**, *28*, 6055 - 6066.
Chapter 4: *Science* **1995**, *268*, 1728 - 1731.
Chapter 5: *J. Am. Chem. Soc.* **1996**, *118*, 3168 - 3181.
Chapter 6: *Science* **1996**, *272*, 1777-1779.
Chapter 7: *Macromolecules* **1996**, *29*, in press.
Chapter 8: *Macromolecules* **1997**, *30*, in press.

All of the papers include the research director, Dr. Adi Eisenberg, as co-author. Chapter 3 (L. Zhang, R. J. Barlow and A. Eisenberg) includes Dr. Raymond J. Barlow who did the DLS experiments and co-wrote this paper. Chapter 6 (L. Zhang, K. Yu and A. Eisenberg) includes Ms. Kui Yu, recognizing that some of the results from PS-*b*-PEO copolymers were used in the paper. Chapter 8 (L. Zhang, H. Shen and A. Eisenberg) includes Mr. Hongwei Shen as a co-author, recognizing that he did some of the light scattering experiments. Other than the supervision, advice and direction of Dr. Eisenberg and the aforementioned contribution to the chapters, all of the work presented in this dissertation was performed by the author.

To my parents and my wife

ACKNOWLEDGMENTS

As this section is the most important part of the thesis, I hope it is complete. My most sincere apologies to anyone I have neglected to mention.

First and foremost, I am grateful for the guidance and support of Dr. Adi Eisenberg who has a tremendous enthusiasm for science, and gives special attention to the growth of scientists. Thanks for his smile, joke and hair.

I would especially like to thank my wife, Wei Gao, for her endless support, encouragement and love.

Most importantly, I must recognize the people who have given me direct assistance, both technical and otherwise, during my time at McGill. Thanks to

Diep, Joon, Karine and *Zhisheng* for their friendship and advice.
Xing-Fu for his help in synthesizing the polymers used in my thesis.
Ray for his friendship and contribution to the chapter 3 of this thesis.
Matthew and *Chris* for useful discussions.
Louis for his friendship and important literature.
Luc for the translation of the abstract.
Neil and *Carl* for their help in preparing the figures.
Drs. J.-F. Revol and *L. Godbout* for using the dark room and the facilities.

In addition, thanks to

all the persons in this group, past and present who made my work place very enjoyable.
Professors and staff members in the chemistry department, McGill University, in particular, Dr. R. B. Lennox, Mr. Fred Kluck, Ms. Renée Charron, Ms. Paulette Henault, Ms. Carol Brown.
Ms. Kathryn Hewitt in EM center of biology department.

Thanks also go out to

Bayer Rubber Inc and Macromolecule Science and Engineering Division of Canada for the 1995 - 1996 Award.
Udho Parsini Diwan and this chemistry department for the 1995 UPD Award .

Table of Contents

Chapter 1. General Introduction

List of Tables

List of Figures

Chapter 1

General Introduction

1.1. INTRODUCTION

The self-assembly of block copolymers in selective solvents to form micelles is a phenomenon of considerable interest to a wide range of scientists. Extensive experimental and theoretical studies have been performed over the past four decades.[1-3] Studies have been focused on the phenomenon of micellization in the solutions of various block copolymers, the developments of new experimental techniques and new theories of micellization, and the recognition that block copolymer micelles may be used in a wide range of industrial and technological applications. The focus of this thesis is on the formation and characteristics of crew-cut micelle-like aggregates of highly asymmetric polystyrene-*b*-poly(acrylic acid) diblock copolymers, formed in solvents composed of mixtures of N,N-dimethylformamide and water and then isolated in water. It emphasizes the effect of various factors, e.g. the copolymer composition and concentration, added electrolytes, etc., on the morphology of the aggregates. The insoluble polystyrene block contents of the block copolymers used in this study range from 80 to 98 wt. %, i.e. the composition region for crew-cut aggregate formation, which has not been investigated before. The principal experimental techniques employed are transmission electron microscopy and light scattering. This chapter begins with a general introduction to polymers, followed by sections dealing with phase separation and aggregate morphologies in various self-assembled systems. The final section is a summary of the aims of this thesis.

1.1.1. Some basic definitions.[4] *Polymers* or *macromolecules* are giant molecules with molar masses ranging from several thousands to millions. Macromolecules can be natural and synthetic. *Natural polymers* usually have more complex structures than *synthetic polymers*. A polymer is usually constructed from many smaller units called *monomers*, covalently bonded together in many conceivable patterns. To qualify as a monomer, a small molecule has to have two or more bonding sites, through which it can be linked to other monomers to form the polymer chain. The number of bonding sites is referred to as the *functionality* of a monomer. Bifunctional monomers form linear macromolecules. If the monomers are polyfunctional, branched polymers can be produced.

When only one species of monomers is used to make a polymer, the product is called *homopolymer*. If the chain is built from two types of monomer unit, the material is known as a *copolymer*. Copolymers prepared from bifunctional monomers can be subdivided further into four main categories according to the arrangements of the monomer units in the chain. Different structures composed of two monomers, A and B, are shown in Figure 1.1. For *random copolymers*, the distribution of two monomers in the chain is essentially random, but influenced by the reactivities of each monomers during the synthesis. In *alternating copolymers*, the A and B monomers are distributed with a regular alternating pattern along the chain. *Block copolymers* consist of substantial sequences or blocks of each monomers. When one sequence of A monomers is attached to a sequence of B monomers, the copolymer is called diblock. Copolymer with a central B block attached to terminal A monomer blocks is called a triblock. In *graft copolymers*, blocks of one monomer are grafted on to a backbone of the other as branches. In this thesis, we deal only with synthetic diblock copolymers.

ABAABBABBBAABBAAAB	*Random copolymer*
ABABABABABABABABAB	*Alternating copolymer*
AAAAAAAAABBBBBBBBB	*Block copolymer*
AAAAAAAAAAAAAAAAA B B B B B B B B B	*Graft copolymer*

Figure 1.1. Types of copolymers synthesized from monomers A and B.

1.1.2. Synthesis of block copolymers. Block copolymers can be synthesized by sequential addition reactions using: (1) ionic initiators where an active site is kept "alive" on the end of the initial block, which is then capable to initiating chain growth of a second monomer on the end of the first chain, or (2) coupling of different blocks with functional terminal units. Ionic reactions are found to be particularly useful since they can provide copolymers of well-defined compositions. Sequential ionic polymerization usually involves three steps: initiation, propagation and termination.[5] As a typical example, the synthesis of polystyrene-*b*-poly(*tert*-butylacrylate) diblock copolymer by sequential anionic polymerization is described below.

In the initiation step, *sec*-butyllithium can be used as an initiator. α-Methylstyrene is used as an indicator and an end-capping agent. *sec*-Butyllithium first titrates any active hydrogen in the reaction system, and then reacts with α-methylstyrene to yield short chain living anions with a deep red color. At room temperature, α-methylstyrene monomer at low concentration does not polymerize because it is above its ceiling temperature.

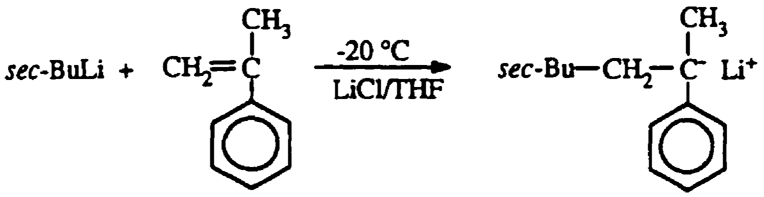

After the styrene monomer is added, the living anions produced in the initiation step initiate the polymerization of the styrene monomer and the anion propagates. The red color of the solution changes to an orange-yellow one. Since the active centers are regenerated at the chain ends of the growing polymers, the process continues until all the styrene monomer is consumed, while the carbanions remain active, indicated by the reappearance of the deep red color due to the end-capping of polystyryllithium anion by α-methylstyrene.

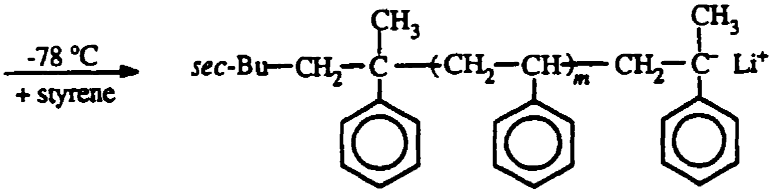

The polymerization is resumed when the second monomer, *tert*-butylacrylate, is added.

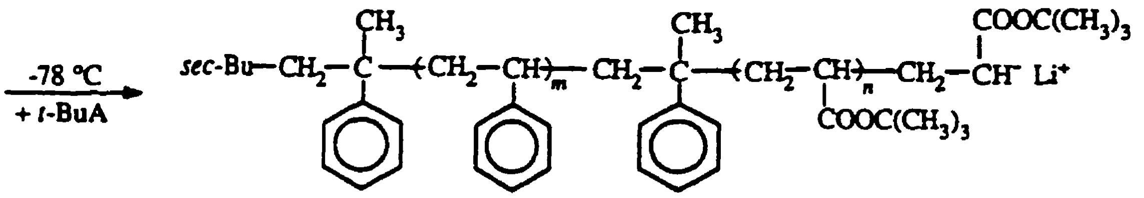

Finally, the polymerization is terminated by adding a small molecule with a labile proton, such as methanol, to kill the living chain end. Thus, one obtains the desired polystyrene-*b*-poly(*tert*-butylacrylate) diblock copolymer. Some technical aspects of this polymerization method should be noted. It is essential to remove all active impurities such as water and oxygen from the reaction medium to keep the anionic chain living. When the initiation step is rapid compared to that of propagation, polymers with a low degree of molecular weight polydispersity can be obtained. In order to avoid a terminating side reaction or chain transfer reaction of the living anionic chains, a stabilizer such as LiCl is usually added to the reaction system.

1.1.3. Some relevant features of polymers.[4] **1.1.3.1. Average molar masses.** One of the most important features which distinguishes a synthetic polymer from a simple molecule is the impossibility to assign an exact molar mass to the polymer. This is a consequence of the fact that in the polymerization reaction, the length of the chain formed is determined entirely by random events. The polymer is characterized best by a molar mass distribution and the associated molar mass averages. The typical distribution, as shown in Figure 1.2, can be described by a variety of averages, i.e. number-average, weight-average and z-average molecular weight.

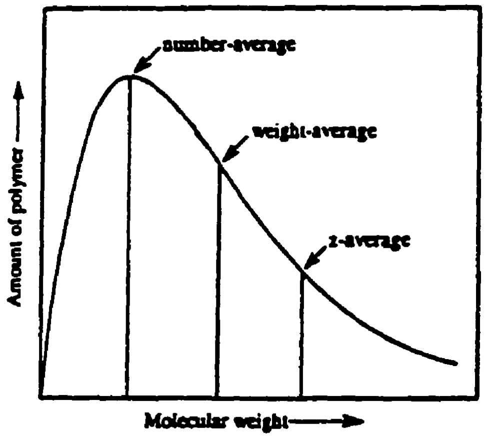

Figure 1.2. Typical distribution of molar masses for a polymer sample.[4]

The number-average molecular weight (M_n) is defined by

$$M_n = \frac{\Sigma_i N_i M_i}{\Sigma_i N_i} = \frac{\Sigma_i W_i}{\Sigma_i (W_i/N_i)}$$

where N_i and W_i refer to the number and weight of the molecules of species i of molar mass M_i, respectively. M_n can be obtained by methods which measure colligative properties such as osmotic and vapor pressure. A weight average molecular weight (M_w) can be obtained from light scattering measurements, a method depending on the size rather than the number of molecules. It is defined as

$$M_w = \frac{\Sigma_i N_i M_i^2}{\Sigma_i N_i M_i} = \frac{\Sigma_i W_i M_i}{\Sigma_i W_i}$$

The z-average molecular weight (M_z) is defined by

$$M_z = \frac{\Sigma_i N_i M_i^3}{\Sigma_i N_i M_i^2} = \frac{\Sigma_i W_i M_i^2}{\Sigma_i W_i M_i}$$

It can be obtained by methods such as sedimentation equilibrium. The molecular weight distribution is also characterized by the polydispersity index (P.I.), which is defined as

$$\text{P.I.} = \frac{M_w}{M_n}$$

when P.I. is equal to unity, the sample is said to be monodisperse. A range of polydispersity indices can be obtained depending on the methods of polymerization.

1.1.3.2. Chain dimensions. The prediction of some average dimension for polymer chains remains a central theme in polymer science. Realistically, a polymer chain is better represented by a flexible chain, which can assume many conformations, loosely coiled into a ball than an extended rod. The random nature results from rotation about the covalent bonds forming the chain backbone. The term "conformation" has been used when referring to a three dimensional geometric arrangement of the polymer, which changes easily when the bonds are rotated.

One of the fundamental problems is to deduce the relations between the end-to-end distance and the chain length. Based on a called "freely-jointed chain model", the most useful statistical result of the dimensions of a linear random coil chain is the mean square end-to-end distance, given by

$$\langle r^2 \rangle = nl^2$$

where n and l represent the number and the length of monomers in polymer chain. The freely-jointed chain model assumes that the bonds act like universal joints, and that complete freedom of rotation about the chain bonds exists. For a real polymer chain, the covalent bonds are not universal joints. The dimensions of the chain will be restricted by the covalent bond angles between each chain atom. For free rotation about a fixed bond angle θ, the expression of the mean square end-to-end distance becomes

$$\langle r^2 \rangle_f = nl^2 \frac{(1-\cos\theta)}{(1+\cos\theta)}$$

For a carbon backbone with tetrahedral bonds, $\theta = 109°28'$, $\cos\theta = -1/3$, and

$$\langle r^2 \rangle_f = 2nl^2$$

Furthermore, because the rotation about most bonds is not free, steric repulsions impose restrictions to bond rotation. Further modifications are needed. Several other models have been suggested, such as the scaling concepts of de Gennes and co-workers.[6] The parameter $\langle r^2 \rangle_0$ is the average mean square of the unperturbed dimension, which is a characteristic parameter for a given polymer chain. For a polystyrene chain, it is known from experimental measurement that

$$\langle r^2 \rangle_0 = 6.76\, N_{PS}\, l^2$$

where N_{PS} is the degree of polymerization of PS chain, and l is the length of styrene monomer.

1.2. PHASE SEPARATION OF POLYMERS IN BULK PHASE.

Block copolymers with their unique mechanical, optical, and structural properties are finding increasing applications in many fields.[7] An important factor contributing to their widespread popularity is the occurrence of phase separation in most block copolymer systems.[8,9] The phase separation and the domain morphology are determined by a number of factors, such as the incompatibility of the blocks, as well as the molecular weight and composition of the copolymers. In this section, we discuss the phase separation phenomena of block copolymers in bulk and of homopolymer/copolymer blends.

1.2.1. Thermodynamic considerations of phase separation. When two polymers are blended, the most likely result is a two phase materials. The reason why two polymers are not usually miscible can be understood from simple thermodynamic considerations. A necessary (but not sufficient) criterion for miscibility is that the free energy of mixing ΔG_m be negative. This is given by

$$\Delta G_m = \Delta H_m - T\, \Delta S_m$$

where ΔH_m is the enthalpy of mixing, ΔS_m is the entropy of mixing and T the absolute temperature. According to the lattice theory of developed by Flory and Huggins,[10] the ΔS_m is very small for high molecular weight polymers, and the ΔH_m, for most polymer mixture, is expected to be positive. Therefore, polymers are not expected to mix. However, mixing can be predicted to occur under three circumstances. (a) If the polymers are not of very high molecular weight, then the entropy will not be negligible and may outweigh an unfavorable enthalpy of mixing. (b) If the enthalpy is positive but very small, then a small entropy of mixing may be sufficient. (c) If the enthalpy of mixing is negative then two polymers would be expected to be miscible. This might occur, for example, if there is a favorable interaction such as hydrogen bonding between the polymers.[11]

1.2.2. Morphology of phase separated microdomains in block copolymer bulk phases. For a mixture of two homopolymers, where the chains of the two polymers have no spatial constraints, and when the enthalpy of mixing is positive, the phase separation may take place on a macro-scale to minimize the unfavorable interfacial energy. [12,13] By contrast, in block copolymers, since the blocks are chemically bonded, even the complete segregation can not lead to a macroscopic phase separation. Phase separation is restricted to small domains, which are referred to as microdomains. The repulsive interaction between A and B blocks in the diblock copolymers tends to increase the domain size. This is opposed by two restrictions; one is uniform segment density requirement, and the second is the stretching (deformation) penalty. The morphology of the system is a result of a balance of these two factors, as described below. Furthermore, the microdomains are not located at random but they may form a regular arrangement giving rise to a periodic structure (macrolattice).[8,9]

Transmission electron microscopy of microtomed samples coupled with heavy-metal staining techniques[14,15] and small angle X-ray scattering[16,17] are useful techniques for the study of block copolymer structures. Many experimental studies have shown that the structures of phase-separated microdomains strongly depend on the copolymer composition, and that a minimum molecular weight is necessary, in general, for the microdomain formation to take place. The microdomains can be spherical, cylindrical, ordered bicontinuous double diamond (OBDD), gyroid or lamellar.[8,9,14-23] The exact composition at which the domain changes shape depends on the copolymer molecular weight and the Flory-Huggins interaction parameter, χ_{AB}, between two blocks. As a typical example, Figure 1.3 shows different structures of microdomains in polystyrene-*b*-polyisoprene (PS-*b*-PI) as a function of the copolymer composition. [9,17] In this figure, it can be seen that up to a volume fraction of polystyrene (φ_{PS}) of 0.17, polystyrene spheres are arranged on a body centered cubic lattice in the polyisoprene matrix. From a φ_{PS} of 0.17 to 0.28, the structure is an hexagonal array formed by cylinders of polystyrene; the OBDD (or gyroid) morphology is observed for a narrow range of φ_{PS} from 0.28 to 0.34. From a φ_{PS} of 0.34 to 0.62, a lamellar structure is formed by alternating layers of polystyrene and polyisoprene. Above this φ_{PS}, similar structures of microdomains made up of the polyisoprene blocks in a matrix of polystyrene blocks are formed.

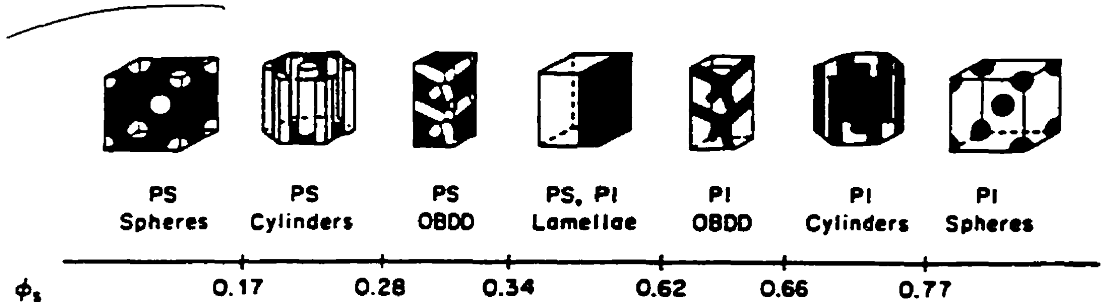

Figure 1.3. Equilibrium morphologies of polystyrene-*b*-polyisoprene diblock copolymer as a function of the volume fraction of the polystyrene. The white domains represent the polystyrene block.

Many theories have been developed which attempt to predict the morphology in terms of fundamental parameters of the block copolymers.[9,12,18] The two most important parameters are the product χN (N is the degree of polymerization) and the volume fractions of the blocks in each copolymer chain (f). Figure 1.4 shows a typical phase diagram for diblock copolymer structures. At present there is no theory capable of predicting the existence of the OBDD or gyroid phase. Furthermore, under the weak segregation limit ($\chi N \sim 10$ for a order-to-disorder phase transition), the microdomain dimensions are predicted to depend on the molecular weight of the domain forming block to the power of 1/2, while the predicted exponent is 2/3 for the strong segregation limit ($\chi N >> 10$).

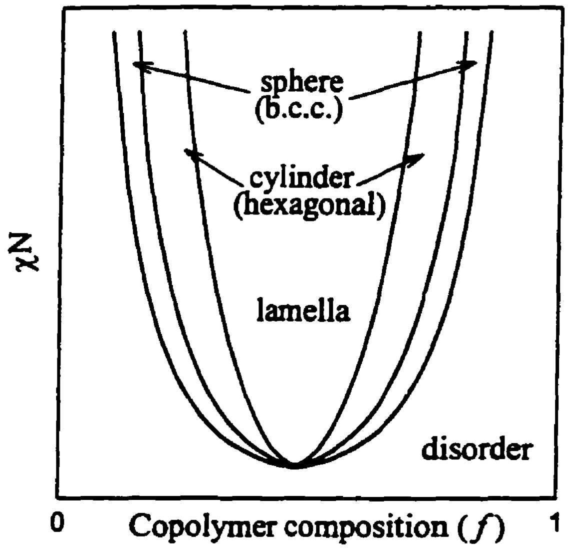

Figure 1.4. Leibler's phase diagram for a diblock copolymer in mean field theory. The regions of the stable equilibrium structures for parameters (χN, f) are indicated in the figure. (Leibler, L. *Macromolecules* **1980**, *13*, 1602)

1.2.3. Phase separation in block copolymer/homopolymer blends. Binary or ternary mixtures of block copolymers with homopolymers can form various microstructures including spherical and cylindrical micelles, vesicles, ordered bicontinuous double diamond (OBDD) and lamellae.[23-31]

The microdomain structures of copolymers are a function of the composition of the blends. [25-27,30,31] For example, for the blends of polystyrene-*b*-polyisoprene (PS-*b*-PI) block copolymers and PS homopolymer, where the PS-b-PI copolymers are the major component and form an alternating lamellar microdomain structure in bulk,[25-27] it was found that as the content of PS homopolymers in the blends increases, the morphology of PI microdomain in the matrix of PS changes progressively from lamellar to OBDD, to cylindrical, and to spherical. The morphological transitions are caused by an increased volume fractions of PS blocks due to the solubilization of PS homopolymers. By contrast, when PI homopolymers are added to the PS-b-PI copolymers, as the added PI homopolymer content increases, the morphology of PI block domains changes from cylindrical to OBDD, to lamellar, i.e. the opposite direction to that seen for the addition of PS homopolymer, because the volume fraction of the PI blocks is increased.

The microdomain structures of the copolymers are also a function of the molecular weight of homopolymers. [24-27] As a typical example, it is shown that blending polystyrene-*b*-polybutadiene diblocks with a large amount of PS homopolymers results in the formation of the microdomains of the butadiene blocks of different structures.[24] For a certain composition of the blends, the morphology of the butadiene block domains changes from spherical to cylindrical and eventually to vesicular by increasing the PS homopolymer molecular weight in the blends. The effect of the homopolymer molecular weight on the domain morphology is ascribed to the different miscibility of the homopolymers and the PS blocks of the copolymers. Since the miscibility decreases as the molecular weight increases, the effective volume fraction of the PS blocks of the copolymers decreases as the homopolymer molecular weight increases, i.e. the PS blocks become less swollen by the PS homopolymers.

1.3. Micellization of Small molecule surfactants.

Because the micellization of amphiphilic block copolymers in solutions is often compared to that of small molecule amphiphiles, a brief introduction to micellization of small molecule amphiphiles is presented in this section. small molecule Amphiphiles consist of a hydrophobic tail (alkyl chain) and a hydrophilic (ionic or non-ionic) head group. The abrupt change in many physicochemical properties of solutions of amphiphilic molecules when a critical concentration is reached is attributed to the formation of micelles.[32,33] The concentration at which the molecules start to form micelles is called the critical micellization concentration (CMC). Because of the relatively high CMC and the liquid-like core of the micelle at room temperature, chain exchange is usually very fast (of the order of ms). Therefore, a dynamic equilibrium exists between the micelles and the single molecules.

It has been known for many years that the micelles of small molecule amphiphiles can be spherical, cylindrical, lamellar or even assume several other morphologies.[34,35] Because the inter-head group repulsion is strong and the surface tension of the core is big, the hydrophobic chains in the cores are highly extended and the core radius is almost equal to the contour length of the alkyl chain. The formation of various morphologies has been explained in terms of a dimensionless packing parameter, v/a_0l_c, where a_0 is the optimal surface area of the hydrophilic head, and v and l_c are the volume and the critical length of the hydrophobic tail. The value of the parameter v/a_0l_c determines the geometry of the aggregates. In particular, if $v/a_0l_c \leq 1/3$, spherical structures are formed. When $1/3 < v/a_0l_c < 1/2$, the structure of the micelles is cylindrical. If $1/2 < v/a_0l_c < 1$, vesicles or lamellar micelles are observed. Finally, when $v/a_0l_c > 1$, inverted spherical micelles form.[34,35] Because a_0 is found experimentally to be dependent of the nature of the head group, but almost independent of the hydrophobic chain length, and l_c can be estimated from semi-empirical equations, the parameter v/a_0l_c can also be used to predict the morphologies of the micelles. For example, most single-chain surfactants form spherical micelles, while most double-chain surfactants form bilayers because of the higher value of v/l_c.

The addition of inert salt has strong effect on the morphology due to a reduction of the thickness of the electron double layer of the head group on addition of salt.[35-41] Consequently, the optimal surface area of the hydrophilic head, a_0, is decreased. The importance of electrostatic interactions among head groups in determining the micelle structure is demonstrated in the studies of micelle formation of mixtures of anionic and cationionic surfactants, in which the optimal area of the head groups is greatly reduced due to the attractive interaction between anionic and cationic heads.[42] Similarly, changing the pH of the solution also affects the aggregation behavior of the amphiphiles, if the ionization of the head group is pH dependent.[43]

1.4. Micellization of Block Copolymers in Two Dimensions.

Another area in which multiple morphologies form is the self-assembly of block copolymer at water surface, i.e. quasi two dimensional micelles.[44-51] The two dimensional micelles were prepared by spreading a solution of the block copolymers in a good solvent at the air-water interface on a Langmuir trough. Langmuir-Blodgett (LB) films of those surface micelles were transferred onto a silicon wafer by dipping. Atomic force microscopy (AFM) [50,51] and TEM [44-51] were used to characterize the micelles. It was shown that the micelles of various morphologies were formed by changing the copolymer composition. The morphologies includes circular micelles, ribbons, large "pancakes" and foams. Both AFM and TEM show that the circular micelles are highly ordered over large distances (several microns). Two dimensional micelles have been prepared from a number of diblock copolymers, such as polystyrene-*b*-poly(4-vinylpyridine), polystyrene-*b*-poly(dimethyl siloxane), polystyrene-*b*-poly(n-butyl methacrylate) and polystyrene-*b*-poly(t-butyl methacrylate). This suggests that two dimensional micellization is a very general phenomenon for hydrophilic-*b*-hydrophobic diblock copolymers at the air-water interface.

A typical example,[47] for the polystyrene-*b*-poly(4-vinylpyridine) (PS-*b*-P4VP) copolymers of a constant PS block length (480 units) but a variable P4VP block (quaternized with decyl iodide), is shown in Figure 1.5. When the P4VP block lengths are 200, 34 and 13, circular micelles, ribbon-like structures and large "pancakes" are formed, respectively. For this particular group of samples, the circular micelles are ~35 nm in diameter and 7 nm high. The ribbons and pancakes have the almost same height but are much larger.

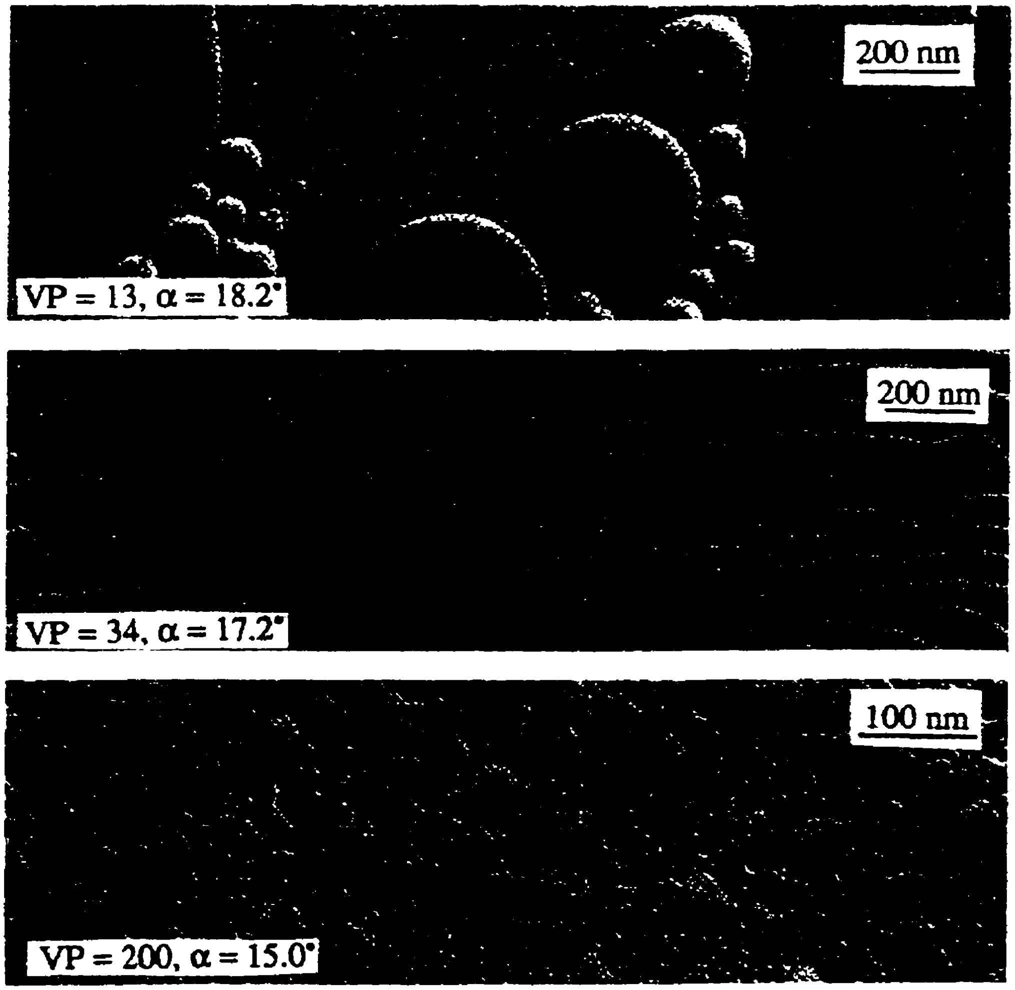

Figure 1.5. Various morphologies of Langmuir-Blodgett films of two dimensional aggregates from PS(480)-*b*-P4VP.$C_{10}I$ copolymer: Pancakes (top); Ribbons (middle); Circular micelles (bottom). The P4VP block length (VP) and the shadowing angle (α) are indicated on each picture.

Two dimensional micelles have been studied with X-ray reflectivity as a function of surface pressure used in the preparation of the Langmuir-Blodgett (LB) films.[50] It was confirmed that long range order in the circular micelles was not an artifact caused by the dipping process when producing LB films. Also, it was found that the hydrophilic chains formed a dense, melt-like layer on the surface of the water, rather than being submerged in the water. The solvent from which the films are cast has an important influence. For example, a phase-inverted form of the circular morphology, i.e. a two dimensional nanofoam, can be produced by changing the casting solvent so that the hydrophobic part forms the continuous phase. [49] Addition of homopolymer to the spreading solution, and of salt to the subphase also have an effect on the micellization process. [48]

1.5. Micellization of Block Copolymers in Solution.

1.5.1. Formation of micelles. For the past four decades,[52] it has been known that when block copolymers are dissolved in a selective solvent, i.e. a solvent which is good for only one of the blocks, micelles or aggregates can form as a result of the association of the insoluble blocks.[1-3] Micelle formation requires the presence of two opposing forces, i.e. an attractive force between the insoluble blocks which leads to aggregation, and a repulsive force between the soluble blocks which prevents unlimited growth of the micelle size into a distinct macroscopic phase. Therefore, each micelle consists of a certain number of copolymer chains, which is called the *aggregation number*, an important parameter of micelle formation. Micelles are stabilized in the solution due to the interaction of the soluble blocks and the solvent.

There are two types of block copolymer micelles. In a polar solvent, such as water, *regular micelles* are formed, which have a hydrophobic core and a hydrophilic corona. In an apolar (or low polarity) solvent, the locations of the blocks are reversed, i.e. the hydrophilic segments form the core surrounded by a hydrophobic corona shell. In this case, the micelles are referred to as *reverse micelles*. Depending on the composition of the block copolymers, each type of the micelles are further divided into *star* and *crew-cut* micelles. Star micelles are made from block copolymers in which the corona-forming blocks are much longer than the core-forming blocks. However, in crew-cut micelles, the corona-forming blocks are much shorter than the core-forming blocks. Therefore, crew-cut micelles are characterized by a bulky core and a relatively thin corona. In the past four decades, star micelles (both regular and reversed) have received much attention, and a considerable amount of information has been accumulated.[1-3] By contrast, crew-cut micelles have been receiving attention experimentally only very recently.[53,54] The concept of crew-cut micelles was proposed by Halperin et al,[55] based on an earlier theoretical study of de Gennes.[56]

1.5.2. Dynamics and thermodynamics. Block copolymers can micellize, in principle, by one of two mechanism, i.e. open (or step-wise) or closed association.[1] Open association is characterized by a series of consecutive equilibria involving all possible sizes of aggregates starting with dimers. The closed association assumes that there is a single-stage equilibrium between unimers and micelles with a certain aggregation number. In general. it has been found that micellization of the block copolymers obeys the closed association mechanism. The closed association model implies the existence of a critical micellization concentration (CMC), from which the free energy of micelle formation (ΔG) can be evaluated by

$$\Delta G = -RT \ln(CMC)$$

where R and T are the gas constant and the temperature. Assuming the association number is independent on temperature, the enthalpy (ΔH) of micellization can be determined from the temperature dependence of the CMC,

$$\Delta H = R\, d\ln (CMC)/d(1/T)$$

The entropy (ΔS) of micellization can be calculated by

$$\Delta S = (\Delta H - \Delta G)/T$$

Based on the above equations, the thermodynamics of micellization in several block copolymer/solvent systems have been studied.[57-59] It was found that in organic solvents, the driving force for block copolymer micellization is the enthalpic contribution to the free energy.[57] The negative enthalpy of micellization results from the replacement of unfavorable polymer(insoluble segment)-solvent interactions by polymer-polymer and solvent-solvent interactions. On the other hand, in aqueous solutions, the driving force becomes entropic.[58] This is ascribed to the change in the structure of water surrounding the hydrophobic segments. That the driving force shifts from enthapic to entropic is demonstrated in a recent study of thermodynamics of block copolymer micellization in DMF/water mixtures with increasing water content.[59]

In a system of micelles of copolymers, an important aspect is the dynamics of the chain exchange between the micelles. An equilibrated system must be in a dynamic equilibrium, in which the micelles can exchange chains with one another. For small molecule amphiphilies, the chain exchange is very fast. However, the chain exchange of copolymer micelles are usually slow due to a number of reasons, such as the high molecular weight, the entanglement and low mobility of the chains in the core, the low CMC, etc. The dynamic process of chain exchange between micelles has been studied by fluorescence,[60,61] sedimentation velocity experiments[62,63] and by theoretical approaches.[64,65] The process was found to depend on the incompatibility of the solvents and the insoluble block. For example, for the micelles of the polystyrene-*b*-poly(methacrylic acid) (PS-*b*-PMAA) copolymers in dioxane/water mixtures,[62] the chain exchange is significant in the time scale of hours when the solvent composition is 80/20 (v/v) for dioxane /water. In this case, the high rate of the chain exchange is due to the fact that the PS core is swollen with dioxane and that the CMC is relatively high. However, when the water content in the solvent mixtures is increased to above 30 %, chain exchange between the micelles is negligible over a period of several days, and the micelle structures are considered to be "frozen" since the chain exchange has become extremely slow. The decreased rate of chain exchange at higher water contents is ascribed to a decreased CMC and less swollen PS cores.

1.5.3. Structural characteristics of block copolymer micelles. Due to a wide range of potential applications of block copolymer micelles in areas such as drug delivery, as catalysts and as microreactors, studies of the structures of the micelles and of their properties have been progressing continuously. Many publications on these subjects exist, which deal with morphology,[66-69] CMC,[70-74] size distribution of the micelles,[75-77] dimensions of both the core and corona shell as a function of the block copolymer composition,[78-80] order-disorder transitions in micellar solutions,[81] etc. Techniques used for the characterization include both dynamic and static light scattering, [75-80] size exclusion chromatography, [82-83] viscosity, [84,85] ultracentrifugation (or sedimentation velocity), [78,86] small angle X-ray (or neutron) scattering, [80,81] fluorescence, [70-74] transmission electron microscopy, [66,68] nuclear magnetic resonance, [87-90] etc.

In general, it was found that the CMC of block copolymer micelles is usually much lower than that of small molecule amphiphilies. The CMC depends on both the insoluble block and the soluble block of the copolymers. In particular, the influence of the insoluble block length is much stronger than that of the soluble block length. The micelle sizes and the aggregation numbers depend on the copolymer composition. The higher the insoluble block length, the larger the aggregation number and the micelle size. The soluble block has an opposite effect. The distributions of the micelle sizes are usually narrow, and are influenced by the polydispersity of the copolymer blocks.

In block copolymer solutions, micelles of spherical geometry are formed in most of the systems studied. A spherical micelle consists of a core surrounded by a spherical corona shell. The micelles take on this structure in a very broad range of the compositions of the block copolymers, especially, where the soluble blocks are the major component. Non-spherical micelles in solutions of block copolymers have been reported in a number of systems. [54, 67-69, 79, 91-96] In light scattering studies of block copolymer micelles, based on the information of gyration radius, hydrodynamic radius, and rotational diffusion coefficient, it was reported that rod-like or cylindrical micelles exist in several systems,[69,79,81,95] depending on the block copolymer composition. In synchrotron SAXS study on solutions of polystyrene-*b*-polyisoprene (PS-*b*-PI) in aniline, where the PI blocks associate to form aggregates, it was found that the vesicle model describes the experimental system much better than the spherical micelle model for the block copolymer with relatively short PS block length.[67] Also, regions of stability of spherical and cylindrical micelles in poly(ethylene oxide)-b-poly(propylene oxide) triblocks were identified by SAXS.[96] While the formation of non-spherical aggregates is based on indirect evidence in most cases, in two cases, the existence of worm-like micelles[92] and of platelet aggregates with copolymer cylinders extending from the edges[68] has been proved by direct TEM observation.

1.5.4. Theoretical approaches to micelle structure. A number of theories deal with spherical block copolymer micelles.[55,97-102] Although those theories were developed using different approaches, they all deal with the relations between structural parameters of the micelles and the molecular characteristics of the constituent block copolymers.

In general, the theories can be divided into two categories, i.e. star and mean-field theories. The star models consider that the density of the core region is uniform, but that the density of the corona decreases with increasing distance from the core. [97,98] The mean-field models assume that each region of the core and the corona shell has a uniform concentration of polymer segments, independent of the distance from the micelle center. [55, 99-102] A simple micelle model was first proposed by de Gennes,[55] which analyzed the formation of diblock copolymer micelles in a selective solvent by minimizing the free energy of an isolated micelle with respect to the aggregation number. On this basis, scaling relations were developed for the core radius, R_{core}. For the case in which the interfacial energy between the core and the solvent is large, it is found that

$$R_{core} \propto N_B^{2/3}$$

where N_B is the degree of polymerization of the core-forming block. When the interfacial energy is low, the micelle core radius R_{core} is related to the core-forming block by

$$R_{core} \propto N_B^{1/2}$$

The model proposed by de Gennes was refined by Leibler, Orland and Wheeler (LOW) for a system of block copolymers in a homopolymer matrix.[100] It was found that when the two blocks of the copolymers show weak incompatibility, the following scaling relation is obtained

$$R_{core} \propto N_B^{0.53}$$

One of the important aspects of the de Gennes and LOW theories is that the free energies of the micelle core-solvent interface and of stretching of the core-forming blocks influence the micellization behavior.

Based on the theoretical treatment of the conformation of star-branched polymers,[103,104] an improved model has been suggested by Zhulina and Birshtein,[97] in which the segment concentration in the micelle shell is allowed to decrease with increasing distance from the core center. Scaling relations are developed relating the micelle characteristics to the lengths of both the core-forming and the corona-forming blocks. Scaling relations for the core radius, the corona shell thickness and the aggregation number are obtained for four different ranges of block copolymer composition. In particular, the micelle core scales only with the insoluble block length when block copolymers are highly asymmetric. In the intermediate region of the copolymer composition, the core size becomes dependent on both the insoluble and the soluble blocks. Halperin[98] also developed a star model of block copolymer micelles. For the case of $N_A >> N_B$, where N_A and N_B are the lengths of the soluble block and the insoluble block, the model predicts that the core radius scales as $aN_B^{3/5}$, a being the typical monomer size; the exponent is in agreement with that of Zhulina and Birstein.

Whitmore and Noolandi [101] extended the theory of Noolandi and Hong [100] to micelles of an A-*b*-B diblock copolymer in homopolymer A. A relationship between the core radius and the copolymer composition, $R_{core} \propto N_B^{\alpha} N_A^{-\gamma}$, was obtained, where N_B and N_A represent the degrees of polymerization of the insoluble and soluble blocks, respectively. In their study, qualitative agreement between experiment and theory was obtained for the system of polystyrene-*b*-polybutadiene copolymer micelles in polybutadiene homopolymer. Theoretical values for the exponents lay in the range $0.67 \leq \alpha \leq 0.76$ and $0 \leq \gamma \leq 0.1$, showing that the soluble block has a relatively weak influence on the size of the micelle core. Bluhm and Whitmore[105] also refined the model of Noolandi and Hong for a particular system, i.e. micelles with polystyrene core and polybutadiene shell in heptane. They obtained

$$R_{core} \propto N_B^{0.67} N_A^{-0.01}$$

Nagarajan and Ganesh [102] also predicted that the soluble block could have a large influence on the micelle structure, specifically if the soluble block is in a good solvent. In their model, the Gibbs energy change in terms of standard chemical potential is expressed by considering all relevant physicochemical changes accompanying the transfer of a copolymer molecule from the unimer state to a micelle. General expressions for the core radius and aggregation number were derived as a function of block copolymer composition, interfacial tension and corona-solvent χ parameter. They found that for polystyrene-*b*-polybutadiene block copolymers in heptane, $R_{core} \sim N_B^{0.70}N_A^{-0.08}$; for poly(oxyethylene)-*b*-poly(oxypropylene) copolymers in water, $R_{core} \sim N_B^{0.73}N_A^{-0.17}$.

The larger dependence of R_{core} on N_A in the latter system is attributed to the fact that water is a good solvent for poly(oxyethylene) under the conditions of the measurement.

While most of the theoretical studies on block copolymer micellization focus on the formation of spherical micelles, some papers[106-111] explored theoretically the stability of block copolymer bilayers, [106-108] and the transition between two different morphologies,[109-111] e.g. from spherical to rod-like, in terms of changes of the molecular parameters of the polymers, such as the degree of polymerization of the component blocks of the copolymer and the size of the solvent molecules. Munch and Gast[109] concluded that the block copolymer will form lamellar micelles in the composition region where the core-forming block is much longer than the corona-forming block. The size of the solvent molecules has a significant effect on the boundary of the morphological transition between the lamellar and the spherical micelles. Specifically, for symmetric copolymers, lamellar micelles are favored as the solvent size increases. The formation of the cylindrical micelles versus spherical micelles in block copolymer/homopolymer blends was studied by Mayes and de la Cruz.[110] As the core-forming block fraction of the copolymers and the homopolymer (solvent) molecular weight increase, cylindrical micelles are favored, and spherical micelles are precluded because of the higher CMC for their formation compared to that for cylindrical micelles. Nagarajan[111] also studied the morphological transitions of block copolymer aggregates. Transitions from spherical to cylindrical, and to bilayer are predicated to occur with increasing insoluble block content of the copolymers. Furthermore, while the core dimensions of the preferred geometry increase with increasing insoluble block content, the core dimensions are predicted to decrease discontinuously in parallel with morphology changes.

1.6. Focus and Purpose of the Present Thesis

Although extensive experimental and theoretical studies of the self-assembly of block copolymers in selective solvents have been conducted over the past four decades, the block copolymers used in the studies had corona forming blocks which were usually much longer than the core-forming blocks. Therefore, the micelles were essentially the star type, with a spherical core-shell structure. The formation of non-spherical micelles, e.g. rods, vesicles, was encountered only on occasion. It was predicated that the formation of non-spherical aggregates of block copolymers in solutions may occur when the major component of the block copolymers is the insoluble block, i.e. for block copolymers which yield crew-cut micelles. This can also be deduced by extrapolating the results of the microdomain structures in block copolymer/homopolymer bends as a function of the homopolymer molecular weight to a small molecule solvent. However, to our knowledge, studies of crew-cut micelles are very limited, in that only two papers dealing with these structures have been published.

This thesis focuses on the formation and characteristics of crew-cut micelle-like aggregates of highly asymmetric polystyrene-*b*-poly(acrylic acid) diblock copolymers. The aggregates are prepared in N,N-dimethylformamide-water mixtures, and are then isolated in water. The contents of the insoluble polystyrene blocks of the copolymers range from 80 to 98 wt. %. The experimental studies presented in this dissertation describe for the first time the preparation of block copolymer aggregates of various morphologies in the low molecular weight solvents.

Chapter 2 is a review of the studies of the crew-cut aggregates presented in the subsequent chapters of this thesis.

Chapter 3 deals with the formation of the spherical crew-cut micelles, the scaling relation between the micelle core size and the copolymer composition in aqueous solutions, and the hydrodynamic radii and the corona shell dimensions of the micelles as a function of added NaCl concentration and pH of the solutions.

Chapters 4 and 5 describe the formation and characteristics of the crew-cut aggregates of various morphologies. The morphologies include small spheres, rods, lamellae, vesicles and the large compound spherical micelles. Specifically, chapter 4 is a brief announcement of the preparation of crew-cut aggregates of various morphologies. Chapter 5 presents the detailed experimental results for the formation of various morphologies. A range of characteristics of the aggregates and their dependence on the compositions of the block copolymers, as well as on the effect of added homopolystyrene on the morphologies of the aggregates is discussed.

Chapters 6 and 7 describe the studies of the morphological transitions induced by added ions. Again, chapter 6 is a brief description of the morphogenic effect of the addition of ions in micromolar ($CaCl_2$ or HCl) or millimolar (NaCl) concentrations. In addition to the morphologies described in chapters 4 and 5, an unusual large compound vesicle (LCV) morphology can be formed from a single block copolymer. The gelation of a dilute spherical micelle solution induced by ions due to the formation of a cross-linked "pearl necklace" morphology is also described. Chapter 7 discusses the detailed study of the morphogenic effects of added ions on the crew-cut aggregates along with some considerations of the causes of added ion effect and the possible mechanism for the formation of LCVs.

Chapter 8 deals with two related topics. One is the phase separation behavior of PS-*b*-PAA block copolymer in DMF/water mixtures as a function of the copolymer concentrations and compositions, as well as the presence of added electrolytes. because the crew-cut aggregates are prepared by adding water to a homogeneous copolymer solution, a phase separation process is involved during micellization. Thus, the study of the phase separation behavior is essential for an understanding of the formation of the aggregates in this system. The second topic deals with the relationship between the lability of the micelle structure and the added water content, to ascertain the conditions under which the formed micelles become structurally frozen aggregates and to bring the consideration of kinetics into the formation of the aggregates.

The final chapter includes the conclusions to the thesis, the contributions to original knowledge and suggestions for the future work.

1.7. REFERENCES

1. Price, C. In *Developments in block copolymers*; I. Goodman, I. Ed.; Applied science publishers: London, 1982; Vol. 1, p 39.
2. Selb, J.; Gallot, Y. In *Developments in block copolymers*; Goodman, I. Ed.; Applied science publishers: London, 1985; Vol. 2, p 27.
3. Tuzar, Z.; Kratochvil, P. In *Surface and Colloid Science*; Matijevic, E. Ed.; Plenum Press: New York, 1993; Vol. 15, p 1.
4. Cowie, J. M. G. *Polymers: Chemistry & Physics of Modern Materials*, 2nd ed., Chapman & Hall, New York, 1991.
5. Noshay, A.; McGrath, J. E. *Block Copolymers Overview and Critical Survey*; Academic Press: New York, 1977.
6. de Gennes, P.-G. *Scaling Concepts in Polymer Physics*, Cornell Univ., Press, 1979
7. *Processing, Structure, and Properties of Block Copolymers*, Folkes, M. J. Ed.; Elsevier, New York 1985.

   Developements in Block Copolymers-1, edited by Goodman, I. Ed.; Applied science, New York, 1982.
8. Brown, R. A., Masters, A. J., Price, C., Yuan, X. F., in *Comprehensive Polymer Science: Polymer Properties*, Allen, S. G.; Bevington, J. C.; Booth, C.; Price, C.; Eds. (Pergamon, Oxford, 1989), vol. 2, p. 155.
9. Bates, F. S.; Fredrickson, G. H. *Annu. Rev. Phys. Chem.* **1990**, *41*, 525.
10. Flory, P. J. "*Principles of Polymer Chemistry*", Cornell University Press, Ithaca, New York, 1953.
11. Bazuin, C. G. In *Multiphase Polymers: Blends and Ionomers*, Utracki, L. A.; Weiss, R. A. eds., ACS Symposium Series 395, ACS, Washington, D. C., 1989, Chapter 21.
12. Helfand, E.; Wasserman, Z. R. In *Developements in Block Copolymers-1*, edited

by I. Goodman; Applied science, New York, 1982.

13. Meier, D. J. In Thermoplastic Elastomers: A Comprehensive Review; Legge, N. R.; Holden, G.; Schroeder, H. E.; eds., Hanser: New York, 1987, Chapter 11.
14. Molau, G. E.; Wittbrodt, W. M. *Macromolecules* **1968**, *1*, 260.
15. Molau, G. E. *Block Polymers*, Plenum Press, 1970, p. 79.
16. Finaz, G.; Skoulios, A.; Sadron, C. *C. R. Acad. Sci.* [Paris] **1961**, *253*, 265; Gallot, B.; Mayer, R.; Sadron, C. *ibid.* **1966**, *263*, 42.
17. Hashimoto, T.; Nagatoshi, K.; Todo, A.; Hasegawa, H.; Kawai, H. *Macromolecules* **1974**, *7*, 364; Hashimoto, T.; Fujimura, M.; Kawai, H. *ibid.* **1980**, *13*, 1660.
18. Meier, D. J. In *Thermoplastic Elastomers*; Legge, N. G., Holden, G., Schroeder, H. E. Eds., Hanser: New York, 1987, Chapter 11.
19. Thomas, E. L.; Alward, D. B.; Kinning, D. J.; Martin, D. C.; Handlin, D. L., Jr.; Fetters, L. J. *Macromolecules* **1986**, *19*, 2197.
20. Hasegawa, H.; Tanaka, H.; Yamasaki, K.; Hashimoto, T. *Macromolecules* **1987**, *20*, 1651.
21. Thomas, E. L.; Anderson, D. M.; Henkee, C. S.; Hoffman, D. *Nature* **1988**, *334*, 598.
22. Förster, S.; Khandpur, A. K.; Zhao, J.; Bates, F. S.; Hamley, I. W.; Ryan, A. J.; Bras, W. *Macromolecules* **1994**, *27*, 6922.
23. Hajduk, D. A.; Harper, P. E.; Gruner, S. M.; Honeker, C. C.; Kim, G.; Thomas, E. L.; Fetters, L. J. *Macromolecules* **1994**, *27*, 4063.
24. Kinning, D. J.; Winey, K. I .; Thomas, E. L. *Macromolecules* **1988**, *21*, 3502.
25. Hashimoto, T.; Tanaka, T.; Hasegawa, H. *Macromolecules* **1990**, *23*, 4378.
26. Tanaka, T.; Hasegawa, H.; Hashimoto, T. *Macromolecules* **1991**, *24*, 240.
27. Winey, K. I.; Thomas, E. L.; Fetters, L. J. *Macromolecules* **1991**, *24*, 6182; *ibid.* **1992**, *25*, 422, 2645.

28. Banaszak, M.; Whitmore, M. D. *Macromolecules* **1992**, *25*, 2757.
29. Whitmore, M. D.; Smith, T. W. *Macromolecules* **1994**, *27*, 4673.
30. Bates, F. S.; Kumar, A.; Schulz, M. F. *J. Polym. Sci., Polym. Phys. Ed.* **1995**, *33*, 1423.
31. Adedeji, A.; Jamieson, A. M.; Hudson, S. D. *Macromolecules* **1995**, *28*, 5255.
32. Shinoda, K.; Nakagawa, T.; Tamamushi, B.-I.; Isemura, T. *Colloidal Surfactants*, Academic Press, New York, 1963.
33. Moroi, Y. *Micelles--Theoretical and Applied Aspects*, Plenum Press: New York, 1992, chapter 4.
34. Israelachvili, J. N. *Intermolecular and surface forces*, 2nd edition, Academic press: London, San Diego, 1992.
35. Mitchell, D. J.; Ninham, B. W. *J. Chem. Soc.; Faraday Trans. II*, **1981**, *77*, 601.
36. Israelachvili, J. N.; Mitchell, D. J.; Ninham, B. W.; *J. Chem. Soc., Faraday Trans.* II, **1976**, *72*, 1525.
37. Ozeki, S.; Ikeda, S. *J. Colloid Interface Sci.* **1982**, *87*, 424.
38. Sein, A.; Engberts, J. B. F. N. *Langmuir* **1995**, *11*, 455.
39. Miyagishi, S.; Kurimoto, H.; Asakawa, T. *Langmuir* **1995**, *11*, 2951.
40. Schepers, F. J.; Toet, W. K.; van de Pas, J. C. *Langmuir* **1993**, *9*, 956.
41. Talmon, Y.; Evans, D. F.; Ninham, B. W. *Science* **1983**, *221*, 1047.
42. Kaler, E. W.; Murthy, A. K.; Rodriguez, B. E. Zasadzinski, J. A. N. *Science* **1989**, *245*, 1371.
43. Ravoo, B. J.; Engberts, J. B. F. N. *Langmuir* **1994**, *10*, 1735.
44. Zhu, J.; Eisenberg, A.; Lennox, R. B. *J. Chem. Soc.* **1991**, *113*, 5583.
45. Zhu, J.; Lennox, R. B.; Eisenberg, A. *Langmuir* **1991**, *7*, 1579.
46. Zhu, J.; Lennox, R. B.; Eisenberg, A. *J. Phys. Chem.* **1992**, *96*, 4727.
47. Zhu, J.; Eisenberg, A.; Lennox, R. B. *Macromolecules* **1992**, *25*, 6547.
48. Zhu, J.; Lennox, R. B.; Eisenberg, A. *Macromolecules* **1992**, *25*, 6556.

49. Meszaros, M.; Lennox, R. B.; Eisenberg, A. *Faraday Discussions* **1994**, *98*, 283.

50. Li, Z.; Zhao, W.; Quinn, J.; Rafailovich, M. H.; Sokolov, J.; Lennox, R. B.; Eisenberg, A.; Wu, X. Z.; Sinha, S. K.; Tolan, M. *Langmuir* **1995**, *11*,.4785.

51. Li, S.; Hanley, S.; Khan, I.; Varshney, S. K.; Eisenberg, A.; Lennox, R. B. *Langmuir* **1993**, *9*,.2243.

    Li, S. Ph.D. Thesis 1995, McGill University, Montreal, Quebec, Canada.

52. Merrett, F. M. *Trans. Faraday Soc.* **1954**, *50*, 759; *J. Polym. Sci.* **1957**, *24*, 467.

53. Gao, Z.; Varshney, S. K.; Wong, S.; Eisenberg, A. *Macromolecules* **1994**, *27*, 7923.

54. Honda, C.; Sakaki, K.; Nose, T. *Polymer* **1994**, *35*, 5309.

55. de Gennes, P. G. In *Solid State Physics*, Liebert, L. Ed.; Academic press, New York, 1978; supplement 14, p. 1.

56. Halperin, A.; Tirrell, M.; Lodge, T. P. *Adv. Polym. Sci.* **1992**, *100*, 31.

57. (a) Quintana, J. R.; Villacampa, M.; Salazar, R.; Katime, I. A. *J. Chem. Soc., Faraday Trans.* **1992**, *88*, 2793; (b) Quintana, J. R.; Villacampa, M.; Katime, I. A. *Macromolecules* **1993**, *26*, 601; (c) Quintana, J. R.; Janez, M. D.; Villacampa, M.; Katime, I. A. *Macromolecules* **1995**, *28*, 4139; (d) Quintana, J. R.; Janez, M. D.; Katime, I. A. *Langmuir* **1996**, *12*, 2196; (e) Price, C.; Chan, E. K. M.; Stubbersfield, R. B. *Eur. Polym. J.* **1987**, *23*, 649; (f) Zhou, Z.; Chu, B.; Peiffer, D. C. *Macromolecules* **1993**, *26*, 1876.

58. Alexandridis, P.; Holzwarth, J. F.; Hatton, T. A. *Macromolecules* **1994**, *27*, 2414; Alexandridis, P.; Nivaggioli, T.; Hatton, T. A. *Langmuir* **1995**, *11*, 1468; Deng, Y.; Yu, G. E.; Price, C.; Booth, C. *J. Chem. Soc., Faraday Trans.* **1992**, *88*, 1441; Zhou, Z.; Chu, B. *Macromolecules* **1994**, *27*, 2025.

59. Shen, H.; Zhang, L.; Eisenberg, A. manuscript in preparation.

60. Prochazka, K.; Bednar, B.; Mukhtar, E.; Svoboda, P.; Trnena, J.; Almgren, M. *J. Phys. Chem.* **1991**, *95*, 4563.

61. Wang, Y.; Kausch, C. M.; Chun, M.; Quirk, R. P.; Mattice, W. L. *Macromolecules* **1995**, *28*, 904.
62. Tian, M.; Qin, A.; Ramireddy, C.; Webber, S. E.; Munk, P.; Tuzar, Z.; Prochazka, K. *Langmuir* **1993**, *9*, 1741.
63. Pacovska, M.; Prochazka, K.; Tuzar, Z.; Munk, P. *Polymer* **1993**, *34*, 4585.
64. Haliloglu, T.; Bahar, I.; Erman, B.; Mattice, W. L. *Macromolecules* **1996**, *29*, 4764.
65. Halperin, A.; Alexander, S. *Macromolecules* **1989**, *22*, 2403.
66. Price, C. *Pure and Appl. Chem.* **1983**, *55*, 1563.
67. Zhou, Z.; Chu, B. *Macromolecules* **1988**, *21*, 2548.
68. Gast, A. P.; Vinson, P. K.; Cogan-Farinas, K. A. *Macromolecules* **1993**, *26*, 1774.
69. Zhao, J. Q.; Pearce, E. M.; Kwei, T. K.; Jeon, H. S.; Kesani, P. K.; Balsara, N. P. *Macromolecules* **1995**, *28*, 1972.
70. Gao, Z.; Eisenberg, A. *Macromolecules* **1993**, *26*, 7353.
71. Astafieva, I.; Zhong, X. F.; Eisenberg, A. *Macromolecules* **1993**, *26*, 7339; and references therein.
72. Karine, K.; Astafieva, I.; Eisenberg, A. *Macromolecules* **1994**, *27*, 6341; **1995**, *28*, 7135.
73. Astafieva, I.; Karine, K; Eisenberg, A. *Macromolecules* **1995**, *28*, 7127.
74. Wilhelm, M.; Zhao, C-L.; Wang, Y.; Xu, R.; Winnik, M. A. *Macromolecules* **1991**, *24*, 1033.
75. Xu, R.; Winnik, M. A. *Macromolecules* **1991**, *24*, 87.
76. Cogan, K. A.; Gast, A. P. *Macromolecules* **1990**, *23*, 745.
77. Alexandridis, P.; Nivaggioli, T.; Hatton, T. A. *Langmuir* **1995**, *11*, 1468.
78. Qin, A.; Tian, M.; Ramireddy, C.; Webber, S. E.; Munk, P. *Macromolecules* **1994**, *27*, 120.
79. Antonietti, M.; Heinz, S.; Schmidt, M.; Rosenauer, C. *Macromolecules* **1994**, *27*,

3276.

80. Nguyen, D.; Williams, C.; Eisenberg, A. *Macromolecules* **1994**, *27*, 5090; Nguyen, D.; Varshney, S. K.; Williams, C.; Eisenberg, A. *Macromolecules* **1994**, *27*, 5086; Nguyen, D.; Zhong, X.-F.; Williams, C.; Eisenberg, A. *Macromolecules* **1994**, *27*, 5173.
81. (a) Huggins, J. S.; Dawkins, J. V.; Maghami, G. G.; Shakir, S. A. *Polymer* **1986**, *27*, 931; (b) McConnell, G. A.; Gast, A. P. Huang, J. S.; Smith, S. D. *Phys. Rev. Let.* **1993**, *71*, 2102; (c) Harkless, C. R.; Singh, M. A.; Nagler, S. E. *Phys. Rev. Lett.* **1990**, *64*, 2285; (d) Shibayama, M.; Hashimoto, T.; Kawai, K. *Macromolecules* **1983**, *16*, 16; (e) Pusey, P. N.; van Megen, W. *Nature(London)* **1986**, *320*, 340; (f) Monovoukas, Y.; Gast, A. P. *J. Colloid Interface. Sci.* **1989**, *128*, 533.
82. Selb, J.; Gallot, Y. *Makromol. Chem.* **1981**, *182*, 1491.
83. Desjardins, A.; Eisenberg, A *Macromolecules* **1991**, *24*, 5779.
84. Periard, J.; Riess, G.; Meyer-Gomez, M. J. *Eur. Polym. J.* **1973**, *9*, 687.
85. Mandema, W.; Zeldenrust, H.; Emeiss, C. A. *Makromol. Chem.* **1979**, *180*, 1521.
86. Plestil, J.; Hlavata, D.; Tuzar, Z. *Polymer* **1990**, *31*, 2112.
87. Nakamura, K.; Endo, R.; Takeda, M. *J. Polym. Sci., Polym. Phys. Ed.* **1977**, *15*, 2087.
88. Heatly, F.; Begum, A. *Makromol. Chem.* **1977**, *178*, 1205.
89. Gao, Z.; Zhong, X.-F.; Eisenberg, A. *Macromolecule* **1994**, *27*, 794.
90. Wu, G.; Zhou, Z.; Chu, B. *Macromolecule* **1993**, *26*, 2117.
91. Utiyama, H.; Takenaka, K.; Mizumori, M.; Fukuda, M.; Tsunashima, Y.; Kurata, M. *Macromolecules* **1974**, *7*, 515.
92. Price, C. *Pure and Appl. Chem.* **1983**, *55*, 1563.
93. Hilfiker, R.; Wu, D. Q.; Chu, B. *J. Colloid Interface Sci.* **1990**, *135*, 573.

94. Tuzar, Z.; Kratochvil, P.; Prochazka, K.; Munk, P. *Collect. Czech. Chem. Commun.* **1993**, *58*, 2362.
95. Schillén, K.; Brown, W.; Johnsen, R. M. *Macromolecules* **1994**, *27*, 4825.
96. Glatter, O.; Scherf, G.; Schillén, K.; Brown, W. *Macromolecules* **1994**, *27*, 6046.
97. Zhulina, E. B.; Birshtein, T. M. *Vysokomol. Soedin.* **1985**, *27*, 511.
98. Halperin, A. *Macromolecules* **1987**, *20*, 2943.
99. Leibler, L.; Orland, H.; Wheeler, J. C. *J. Chem. Phys.* **1983**, *79*, 3550.
100. Noolandi, J.; Hong, K. M. *Macromolecules* **1983**, *16*, 1443.
101. Whitmore, M. D.; Noolandi, J. *Macromolecules* **1985**, *18*, 657.
102. Nagarajan, R.; Ganesh, K. *J. Chem. Phys.* **1989**, *90*, 5843.
103. Daoud, M.; Cotton, J. P. *J. Physique* **1982**, *43*, 531.
104. Birshtein, T. M.; Zhulina, E. B. *Polymer* **1984**, *25*, 1453.
105. Bluhm, T. L.; Whitmore, M. D. *Can. J. Chem.* **1985**, *63*, 249.
106. Ajdari, A.; Leibler, L. *Macromolecules* **1991**, *24*, 6803.
107. Wang, Z.-G. *Macromolecules* **1992**, *25*, 3702.
108. Dan, N.; Safran, S. A. *Macromolecules* **1994**, *27*, 5766.
109. Munch, M. R.; Gast, A. P. *Macromolecul* **1988**, *21*, 1360.
110. Mayes, A. M.; de la Cruz, M. O. *Macromolecules* **1988**, *21*, 2543.
111. Nagarajan, R. in *Solvents and Self-organization of Polymers*, NATO ASI Series, S. E. Webber Ed, in preparation.

Chapter 2

Structures of "Crew-Cut" Aggregates of Polystyrene-*b*-Poly(acrylic acid) Diblock Copolymers

ABSTRACT

"Crew-cut" aggregates of polystyrene-*b*-poly(acrylic acid) block copolymers can be prepared by dissolving the copolymers in N,N-dimethylformamide (DMF) and adding water to the solution to induce aggregation of the styrene segments of the copolymer chains. The aggregates are formed at near-equilibrium conditions, and their structures are subsequently frozen by isolating them into aqueous solution by dialysis. Aggregates of a number of different morphologies have been prepared. The morphologies, identified by transmission electron microscopy, consist of spheres, rods, vesicles, lamellae, large compound vesicles, large compound micelles, etc. The formation of aggregates of different morphologies can be controlled by varying the copolymer composition, by changing the initial copolymer concentration in DMF, by adding ions (e.g. NaCl, $CaCl_2$, HCl and NaOH, etc), or by adding homopolystyrene.

2.1. INTRODUCTION

It is well-known that small molecule amphiphiles form self-assembled aggregates of various morphologies.[1] The manipulation of the aggregate morphology involves changing the nature of the head group, varying the length and the number of tails, adding electrolytes, etc. The formation of different morphologies is well explained in terms of a dimensionless packing parameter, v/a_0l_c, where a_0 is the optimal surface area of the polar head, and v and l_c are the volume and the critical length of the hydrophobic part (tail) of the surfactant molecule. As the value of parameter v/a_0l_c increases, the aggregates change from spherical, to rod-like, to vesicular or lamellar, etc. Thus, most single-chain surfactants commonly form spherical micelles, while most double-chain surfactants, because of a higher value of v/l_c, form bilayers.

Apart from aggregates in solutions, the phase-separated domains of block copolymers in bulk can be spherical, cylindrical, planar/lamellar, and ordered bi-continuous (double diamond or gyroid), depending on the copolymer composition. [2-5] The formation of different structural domains is mainly determined by the relative volume fraction of the copolymer blocks. Specifically, highly asymmetric copolymers form spherical domains by aggregation of the short blocks, while symmetric copolymers usually yields lamellae. In bulk block copolymer/homopolymer blends, depending on the composition of the block copolymer, the molecular weight of the homopolymer and the block copolymer to homopolymer ratio, aggregates of different morphologies have also been observed. [6,7] Four morphologies (starfish, rod, planar and foam) were observed for two dimensional or surface aggregates of polystyrene/decylated poly(vinylpyridinium) block polyelectrolytes of different compositions. [8,9] Very recently, it was found that amphiphilic dendrimers of different generations with an attached polystyrene tail form aggregates of different morphologies. [10]

In contrast to the above, micelle-like aggregates of block copolymers in solutions are usually spherical over a very broad range of the compositions of the copolymer. [11-15]

Non-spherical micelles in solutions of block copolymers have been observed only rarely by transmission electron microscopy (TEM); their structures were mostly deduced from studies by other techniques. [16-20] For example, the existence of worm-like micelles [16] and of platelet aggregates with copolymer cylinders extending from the edges [18] has been proved by direct TEM observation. On the other hand, synchrotron SAXS measurements on solutions of polystyrene-b-polyisoprene in aniline suggested that vesicles were very probably formed as the content of the soluble polystyrene (PS) block decreased. [17]

Recently, it was found that aggregates of various morphologies can be prepared from amphiphilic block copolymers in solutions of small molecule solvents. [21-25] These aggregates are made from one family of highly asymmetric polystyrene-*b*-poly(acrylic acid) (PS-*b*-PAA) or polystyrene-*b*-poly(ethylene oxide) (PS-*b*-PEO) diblock copolymers, in which the lengths of the insoluble PS blocks are much longer than those of the soluble PAA (or PEO) blocks. The aggregates are therefore described as "crew-cut". The observed morphologies include spheres, rods, vesicles, elongated vesicles, lamellae, large compound vesicles, large compound micelles, and several others. Basically, the formation of the aggregates of different morphologies depends on the copolymer composition, the initial copolymer concentration in solution, and the type and concentration of added ions (as salt, acid or base). This chapter reviews the formation of PS-*b*-PAA block copolymer "crew-cut" aggregates with various morphologies in low molecular weight solvents.

2.2. PREPARATION OF AQUEOUS SOLUTIONS OF BLOCK COPOLYMER AGGREGATES

The PS-*b*-PAA copolymers were synthesized by sequential anionic polymerization. A detailed description of the procedures can be found elsewhere. [22] The core-forming block (PS) contents ranged from 80 to 98 wt.-%. The polymers are identified by the notation used previously, e.g. PS(410)-*b*-PAA(16) represents a diblock copolymer with a degree of polymerization of the PS block of 410 and the PAA block of 16, respectively.

To prepare stable aqueous aggregate solutions, the diblock copolymers were first dissolved in N,N-dimethylformamide (DMF), a common solvent for both PS and PAA blocks. Deionized water was added to the copolymer/DMF solution to induce micellization. The aggregates were isolated in aqueous solution by dialysis to remove the DMF. For studies of the effects of added ions or of added homopolystyrene on the morphology, additives in different amounts were mixed with the copolymer/DMF solution before the addition of deionized water. At the point of micellization, the cores of the aggregates are swollen by a DMF-rich solvent. Thus, the mobility of copolymer chains into and out of the aggregates may be still high, and a dynamic equilibrium between micelles and unimers undoubtedly exists. The plasticizing effect is lost as DMF is removed from the core during further addition of water and subsequent dialysis. Therefore, the structures of the aggregates in the final aqueous solutions are kinetically locked because of the glassy nature of the PS chains. However, the morphologies are still a manifestation of thermodynamics of micellization under equilibrium conditions. [15,22]

2.3. FACTORS CONTROLLING MORPHOLOGY

2.3.1. Copolymer composition.

Usually, the PS-*b*-PAA copolymers with relatively high contents of PAA blocks form spherical micelles, as shown in Figure 2.1-A. The micelle sizes are measured directly from the prints. Because the corona-forming block (PAA) contents in the copolymers are low in general, the corona layer on the core surface of the dry micelles must be thin (its thickness can be calculated from the copolymer composition and the aggregation number). The observed particle size thus represents the core dimension to a very good approximation. The number-average core radii depend on the chain lengths of both the insoluble PS block (N_{PS}) and the soluble PAA block (N_{PAA}), and scale in the manner of a power law: [15]

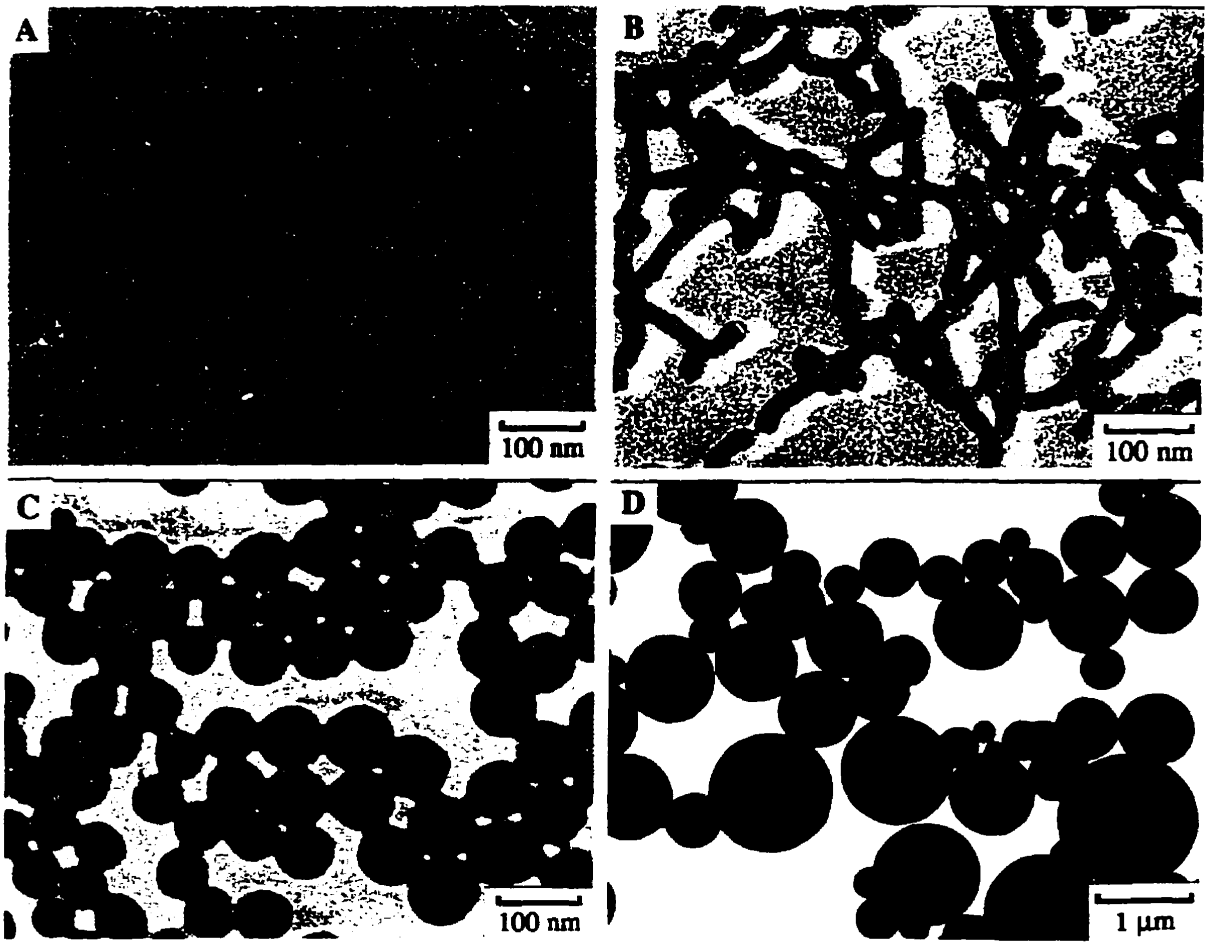

Figure 2.1. (A) spherical micelles from PS(500)-*b*-PAA(60), (B) rod-like micelles from PS(180)-*b*-PAA(15), (C) vesicles from PS(410)-*b*-PAA(20), and (D) large compound micelles from PS(200)-*b*-PAA(4). The initial copolymer concentration in DMF is 2 wt.-%.

$$R_{core} \sim N_{PS}^{0.4}\, N_{PAA}^{-0.15} \tag{2.1}$$

Equation (2.1) shows that the dependence of R_{core} on PS block length is weaker than that suggested from theoretical studies. [26-31] The difference is not surprising because the present scaling law only applies to the dry micelles, while theoretical predictions are based on thermodynamic equilibrium conditions.

It was found that as the block length ratio of PAA to PS decreases, the aggregates become rod-like. [21,22] The rod-like micelles have a relatively narrow distribution of diameters, but a widely variable length (Figure 2.1-B). As the ratio of PAA to PS block lengths drops further, vesicular aggregates are formed, as shown in Figure 2.1-C. The PS wall thicknesses of the vesicles are very uniform and independent on the overall sizes of the vesicles. Lamellar aggregates are found on occasion. Although it has been known for a long time that some small molecule surfactants form vesicles, it is believed to be the first time that the glassy vesicles of block copolymers have been isolated into water and observed directly by TEM.

When the PAA block length becomes very short, the copolymers form highly polydisperse spheres, with diameters exceeding one micron, as shown in Figure 2.1-D. A study of their internal structure by TEM of microtomed embedded specimens reveals that these polydisperse spheres consist of a large number of reverse micelles with the polar PAA cores in a PS matrix. The outer surface of these spheres should be hydrophilic because of the presence of the short PAA chains. This gives them considerable stability, and allows even those which have settled to the bottom of the container to be resuspended. These aggregates are called large compound micelles (LCMs), and appear to be a new morphology. [21,22]

The morphology of the aggregates is determined by many factors. An important aspect is believed to be the force balance among three factors, i.e. the deformation (stretching) of the PS blocks in the core, the surface tension between the core and the solvent, and the repulsion among the corona chains. [22] In order to decrease the interfacial energy between the core and the solvent, the aggregates increase the core size, which is opposed by increases of both PS chain stretching and repulsion among the corona chains. Clearly, the strength of the interactions among the corona chains is related to the PAA block lengths (or coil dimensions). As the length of PAA blocks decreases, the repulsion among the PAA corona chains decreases, and the core size increases. As a result, the stretching of the PS chains in the cores should increase. However, the increase of the stretching cannot continue indefinitely due to the penalty from the decreased entropy of the PS chains in the micelle core. Thus, in order to minimize the total free energy of the system with decreasing the PAA chain length, the aggregates change their morphology progressively from spherical to rod-like, to bilayer and to large compound micelle.

2.3.2. Added ions.

The morphology of the aggregates can also be controlled by the addition of either acid or base in different amounts. Thus, from a block copolymer with a certain composition, one can produce aggregates of several different morphologies. [23,24] For example, when a 1 wt.-% PS(410)-*b*-PAA(25) copolymer/DMF solution is used, the addition of water to the solution yields small spherical micelles of the copolymers with an average diameter of 29 nm. When HCl is added to a concentration of 190 μM (or a molar ratio, R, of added HCl to acrylic acid repeat units of 0.035), the aggregates are still spherical, but with an average diameter of 38 nm. As the HCl concentration is increased to 210, 240 and 270 μM (R = 0.04, 0.045 and 0.05), the dominant aggregates become rods, vesicles, and large compound vesicles (LCVs), respectively. The LCVs are aggregates of many single vesicles, and their structure bears some resemblance to that of aggregated soap bubbles.

The effect of added HCl on the morphology is parallel to that of a decrease in the PAA block length of the copolymer. Thus, it can be ascribed to a decreased repulsion among the PAA chains. The repulsion among the PAA chains is believed to arise not only from steric repulsion associated with the chain dimensions, but also from electrostatic interactions due to partial ionization of the PAA chains. [23] Because HCl is a strong acid and the PAA is a weak acid, the addition of HCl may protonate the PAA, leading to a lower degree of ionization. Thus, the repulsion among the PAA chains is decreased, and the morphology changes progressively from spheres, to spheres with increased sizes, to rods, to vesicles, and eventually to LCVs. When NaOH is used, the morphology is found to change in the opposite direction with increasing NaOH concentration, i.e. from vesicles, to spheres, and to spheres of smaller sizes. This is not surprising, since the added NaOH neutralizes the PAA segments, increases the degree of ionization, and therewith increases the repulsion among the corona chains.

Added salt also has a morphogenic effect on the aggregates. [23,24] Table 2.1 gives some of the results for PS(410)-*b*-PAA(13). One can see that changes in the aggregate morphology can be achieved with much lower concentrations of $CaCl_2$ than of NaCl. The remarkably strong effect of $CaCl_2$ on the morphology is ascribed to strong Ca^{2+} binding to PAA segments. The effect of added NaCl on the morphology is ascribed to a weak Na^+ binding to the PAA segments and possibly a screened electrostatic field of the weakly charged PAA segments in the presence of NaCl.

Table 2.1. Summary of the effect of added salt concentration (moles/litre) on aggregate morphology of the PS(410)-*b*-PAA(13) copolymer. In the table, the numbers in brackets represent the molar ratio of added salt or acid to acrylic acid repeat units.

	Dominant Morphology		
Added salt	Spheres	Vesicles	LCVs
NaCl	$< 2.3 \times 10^{-3}$	$2.8 \sim 4.2 \times 10^{-3}$	5.6×10^{-3}
	(0.80)	(1.0 ~ 1.5)	(2.0)
$CaCl_2$	$< 8.5 \times 10^{-5}$	$9.0 \sim 11 \times 10^{-5}$	$1.3 \sim 1.7 \times 10^{-4}$
	(0.03)	(0.032 ~ 0.04)	(0.045 ~ 0.06)

2.3.3. Other factors.

Under certain conditions, homopolystyrene can be solubilized into the core during micellization. [22] Upon addition of homopolystyrene, the block copolymers which give spherical micelles without added homo-PS, still form spherical micelles. However, the addition of homopolystyrene changes the vesicular or rod-like aggregates to spherical micelles. For example, vesicles are formed from 2 wt.-% PS(410)-*b*-PAA(16) copolymer/DMF solution, but spherical micelles are obtained upon addition of 10 wt.-% PS(180) homopolymer to the copolymer. One of the reasons for the morphological change caused by the addition of homopolystyrene may be the reduced degree of stretching of the PS blocks due to the accumulation of even a small amount of the homopolystyrene in the center of the core.

The morphology of the aggregates also depends on the initial copolymer concentration in DMF. Figure 2.2 shows different morphologies of the aggregates prepared from the same copolymer, PS(410)-*b*-PAA(25), but at different initial concentrations. When the concentration is 2 wt.-%, spherical micelles are formed (Figure 2.2-A). Rod-like micelles are formed from a 2.6 wt.-% copolymer/DMF solution (Figure 2.2-B). When the concentration is 3.0 wt.-%, rod-like micelles and vesicles coexist in the solution (Figure 2.2-C). As the copolymer concentration increases to 4.0 wt.-%, most of the aggregates are vesicles, while the rod-like micelles are seen only rarely (Figure 2.2-D). At this point, the sizes of the vesicular aggregates are highly polydisperse, ranging from 50 to 500 nm outer diameters.

2.4. STRUCTURAL CHARACTERISTICS OF VARIOUS MORPHOLOGIES

2.4.1. PS chain extension in the cores.

For a compact micelle core, some of the core-forming blocks must span the distance from the core/corona interface to the core center. The degree of PS chain stretching, S_c, is defined as the ratio of the micelle core radius to the PS chain end-to-end

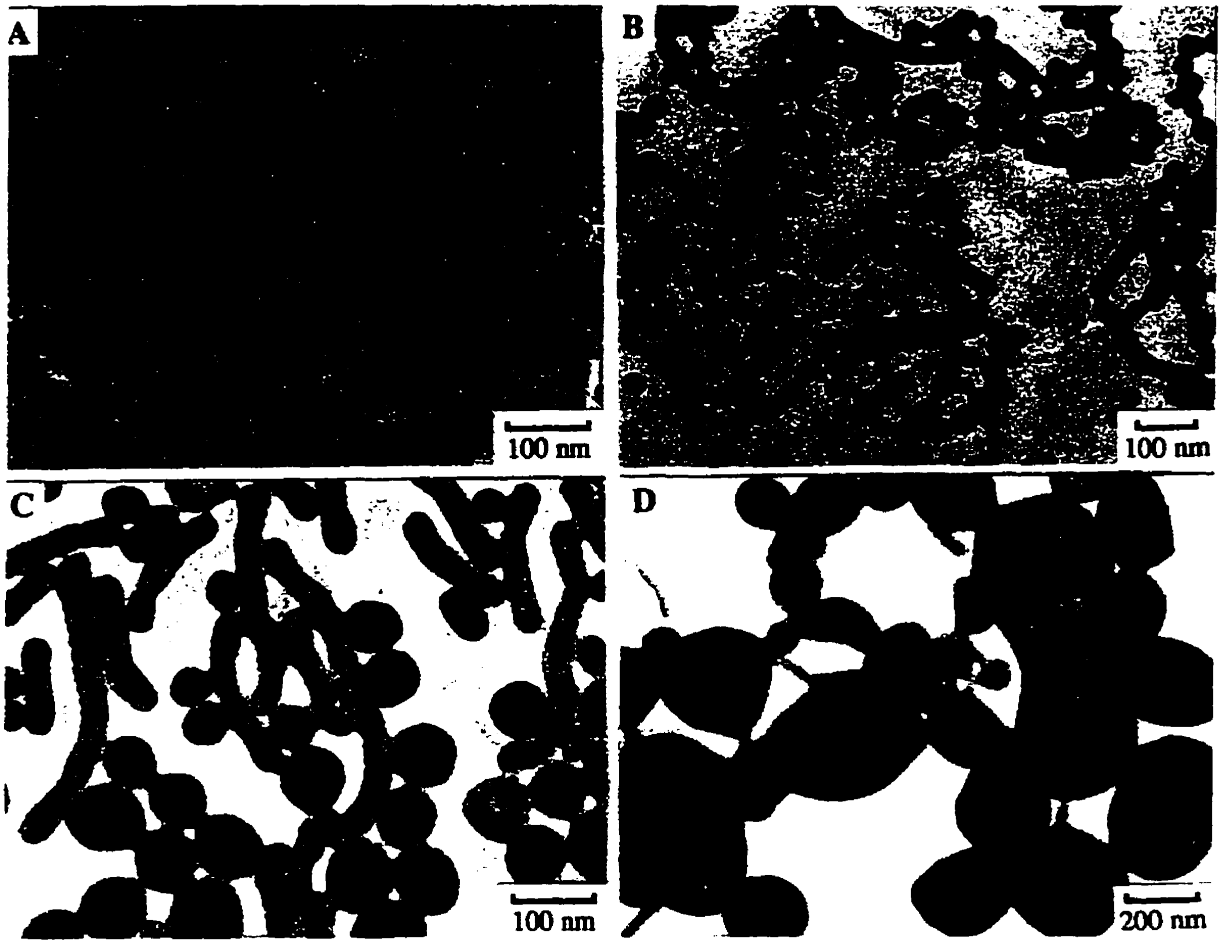

Figure 2.2. Aggregates of various morphologies made from PS(410)-*b*-PAA(25) copolymers with different initial concentrations in DMF: (A) 2.0, (B) 2.6, (C) 3.0, and (D) 4.0 wt.-%.

distance in the unperturbed state. Clearly, not all chains are stretched to the full extent (i.e. from the core center to the surface), but some must be. Because the end-to-end distance of a polymer chain in the unperturbed state is proportional to $N_{PS}^{1/2}$, the dependence of S_c on the copolymer composition is given by [22]

$$S_c \sim N_{PS}^{-0.1} N_{PAA}^{-0.15} \qquad (2.2)$$

It is clear that the degree of stretching decreases as the PS and/or the PAA block lengths increase. Equation (2.2) applies only to spherical micelles in aqueous solution. However, it has to be pointed out that, at the moment of the formation of the micelles, the cores are expected to be swollen by a DMF rich solvent mixture. The degrees of stretching of the PS blocks at the onset of micellization are, therefore, higher than those of the micelles in aqueous solution. Since the micelle cores become totally deswelled in aqueous solutions, the degrees of stretching of the PS blocks decrease.

While the value of S_c in the spherical micelle cores depends on the composition of the copolymers, it is found that it decreases as the morphology changes from sphere to cylinder, and to vesicle. Table 2.2 gives some typical data. For example, the block copolymers 200-*b*-21, 200-*b*-15 and 200-*b*-8 have the same PS block, and yield, respectively, spherical micelles, cylindrical micelles and vesicles. The degrees of stretching of the PS chains are 1.41, 1.26 and 0.99, respectively. If the last two copolymers were to form spherical micelles, the stretching would be expected to increase as PAA block length decreases. According to equation (2), the values of S_c would be 1.47 and 1.62, respectively (rather than 1.26 and 0.99).

Table 2.2. Some characteristics of the rod-like micelles and the bilayer aggregates of the block copolymers

PS-*b*-PAA/PS	Morphology	Dimension of PS core (nm) [b]	S_c [c]	A_c [d] (nm^2)
200-*b*-21	spheres	26	1.41	8
200-*b*-15	rods	23	1.26	5.8
200-*b*-8	vesicles	18	0.99	4.2
200-*b*-8/38 (95 : 5) [a]	spheres	33	1.79	6.4
410-*b*-46	spheres	30	1.14	14
410-*b*-16	vesicles	22	0.84	6.6
410-*b*-16/180 (90 : 10)	spheres	37	1.42	12

[a] The numbers in the brackets indicate the ratio of the copolymer and the homopolymer(w/w).

[b] Average diameter of the spherical and cylindrical micelles or wall thickness of the vesicles.

[c] Degree of stretching of the PS blocks; for the sphere and rod, it is defined as a ratio of the radius to the end-to-end distance of the PS block in the unperturbed state; for the vesicle, half of the wall thickness is used.

[d] Surface area per corona chain at the core/corona interface.

2.4.2. Area per corona chain at the core surface.

The area per corona chain on the core surface appears to be an important factor among those controlling the aggregation number and the structure of the micelles because it is related inversely to the strength of the repulsive interactions among the corona chains. Because of the chemical bond between the two blocks of the copolymer, one can calculate the A_c value from the average core diameter and the density of the core. [22] For spherical micelles, it can be shown that

$$A_c \sim N_{PS}^{0.6} N_{PAA}^{0.15} \qquad (2.3)$$

Thus, A_c increases with the PS block length, and for a constant PS block length, it also increases as the PAA block length increases. The large dependence of A_c on the PS block length is related to low degrees of PS chain stretching in the cores.

The dependence of A_c on the PAA block length is related to the strength of the repulsive interaction among corona chains during micellization. The major contributions to the repulsion can be both steric and electrostatic since the PAA blocks are ionizable. In order to estimate the relative importance of the two repulsive components, a dimensionless parameter, $\sigma N_{PAA}^{6/5}$, is used to evaluate the density of the corona chains on the core surface. [22] σ is defined as the number of corona chains per unit area times a^2, where a is the length of the repeat unit. The condition for low surface density is $\sigma N_{PAA}^{6/5} < 1$. When $\sigma N_{PAA}^{6/5}$ becomes greater than 1, the corona chains have to adopt conformations which are extended in the direction perpendicular to the surface due to steric repulsion between the corona chains. [22] A calculation shows that the values of $\sigma N_{PAA}^{6/5}$ for most of micelles fall in the range 0.2 to 0.6, except for a few samples with relatively long PAA blocks, where the values of $\sigma N_{PAA}^{6/5}$ are near or slightly higher than unity. This suggests that the surface density of the corona chains is low. Thus, the repulsion among the corona chains may come mainly from the electrostatic interactions.

While the A_c value depends on the lengths of both the PS and the PAA blocks, it also decreases as the morphology changes from spherical to cylindrical, and to vesicular (Table 2.2). The A_c value is undoubtedly determined by the force balance among several factors during the aggregation. However, it can be shown [22] that the A_c value is also related to the geometric shapes of the aggregates of the different morphologies. A more detailed discussion can be found in Ref. 22.

2.5. CONCLUDING REMARKS

The formation of PS-*b*-PAA block copolymer aggregates of different morphologies has been explored by transmission electron microscopy. Spherical micelles, usually monodisperse in size, are formed when the copolymers have relatively high soluble block (PAA) contents. As the content of the soluble block (PAA) in the block copolymer decreases, the morphology of the aggregates changes progressively from spheres to cylinders, to vesicles or lamellae, and eventually to large compound micelles. The morphology of the aggregates can also be controlled by using solutions of different copolymer concentrations, or by adding homopolystyrene, or by adding ions (e.g. NaCl, $CaCl_2$, HCl and NaOH, etc). The effect of added salt or acid on the morphology is parallel to that of a decrease in the PAA block length of the copolymer. In addition, aggregates of a new morphology, consisting of large compound vesicles, have been prepared. The large compound vesicles may be useful as possible drug delivery vehicles, and as models of stable microstructured biomaterials. The morphology of the aggregates appears to be determined mainly by the force balance among three components, i.e. the stretching of the PS blocks in the core, the surface tension between the core and the solvent, and the repulsion among the corona chains.

2.6. ACKNOWLEDGMENTS

We would like to thank The Natural Sciences and Engineering Research Council of Canada(NSERC) for continuing support of this research.

2.7. REFERENCES

1. J. N. Israelachvili, "*Intermolecular and surface forces*", 2nd edition, Academic press, London 1992.
2. D. J. Meier, In *Thermoplastic Elastomers*, Hanser, New York 1987, Chapter 11.
3. H. Hasegawa, H. Tanaka, K. Yamasaki, T. Hashimoto, *Macromolecules* **20**, 1651 (1987).
4. S. Förster, A. K. Khandpur, J. Zhao, F. S. Bates, I. W. Hamley, A. J. Ryan, W. Bras, *Macromolecules* **27**, 6922 (1994).
5. D. A. Hajduk, P. E. Harper, S. M. Gruner, C. C. Honeker, G. Kim, E. L. Thomas, L. J. Fetters, *Macromolecules* **27**, 4063 (1994).
6. D. J. Kinning, K. I. Winey, E. L. Thomas, *Macromolecules* **21**, 3502 (1988).
7. F. S. Bates, A. Kumar, M. F. J. Schulz, *Polym. Sci., Polym. Phys. Ed.* **33**, 1423 (1995).
8. J. Zhu, R. B. Lennox, A. Eisenberg, *J. Phys. Chem.* **96**, 4727 (1992).
9. M. Meszaros, A. Eisenberg, R. B. Lennox, *Faraday Discuss.* **98**, 283 (1994).
10. J. C. M. van Hest, D. A. P. Delnoye, M. W. P. L. Baars, M. H. P. van Genderen, E. W. Meijer, *Science* **268**, 1592 (1995).
11. Z. Tuzar, P. Kratochvil, In *Surface and Colloid Science*, Plenum Press, New York, 1993, Vol. 15, p 1.
12. M. Wilhelm, C.-L. Zhao, Y. Wang, R. Xu, M. A. Winnik, *Macromolecules* **24**, 1033 (1991).
13. I. Astafieva, X. F. Zhong, A. Eisenberg, *Macromolecules* **26**, 7339 (1993).
14. A. Qin, M. Tian, C. Ramireddy, S. E. Webber, P. Munk, *Macromolecules* **27**, 120 (1994).
15. L. Zhang, R. J. Barlow, A. Eisenberg, *Macromolecules* **28**, 6055 (1995) (chapter 3 of this thesis).
16. C. Price, *Pure and Appl. Chem.* **55**, 1563 (1983).

17. Z. Zhou, B. Chu, *Macromolecules* **21**, 2548 (1988).
18. A. P. Gast, P. K. Vinson, K. A. Cogan-Farinas, *Macromolecules* **26**, 1774 (1993).
19. M. Antonietti, S. Heinz, M. Schmidt, C. Rosenauer, *Macromolecules* **27**, 3276 (1994).
20. O. Glatter, G. Scherf, K. Schillén, W. Brown, *Macromolecules* **27**, 6046 (1994).
21. L. Zhang, A. Eisenberg, *Science* **268**, 1728 (1995) (chapter 4 of this thesis).
22. L. Zhang, A. Eisenberg, *J. Am.Chem. Soc.* **118**, 3168 (1996) (chapter 5 of this thesis).
23. L. Zhang, K. Yu, A. Eisenberg, *Science* **272**, 1777 (1996) (chapter 6 of this thesis).
24. L. Zhang, A. Eisenberg, *Macromolecules* **1996**, *29*, in press (chapter 7 of this thesis).
25. K. Yu, A. Eisenberg, *Macromolecules* **1996**, in press.
26. P. G. de Gennes, In *Solid State Physics*, Academic press, New York 1978; supplement 14, p. 1.
27. L. Leibler, H. Orland, J. C. Wheeler, *J. Chem. Phys.* **79**, 3550 (1983).
28. M. D. Whitmore, J. Noolandi, *Macromolecules* **18**, 657 (1985).
29. E. B. Zhulina, T. M. Birshtein, *Vysokomol. Soedin.* **27**, 511 (1985).
30. A. Halperin, *Macromolecules* **20**, 2943 (1987).
31. R. Nagarajan, K. Ganesh, *J. Chem. Phys.* **90**, 5843 (1989).

Chapter 3

Scaling Relations and Coronal Dimensions in Aqueous Block Polyelectrolyte Micelles

ABSTRACT

Polystyrene-*b*-poly(acrylic acid) block copolymers, PS-*b*-PAA, prepared by sequential anionic polymerization, were found to associate to form spherical, water soluble micelle-like aggregates. The micelle core radii were measured by transmission electron microscopy (TEM). It was found that the PS core radii scaled as $R_{core} \sim N_B^{0.4} N_A^{-0.15}$ (where N_B and N_A are the length of the insoluble and soluble blocks, respectively), illustrating that the soluble block exerted a considerable influence on the colloidal structure of the micelles. The micellar solutions were also studied by dynamic light scattering (DLS), yielding values of the micelle hydrodynamic radius, r_h. These studies showed that, in the absence of salt, the ionized form of the poly(acrylic acid) chains in the coronal layer of the micelles had a highly extended conformation.

3.1. INTRODUCTION

The self-assembly of block copolymers in selective solvents is a phenomenon of considerable interest to a wide range of scientists. The ability of block copolymers to undergo self-assembly in selective solvents imparts them with a number of unique properties, and extensive experimental and theoretical work has been performed over the past two decades. The proliferation of studies in the field has had several impetuses, including: the advent of new experimental techniques, which enable the micelle structure to be determined and the micellization phenomenon to be investigated; the development of new theories of micellization; and the recognition that block copolymer micelles may be used in a wide range of industrial and technological applications. The field is reviewed in a number of publications.[1-4]

In a recent paper, we reported on the preparation and characterization of a new type of micelle-like structure formed by the association of block copolymers composed of relatively long polystyrene blocks and relatively short poly(4-vinyl-pyridinium methyl iodide) blocks.[5] It was found that the copolymers associated to form spherical micelle-like structures with a polystyrene core and an ionic corona which renders the system water soluble. The description "crew-cut" was applied to these copolymers on account of the fact that the length of the core-forming block was much longer than the length of the corona-forming block. One of the novel features of these colloids was that the micelles had large hydrophobic cores (40-65 nm in diameter) because of the large number of polystyrene repeat units in the copolymer. Preliminary results indicated that the distribution of core radii was narrow, and that the average aggregation numbers and average core radii scaled as a function of the hydrophobic block length, N_B, in a manner predicted by theory.[4]

More recently, we have studied the association of block copolymers composed of long polystyrene blocks and short poly(acrylic acid) blocks. These systems have proven to be extremely interesting, and a number of aspects of their colloidal behavior will be reported in the near future.[6,7] In this chapter, we describe the colloidal structure of spherical micelles formed from these copolymers. In particular, we have studied the relationship between core size and the relative lengths of the polystyrene and poly(acrylic acid) blocks. Furthermore, by measuring the hydrodynamic diameter of the micelles, it was possible to obtain information about the conformation of the poly(acrylic acid) chains in the coronae of the micelles. The major results of this study are that the water soluble poly(acrylic acid) block has a large effect on the micelle formation process and on the structure of the resulting micelles, and that, in the absence of salt, the ionized form of the poly(acrylic acid) chains in the coronal layer of the micelles have a highly extended conformation.

3.2. EXPERIMENTAL

3.2.1. Synthesis of block copolymers.

The anionic polymerization method used to synthesize the polystyrene-*b*-poly(acrylic acid) block copolymers has been previously reported in detail.[8] A complete list of the copolymers studied in this paper is presented in Table 3.1. In Table 3.1, N_B is the number of styrene repeat units and N_A is the number of acrylic acid repeat units. In the text, block copolymer samples are differentiated by the notation developed previously, i.e. the copolymer 500-*b*-60 is copolymer containing 500 styrene repeat units and 60 acrylic acid repeat units. All copolymers had a relatively narrow distribution of molecular weights, with polydispersity indices (M_w/M_n), estimated by gel permeation chromatography (GPC), in the range 1.04 - 1.10 (see Table 3.1).

3.2.2. Preparation of micelles.

Aqueous solutions of the block copolymers were prepared by dialysis. To a solution of the copolymer in DMF (20 cm^3, 2 %-wt.) was added deionized water at a rate of 1 drop every 10 seconds. Addition of water was continued until 25 %-wt. water had

Table 3.1. Molecular and micellar characteristics of polystyrene-*b*-poly(acrylic acid) copolymers[a]

PS-*b*-PAA Copolymer			Micelles in water			
N_B(S)	N_A(AA)	(M_w/M_n)	$(R_{core})_n$ /nm	s.d./nm	N_{agg}	A_c/nm^2
170	33	1.08	13	0.7	268	7
180	28	1.05	12	1.1	217	8
390	40	1.06	16	1.6	246	13
390	80	1.07	14	1.2	175	15
410	46	1.06	15	1.0	190	14
500	60	1.04	15	1.2	160	17
740	55	1.08	20	1.3	268	19
740	180	1.08	16	1.2	125	24
1140	170	1.06	20	1.1	188	30
1400	120	1.09	21	2.9	159	34
1400	310	1.10	18	1.7	87	43
1400	310[b]	1.10	19	2.0	105	42

[a]. The error in N_A and N_B is approximately 5%; the error in R_{core} is approximately 1 nm.

[b]. Prepared by dialysis against deionized water, all other samples prepared by dialysis against distilled water.

been added. The resulting micellar solution was placed in a dialysis bag (Spectra/Por. molecular weight cut-off 8,000) and dialyzed against distilled (and, in one case, deionized) water for at least 4 days.

3.2.3. Transmission electron microscopy (TEM).

TEM was performed using a Phillips EM410 electron microscope operating at an acceleration voltage of 80 kV. Samples were transferred to copper EM grids which had been coated firstly, with a thin film of Formvar™ (J.B. EM services Inc., Que., Canada), and then with a thin film of carbon. Water was evaporated from the grid over 1 day at atmospheric pressure, and the grids were then shadowed with a palladium/platinum alloy at a shadowing angle of *ca.* 33°. Number-average micelle core radii, $(R_{core})_n$, the distribution of core radii, $(R_{core})_w/(R_{core})_n$), and the standard deviation of core radii about the mean, *s.d.*, were obtained for each sample, by measuring the micelle size directly from prints of the microscope negatives. It was assumed in data analysis that the measured micelle radius corresponded to the radius of the core, i.e. in the dried state, the thickness of the collapsed poly(acrylic acid) corona was negligible in comparison to the core radius. Simple calculations showed that in the extreme case of the sample with the longest poly(acrylic acid) block, 1400-*b*-310, the thickness of the collapsed corona was equal to 6% of the total radius. The accuracy of the microscope magnification was assessed by using a polystyrene latex standard (1.09 μm, Dow diagnostics). The measured number-average core diameter and the manufacturer's quoted number-average core diameter were the same within the error of the measurement.

3.2.4. Dynamic light scattering (DLS).

DLS experiments were performed on a Brookhaven Instruments Corporation photon correlation spectrometer fitted with a Brookhaven Instruments BI-2030 digital correlator and a Spectra Physics 120 He/Ne laser, which operated at a power of 50 mW and supplied vertically polarized light with a wavelength of 632.8 nm. All experiments were performed at a temperature of 25.0 ± 0.1 °C. The angle of detection could be varied between 35° and 150°, enabling the determination of $\Gamma(s^{-1})$ [the relaxation rate of the normalized intensity autocorrelation function, $g_2(\tau)$] over a range of angles. Γ was determined a total of five times, for each angle and concentration, using the single exponential and cumulant methods of data analysis; further details are given in Section 3.3.4.1. From these measurements it was possible to obtain the average z-average relaxation rate, $(\overline{\Gamma})_z$.

Great care was taken to ensure that the DLS measurements were not affected by dust. All glassware was cleaned thoroughly with filtered (0.2 mm, x 5), reagent-grade acetone, which had been condensed from the vapor. All solvents and micelle solutions were filtered through surfactant-free, aqueous filters (0.2 μm and 0.45 μm; Chromatographic Specialties Inc., Ont., Canada). Any data which showed the presence of dust were discarded. The concentrations of the micellar solutions were determined gravimetrically after filtration by evaporation of water.

3.3. RESULTS AND DISCUSSION

The Results and Discussion section of this paper is organized in the following manner. In the first section (Section 3.3.1), a qualitative discussion of the micelle formation process is presented. In Section 3.3.1, the physical conditions which are applicable during copolymer association are discussed, as well as a discussion of the colloidal structure of the resulting micelles. In Section 3.3.2, results obtained by TEM are presented, including the average core radii and the distribution of core radii of the different copolymer samples. In Section 3.3.3, the dependence of the core radii on the length of the insoluble block and the length of the soluble block is discussed, using an empirically determined scaling relationship. As part of this discussion, brief comparisons are made between the empirical scaling relation obtained here, and a number of theoretical scaling relations.

In Section 3.3.4, results obtained by DLS are presented and discussed. This section includes a brief introduction to the basic theory of DLS (Section 3.3.4.1) and a presentation of the experimental DLS results (Section 3.3.4.2). In Section 3.3.4.3, results obtained by DLS are compared with results obtained by TEM. From this comparison, it was possible to determine the coronal thickness and the degree of extension of the coronal chains for a number of different micellar samples.

In Section 3.3.5, the factors which are known to affect the conformation of polymer chains in the coronae of micelles are discussed. An integral part of this discussion is a comparison of experimental results obtained here with experimental and theoretical results obtained previously by other workers. Section 3.3.5 begins with a selective summary of the previous literature on the stretching of chains in the coronae of non-ionic micelles in organic solvents (Section 3.3.5.1). This section is followed by a discussion of the effect of various parameters on the stretching of coronal chains. The parameters discussed are the following: the effect of the surface density of coronal chains (Section 3.3.5.2); the effect of the curvature of the micelle core to which the chains are attached (Section 3.3.5.3); the effect of the chemical nature of the coronal chains (Section 3.3.5.4); and the effect of the quality of the solvent for the coronal chains (Section 3.3.5.4). Finally, in Section 3.3.5.5, a comparison is made between the experimental results obtained here and a number of theoretical and experimental studies of colloids which contain ionic polymer chains attached to the colloid surface.

3.3.1. The micelle formation process and the structure of the resulting micelles.

Before presenting specific results, it is necessary to consider the conditions under which the block copolymer molecules associate. It was not possible to prepare stable micellar solutions by direct dissolution of the copolymer molecules into water. This is a consequence of the large weight-fraction of polystyrene in the copolymer samples, which renders them insoluble in water. In order to form stable micelles in a completely aqueous environment, it was necessary to first dissolve the copolymer samples in DMF (which is a good solvent for both polystyrene and poly(acrylic acid) blocks), and then gradually decrease the quality of the solvent for the polystyrene blocks by adding deionized water very slowly. Gradual addition of deionized water was continued until 25 %-wt. of water had been added. Micelle formation, as indicated by turbidity in the solution, typically occurred at 3-6 %-wt. water addition, i.e. well before dialysis was started. DMF was then removed from the system by dialysis against distilled (and, in one case, deionized) water over a period of at least 4 days.

Under the experimental conditions outlined above, it is reasonable to assume that, in the early stages of water addition, the micelle formation process is a reversible process, i.e. at a given DMF/water concentration, there will be a true equilibrium between the free chain form of the copolymer and the associated form of the copolymer in the micelle. We outline our reasoning below.

All copolymer samples formed clear, molecularly dispersed solutions in DMF. The fact that copolymer molecules were unassociated in DMF was confirmed by light scattering: the molecular weight of the copolymer 500-*b*-60, determined by light scattering in DMF, corresponded to the molecular weight determined by GPC. As the quality of the solvent for polystyrene is decreased further, by adding more water, the solubility of the copolymer decreases and, in order for the free energy of the system to be minimized, association of free chains occurs.

At this stage of the discussion, it is useful to introduce the concept of a critical water concentration, i.e. the concentration of water at which micelles are first formed. At the critical water concentration, different copolymer chains begin to associate reversibly to form micelles, and there is an increase in the turbidity of the solution which can be monitored by light scattering. In a future publication we will present detailed experimental results on the phase behavior of solutions of these copolymers.[7] The various factors investigated in that study include the dependence of the critical water concentration on the polystyrene and poly(acrylic acid) block lengths, the dependence of the critical water concentration on the pH of the precipitating solvent, the dependence of the critical water concentration on the polymer concentration, and an NMR study of the micro-environment experienced by the water molecules during the initial stages of water addition.

At concentrations of water close to the critical water concentration, association of polymer chains is an equilibrium process, i.e. there is a dynamic equilibrium between the single-chain form of the copolymer molecules and the associated form, such that the associated copolymer would become molecularly dispersed if the quality of solvent for the polystyrene blocks were to be improved. Because of the presence of an appreciable amount of DMF in the solution (in the region of 95%), it is expected that the hydrophobic micelle cores will be highly swollen.

As the concentration of water in the solution is increased well above the critical water concentration, the solvent becomes worse for the relatively long polystyrene blocks. As a result, the continuous medium becomes an extremely poor solvent for the free-chain form of the copolymer, and the dynamic equilibrium between the associated micelle form and free-chain form of the copolymer will be shifted in favor of the micelle. The thermodynamics of the system will be such that the lowest free energy state will be the associated state. As the water content is increased further, the micelle core will become less swollen with DMF, and may even become glassy. Once most of the DMF is removed from the system, the micelles will have a kinetically frozen structure, i.e. the copolymer chains will be "locked" into the micelle, and there will no longer be a dynamic equilibrium between micelles and free-chains. The frozen micelle structure is a consequence of the strong hydrophobic interaction between different polystyrene chains, the relatively high glass transition temperature of polystyrene, and the low solubility of the copolymer in water. Furthermore, once the micelle has been transferred to a completely aqueous solvent, it is reasonable to assume that the polystyrene core will not be swollen with solvent.

One aspect of this micellization process that needs to be addressed is at what stage of water addition is there a transition from an equilibrium micelle system (an associate) to a non-equilibrium system (an aggregate). If the micelle structure becomes frozen instantaneously at one equilibrium state, then the structure of the micelles in the frozen state will reflect the structure of the micelle in that equilibrium state. However, the instantaneous freezing of the micelle may not be entirely realistic. For example, during the addition of water, there may be a change in the kinetics of micellization, which is a consequence of the progressive removal of DMF from the micelle core with increasing water content. Therefore, it is possible to propose that as more and more solvent is leached from the micelle core, there will be a gradual slowing down of the rate of micellization. Therefore, as the water content is increased there is a simultaneous change in the kinetics of micellization and the thermodynamics of micellization. If the rate of micellization approaches, or becomes slower than, the rate at which the equilibrium constant changes with the addition of water, then it will no longer be possible for the micellar solution to adjust to a new equilibrium state. In this situation, we would expect that the final frozen structure of the micelle will be a function of the change in the micellization kinetics, along with the state of the micelle equilibrium near the freezing point.

We are, at present, attempting to resolve the question of what conditions pertain during micellization using various quenching techniques. The determination of the actual thermodynamic and kinetic conditions which are operative, at the point at which the micelle structure becomes frozen, may be a difficult task. We have not attempted to resolve this question in the present study. We do, however, note two things associated with this aspect of the work. Firstly, at most stages of the micelle formation process, the associated copolymer molecules were equilibrium micellar associates; we use the word micelle to describe the final frozen aggregates because of this fact. Secondly, the distribution of core radii in the final micellar solutions is narrow (see Section 3.3.2). This fact indicates that relatively few micellization equilibria are operative at the point at which the micelle structure becomes frozen. One fortunate aspect of the frozen structure of these micelles, from an experimentalist's viewpoint, is that systems of this type are readily characterized, i.e. their aggregation number is fixed and not influenced by dilution, or by changing the temperature below the glass transition temperature of the polystyrene block.

Of importance to the second part of this study is the extent of neutralization of the poly(acrylic acid) chains in the coronal layer of the micelles. As mentioned in Section 3.2, most samples were dialyzed against distilled, but not deionized, water. The pHs of the resulting micellar solutions after dialysis were in the region 6.5-7.1 (see Table 3.2). From literature data on the acid-base behavior of poly(acrylic acid) [9,10] it is possible to estimate that the degree of ionization (α) of the poly(acrylic acid) chains in the coronae of these micelles is in the region of $0.8 > \alpha > 0.5$. The high pHs of the micellar solutions suggest a processes of cation-exchange during the extended dialysis. This ion-exchange, between cations in the distilled water and protons on the polymer chain (obviously subject to a Donnan equilibrium), produces neutralized polyelectrolyte chains in the coronae of the micelles. That cation-exchange occurs during extended dialysis against distilled water can be corroborated by the fact that a micellar solution of the polymer 1400-*b*-310, prepared by dialysis against deionized water, had a pH of 4.5.

It is reasonable to assume that cation-exchange occurs after the micelles have been formed, and that the polymer chains in the corona do not become charged until after the micelle structure has been established. It is thus assumed that neutralization of the polymer chains does not influence the micelle formation process. This assumption is upheld by core radius measurements (see Table 3.1). The average core radii of micelles formed from the polymer 1400-*b*-310 in distilled and deionized water were essentially identical (18 and 19 nm, respectively) even thought the pHs of the micellar solutions were, respectively, 6.8 and 4.5.

Table 3.2. Micelle hydrodynamic and structural information[a]

Sample	pH	$[(1/r_h)_z]^{-1}$ (nm)	$[(1/r_h)_z]^{-1} - (R_{core})_z$ (nm)	extension %
500-*b*-60	6.6	23	9	60
1140-*b*-170	7.0	52	32	75
1400-*b*-120	7.1	50	29	97
1400-*b*-310	6.8	90	72	96
1400-*b*-310[b]	4.5	38	20	25
1400-*b*-310[c]	5.3	48	30	39

[a]. The error in r_h is approximately ± 5%; the error in R_{core} is approximately ± 1 nm

[b]. Prepared by dialysis against deionized water, all other samples prepared by dialysis against distilled water

[c]. NaCl added to this sample, total concentration of NaCl equal to 1.0 M.

3.3.2 Distribution of core radii.

All of the copolymer samples prepared in this study associated to form completely spherical micelle-like structures. A typical micrograph of micelles formed from the copolymer 1140-*b*-170 presented in Figure 3.1. The use of electron microscopy to measure micelle core radii directly alleviates many of the problems associated with the use of other methods of measuring core radii, such as small-angle X-ray scattering (SAXS). For example, in order to obtain the core radius it is not necessary to use any particular theoretical model to fit the experimental data. The number-average core radii, $(R_{core})_n$, of the different copolymer samples are presented in Table 3.1, along with the standard deviation of core radii about the mean (s.d.), and the aggregation numbers (N_{agg}) calculated from the core radii, assuming an unswollen core. It is clear that the majority of samples had a relatively narrow distribution of micelle core radii, with standard deviations from the mean (s.d.) in the range 0.7 to 2.9 nm (5-14%).

3.3.3 Dependence of the core radii on the length of the insoluble block (N_B) and the length of the soluble block (N_A).

One of the goals of this work was to compare experimentally determinable quantities (e.g. number-average core radii, aggregation numbers and hydrodynamic radii) with the predictions from the various scaling theories which are now in place.[4,11-17] Because of the versatility of the copolymer synthesis and the relatively large range of samples, it was hoped that the effect of the length of the polystyrene and poly(acrylic acid) blocks on the micelle structure could be investigated in detail. It should be noted, especially in relation to Section 3.3.1, that the micelles studied here are non-equilibrium structures. However, the micelles were formed under equilibrium conditions, and as such the structure of the micelles should reflect the structure which pertained under equilibrium conditions. This study is in the spirit of an earlier study by Qin et al., in which the aggregation numbers and hydrodynamic diameters of micelles, formed from a relatively wide range of polystyrene-*b*-poly(methacrylic acid) copolymers in a water/dioxane mixture, were investigated.[18]

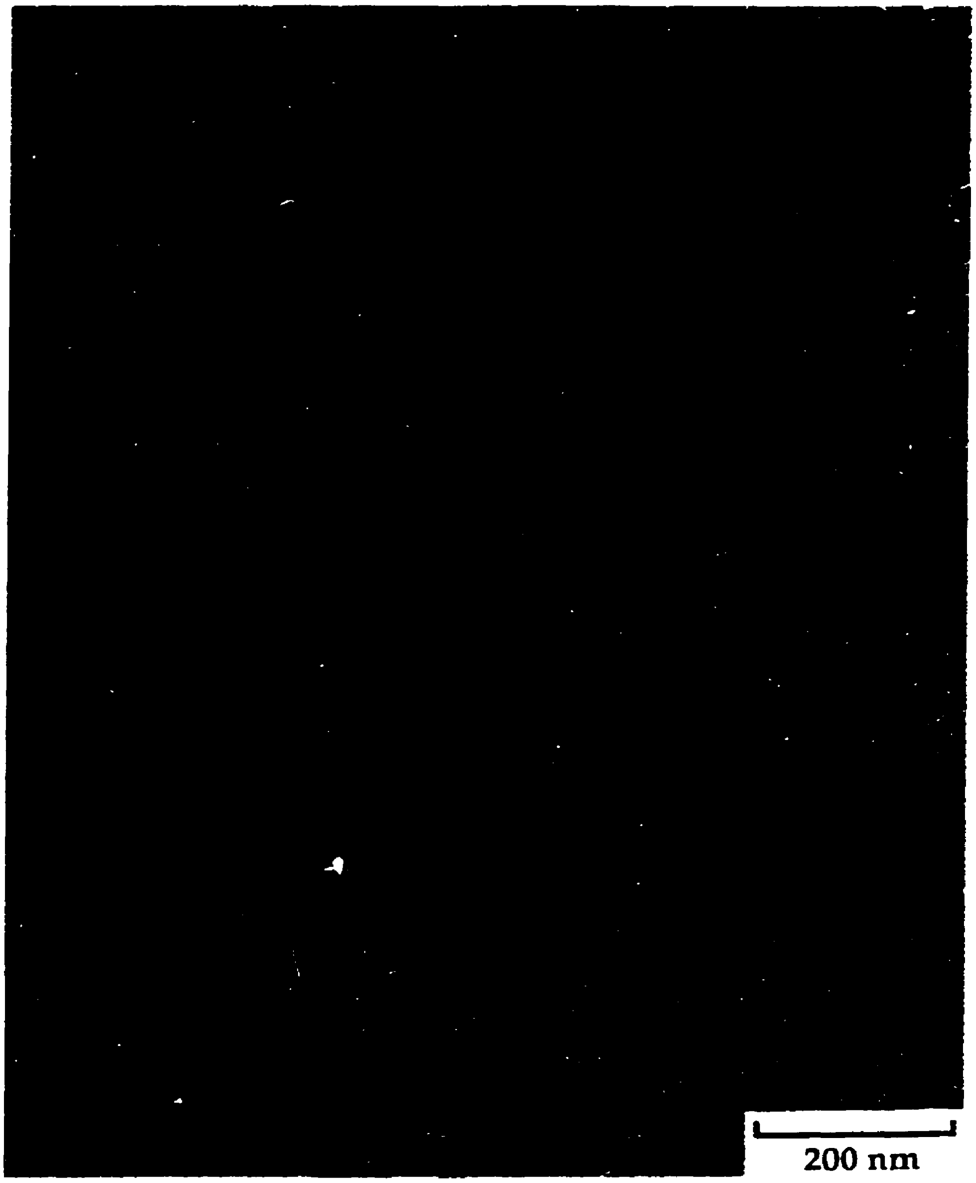

Figure 3.1. Transmission electron micrograph showing micelles formed from the copolymer 1140-*b*-170.

It was found that none of the theoretical scaling relations used, nor a variety of empirical scaling relations[18,19] could scale the core radius and aggregation number data cleanly. In particular, it was found that those scaling relations in which only the length of the insoluble block is considered to influence the structure of the micelle could not be used to scale the data. Therefore, in order to scale the average core radii data, we had to fit the data empirically. The results of this fitting are shown in Figure 3.2, where the measured number-average core radii are plotted against $N_B^{\ 0.4} N_A^{-0.15}$. The value of the exponents was determined by trial and error: the values were altered relative to each other and the combination which gave the best linear regression fit to the experimental data (0.4 and -0.15) was chosen.

Included in Figure 3.2 are weight-average core radii for block ionomer micelles in toluene, obtained by Nguyen *et al.*[20] using small-angle X-ray scattering (open circles). These copolymers are composed of a polystyrene block and either a poly(cesium acrylate) or poly(4-vinyl pyridinium methyl iodide) ionic block, and associate in organic solvents to form reverse micelles with ionic cores. From Figure 3.2, it is clear that there is a linear relationship between the core radius and $N_B^{\ 0.4} N_A^{-0.15}$ for both sets of data.

We do not consider the scaling relation obtained here to be universal in nature. The fact that the core radii data from these two very different micellar systems scaled well with $N_B^{\ 0.4} N_A^{-0.15}$ may illustrate that the various energy contributions for the different copolymer/solvent systems balance in a way to lead to an apparent similarity in the numerical value of the exponents. The proposition that the dependence of R_{core} on N_A and N_B may be system specific, is corroborated by the fact that we could not use the empirical scaling relation obtained here to scale cleanly the weight-average core radii data obtained by McConnell et al.[21] The core radii of polystyrene-*b*-polyisoprene micelles in decane, obtained by McConnell et al. using small-angle neutron scattering (SANS), are, to the best of our knowledge, the only other comprehensive data on the dependence of the core radii on the length of the soluble and insoluble blocks, other than those presented here.

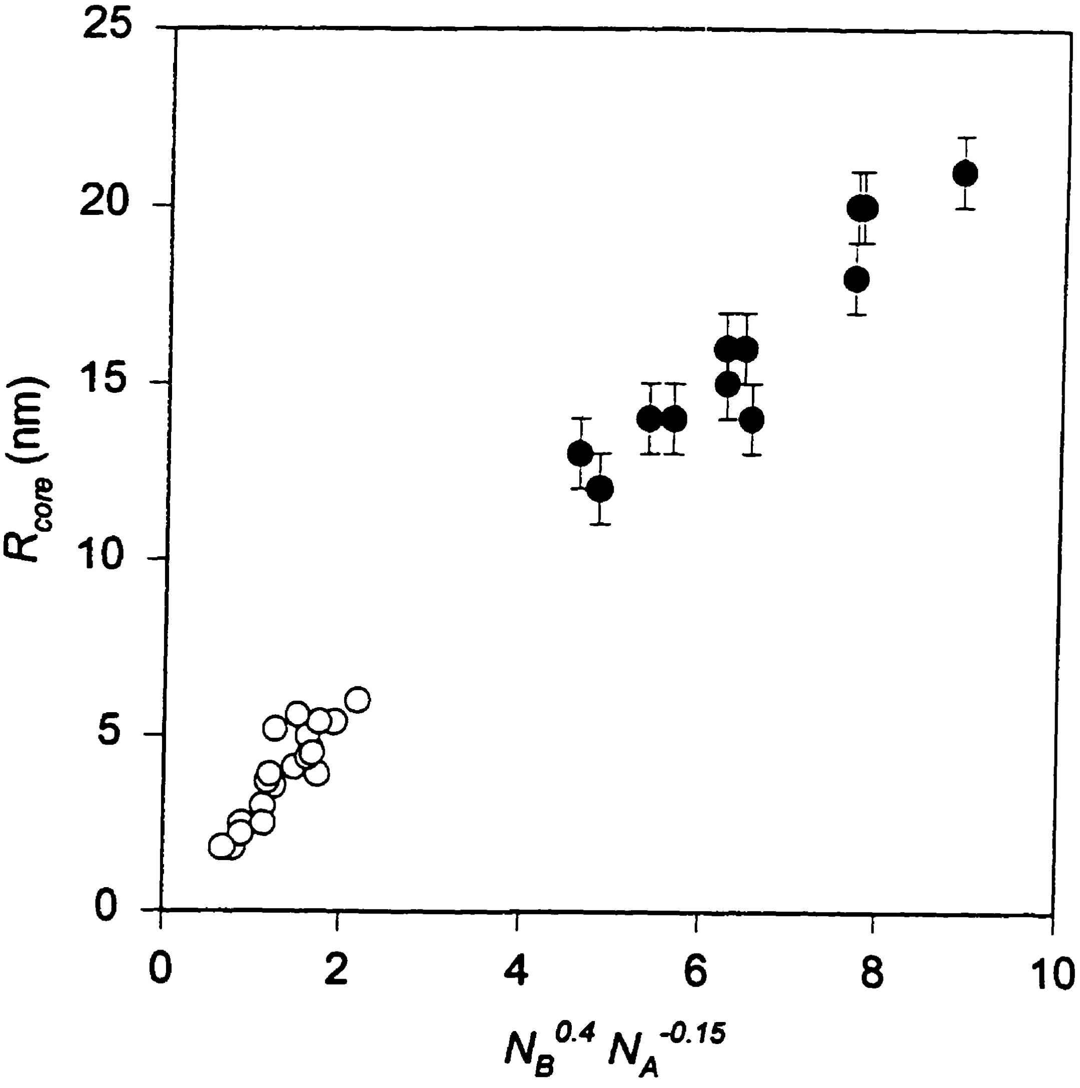

Figure 3.2. Plot of average core radius (R_{core}/nm) versus $N_B{}^{0.4}\ N_A{}^{-0.15}$ for different micelle systems. N_B is the length of the insoluble block and N_A is the length of the soluble block. Filled circles are number-average data for polystyrene-*b*-poly(acrylic acid) micelles in water obtained by TEM. Open circles are weight-average data obtained by Nguyen et al. using small-angle X-ray scattering.[20] to study polystyrene-*b*-poly(cesium acrylate) and polystyrene-*b*-poly(4-vinyl pyridinium methyl iodide) reverse micelles in toluene.

We found that the data of McConnel et al. did not fit our empirical scaling relation in a quantitative sense, i.e. the measured core radii did not coincide exactly with the data points shown in Figure 3.2. However, it was found that their core radii data did show a soluble block dependence. In particular, we found that their data scaled better when the length of the soluble block was considered.

Whilst it is recognized that the empirical scaling relation obtained here is not applicable to every block copolymer/solvent system, our results do illustrate that the micelle core radius depends on both the length of the insoluble block and the length of the soluble block, scaling in the manner:

$$R_{core} \sim N_B^{\alpha} N_A^{-\gamma}$$

The fact that samples of very different chemical composition (which associate in very different solvent media) show a linear relationship between the average micelle core radii and a quantity of the type $N_B^{\alpha} N_A^{-\gamma}$ suggests that the soluble block plays a role in the micelle formation process and influences the structure of the resulting micelles. This further suggests that in any theoretical treatment of the micellization of block copolymers the influence of the soluble block should be considered.

Theoretical expressions relating the core radius to a quantity of the type $N_B^{\alpha} N_A^{-\gamma}$ were first obtained by Whitmore and Noolandi using a free energy minimization approach.[14] Their theory is based on micelle formation in block copolymer-homopolymer blends and was applied specifically to experimental data obtained on polystyrene-*b*-polybutadiene copolymer micelles dissolved in polybutadiene homopolymers. In their study, qualitative agreement between experiment and theory was obtained. Theoretical values for the exponents lay in the range $0.67 \leq \alpha \leq 0.76$ and $0 \leq \gamma \leq 0.1$, showing that the soluble block has a relatively weak influence on the size of the micelle core. This conclusion is in contrast to the theory of Nagarajan and Ganesh.[17]

They predicted that the soluble block can exert a large influence on the structure of the micelle, particularly in the case of copolymer molecules in which the soluble block is in a good solvent. Generalized scaling relations were developed for R_{core} and N_{agg}, as well as the molecular properties of the solvent and copolymer. To facilitate quantitative calculations, two model systems and three specific block copolymer/solvent systems were chosen. They scaled the data in terms of the effective number of repeat units, m_B and m_A [$m_B = (N_B V_B / V_S)$, where V_B and V_S are the molecular volume of the insoluble copolymer block repeat unit and solvent, respectively]. The values of the exponents which they obtained depended on the copolymer/solvent system. For polystyrene-*b*-polybutadiene block copolymers in heptane they found $R_{core} \sim m_B^{0.70} m_A^{-0.08}$; for poly(oxyethylene)-*b*-poly(oxypropylene) copolymers in water they found $R_{core} \sim m_B^{0.73} m_A^{-0.17}$. The larger dependence of R_{core} on N_A in the latter system was attributed to the fact that water is a good solvent for poly(oxyethylene), under the conditions of the measurement. Zulina and Birshtein[15] also proposed an expression for R_{core} in a specific copolymer composition region, roughly corresponding to the composition of the polystyrene-*b*-poly(acrylic acid) copolymers studied here, in which the micelle core radius scaled as $N_B N_A^{-\gamma}$. The value of g depended on the quality of the solvent, being equal to 0.5 in a θ solvent and equal to 0.545 in a good solvent.

The basic difference between our empirical fit and the theoretical expressions of Whitmore and Noolandi, Nagarajan and Ganesh, and Zulina and Birshtein, is quantitative, i.e. the experimental values of the exponents are different to the theoretical values. In particular, our experimental data suggest that the dependence of the core radius on the length of the insoluble block is weaker than predicted by theory. The difference in the value of the exponents obtained here to those predicted by theory is probably due to the interplay of several different contributions. As already mentioned, differences in the physicochemical nature of the specific interactions in different block copolymer/solvent systems may lead to different values of the exponents. Differences in the manner in which block copolymers systems associated may also be of importance. For example, it has been noted that in order for equilibrium micellar structures to be formed it is necessary to ensure that micelles associate under conditions in which there is a dynamic equilibrium between the free-chain form of the copolymer and the associated micellar form.[22] Furthermore, most theoretical predictions of the core radius R_{core} are obtained for a constant value of the interaction parameter, χ. However, in present system, the values of χ at which the micelles formed were to decrease with increasing N_B, then the values of R_{core} may scale more slowly with N_B than at fixed χ. Finally, the influence of experimental error on the values of the exponents should not be underestimated. For example, in their study Whitmore and Noolandi[14] estimate that an uncertainty of ± 0.2 nm in the measured values of R_{core} produced an uncertainty of ~ ± 0.05 in g and ~ ± 0.1 in a. At this point of our study it is not clear whether there is a discrepancy between experiment and theory, or an agreement. Future work with other copolymer systems, or different procedures for the micelle preparations may help resolve this question.

3.3.4 An investigation of the micelle structure by DLS.

3.3.4.1 Basic DLS theory. The basic quantity measured in the DLS experiment is the intensity autocorrelation function, $G_2(\tau)$, which, in a dilute solution of monodisperse particles, is an exponentially decaying function of the decay time, τ(s). $G_2(\tau)$ is related to the normalized electric field autocorrelation function, $g_1(\tau)$, via the Siegert relationship:

$$G_2(\tau) = B\,(1+\beta\,|g_1(\tau)|^2) \qquad (3.1)$$

where B is the measured baseline of the decaying autocorrelation function and β is the coherence factor which can be used as an adjustable parameter in data analysis. In the simplest case of monodisperse non-interacting particles, $g_1(\tau)$ is a simple, single exponential function:

$$g_1(\tau) = \exp^{-\Gamma\tau} \tag{3.2}$$

where Γ is the relaxation rate of the decaying autocorrelation function (s^{-1}). Γ is related to the diffusion coefficient, D ($m^2\ s^{-1}$), by :

$$\Gamma = D\, q^2 \tag{3.3}$$

where q is the scattering vector:

$$q = (4\pi n/\lambda)\ \sin(\theta/2). \tag{3.4}$$

Here n is the refractive index of the scattering medium (water), λ is the wavelength of the incident light (m), and θ is the scattering angle.

It is often found that the experimental autocorrelation function is not a single exponential function, and that there is a distribution of relaxation rates. The analysis of experimental data in these circumstances can become much more complicated and is, in many respects, a developing field. Various methods of data analysis have been developed; a review of the field is given by Štêpánek.[23] In the present study, data were fitted by a single exponential method and by the method of cumulants developed by Koppel,[24] using the Brookhaven correlator software. Because of the more reliable fitting of the experimental data by the cumulant method, all subsequent quantitative analyses were performed using values of the mean z-average relaxation rate $(\overline{\Gamma})_z$ obtained by this technique.

In the method of cumulants the correlation function is expanded about a z-average relaxation rate, $(\overline{\Gamma})_z$. The result is a polynomial expansion in the sample time with cumulants (moments about $(\overline{\Gamma})_z$) as the parameters to be fitted. For polydisperse, point like, isotropic particles without intermolecular interactions the expansion may be written:

$$| g_1(\tau) | = \exp \{- \bar{\Gamma}\tau + (\mu/2!)\tau^2 + ...\} \qquad (3.5)$$

where $\bar{\Gamma}$ is the intensity (I)-weighted mean relaxation rate, sometimes referred to as the initial slope: $\bar{\Gamma} = \sum_i I_i(\Gamma_i - \Gamma)$; and μ is the second moment of the distribution of the relaxation rates about the mean: $\sum_i I_i(\Gamma_i - \Gamma)^2$. The logarithm of equation 3.5 can be fitted by a non-negative least squares routine. The ratio $\mu/(\bar{\Gamma})_z^2$ is a measure of the width the intensity distribution of relaxation rates, which can be used to give an indication of the polydispersity of the sample under investigation.

3.4.2 DLS results. In the present study, all micelle samples gave values of $\mu/(\bar{\Gamma})_z^2$ in the range of 0.07 - 0.20, illustrating that there was a distribution of relaxation rates contributing to the correlation function. These results also suggest that a more sophisticated data analysis technique, such as the CONTIN method due to Provencher,[25] should be used to extract information on the distribution of relaxation rates. It should be noted that correlation curves obtained in the present study were exponential, and did not have any bi-exponential character. Therefore, we feel that the polydispersity observed in the concentration ranges studied here is due mainly to polydispersity in micelle size, rather than to the formation of ordered structures in solution (as has been previously observed for ionized polystyrene-*b*-poly(methacrylic acid) micelles[26]) or because of strong electrostatic interactions between micelles.[27] This assertion is corroborated by the fact that the sample 1400-*b*-310, which was prepared by dialysis against deionized water, also exhibited appreciable micelle polydispersity by DLS. This sample should have the lowest degree of ionization of all samples, and therefore should be least affected by strong electrostatic intermicellar interactions. A number of explanations can be proposed for the observed polydispersity in micelle size. For example, the micelle polydispersity may be due to compositional polydispersity in the corona-forming blocks. However, we prefer to await results obtained by the CONTIN method before discussing this observation further. These studies are currently underway in our laboratory.

Angular dependence data obtained on the present micellar solutions also suggest that strong intermicellar interactions did not influence the DLS results. Data for micelles formed from the sample 1400-*b*-310, prepared by dialysis against distilled water, are shown in Figure 3.3. This pH of this sample was 6.5, illustrating that the acid groups in the coronal layers of the micelles were ionized. The different plots of $(\bar{\Gamma})_z$ versus q^2 are straight lines which, within the variation of $(\bar{\Gamma})_z$, pass through the origin. This illustrates that the relaxation mode was diffusive in nature, i.e. free diffusion of the micelle was investigated in the concentration range studied. The simple angular dependence of the measured relaxation rate suggests that long-range interactions were not probed in the experiments.

From the slopes of the plots of $(\bar{\Gamma})_z$ versus q^2, it is possible to obtain a value of the diffusion coefficient, D. We define the diffusion coefficient thus obtained as the effective diffusion coefficient, D_{eff}. It is clear that the value of D_{eff} obtained depended on the concentration of the solution. In particular, as the concentration of the solution was increased, the value of D_{eff} increased. This is shown more clearly in Figure 3.4, where a plot of D_{eff} versus polymer concentration (C/g.cm^{-3}) is presented for different micellar systems. The data in Figure 3.4 clearly illustrate that, within the variation of D_{eff} (~ ± 5%) and the error in C (± 3%), there is a linear variation of D_{eff} with respect to concentration, in the concentration ranges studied. From theory, it can be shown that the mutual diffusion coefficient, D,[28] obtained at finite concentration, is characterized by the concentration coefficient, k_D, in the expansion:[29]

$$D = D_0 (1 + k_D C + \ldots) \qquad (3.6)$$

where D_0 is the diffusion coefficient, obtained by extrapolating vales of D obtained at finite concentrations to infinite dilution.

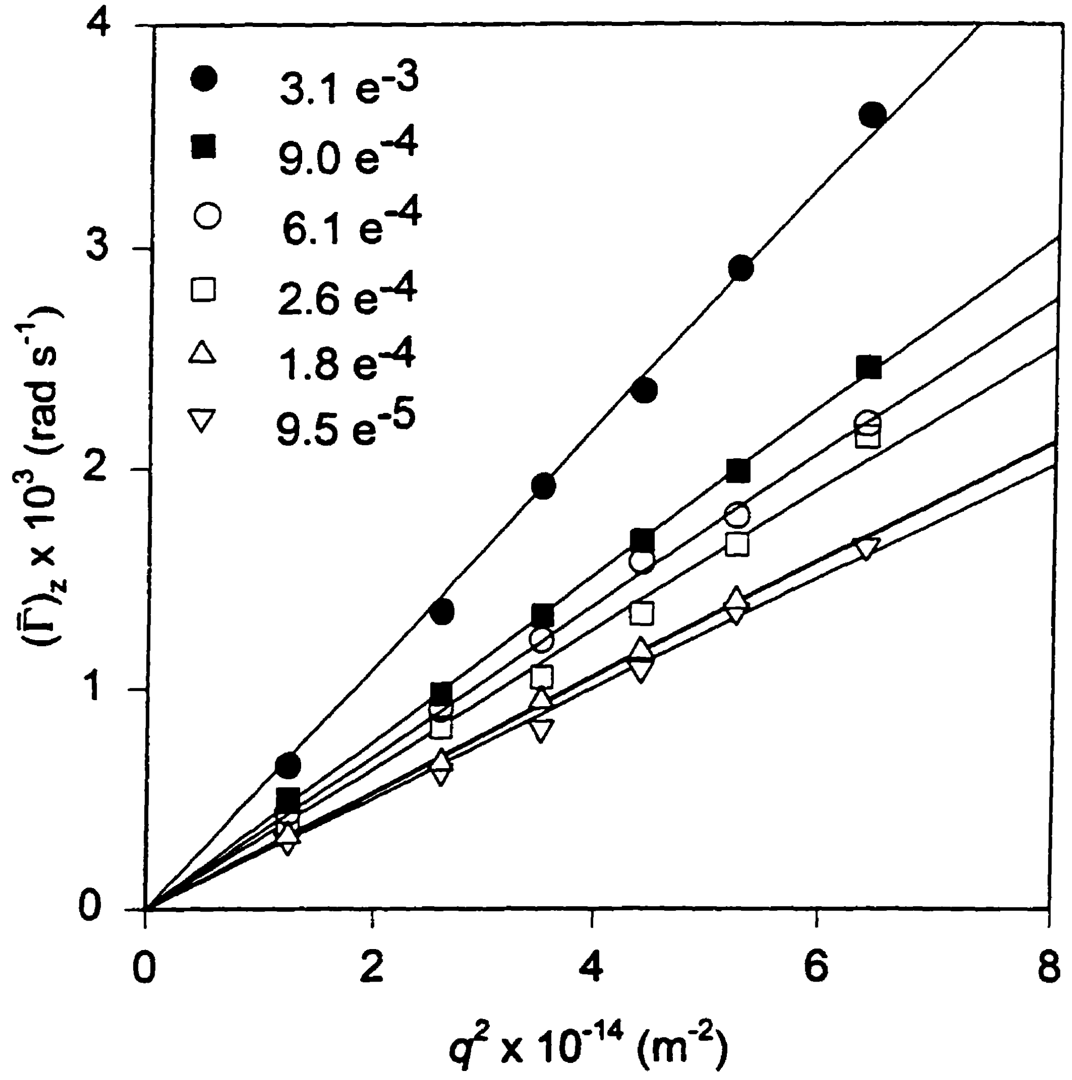

Figure 3.3. Plot of the average z-average relaxation rate $[(\bar{\Gamma})_z$ / rad $s^{-1}]$ versus the square of the scattering vector (q^2/m^{-2}) for different concentrations of micellar solutions of the block copolymer 1400-*b*-310. The concentrations shown are: (●) 3.1e^{-3} g cm^{-3}; (■) 9.0e^{-4} g cm^{-3}; (○) 6.1e^{-4} g cm^{-3}; (□) 2.6e^{-4} g cm^{-3}; (△) 1.8e^{-4} g cm^{-3}; and (▽) 9.5e^{-5} g cm^{-3}.

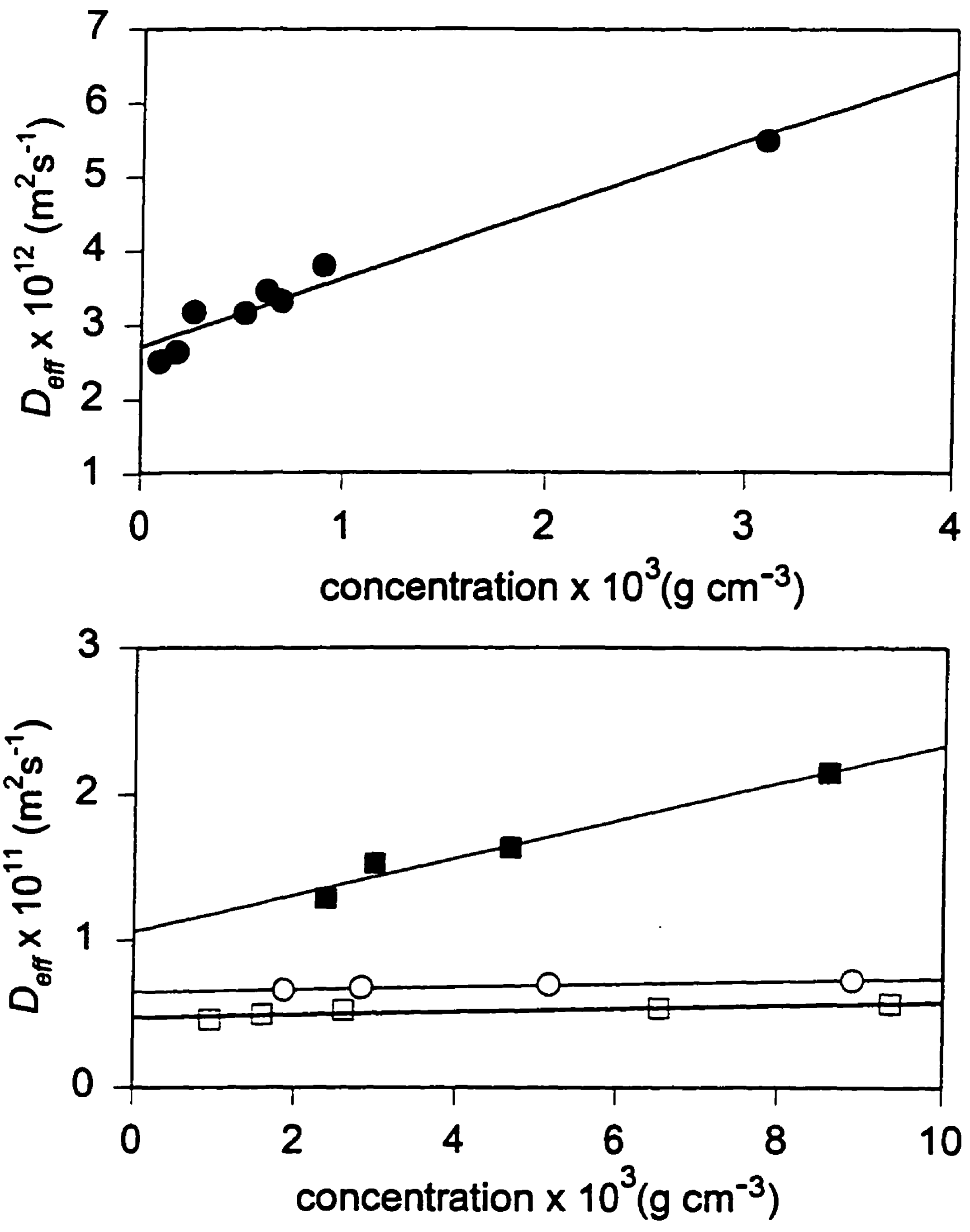

Figure 3.4. Plot of the effective diffusion coefficient (D_{eff}/m^2s^{-1}) versus concentration (C/g cm^{-3}) for different micellar solutions: (●) 1400-*b*-310 prepared by dialysis against distilled water; (■) 500-*b*-60; (○) 1400-*b*-310 prepared by dialysis against deionized water; and (□) 1140-*b*-170.

For dilute solutions, k_D contains thermodynamic and hydrodynamic (frictional) components: [29]

$$k_D = 2A_2 M_w - K_f - \nu \qquad (3.7)$$

where A_2 is the second virial coefficient , M_w is the weight-average molecular weight of the diffusing species, K_f is the frictional coefficient and ν is the partial specific volume of the polymer in the solvent.

One quantity that is readily obtained from the plots of D_{eff} versus C is the diffusion coefficient at infinite dilution, D_0. Furthermore, by substituting the experimentally determined values of D_0 into the Stokes-Einstein equation, it is possible to obtain the hydrodynamic radius of the micelle, r_h :

$$r_h = kT/6\pi\eta\, D_0 \qquad (3.8)$$

where k is the Boltzmann constant (JK^{-1}), T is the absolute temperature (K), and η the viscosity of the solvent ($Nm^{-2}s$). Values of the hydrodynamic radii of different samples are listed in Table 3.2. The notation used, i.e. $[(1/r_h)_z]^{-1}$, illustrates that the average radius obtained by DLS is the inverse reciprocal z-average hydrodynamic radius.

3.3.4.3 coronal thickness and the degree of extension of coronal chains. One of the major reasons for accumulating these data was to gain an estimate of the thickness of the coronal layer in micelles of this type. From these data, it is also possible to calculate the degree of extension of the poly(acrylic acid) chains in the corona, by comparing the thickness of the corona with the fully extended contour length of the poly(acrylic acid) chains. The thickness of the corona may be obtained by subtracting the z-average core radius $[(R_{core})_z]$ from the inverse reciprocal z-average hydrodynamic radius. The percentage extension can be calculated from equation 3.9:

$$\%\,extension = \frac{100\,\{[(1/r_h)_Z\,]^{-1} - (R_{core})_Z\,\}}{a\,N_A} \qquad (3.9)$$

where a is the length of one fully extended acrylic acid repeat unit (assumed to be 0.25 nm). Values of the coronal thickness, $[(1/r_h)_Z\,]^{-1}$ - $(R_{core})_Z$], and the % extension of poly(acrylic acid) chains are presented in Table 3.2.

Before discussing these results, it is necessary to consider the various factors which influence the magnitude of the coronal thickness and % extension values. As already mentioned, the average radius obtained by DLS is the inverse reciprocal z-average hydrodynamic radius, which, in the case of polydisperse samples, is larger than the weight- and number-average hydrodynamic radius. Whenever possible, the same type of averages should be compared. It is possible to calculate the z-average core radius, $(R_{core})_Z$, from the distribution of measured core radii; however, since the distribution of core radii is relatively narrow, the calculated z-average radius is not very different than the number-average radius. Unfortunately, in the present experiments, we did not have access to data analysis software from which we could calculate the number-average hydrodynamic radius. As a consequence, the intensity (I) -weighted values of the coronal thickness and % extension quoted in Table 3.2 represent the upper limit to the possible values.

Other factors which influence the magnitude of the values in Table 3.2 are the variation and errors in the different parameters. Obviously $[(1/r_h)_Z\,]^{-1}$, $(R_{core})_Z$ and N_A are averages which are subject to experimental uncertainty: the uncertainty in $[(1/r_h)_Z\,]^{-1}$ is approximately equal to the variation in D_{eff} (~ ± 5%), the error involved in measuring R_{core} is around ± 1nm (5-8%), and the error in N_A is around ± 5%. It must be recognized, therefore, that a combination of all these errors leads to a rather large error in the value of the coronal thickness and the value of the % extension.

Having recognized the factors which influence the values in Table 3.2, it is now possible to state, with confidence, that the poly(acrylic acid) chains in the coronae of micelles formed at high pH and at low ionic strength have an extremely extended conformation.

3.3.5 Factors affecting the stretching of coronal chains.

In this section, we discuss the various factors which are known to influence the conformation of chains in the coronal layer of micelles. The conformation of chains in the corona of a micelle is known to be affected by a variety of parameters, including the curvature of the micelle core to which the chains are attached, the concentration of chains in the corona, the chemical nature of the coronal chains, the quality of the solvent for the coronal chains, and the macroscopic concentration of micelles.[4,11-17, 48-60] How each of these variables may contribute to the stretching of the coronal chains observed in the present experiments is discussed below. As part of this discussion we present results obtained on the present micellar systems, as well as a comparison of our results with results available for other micellar systems.

3.3.5.1 Stretching of coronal chains: a selective summary of the available literature. We begin our discussion by briefly overviewing some of the literature relevant to this study. Whilst there have been quite a few studies of the dimensions of micelle cores,[20,21,30-37] direct determination of the coronal thickness in micellar aggregates is more difficult,[21,33,34,38-40] since it involves the measurement of both the core and micelle radii. One study of this type was performed by McConnell et al. on polystyrene-*b*-polyisoprene micelles in decane, using a combination of small-angle X-ray scattering (SAXS), small-angle neutron scattering (SANS) and DLS experiments.[21] By subtracting core radii, obtained using SAXS and SANS, from hydrodynamic radii, they were able to obtain coronal thicknesses for a range of samples. Their experiments showed that the conformation of chains in the coronal layer of micelles is perturbed in comparison to the free homopolymer, i.e. the coronal thickness is larger than the root-mean-squared end-to-end distance of equivalent free homopolymer chains of the same molecular weight in the same solvent. This result has also been obtained by other authors.[33,34,38,39] For the polystyrene-*b*-polyisoprene micelles in decane studied by McConnell et al. , the chains in the micelle coronae were much less extended than those in the present study, with % extension values in the range 16%-35%, depending on the sample.[21]

The results obtained by McConnell et al. were consistent with results obtained by Cogan et al. in an earlier study of micelles formed from polystyrene-*b*-poly(oxyethylene) block copolymers in cyclohexane.[39] In the study of Cogan et al., the degree of stretching of the coronal chains in the micelles was found to depend on the relative balance between the composition of the copolymer, the size of the micelle core, the aggregation number and the length of the coronal chains. For example, micelles formed from copolymers consisting of relatively short core-forming blocks and relatively long corona-forming blocks formed micelles which resembled star polymers, e.g. their scattering profiles were consistent with a concave coronal density profile.[16] Micelles formed from copolymers consisting of relatively long core-forming blocks and relatively short corona-forming blocks had a very different structure which could not be described by the star model. For those systems, it was found that as a consequence of the higher concentration of chains in the corona, the coronal chains had a highly extended conformation. Using experimental values of r_h and N_A obtained by Cogan et al. for this sample, and an estimated value of R_{core}, we calculated that the coronal chains in micelles of a poly(oxyethylene)-*b*-polystyrene block copolymer (65-*b*-80) were approximately 70% extended.

In other studies of the micelle structure, a structural parameter of the micelle was measured, e.g. r_h, and a structural model was invoked to calculate the unknown parameter, e.g. R_{core}.[18,31,33,41,42] Two examples of this approach are outlined below. In a recent SANS study of block copolymers micelles formed from triblock copolymers of poly(oxyethylene)-*b*-poly(oxypropylene)-*b*-poly(oxyethylene) micelles in water, Pospisil et al. used the spherical core/shell micelle model to estimate micelle structural parameters.[42] From SANS measurements, the authors were able to show that the micelle core was swollen. One controversial result that was obtained was that the shell thickness was 20% bigger than the fully extended length of the poly(oxyethylene) chain. The authors attributed this result to micelle and compositional polydispersity, or to the existence of a poorly defined core-shell interface.

In another study, Qin et al. studied micelles formed from polystyrene-*b*-poly(methacrylic acid) copolymers in a mixed solvent of 80%-vol. dioxane and 20 %-vol. water by a wide range of experimental techniques.[18] The micelles were found to behave thermodynamically and hydrodynamically as impermeable spheres. By modeling their micelles as hard spheres, they were able to calculate the micelle core radii for two different cases: a completely unswollen core and a core with extensive swelling. Furthermore, from the measured values of r_h and the calculated values of R_{core}, they were able to estimate the degree of extension of chains in the corona. The results depended on whether it was assumed that the core was swollen or unswollen, and varied for different samples. For a dry core, the % extension varied between 39%-94%; for the more realistic case of a swollen core, the authors calculated that the % extension varied between 32 -58%.

3.3.5.2. Surface area per coronal chain (A_c/nm^2). The conformation of chains adsorbed at, or tethered to, a surface is known to be influenced by the density of chains at the surface. The influence of surface density on the conformation of chains has received both theoretical[43,44] and experimental[45] attention in recent years. The density of attached chains is considered low if the attached chains do not overlap. We can obtain an estimate of the surface (interface) area per coronal chain (A_c/nm^2) from the equation:

$$A_c = 4\pi(R_{core})^2 / N_{agg} \qquad (3.10)$$

A complete list of values of A_c is given in Table 3.1.

It has been argued that the surface area per coronal chain may be an important factor among those controlling aggregation number and the structure of the micelles.[18,19] In particular, it has been suggested that in micelle formation, the interface energy between the core-forming block and solvent, and the osmotic force acting on the corona-forming chains, balance in a way so that a constant interface area per chain is maintained. This is clearly not observed in the present experiments. Our results suggest that the value of A_c increases as the total length of the block copolymer is increased. However, it must be remembered that the aggregation numbers contained in Table 3.1 were calculated from the micelle core radius. As such, we prefer to await results obtained from static light-scattering, which will give a direct measure of N_{agg}, before discussing this observation further.

Using the approximate values of A_c contained in Table 3.1 it is possible to gain an *estimate* of the surface density of coronal chains for different micellar systems. Using the approach of Hadziioannou et al.,[45] the dimensionless surface density for a planar surface, σ , is defined as: $\sigma = A_c^{-1} a^2$, where a^2 is the area taken up by a single monomer segment (0.25^2 nm^2). For a polymer in a good solvent, the condition for low surface density is $\sigma < N_A^{-6/5}$. As σ becomes greater than $N_A^{-6/5}$, chains adopt conformations extended in a direction perpendicular from the surface, in order to accommodate the higher lateral packing of anchored chains at the surface. For the samples studied in the present experiments, the calculated value of the ratio $\sigma / N_A^{-6/5}$ was greater than unity only in three cases, i.e. for micelles formed from the polymers 740-*b*-180, 1140-*b*-170 and 1400-*b*-310; all micelles with relatively small core radii and relatively long coronal chains. However, the density of coronal chains obtained for all the micelles in the present study were low in comparison to micelles formed by other block copolymers, for example, the ratio $\sigma / N_A^{-6/5}$ lies in the range 9-200 for the star-like micelles studied by Nguyen et al.[20] The high degree of extension observed in the present experiments cannot, therefore, be attributed to a high density of coronal chains at the micelle core. If anything, the surface density of coronal chains is rather low.

3.3.5.3 curvature of the micellar surface. Another factor which influences the thickness of the coronal layer is the degree of curvature of the surface to which the coronal chains are attached. Dan and Tirell[46] have treated this effect theoretically using a self-consistent field model to compute the segment density profiles, layer thicknesses and the distribution of chain ends, for chains tethered by one end to a curved impenetrable surface. The influence of geometry of the surface, the length of the tethered chain, the surface density of chains, and the radius of curvature can be seen in the relation for the average brush height, $<L>$:

$$<L> \sim a\, N_A^{3/(3+D)}\, \sigma^{1/(3+D)}\, (R/a)^{D/(3+D)} \tag{3.11}$$

where R is the interface radius (R_{core} for spherical micelles). D is related to the dimensionality of the curvature for a particular geometry, and is equal to 0 in planar geometry, 1 for cylinders and 2 for spheres. From this relation, it can be seen that a spherical micelle with a large core (large value of R/a) will have a larger average brush height than a spherical micelle with a small core (small value of R/a). In the limit of very large spherical micelles, the curvature of the core becomes small and the average brush height approaches that of the planar brush attached to a flat surface. From experimentally determined values of R_{core} it is possible to calculate an approximate value of the ratio (R/a) for different micellar systems. These calculations show that as a consequence of their relatively large core radii, the micelles in the present study have (R/a) values in the range of 48-84, comparable to the calculated range of values of (R/a) obtained by McConnell et al.[21] for polystyrene-*b*-polyisoprene micelles in decane (30-82), but bigger than the range of (R/a) values obtained by Nguyen et al.[20] for polystyrene-*b*-poly(cesium acrylate) and polystyrene-*b*-poly(4-vinyl pyridinium methyl iodide) reverse micelles in toluene (7-24).

3.3.5.4 Chemical nature of the coronal chains and the quality of the solvent for the coronal chains. Whilst the surface density of coronal chains and the core curvature undoubtedly affect the conformation of chains in the coronae of micelles, it seems that, considering the high degree of extension observed in the present experiments, the most important factors have not been addressed, i.e. the chemical nature of the coronal chains and the quality of the solvent for the coronal chains. It has already been noted that in the present experiments, as a consequence of the way the micelle systems were prepared, different micellar solutions had different pHs (see Table 3.2). This aspect of the study is rather unfortunate, since the pH of the solution determines (and gives an indication of) the degree of ionization, α, of the poly(acrylic acid) chains. It is, in principle, possible to calculate the degree of ionization of the coronal chains from data on the acid-base behavior of poly(acrylic acid) in water.[9,10] However, the acid-base behavior of poly(acrylic acid) in the corona of a micelle is undoubtedly different from the behavior of the free homopolymer in solution;[47] an unambiguous estimate of α is therefore difficult. We can, however, make the general statement that the chains in the coronae of the micellar samples prepared by dialysis in distilled water are neutralized by counterions introduced during the dialysis, and, as a result, have an appreciable degree of polyelectrolyte character.

The principal difference between grafted neutral polymer and grafted polyelectrolyte layers is related to the difference in the nature of the interpolymer interactions in the two system, i.e. short-range excluded volume type interactions in the case of neutral polymers, and long-range electrostatic interactions in the case of ionic polymers. As a consequence of long-range electrostatic repulsion, the chains in adsorbed or tethered polyelectrolyte adopt a highly extended conformation at relatively low surface densities.[48]

3.3.5.5 Comparison of experimental results to other theoretical and experimental studies of polyelectrolyte colloids. 3.3.5.5.1 Theoretical studies. There are a number of theoretical studies of polyelectrolytes adsorbed, or attached, to a planar surface [48-55] or attached to the surface of a spherical colloid particle.[48,53,55-61] In the case of a polyelectrolyte grafted to a flat surface with no added electrolyte, Pincus found that the brush thickness, L, was determined by a balance between the swelling effect of the counterions trying to increase their entropy by mixing, and the chain elasticity.[48] He also found for this case that the chains were highly stretched for low degrees of ionization, and that the brush thickness was independent of the grafting density. For the case of polyelectrolyte chains attached to a spherical colloidal particle, many theoretical treatments predict that the polymer chains will be strongly stretched radially. Using a self-consistent mean-field Monte Carlo approach to probe the conformational equilibria of chains in the corona of spherical polyelectrolyte micelles, Ronis predicted that the chains in the coronal layer do not adopt a single conformation.[57] Rather, the coronal layer is composed of three subregions: a rigid rod-like region near the core, followed by a flexible-rod region and a continuum region at the end of the chain. He also showed that the extent of rod-like or coil-like conformational behavior depended on the length of the chain, the core size, the aggregation number and the screening length.

The high degrees of extension of coronal chains which we observed experimentally in samples prepared by dialysis against distilled water (which have a high degree of neutralization) are therefore reasonable. In water, the intramolecular repulsion between chains in the corona causes the chains to adopt a highly extended conformation. Using the terminology of Pincus,[48] the coronal chains resemble porcupine quills.

Another feature of some of the theoretical models is that the conformation of the polymer chains attached to spherical colloidal particles is strongly affected by the presence of added electrolyte, and by changes in the degree of ionization of the polyelectrolyte chains.[48,52,53,55,57,58] These studies are allied with a substantial body of literature on the conformation of polyelectrolytes,[27] which shows that, in the presence of salt, the range of electrostatic repulsion is reduced and the chains adopt a more random coil conformation. In a recent paper Ronis also considered the effect of micelle-micelle interactions at finite colloid concentrations.[58] For the concentrations and surface coverage studied, he found that the conformation of chains was mainly affected by intra-aggregate interactions; inter-aggregate interactions did not perturb the conformation appreciably. It is worthwhile to note that all hydrodynamic radii were calculated from the extrapolated value of the diffusion coefficient at infinite dilution. At the limit of infinite dilution, inter-aggregate interactions should not influence the size of the micelle.

The data presented in Table 3.2 provide a test of the theoretical studies outlined above. For example, by studying the variation of the hydrodynamic radius with respect to salt concentration, or degree of neutralization, it should be possible to investigate the balance of physical forces which influence the conformation of polyelectrolyte chains attached to a colloidal surface. We have recently compared our experimental results to the theoretical model developed by Ronis.[57,58] Preliminary results suggest that theoretical predictions of the degree of chain extension are in agreement with experiment. Future work will involve probing the conformation of the chains in the coronae of a wider range of samples, spanning a broader range of copolymer compositions. It should be noted that in water, or in aqueous salt solutions, the micelles have a frozen structure, and that changes to the ionic strength or degree of neutralization should not influence parameters which depend on the dimensions of the core; therefore, R_{core} and N_{agg} will not change.

As part of a preliminary study of the effect of the salt concentration and degree of neutralization of the coronal chains on the degree of extension of coronal chains, we present results obtained on micelles formed from the copolymer 1400-*b*-310. This copolymer was chosen since it contains micelles which have the longest coronal chains. The micelles formed from this copolymer also have largest hydrodynamic radius of all the different samples studied here; any effects due to the dimensions of the coronal chains should be most easily measured in this sample. When the micelle sample was prepared in deionized water, the resulting micellar solution had a pH of ~4.5. This indicates that the degree of ionization of the polymer chains was low. For this sample the micelle hydrodynamic radius was 38 nm, which is two times smaller than that at pH 7. The corresponding value for the % extension of coronal chains was 25 %, comparable to the values obtained by McConnell et al. for polystyrene-*b*-polyisoprene micelles in decane.[21] The influence of the degree of neutralization is thus clear: introducing ionic charges to the polymer chain results in an appreciable expansion of the coronal chains. The resemblance of micelles formed from copolymers with essentially unionized poly(acrylic acid) to neutral polymers is also apparent.

Another way of influencing the conformation of polyelectrolyte chains is to add an inert electrolyte to the solution. Preliminary data for the sample 1400-*b*-310 in 1M NaCl also show that the hydrodynamic radius of the micelle decreases in the presence of an electrolyte. One interesting aspect of this study is that the hydrodynamic radius in the presence of salt (48 nm) was smaller than the hydrodynamic radius in the absence of salt (90 nm), but larger than the hydrodynamic radius of the sample at pH 4.5 (38 nm) (it should be noted that the hydrodynamic radius for the sample with added salt was obtained by extrapolation through only three data points; this is because on dilution of this sample flocculation occurred: see below). This result suggests that ionized coronal chains, in the presence of salt, are more stretched than coronal chains with a low degree of ionization. This effect has been predicted theoretically by Pincus,[48] who suggested that the addition of electrolyte (Debye screening) reduces the counterion osmotic pressure, which stretches the polymer chains.

The effect of the addition of salt on the dissociation equilibrium of the carboxylic acid groups and the neutralized carboxylic acid groups is also of importance. For example, it is well known that the addition of a salt to a polyelectrolyte solution leads to a decreases in the pKa of the polyelectrolyte.[10] This effect, reflected in the lower pH of the sample in the presence of salt (see Table 3.2), illustrates that the activity of the proton is increased in the presence of NaCl. The addition of salt to a solution of an ionized polyelectrolyte micelle thus leads to a number of component effects: Debye screening and a change in the acid-base equilibria. This result also illustrates that in order to study the effect of the addition of salt on the degree of stretching of the coronal chains, it is necessary to ensure that the ionic strength and degree of ionization of the initial polyelectrolyte solution are known.

Another interesting observation for the sample in the presence of salt was that flocculation occurred on dilution of this sample with 1M NaCl. It was possible to re disperse the flocs by placing the sample in a sonic bath, but the flocculated structure was formed again when the sample was left to stand for a few hours. After an extended period of standing (10 days), the cloudy solution eventually settled to form a two phase system. It was not possible to form a one-phase system by increasing the pH of the continuous medium. We consider the loss of colloidal stability observed for this sample to be a consequence of the relatively low density of coronal chains at the surface. This effect, noted in our previous study of micelles formed from polystyrene-*b*-poly(4-vinyl-pyridinium methyl iodide) block copolymers,[5] has also been predicted by theory.[48] The critical dimension in determining the degree of screening is the density of chains at the surface, i.e. the grafting density: the lower the grafting density, the more sensitive the colloid is to added electrolyte.

3.3.5.5.2 Experimental studies. Whilst the direct determination of the thickness of the coronal layer in spherical polyelectrolyte micelles is certainly one novel aspect of this work, the observation that the structure of block copolymer micelles composed of a hydrophobic core and ionogenic corona depends on the pH and the ionic strength is not new. The fact was recognized early in the development of the field,[62,63] but was not studied systematically. More recently Tuzar, Munk and co-workers[26,47,64] have studied micelles formed from polystyrene-*b*-poly(methacrylic acid) block copolymers by a variety of experimental techniques, including DLS. In the first of these studies, they found that the apparent hydrodynamic diameter of the micelles increased as the degree of neutralization increased.[26] They attributed this result to the expansion of the poly(methacrylic acid) blocks in the shell of the micelle. Core dimensions were not determined in this study, but from a knowledge of the block lengths and the aggregation number we estimate that the % extension of coronal chains at a degree of neutralization $\alpha = 1$ was ~ 45%-70%, depending on the concentration. For ionized micelles at concentrations $\geq 5 \times 10^{-3}$ g cm^{-3} , DLS experiments were affected by order formation in solution. The distribution of apparent hydrodynamic radii became broad, and the autocorrelation curve became non-exponential.

In another study, the hydrodynamic radius of micelles was measured as a function of pH for polystyrene-*b*-poly(methacrylic acid) block copolymer micelles in various buffer solutions.[64] Again, the authors found that as the pH of the solution was increased, the hydrodynamic radius increased. The coronal dimensions were not determined in this study. However, we estimate that the degree of expansion of the coronal chains observed in these experiments was smaller than that observed in our experiments. For example, as the pH was changed from 5 to 7.8, using buffers, the % extension increased from ~25 % to ~32% for one sample, and from ~25% to ~38% for another sample. We consider the lower values of the % extension observed in these studies to be a consequence of the fact that buffer solutions contain an appreciable concentration of salt. It is thus difficult to separate the effect of an increase in pH on the extension of coronal chains from the effect of an increase in the ionic strength. The different chemical nature of the coronal chains will also be of influence. In particular, it is known that poly(methacrylic acid) has very different acid-base and solubility behavior than poly(acrylic acid).[10]

3.4. SUMMARY

In this study, we have been able to gain valuable information about the structure of polystyrene-*b*-poly(acrylic acid) micelles in water. Because of the versatility of the synthetic method, it was possible to synthesize a wide range of different copolymer samples, and study the effect of the length of the insoluble block (N_B) and the length of the soluble block (N_A) on the structure of the micelles. One of the important aspects of this work is that the micelle core radius, R_{core}, appears to depend not only on the length of the insoluble polystyrene block , but also on the length of the soluble poly(acrylic acid) block. Although an extensive comparison of our experimental data with theory was not attempted, our experimental results suggest that the length of the soluble block is an important parameter among those determining the structure of micellar associates. It is worthwhile to note that the inverse dependence of the core radius on the coronal block length has been observed previously,[35] and that the value of the exponent, γ, describing this dependence is similar to that predicted by some theories.[14]

From values of the core radius, R_{core}, and the hydrodynamic radius, r_h, it was possible to obtain an estimate of the thickness of the coronal layer of the micelles, and the degree of extension of the coronal chains. It was found that the poly (acrylic acid) chains were highly extended in samples at a pH of ~7. A brief overview of some of the current literature on coronal dimensions in micelles was presented, as was a discussion of the various parameters which are know to influence the dimension of chains in the coronae of micelles. Results obtained here were compared with various data from other experimental studies of micelle structure, and a discussion of results in relation to a number of theoretical studies was presented. We consider the high degree of extension of coronal chains observed in the present experiments to be due to the charged nature of the poly(acrylic acid) chains, the low degree of curvature of the surface to which the chains are attached, and the relatively low macroscopic concentration of micelles in the DLS experiments. In many ways the coronal chains resemble the polyelectrolyte brushes which currently excite much interest.[55]

Data of these type provide a test of many of the theoretical models available in the literature. We have recently compared our results with a theoretical model developed by Ronis,[57,58] which uses a self-consistent mean-field Monte Carlo approach to probe the conformational equilibria of chains in the coronal layer of spherical polyelectrolyte micelles. Preliminary results suggest that theoretical predictions of the chain conformation are in agreement with experiment. Future work will involve probing the conformation of the chains in coronae of a wider range of samples, spanning a broader range of copolymer compositions. The influence of the degree of ionization and the pH of the micellar solution on the conformation of the coronal chains will also be investigated. These studies are currently underway in our laboratory, and results will be reported in the near future.

3.5. ACKNOWLEDGMENTS

We would like to acknowledge the National Sciences and Engineering Research Council of Canada (NSERC) for funding this work. We would like to thank Dr. T. G. M. van de Ven, director of the Pulp and Paper Research Institute of Canada, for permission to use the center's DLS equipment. The various contributions of Matthew Moffitt during the writing of this paper are also gratefully acknowledged.

3.6. REFERENCES AND NOTES

1. Tuzar, Z.; Kratochvil, P. *Adv. Colloid Interface Sci.* **1976**, *6*, 201.
2. Price, C. In: *Developments in Block Copolymers*; Goodman, I., Ed.; Applied Science Publishers: London and New York, 1982, Vol. 1, Chapter 2, p. 39.
3. Reiss, G.; Hurtez, G.; Bahadur, P. In: *Encyclopedia of Polymer Science and Engineering* 2nd ed.; Mark, H. F.; Bikales, N. M.; Overberger, Ch. G.; Menges, G., Eds.; John Wiley & Sons: New York, 1985; Vol.2, p. 324.
4. Tuzar, Z.; Kratochvil, P. *Surface and Colloid Science*; Matijevic, E., Ed.; Plenum Press; New York, 1993; Vol. 15, p. 1.
5. Gao, Z.; Varshney, S. K.; Wong, S.; Eisenberg, A. *Macromolecules* **1994**, *27*, 7923.
6. Zhang, L.; Eisenberg, A. *Science* **1995**, *268*, 1728 (chapter 4 of this thesis).
7. Zhang, L.; Eisenberg, A. *J. Am. Chem. Soc.* **1996**, *118*, 3168 (chapter 5 of this thesis). Zhang, L.; Shen, H.; Eisenberg, A. *Macromolecules* **1997**, *30*, in press (chapter 8 of this thesis).
8. Zhong, X-F.; Varshney, S.K.; Eisenberg, A. *Macromolecules* **1992**, *25*, 7160.
9. Arnold, R. *J. Colloid Sci.* **1957**, *12*, 549.
10. Nagasawa, M.; Murase, T.; Kondo, K. *J.Phys. Chem.* **1965**, *69*, 4005.
11. de Gennes, P. G. In: *Solid State Physics*; Liebert, J. , Ed.; Academic Press: New York, 1977; supl. 14, p. 1.
12. Noolandi, J.; Hong, K.M. *Macromolecules* **1983**, *16*, 1443.
13. Liebert, L.; Orland, H.; Wheeler, J. C. *J.Chem. Phys.* **1983**, *79*, 3550.
14. Whitmore, M.; Noolandi, J. *Macromolecules* **1985**, *18*, 657.
15. Zhulina, E. B.; Birshtein, T. M. *Vysokomol. Soedin.* **1985**, *27*, 511.
16. Halperin, A. *Macromolecules* **1987**, *20*, 2943.
17. Nagarajan, R.; Ganesh, K. *J.Chem. Phys.* **1989**, *90*, 5843.
18. Qin, A.; Tian, M.; Ramireddy, C.; Webber, S. E.; Munk, P.; Tuzar, Z.

Macromolecules **1994**, *27*, 120.

19. Antonietti, M.; Heinz, S.; Schmidt, M.; Rosenauer, C. *Macromolecules* **1994**, *27*, 3267.
20. Nguyen, D.; Varshney, S. K.; Williams, C. E.; Eisenberg, A. *Macromolecules* **1994**, *27*, 5086. Nguyen, D.; Williams, C. E.; Eisenberg, A. *Macromolecules* **1994**, *27*, 5090. Nguyen, D.; Zhong, X-F.; Williams, C. E.; Eisenberg, A. *Macromolecules* **1994**, *27*, 5173.
21. McConnell, G. A.; Gast, A. P.; Huang, J. S.; Smith, S. D. *Physical Review Letters* **1993**, *71*, 2102.
22. Stejskal, J.; Koňák, C.; Helmstedt, M.; Kratochvil, P. *Collect.Czech. Chem.Comm.* **1993**, *58*, 2282.
23. Štêpánek, P. In: *Dynamic Light Scattering:The Method and Some Applications*; Brown, W., Ed.; Claredon Press: Oxford, 1993; chapter 4, p. 177.
24. Koppel, D. E. *J. Chem. Phys.* **1972**, *57*, 4814.
25. Provencher, S. W. *Computer Phys. Comm.* **1982**, *27*, 213.
26. Kiesrow, D.; Prochazka, K.; Ramireddy, C.; Tuzar, Z.; Munk, P.; Webber, S. E. *Macromolecules* **1992**, *25*, 461.
27. Mandel, M. In: *Dynamic Light Scattering:The Method and Some Applications*, Brown, W., Ed.; Claredon Press: Oxford, 1993; chapter 7, p. 319.
28. The corresponding relation for the concentration dependence of D_{eff} is more complicated and contains a number of q-dependent terms (see, e.g. Ref. 27). However, values of D_{eff} extrapolated to zero concentration give the same value of the diffusion coefficient, D_0 .
29. Brown, W.; Nicolai, T. In: *Dynamic Light Scattering:The Method and Some Applications*; Brown, W. , Ed.; Claredon Press: Oxford, 1993; chapter 6, p. 272.
30. Tuzar, Z.; Kratochvil, P. *Macromol.Chem.* **1972**, *160*, 301.
31. Plestil, J. ; Baldrian, J. *Macromol.Chem.* **1973**, *174*, 183.

32. Plestil, J.; Baldrian, J. *Macromol.Chem.* **1975**, *176*, 1009.
33. Rigby, D.; Roe, R.-J. *Macromolecules*, **1984**, *17*, 1778.
34. Rigby, D.; Roe, R.-J. *Macromolecules*, **1986**, *19*, 721.
35. Selb, J.; Marie, P.; Rameau, A.; Duplessix, R.; Gallot, Y. *Polym. Bull.* 1983, *10*, 444.
36. Broadbent, G.; Brown, D. S.; Dawkins, J. V. *Polym. Commun.* **1987**, *28*, 1987.
37. Edwards, Ch. C. J.; Richards, R. W.; Stepto, R. F. T. *Polymer* **1986**, *27*, 643.
38. Brown, D. S.; Dawkins, J. V.; Farnell, A. S.; Taylor, G. *Eur. Polym. J.* **1987**, *23*, 463.
39. Cogan, K. A.; Gast, A.; Capel, M. *Macromolecules* **1991**, *24*, 6512.
40. Wu, G.; Chu, B.; Schnider, D. K. *J.Phys. Chem.* **1994**, *98*, 12018.
41. Xu, R.; Winnik, M.A.; Riess, G.; Chu, B.; Croucher, M. D. *Macromolecules* **1992**, *25*, 644.
42. PospíŠil, H. ; PleŠtil, J.; Tuzar, Z. *Collect.Czech. Chem.Comm.* **1993**, *58*, 2428.
43. Milner, S. T.; Witten, T. A.; Cates, M. E. *Macromolecules* **1988**, *21*, 2610.
44. Lai, P. Y.; Halperin, A. *Macromolecules* **1992**, *25*, 6693.
45. Hadziioannou, G.; Patel, S.; Granick, S.; Tirrell, M. J. *J. Am. Chem. Soc.* **1986**, *108*, 2869.
46. Dan, T.; Tirrell, M. *Macromolecules* **1992**, *25*, 2890.
47. Tuzar, Z.; Prochazka, K.; Zuzkova, I.; Munk, P. *Polymer Preprints* **1993**, *34*, 1038.
48. Pincus, P. *Macromolecules* **1991**, *24*, 2912.
49. Miklavic, S. J. ; Marcelia, S. J. *J.Phys. Chem.* **1988**, *92*, 6718.
50. Borisov, O. V.; Birshtein, T. M.; Zhulina, E. B. *J. Phys. Fr.II* **1991**, *1*, 521.
51. Zhulina, E. B.; Birshtein, T. M.; Borisov, O. V. *J. Phys. Fr.II* **1992**, *2*, 63.
52. Ross, R. S.; Pincus, P. *Macromolecules* **1992**, *25*, 2177.
53. Dan, N.; Tirrell, M. *Macromolecules* **1993**, *26*, 4310.

54. Seidel, C. *Macromolecules* **1994**, *27,* 7085.

55. Misra, S.; Mattice, W. L.; Napper, D. H. *Macromolecules* **1994**, *27,* 7090.

55. Khan, S.; Morton, T. L.; Ronis, D. *Physical Review A* **1987**, *35 (10),* 4295.

56. Ronis, D. *Physical Review A* **1991**, *44 (6),* 3769.

57. Ronis, D. *Macromolecules* **1993**, *26,* 2016.

58. Ronis, D. *Physical Review E* **1994**, *49(6)*, 5438.

59. Marko, J. F.; Rabin, Y. *Macromolecules* **1993**, *25,* 1503.

60. Whitmer, J.; Joanny, J. F. *Macromolecules* **1993**, *26,* 2691.

61. Zhulina, E. B. *Macromolecules* **1993**, *26,* 6273.

62. Selb, J.; Gallot, Y. In: *Polymeric Amines and Ammonium Salts*; Goethals, E.J. Ed.; Pergammon Press: New York, 1980; p.205.

63. Selb, J.; Gallot, Y. In: *Developments in Block Copolymers*; Goodman, I. Ed.; Applied Science Publishers: London and New York, 1985; Vol. 2, p.. 27.

64. Tuzar, Z.; Kratochvil, P.; Procházka, K.; Munk, P. *Collect.Czech. Chem.Comm.* **1993**, *58*, 2362.

Chapter 4

Multiple Morphologies of "Crew-cut" Aggregates of Polystyrene-*b*-Poly(acrylic acid) Block Copolymers

ABSTRACT

The observation by transmission electron microscopy of six different stable aggregate morphologies is described for the same family of highly asymmetric polystyrene-*b*-poly(acrylic acid) block copolymers prepared in a low molecular weight solvent system. Four of the morphologies consist of spheres, rods, lamellae, and vesicles in aqueous solution, whereas the fifth consists of simple reverse micelle-like aggregates. The sixth consists of up to micrometer-size spheres in aqueous solution that have hydrophilic surfaces, and are filled with the reverse micelle-like aggregates. In addition, a needle-like solid, which is highly birefringent, is obtained on drying of aqueous solutions of the spherical micelles. This range of morphologies is believed to be unprecedented for a block copolymer system.

4.1. INTRODUCTION

Small molecule amphiphile surfactant systems can form aggregates or micelles of various morphologies.[1] Also, depending on the block copolymer composition, multiple morphologies exist in the bulk phase of block copolymers, [2,3] in block copolymer/homopolymer blends, [4] and in two-dimensional micelle systems of amphiphilic block copolymers on water surfaces. [5] In block copolymer solutions, spherical micelles have been identified in many studies. [6,7] However, nonspherical micelles in solution have been observed only rarely and mostly indirectly. [8,9] To our knowledge, multiple morphologies, that is, spheres, rods, and vesicles or lamellae, have not yet been seen for the same block copolymer family in solutions of low molecular weight solvents. In this chapter, we describe the preparation and observation of six different morphologies. All of these were prepared in a low molecular weight solvent system from block copolymers of the same type differing only in the relative block lengths. This factor may allow for more precise modeling studies of the dependence of the morphologies on the molecular architecture in such system in solution. Four of the morphologies consist of spheres, rods, lamellae and vesicles in aqueous solution, while the fifth consists of simple reverse micelle-like aggregates in organic solvents. The sixth is new and consists of large spheres in aqueous solution which have hydrophilic surfaces, and are filled with the reverse micelle-like aggregates. In addition to these six different morphologies, a needle-like solid, which is highly birefringent, was obtained by drying aqueous solutions of the spherical micelles of the block copolymers. This range of morphologies is unprecedented for block copolymer systems.

4.2. RESULTS AND DISCUSSION

The polymers used in this study are diblocks of polystyrene (PS) and poly(acrylic acid) (PAA), which we synthesized by anionic polymerization as described before. [10] The polydispersity indices of the copolymers, estimated by gel permeation chromatography, were between 1.04 to 1.05. To prepare the colloidal aqueous solutions, deionized water at a rate of 1 drop every 10 s was added with vigorous stirring to a solution of the copolymer (2 wt.%, 10 ml) in N,N-dimethylformamide (DMF). Addition of water was continued until 25 wt.% of water had been added. The quality of the solvent for the PS block worsened as the addition of water progressed. Micellization occurred when the water content reached ca. 5 wt.%. The resulting solution was placed in a dialysis bag (Spectra/Por; molecular weight *MW* cut-off of 8000) and dialyzed against distilled water for 4 days to remove DMF. Transmission electron microscopy (TEM) was performed with a Phillips EM410 microscope operating at an acceleration voltage of 80 kV. [11]

Several of the morphologies described here (with the exception of the vesicles) resemble micelles; however, they should be referred to as micelle-like aggregates (*mlas*) because, after preparation under equilibrium conditions and subsequent isolation in water, they are no longer in thermodynamic equilibrium; once the organic solvent is removed, the PS cores are below their glass transition temperature, T_g. However, much of the block copolymer literature refers to the non-equilibrium block copolymer *mlas* as micelles, in recognition of the structural similarities to equilibrium micellar associates. This convention is adopted in this report. The name "crew-cut" [12,13] was suggested for the system under study because the length of the corona-forming block (PAA) of the aggregates is very short compared to that of the core-forming block (PS). The compositions of the blocks are indicated by x-*b*-y, where x is the number of styrene units and y is the number of acrylic acid units in the chain.

Figure 4.1 shows the four morphologies of the aggregates prepared from block copolymers of different compositions that contain the same polystyrene block. The least asymmetric diblock copolymer (200-*b*-21) gives spherical micelles of low polydispersity (Figure 4.1-A). They consist of a PS core (26 nm average diameter) with the surface covered by the PAA chains forming the corona. This is the most common morphology reported for block copolymer micelles in which, in contrast with the present system, the corona is

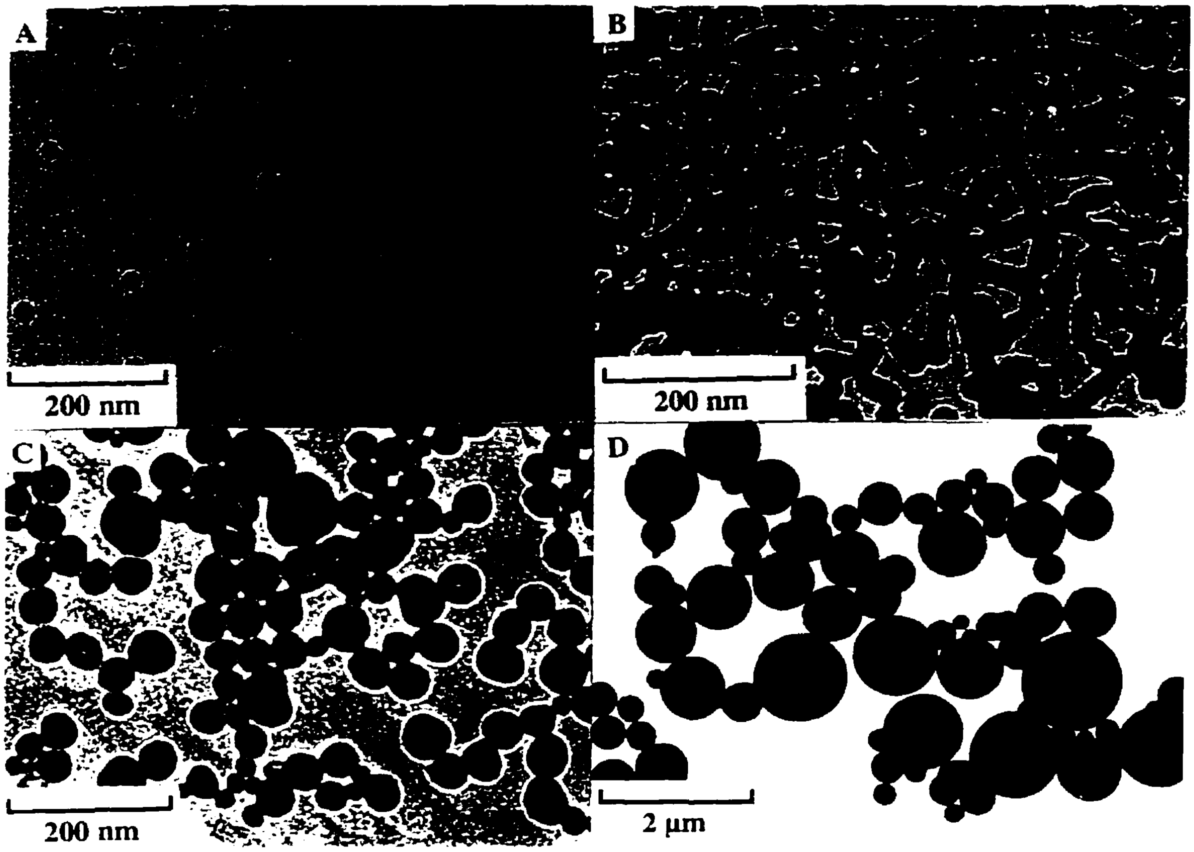

Figure 4.1. Multiple morphologies of the crew-cut aggregates from block copolymers of (A) 200-*b*-21, (B) 200-*b*-15, (C) 200-*b*-8, and (D) 200-*b*-4.

normally larger than the core. Very recently, the preparation of spherical "crew-cut" micelles of the type encountered here but made from polystyrene-*b*-poly(4-vinylpyridinium methyl iodide) was reported. [13] As the PAA block length decreases to 15 (200-*b*-15), the morphology changes from spherical to rod-like (23 nm in diameter) (Figure 4.1-B). The morphology changes again from rod-like to vesicular (Figure 4.1-C) when the PAA block length decreases still further (200-*b*-8). The vesicular nature is evidenced from a higher transmission in the center of the aggregates than around their periphery, coupled with height measurements (from shadowing) which show the aggregates to be spherical. The sizes of the vesicles are quite polydisperse, with diameters up to 100 nm. However, the PS wall thickness of the vesicles is very uniform (18 ± 2 nm). Finally, Figure 4.1-D shows the micelles from the block copolymer with the shortest PAA block length (200-*b*-4). These micelles are spherical, solid, highly polydisperse and contain some very large specimens (up to 1200 nm diameter in this image). A micrograph of a section of one of the smaller spheres, along with a schematic picture (Figure 4.2), shows that the sphere has an internal structure similar to that of block copolymers cast from a solution in a solvent in which the blocks form reverse micelles, with the polar cores on the inside and the styrene in the corona. [2] These inverse micelles are, in principle, the phase-inverted versions of the aqueous crew-cut micelles. Such reverse micelles in salt form are soluble in a range of organic solvents and retain their identity in solution indefinitely at room temperature. [14] Because this block ionomer reverse micelle morphology has been explored extensively in bulk and in solution, [14,15] it will not be described further. The large spheres with hydrophilic surfaces, which makes them stable in aqueous solution, however, are new. Note that the schematic shows a superficial resemblance to a mammalian cell, as well as to the structure of high impact polystyrene (HIPS). [16]

Examination of micrographs of the aggregates in the range of compositions that give vesicles occasionally reveals lamellar micelles. An example is shown in Figure 4.3 for the block copolymer 410-*b*-16. The thickness of the lamella (24 nm) is of the same order as the wall thickness of the vesicles (22 nm), as evidenced from the length of the shadowed region.

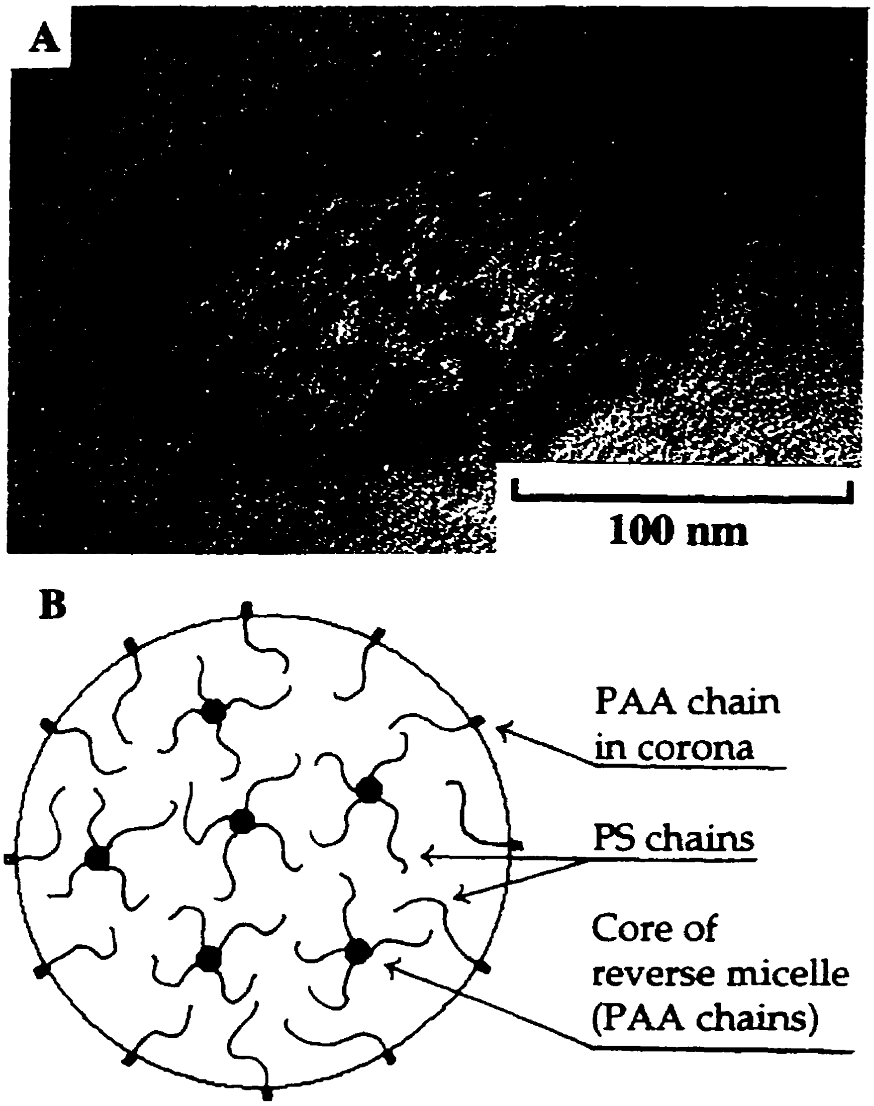

Figure 4.2. (A) The internal morphology of the large complex micelle made from the block copolymer (200-*b*-4) in Figure 4.1-D. The elongation of the particle shape in one direction is probably caused by the strong shear forces during microtoming. (B) A schematic structure of the large complex micelle filled with bulk reverse micelles.

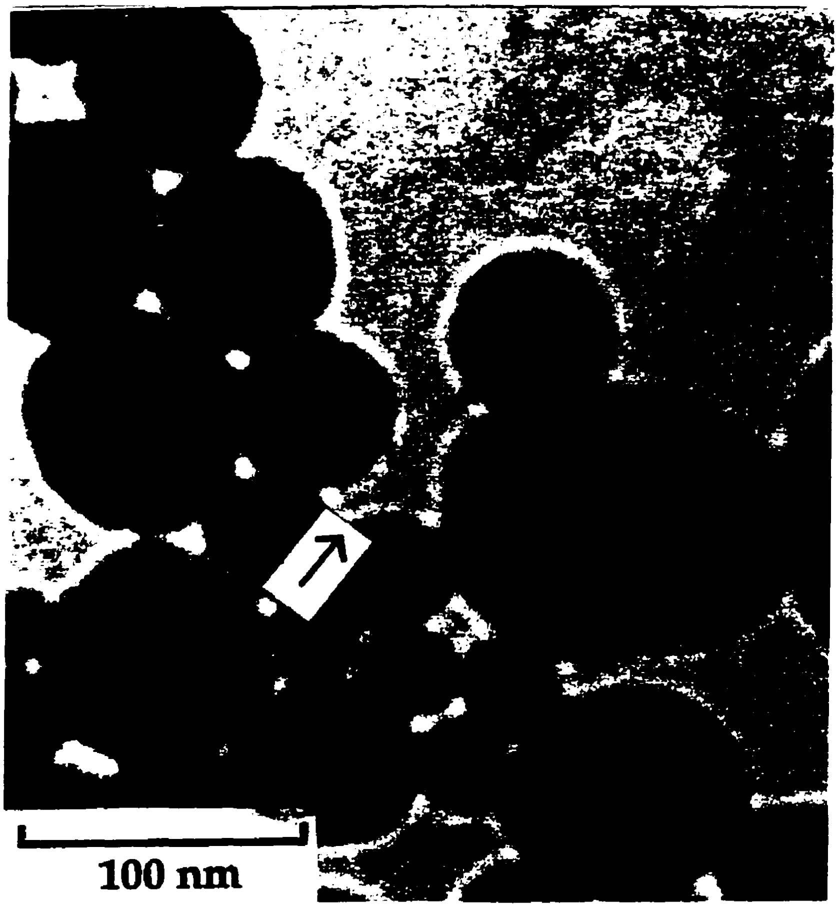

Figure 4.3. The morphologies of the aggregates made from the diblock copolymer 410-*b*-16. One lamellar micelle can be seen among the vesicles. The lamellar nature is evidenced by the uniformity of the light intensity over the entire feature. The wall thickness of the vesicles and the thickness of the lamellar micelle are consistent (22 versus. 24 nm). The arrow indicates he direction of shadowing.

Although the existence of vesicles made of block copolymers in low molecular weight solvents has been postulated individually on the basis of indirect evidence, [9] these structures have been observed directly by electron microscopy. Furthermore, we are not aware of any method of preparing glassy ($T_g \approx 100°C$) vesicles of this type (that is, size, wall thickness, and composition) by techniques other than that described here. The preparation of all of the morphologies (except the lamellae) is very reproducible. Furthermore, depending on the soluble chain length, the same morphologies can be observed for block copolymer series with different PS chain lengths. The boundaries, in terms of percent by mole of PAA block content between the different morphological regions, do not appear to change with PS block length for the samples we have studied.

For blends of poly(styrene-*b*-butadiene) diblocks with homopolystyrene (in which the butadiene forms the discontinuous phase), Kinning *et al.* [4] reported that the morphology can change from spherical to cylindrical and eventually to vesicular, by increasing either the insoluble butadiene block content in the block copolymer or the homopolystyrene molecular weight. By extrapolating the reported trends, nonspherical morphologies of block copolymer aggregates can be expected in low molecular weight solvents only if the soluble block of the copolymer is very short, with the long block remaining insoluble. However, for these very short block lengths, differential solubility in non-aqueous block copolymer systems may be very difficult to achieve. Furthermore, even if it is achieved, the isolation of the aggregates into a form in which they can be stabilized and dried may be even more difficult. Therefore, it has not been possible to make stable block copolymer vesicles (which can be isolated and dried), either in water or in other small molecule solvents. In the present system, however, it is possible to do so because of the large difference in the solubilities of the hydrophilic and hydrophobic blocks. Once formed in their various morphologies at equilibrium, the aggregates can be deswelled in water, which makes them very stable because of the strong interactions between the acidic or ionic aqueous corona-forming PAA blocks and the water. Also, at room temperature, the deswelled cores are probably well below the T_g of bulk polystyrene.

Thermodynamically, the present system in aqueous solution is not an equilibrium system. However, the multiple morphologies, as well as the dimensions, are a result of a thermodynamic equilibrium which prevailed while the equilibrium micelles or vesicles were being formed in DMF at low water contents during water addition. The different morphologies are thus a manifestation of the thermodynamics during the aggregation process. During aggregation, the cores (styrene rich regions) would be expected to be swollen by a DMF-rich solvent mixture. As the solvent is removed from the swollen PS cores during the addition of water and the subsequent dialysis, the cores pass the glass transition at room temperature, at which point the core structures become locked. In view of the above, it seems reasonable to think that the morphologies and dimensions seen in Figure 4.1 are directly related to those of the swollen cores in the equilibrium state, although they are obviously not identical.

In the block copolymer micelles, the major contributions to the thermodynamics of aggregation are considered to originate mainly from three sources, namely, the core, the interaction between the corona and the solvent, and the core-solvent interface. [7] Among these, the contribution of the core, which is influenced by a number of factors, may be the most variable, considering the range of core dimensions and morphologies seen here. The PS chains in the spherical core are stretched in the radial direction compared with their dimensions in the unperturbed state. The degree of stretching is probably proportional to the radius of the micelle core. Therefore, from the dimensions of the various structures in Figure 4.1, it is of interest to estimate how the degree of the stretching of the core-forming PS chains (in the unswollen state) changes as the morphologies change. The stretching of the PS chains is greatest in the spherical micelles (the ratio of the core radius to the chain end-to-end distance in the unperturbed state being 1.4); the stretching decreases as the shape changes from spherical to rod-like (ratio =

1.25), and decreases still further as vesicles or lamellae are formed (ratio = 1.0). These ratios are expected to be related to a comparable stretching parameter while the micelles are formed under equilibrium conditions. It has been found experimentally, [17] and also suggested on theoretical grounds, [18] that the radius of the spherical core increases with a decrease of the corona-forming block length at a constant PS block length, implying a corresponding increase of the degree of stretching of the PS block. Because the stretching results in a decrease in the entropy of the PS chains in the micelle core, it cannot continue indefinitely as the soluble block (PAA) length decreases. At some point, the system becomes unstable. [18] This might explain qualitatively the behavior of the present system. Beyond a certain degree of stretching, the morphology changes first from spherical to rod-like, and eventually to lamellar or vesicular, presumably to reduce the thermodynamic stretching penalty.

It is of interest to study theoretically the relations between structural parameters of block copolymer micelles, [7,18,19] the transition between the different morphologies [20] and the molecular characteristics of the constituent block copolymers. The present system can serve as an experimental reference point for these studies because all of the transitions have been identified. From a practical point of view, it is anticipated that, because of the size and the degree of control which can be exercised over the organic core, the crew-cut micelles may adsorb or release organic chemicals (such as drugs) from or into aqueous solutions with a range of rates. They may thus be useful in the treatment of waste water, or serve as controlled delivery vehicles for hydrophobic drugs. In connection with the latter, the large spheres filled with inverse micelles might be most interesting. They are hydrophilic; however, depending on the composition of the long block, they might be expected to break down into their constituent reverse micelles in a hydrophobic environment, such as in lipids, thus providing a possible targeting mechanism. The intravesicular cavities might also be useful in drug delivery. Finally, the formation of vesicles and especially of the large complex micelles which have a superficial resemblance to cells, not only in appearance but also in size, may be of some interest in the life sciences, since hydrophilic regions form in a hydrophobic matrix which, in turn, is surrounded by a hydrophilic surface.

In addition to the six morphologies described above, we have also prepared a needle-like solid, which forms at the glass-air interface when a solution of the spherical micelles is dried. An optical micrograph (Figure 4.4-A) of the appearance of the crack pattern in the dried layer shows that the arrangement of these features is very regular. Soaking the cracked film in water results in a desorption of the needles, which are now highly birefringent (Figure 4.4-B). The first-order birefringence colors (yellow and blue) can be observed by using a first-order red plate, which indicates that the needles have either a strained or ordered structure, possibly similar to that encountered in crystals. An important aspect here is that the repeat unit is a large micelle ball, which is several tens of nanometers in diameter. Although, both latex particles and block copolymer micelles in solution show a tendency to order into crystal-like structures in certain ranges of temperature and concentration, [21] we are not aware any micelle or latex systems which spontaneously forms macroscopic needles on drying.

4.3. ACKNOWLEDGMENTS

We thank R. J. Barlow and M. Topors for useful discussions. We also thank The Natural Sciences and Engineering Research Council of Canada(NSERC) for continuing support of this research.

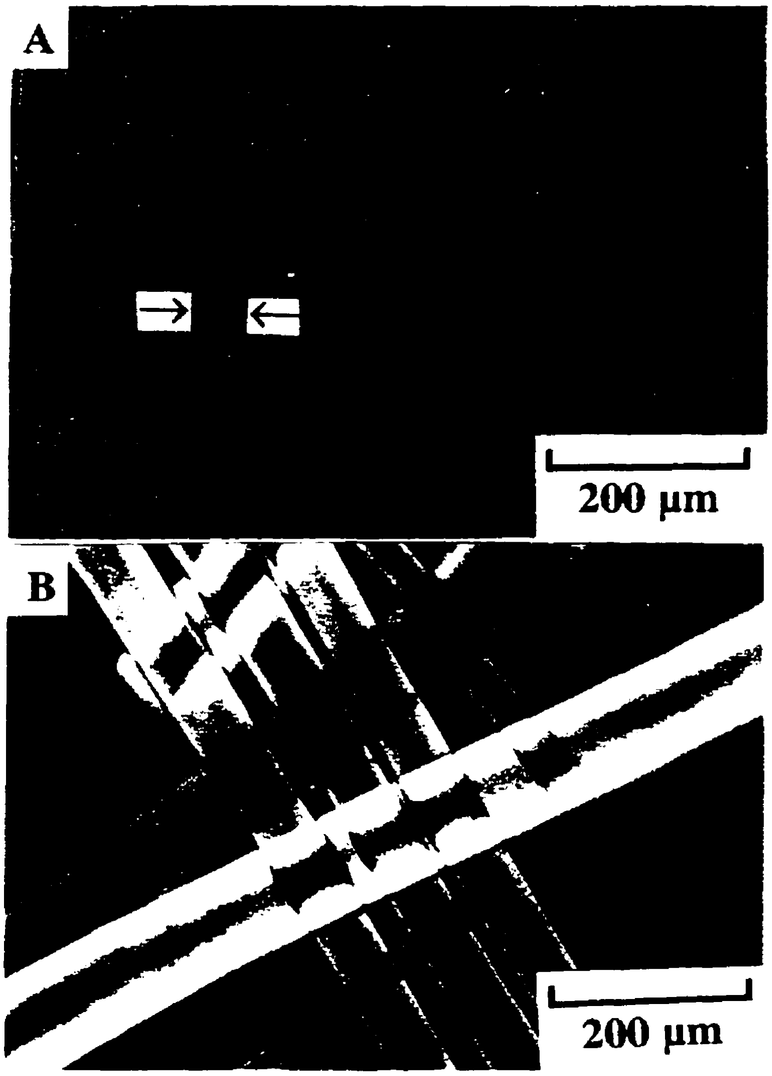

Figure 4.4. The needle-like solid formed by drying an aqueous solutions of the spherical micelles of the 180-*b*-28 diblock copolymer at 60 °C. (A) An optical micrograph shows the crack pattern which forms the needles. The arrows indicate the dimension of a single needle. (B) An optical micrograph (taken using crossed polarized light) of the needles after soaking in water.

4.4. REFERENCES AND NOTES

1. D. W. R. Gruen, *J. Phys. Chem.* **89**, 146 (1985); E. W. Kaler, A. K. Murthy, B. Rodriguez, J. A. N. Zasadzinski, *Science* **245**, 1371 (1989); S. A. Safran, P. Pincus, D. Andelman, *ibid.* **248**, 354 (1990); J. N. Israelachvili, *Intermolecular and Surface Forces*, (Academic Press, London, ed. 2, 1992).
2. T. Inoue, T. Soen, T. Hashimoto, H. Kawai, in *Block Polymers*, S. L. Aggarwal, Ed. (Plenum, New York, 1970), pp. 53-78; R. A. Brown, A. J. Masters, C. Price, X. F. Yuan, in *Comprehensive Polymer Science: Polymer Properties*, S. G. Allen, J. C. Bevington, C. Booth, C. Price, Eds. (Pergamon, Oxford, 1989), vol. 2, pp. 155-198.
3. E. L. Thomas *et al.*, *Macromolecules* **19**, 2197 (1986); H. Hasegawa, H. Tanaka, K. Yamasaki, T. Hashimoto, *ibid.* **20**, 1651 (1987); S. Forster *et al.*, *ibid.* **27**, 6922(1994).
4. D. J. Kinning, K. I. Winey, E. L. Thomas, *ibid.* **21**, 3502 (1988).
5. J. Zhu, R. B. Lennox, A. Eisenberg, *J. Phys. Chem.* **96**, 4727 (1992).
6. C. Price, in *Developments in Block Copolymers*, I. Goodman, Ed. (Applied Science, London, 1982), vol. 1, pp. 39-80; J. Selb, and Y. Gallot, *ibid.*, I. Goodman, Ed. (Applied Science, London, 1985), vol. 2, pp. 27-96.
7. Z. Tuzar, and P. Kratochvil, in *Surface and Colloid Science*, E. Matijevic, Ed. (Plenum, New York, 1993), vol. 15, pp. 1-83.
8. C. Price, *Pure Appl. Chem.* **55**, 1563 (1983); A. P. Gast, P. K. Vinson, K. A. Cogan-Farinas, *Macromolecules* **26**, 1774 (1993); M. Antonietti, S. Heinz, M. Schmidt, C. Rosenauer, *ibid.* **27**, 3276 (1994).
9. R. Hilfiker, D. Q. Wu, B. Chu, *J. Colloid Interface Sci.* **135**, 573 (1990); C. Honda, K. Sakaki, T. Nose, *Polymer* **35**, 5309 (1994).
10. X. F. Zhong, S. K. Varshney, A. Eisenberg, *Macromolecules* **25**, 7160 (1992).
11. For the observations of the size and size distribution of the block copolymer

aggregates, solution samples were deposited from solution onto copper EM grids that had been precoated with a thin film of Formvar (J.B.EM services Inc.) and then coated with carbon. Water was evaporated from the grid for 1 day at atmospheric pressure, and the grids were shadowed with a palladium/platinum alloy at a shadowing angle of 33°. Core diameters were measured directly from prints of the microscope negatives, and confirmed by measurement of the shadow length. For the observation of the internal morphology of the complex micelles, a powder sample of the complex micelles was embedded in epoxy resin (Epon), and thin sections of about 60 nm in thickness were obtained by microtoming the resin sample at room temperature. In order to increase the contrast between the PAA and the PS regions, the sections were stained with CsOH (aq), and washed with deionized water to remove excess CsOH.

12. A. Halperin, M. Tirrell, T. P. Lodge, *Adv. Polym. Sci.* **100**, 31 (1992).
13. Z. Gao, S. K. Varshney, S. Wong, A. Eisenberg, *Macromolecules* **27**, 7923 (1994).
14. A. Desjardins and A. Eisenberg, *ibid.* **24**, 5779 (1991).
15. D. Nguyen, C. Williams, A. Eisenberg, *ibid.* **27**, 5086 (1994).
16. A. E. Platt, in *Comprehensive Polymer Science: Polymer Reactions*, S. G. Allen, J. C. Bevington, G. C. Eastmond, A. Ledwith, S. Russo. P. Sigwalt, Eds. (Pergamon, Oxford, 1989), vol. 6, chap. 14.
17. L. Zhang, R. J. Barlow, A. Eisenberg, *Macromolecules* **28**, 6055 (1995) (chapter 3 of this thesis).
18. M. D. Whitmore and J. Noolandi, *Macromolecules* **18**, 657 (1985); R. Nagarajan, K. Ganesh, *J. Chem. Phys.* **90**, 5843 (1989).
19. A. Halperin, *Macromolecules* **20**, 2943 (1987); D. Ronis, *Phys. Rev. E* **49(6)**, 5438 (1994).
20. M. R. Munch and A. P. Gast, *Macromolecules* **21**, 1360 (1988); A. M. Mayes and

M. O. de la Cruz, *ibid.* **21**, 2543 (1988); A. Ajdari and L. Leibler, *ibid.* **24**, 6803 (1991); Z.-G. Wang, *ibid.* **25**, 3702 (1992).

21. M. Shibayama, T. Hashimoto, H. Kawai, *Macromolecules* **16**, 16 (1983); N. Ise, *Angew Chem. Int. Ed. Engl.* **25**, 323 (1986); P. N. Pusey and W. van Megen, *Nature* **320**, 340 (1986); G. A. McConnell, A. P. Gast, J. S. Huang, S. D. Smith, *Phys. Rev. Lett.* **71**, 2102 (1993).

Chapter 5

Multiple Morphologies and Characteristics of "Crew-Cut" Micelle-like Aggregates of Polystyrene-*b*-poly(acrylic acid) Diblock Copolymers in Aqueous Solutions

ABSTRACT

Crew-cut micelle-like aggregates of various morphologies prepared from polystyrene-*b*-poly(acrylic acid), PS-*b*-PAA, diblock copolymers under near-equilibrium conditions, were studied by transmission electron microscopy (TEM). The insoluble block (PS) contents in the copolymers ranged from 80 to 98 wt. %. In spherical micelles, the micelle cores, formed by aggregation of the PS blocks, were generally monodisperse. A comparison between star and crew-cut micelles showed that the latter are distinguished by a low density of corona chains on the core surface, and a low degree of stretching of the PS blocks in the cores. As the PAA content in block copolymer decreased, the morphology of the aggregates changed progressively from spheres to cylinders, to bilayers (both vesicles and lamellae), and eventually to compound micelles consisting of an assembly of inverted micelles surrounded by a hydrophilic surface. The compound micelles are believed to be a new morphology for block copolymers. The addition of homopolystyrene to the diblocks changed the morphologies from bilayers or cylinders to spheres. The present system provides the first instance in which all these multiple aggregate morphologies have been observed directly in block copolymers in a low molecular weight solvent with changing copolymer composition. It is believed that this is the only way so far to prepare stable nanosize glassy vesicles of block copolymers which form spontaneously, and can be isolated in water and studied directly by electron microscopy.

5.1. INTRODUCTION

It has been known for many years that when diblock copolymers are dissolved in a solvent which is selective for one of the blocks, colloidal size aggregates or micelles can form as a result of the association of the insoluble blocks.[1-3] Depending on the composition of the block copolymers, the polarity of the solvent, and the relative solubilities of the blocks in the solvent, the materials can form regular micelle-like aggregates (in aqueous media), which have a hydrophobic core and a hydrophilic corona,[4-9] or aggregates resembling reverse micelles[10-12] when the amphiphilic block copolymers are dissolved in a solvent of low polarity. Because of the range of relative block lengths of most of the block copolymer systems which have been studied to date, either as regular or as reverse micelles, the aggregates have a core which is much smaller than the corona; such assemblies are sometimes referred to as star micelles. Micelles of another kind, namely crew-cut micelles, have been receiving attention only recently.[13-15] The concept of crew-cut micelles was proposed by Halperin et al,[16] based on an earlier theoretical study of de Gennes.[17] Crew-cut micelles are characterized by a bulky core and a relatively short corona.

In block copolymer solutions, micelle-like aggregates of spherical geometry have been identified in many studies.[1-15] The structure of a spherical micelle consists of a core of radius R_{core}, formed by the aggregated insoluble blocks of the copolymers, surrounded by a spherical corona shell formed by the soluble blocks. The aggregates take on this spherical geometry in a very broad range of the compositions of the block copolymer.

Non-spherical micelles in solutions of block copolymers have been observed only rarely, and mostly indirectly.[7,14,18-26] On the basis of light scattering studies, it was reported that rod-like or cylindrical micelles existed in systems of polystyrene-*b*-poly(methyl methacrylate) in mixed solvents[18] and polystyrene-*b*-poly(4-vinylpyridine) in dilute solution,[23] depending on the block copolymer composition. Synchrotron SAXS measurements on solutions of polystyrene-*b*-polyisoprene in aniline suggested that vesicles were very probably formed as the content of the soluble polystyrene (PS) block decreased.[20] Very recently, studies of crew-cut micelles from an asymmetric block copolymer, in mixed selective solvents for the short block, also suggested the possible existence of block copolymer vesicles, although that possibility was discounted on the basis of other evidence.[14] The existence of worm-like micelles[19] and of platelet aggregates with copolymer cylinders extending from the edges[22] has been proved by direct TEM observation. Also, regions of stability of spherical and cylindrical micelles in poly(ethylene oxide)-b-poly(propylene oxide) triblocks were identified by SAXS and other indirect methods.[25,26]

The existence of various morphologies in block copolymers in bulk has been known for many years. Originally, the three most common morphologies were spherical, cylindrical and planar/lamellar, depending on the block copolymer composition.[27,28] Later, a new one, the ordered bi-continuous double diamond or gyroid morphology, was added.[29-32] Multiple morphologies have also been observed in block copolymer/homopolymer blends in bulk.[33,34] Depending on the compositions of the block copolymers and the molecular weight of the homopolymer, the aggregates of copolymers can be spherical, cylindrical, lamellar and vesicular. Three morphologies (starfish, rod, and planar) adopted by two dimensional or surface aggregates were observed in polystyrene/decylated poly(vinylpyridinium) block polyelectrolytes within well-defined composition ranges.[35,36] Very recently, three different morphologies, i.e. sphere, rod, and vesicle, have been observed in a polystyrene amphiphilic dendrimer system.[37] Furthermore, it is well-known that small molecule amphiphile surfactant systems form self-assembled aggregates of multiple morphologies.[38-41]

To our knowledge, multiple morphologies of block copolymer aggregates, i.e. spheres, rods and vesicles or lamellae, have not been observed for the same block copolymer family in solvents of low molecular weight. In a very recent preliminary report,[42] we described the preparation and observation of various morphologies of aggregates made from the diblock copolymers of polystyrene-*b*-poly(acrylic acid), PS-*b*-PAA. Aggregates of several different morphologies were prepared in a low molecular weight solvent system from the block copolymers of the same type differing only in the relative block lengths. Four of these morphologies are spheres, rods, lamellae and vesicles in aqueous solution. The fifth is new and consists of large spheres in aqueous solution which have hydrophilic surfaces of PAA blocks, and are filled with reverse micelle-like aggregates of the copolymers. Regular reverse micelles would, of course, exist in solvents of low polarity. The PS-*b*-PAA system in aqueous solution is believed to provide the first instance in which the existence of all of these aggregates formed from the same block copolymer family in low molecular weight solvents has been proven by direct electron microscope observation. In that report, the preparation of a needle-like solid, which was obtained by drying an aqueous solution of the spherical crew-cut micelles, and which is highly birefringent after soaking in water, was also described.

In this chapter, we present the detailed experimental results concerning the general preparation of the "crew-cut" aggregates and the formation of the various morphologies of the diblock copolymers of polystyrene-*b*-poly(acrylic acid) in low molecular weight solvents. In particular, we report on a range of characteristics of the aggregates and their dependence on the compositions of the block copolymers, as well as on the effect of added homopolystyrene on the morphologies of the aggregates. Finally, a possible mechanism underlying the formation of the different morphologies is discussed.

5.2. EXPERIMENTAL SECTION

5.2.1. Synthesis of the Block Copolymers.

The polystyrene-*b*-poly(*tert*-butyl-acrylate) diblock copolymers were synthesized by sequential anionic polymerization of styrene monomer followed by *tert*-butyl-acrylate (*t*-BuA) monomer. *sec*-Butyllithium was used as an initiator. Styrene, α-methylstyrene, and *t*-BuA monomers were pre-dried overnight using calcium hydride (CaH_2), distilled under vacuum, and stored under nitrogen at -20 °C. Before polymerization, styrene was treated with fluorenyllithium for 15 min and distilled under vacuum (mechanical pump). *t*-BuA was diluted with toluene and then treated with 10% triethylaluminum solution in hexane until a persistent greenish-yellow color was observed; then, it was distilled under vacuum prior to polymerization. The polymerization was carried out in tetrahydrofuran (THF) at -78°C under nitrogen gas. α-Methylstyrene was used as the end-capping agent for the polystyryllithium anion. A 5 to 10 fold excess of LiCl relative to the number of the living anionic chains was added to serve as a stabilizer for the poly(*tert*-butyl-acrylate) living end. After the polystyrene block was formed, an aliquot of the reaction medium was withdrawn to obtain a sample of the homopolystyrene for characterization. After the PS was polymerized and end-capped with α-Methylstyrene, a series of diblocks with that polystyrene block length was obtained by withdrawing aliquots of the reaction mixtures after each *t*-BuA monomer addition. A more detailed description of the procedures can be found elsewhere.[43]

Gel Permeation Chromatography (GPC) was used to measure the degree of polymerization and the polydispersity of the polymers. All the homopolystyrenes and their diblock copolymers in the form of *t*-butyl-acrylate gave one narrow GPC peak. The degree of polymerization of the poly(*t*-butyl-acrylate) block was measured by FTIR.[43]

5.2.2. Hydrolysis.

The poly(*t*-butyl-acrylate) block in the block copolymers was hydrolyzed to its acid form, poly(acrylic acid), by using *p*-toluene sulfonic acid as the catalyst (10 mol% relative to the *t*-butyl acrylate content). For this procedure, the copolymers were dissolved in toluene, and the solutions were heated at reflux (110 °C) overnight. Finally, after cooling, the block copolymers were precipitated into methanol, washed with methanol several times, and dried overnight under vacuum at 60 °C. FTIR studies[43] showed that the hydrolysis was essentially complete. The polymers are identified by the notation used previously, i.e. PS(180) is homopolystyrene with 180 repeat units (number average). The diblock copolymer samples are denoted as x-*b*-y, where x and y represent the degrees of polymerization of the PS block and the PAA block, respectively. For example, 200-*b*-4 represents a diblock copolymer containing 200 styrene repeat units and 4 acrylic acid repeat units (number average). The homopolystyrenes and the block copolymers used in this study, along with their molecular characteristics, are given in Table 5.1.

Table 5.1. Molecular characteristics of homopolystyrene and of polystyrene-*b*-poly(acrylic acid) diblock copolymers.

PS-*b*-PAA[a]	Mw/Mn[b]	PS-*b*-PAA[a]	Mw/Mn[b]
170-*b*-33	1.08	500-*b*-58	1.04
180-*b*-15	1.05	630-*b*-18	1.05
180-*b*-28	1.05	705-*b*-22	1.05
200-*b*-4	1.05	740-*b*-55	1.09
200-*b*-8	1.05	740-*b*-180	1.09
200-*b*-15	1.05	1140-*b*-165	1.06
200-*b*-21	1.05	1400-*b*-120	1.08
390-*b*-41	1.06	1400-*b*-306	1.10
390-*b*-79	1.07	PS(38)	1.08
410-*b*-16	1.06	PS(180)	1.05
410-*b*-46	1.06	PS(500)	1.04

[a]. Degree of polymerization of the polystyrene from SEC measurements. Poly(acrylic acid) chain length determined by FTIR.[43]

[b]. Polydispersity index, measured by SEC, of the whole diblock copolymer in the form of PS-*b*-P-*t*-BuA, and of the homopolystyrene.

5.2.3. Preparation of the Aqueous Solutions.

Generally, star type micelles can be prepared directly by dissolving a highly asymmetric block copolymer in a solvent selective for the long block. During the dissolution of the block copolymers, the insoluble (short) blocks form the core while the long blocks form the corona of the micelles. However, because the block copolymers in the present study have a very large weight-fraction of polystyrene, it is impossible to prepare stable solutions by direct dissolution of the block copolymer molecules in water. Therefore, in order to prepare stable aqueous solutions, the diblock copolymers were first dissolved in N,N-dimethylformamide (DMF), which is a common solvent for both polystyrene and poly(acrylic acid) blocks. Subsequently, deionized water was added to the polymer/DMF solutions (*ca.* 10 ml) at a rate of 1 drop every 5 ~ 10 seconds with vigorous stirring. As the addition of water progressed, the quality of the solvent for the PS block decreased gradually. The aggregations of the PS blocks of the copolymers, as indicated by the appearance of turbidity in the solution, typically occurred when the water content reached 3~6 wt.%, depending on the composition of the block copolymers. The addition of water was continued until 25 wt.% of water had been added, i.e. well after the aggregations occurred. The resulting colloidal solutions were placed in dialysis bags and dialyzed against distilled water to remove the DMF. In the present studies, the initial polymer concentration in DMF (before the addition of water) was 2 wt.% unless specified otherwise.

5.2.4. Transmission Electron Microscopy.

Transmission electron microscopy (TEM) was performed on a Phillips EM410 microscope operating at an acceleration voltage of 80 kV. For the observations of the size and distribution of the copolymer aggregates, samples were deposited from aqueous solutions (about 0.5 mg/ml) onto copper EM grids, which had been pre-coated with a thin film of Formvar (J.B.EM services Inc) and then coated with carbon. Water was allowed to evaporate from the grids at atmospheric pressure and room temperature. Finally, the grids were shadowed with palladium/platinum alloy at a shadowing angle of about 33°. The sizes of the copolymer aggregates were measured directly from prints of the microscope negatives. For the observation of the internal morphology of the compound micelles, a powder sample of the compound micelles was embedded in epoxy resin (Epon), and sections of about 60 nm thickness were obtained by microtoming the resin sample at room temperature. In order to increase the contrast between the PAA and the PS regions, the sections were stained with CsOH(aq), and washed with deionized water to remove excess CsOH.

5.3. RESULTS AND DISCUSSION

The Results and Discussion section consists of six parts. In the first, TEM pictures are presented which illustrate the multiple morphologies of the aggregates made from the block copolymers of different compositions. In parts two and three, two characteristics of the crew-cut aggregates are addressed, i.e. the degree of stretching of the PS block in the core region and the surface area per corona chain at the interface of the core/corona shell. These two aspects are thought to be very important in controlling the formation of aggregates. Part four deals with the effect of added homopolystyrene on the morphologies; this is followed by a comparison of multiple morphologies in the present system with those in other systems. Finally, in part six, some additional considerations of the formation of the aggregates are presented.

When block copolymers are dissolved in a solvent selective for one of the blocks, thermodynamic equilibrium may not be operative between the unimers and the aggregates, especially if the glass transition temperature, T_g, of the core forming blocks is above room temperature. Under those circumstances, the structures should be called micelle-like aggregates (*mlas*). This point is relevant to the present discussion. In the course of preparation of the aggregates in the present system, the copolymers are unimolecular in the DMF before the addition of water. While deionized water is added to the polymer/DMF solution, the solvent becomes progressively worse for the PS block. At a certain water content, the PS blocks start to associate. It appears that there is a true equilibrium between the aggregates and the copolymer unimers at that stage of the aggregation. However, after the formation of the polymer aggregates and subsequent isolation into water, the structures of the aggregates become locked because the PS chains are below their T_g. Thus, they are no longer in thermodynamic equilibrium. Because several of the morphologies described here (with the exception of the vesicles) resemble micelles, and much of the block copolymer literature refers to the non-equilibrium block copolymer *mlas* as micelles, this convention is adopted in the present work also.

5.3.1. Various Morphologies of the Crew-cut Aggregates.

5.3.1.1. Spherical Micelles. The spherical morphology for crew-cut micelles has been described recently for polystyrene-*b*-poly(4-vinylpyridinium methyl iodide) in aqueous solutions[13] and for poly(α-methystyrene)-*b*-poly(vinyl-p-phenethyl alcohol) (PαMS-*b*-PVPA) in a mixed solvent consisting of *m*-chlorobenzyl chloride and *m*-chlorobenzyl alcohol.[14] In present systems, the aqueous solutions of the micelles show a pale blue color because of the sizes of the micelles (25 ~ 45 nm, see below). The aggregates are readily observable by TEM because of the high Tg of polystyrene, and their sizes are measurable directly from the prints. Most of the block copolymers studied to date yield spherical micelle-like aggregates. Very recently, we reported that the core radii of these spherical micelles have a narrow size distribution.[15] The dimensions of the core radii depend on the chain lengths of both the insoluble (core-forming PS) block and the soluble (corona-forming PAA) block, and scale in the manner of a power law:[15]

$$R_{core} \propto N_{PS}^{0.4} N_{PAA}^{-0.15} \qquad (5.1)$$

where R_{core} is the core radius, and N_{PS} and N_{PAA} are the degrees of polymerization of the PS and the PAA blocks, respectively.

Figure 5.1 shows a micrograph of the spherical micelles of a typical sample of the block copolymer, 500-*b*-58, along with a graph of the size distribution which yields an average diameter of 30.3 nm with a standard deviation of 2.4 nm. The dotted line represents a Gaussian fit with the same average diameter and standard deviation. Because the corona-forming block content in the copolymers is low, and because the contrast in the electron density between the copolymer blocks is low, it is not possible to distinguish the micelle corona layer from the core region. However, in view of the composition, it is clear that the corona layer on the core surface must be very thin, and its thickness can be calculated from the composition and the density. In this case, it is 0.3 nm. The observed particle size thus represents the core dimension to a very good approximation. From the size distribution of the micelles, one can readily obtain the average and the standard deviation of the core sizes, the polydispersity index of the micelle molecular weight, etc. The values of these parameters are summarized in Table 5.2.

5.3.1.2. Rod-like Micelles. As the block length ratio of PAA to PS decreases, it is found that, below some value of the ratio, the block copolymers associate to form rod-like micelles. Figure 5.2 shows one example for 180-*b*-15. Most of the micelles appear to be bent rather than straight cylinders. Also, the micrograph suggests a relatively narrow size distribution of the cylindrical micelle diameters, but a widely variable length. Hemispherical caps form at the cylinder ends. The cylindrical micelles are usually found to coexist with aggregates of other morphologies. Preliminary results suggest that the cylindrical micelles are formed only in a relatively narrow range of copolymer compositions. Some characteristics of the cylindrical micelles are listed in Table 5.3. In the calculations of the surface area per corona chain, the number-average diameters were used, with the lengths of the cylindrical micelles assumed to be infinite.

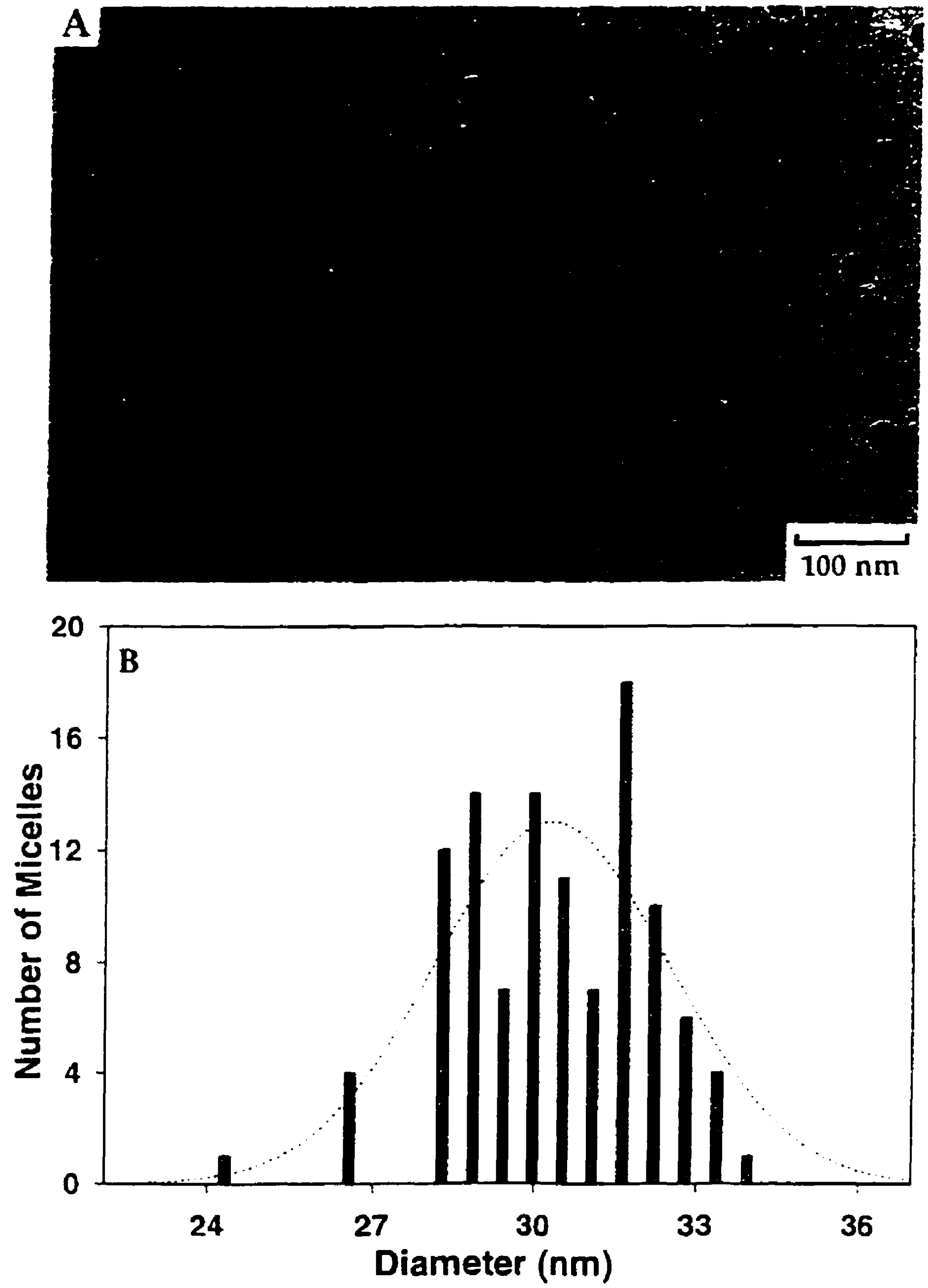

Figure 5.1. (A): TEM picture of the spherical micelles from the block copolymer 500-*b*-50; (B): The size distribution of the spherical micelles in (A); the dotted line represents a Gaussian fit (average diameter: 30.3 nm and standard deviation: 2.4 nm).

Table 5.2. Some characteristics of the spherical micelles.

PS-*b*-PAA	PAA (mol)%	D[a] (nm)	*s.d.*[b] (± nm)	A_c[c] (nm^2)	S_c[d]	P. I.[e] (Mw/Mn)
170-*b*-33	16.3	25	1.4	7	1.47	1.02
180-*b*-28	13.5	24	2.2	8	1.38	1.07
200-*b*-21	9.5	26	2.0	8	1.41	1.04
390-*b*-41	12.4	32	3.2	12	1.25	1.09
390-*b*-79	16.8	28	2.4	14	1.13	1.05
410-*b*-46	10.1	30	2.0	14	1.14	1.04
500-*b*-58	10.4	30	2.4	17	1.01	1.04
630-*b*-18	2.8	43	3.8	15	1.32	1.07
705-*b*-22	3.0	41	3.6	17	1.20	1.06
740-*b*-55	6.9	40	2.6	19	1.13	1.03
740-*b*-180	19.6	32	2.4	24	0.90	1.05
1140-*b*-165	12.6	40	2.2	30	0.91	1.03
1400-*b*-120	7.9	42	5.8	34	0.86	1.18
1400-*b*-306	17.9	35	3.4	43	0.72	1.08

a. Number average diameter of the cores from TEM.

b. Standard deviation of the distribution of the core diameters.

c. Surface area per corona chain at the core/corona interface.

d. Degree of stretching of the PS blocks in the core, taken as a ratio of the core radius to the end-to-end distance of the PS block in the unperturbed state, $(6.76\ N_{PS})^{0.5}l$, where N_{PS} is the degree of polymerization of PS chain, and l is the length of styrene monomer.

e. Polydispersity index of the micelle molecular weight.

Figure 5.2. TEM picture of the rod-like micelles from the block copolymer 180-*b*-15.

Table 5.3. Some characteristics of the rod-like micelles and the bilayer Aggregates of the block copolymers.

PS-*b*-PAA	PAA (mol)%	Morphology	Cylinder diameter or wall thickness[a] (nm)	A_c [b] (nm^2)	S_c [c]
180-*b*-14	7.2	rods	23	5.2	1.32
200-*b*-15	7.0	rods	23	5.8	1.26
410-*b*-25 [d]	5.9	rods	36	7.5	1.39
200-*b*-8	3.8	vesicles	18	4.2	0.99
410-*b*-20	4.7	vesicles	22	6.3	0.83
410-*b*-16	3.8	vesicles	22	6.6	0.84
410-*b*-16	3.8	lamellae	24	5.7	0.91

a. Average diameter of the cylindrical micelles or wall thickness of the vesicles.

b. Surface area per corona chain at the core/corona interface.

c. Degree of stretching of the PS blocks; for the cylinder, it is defined as a ratio of the radius to the end-to-end distance of the PS block in the unperturbed state; for the vesicle, half of the wall thickness is used.

d. The initial copolymer concentration in DMF is 2.8 wt.%.

5.3.1.3. Vesicles and Lamellar Micelles. As the ratio of PAA to PS block lengths drops further, vesicular aggregates can form from the block copolymers. Figure 5.3 shows the morphology of the vesicular aggregates made by the block copolymer 410-*b*-20. The vesicular nature is evidenced from a higher transmission in the center of the aggregates than around their periphery, coupled with height measurements (from shadowing) which show the aggregates to be spherical. The overall sizes of vesicles are found to be sensitive to the initial copolymer concentration in DMF. For example, the vesicles, formed from 2 wt.% 410-b-20 copolymer/DMF solution, are quite uniform (Figure 5.3). For vesicles formed from 3 wt.% solution of this copolymer, the sizes are very polydisperse (with the outer diameters ranging from 50 to 500 nm). However, the PS wall thicknesses of the vesicles are very uniform and independent of the overall size of the vesicles. Some structural properties of the vesicles are listed in Table 5.3. The wall thickness of the vesicles increases with the PS block length.

In examining micrographs of the aggregates in the range of compositions which give vesicles, one also sees lamellar micelles on occasion. The lamellar nature is evidenced by the uniformity of the light intensity over the entire feature. From the measurement of the length of the shadowed region, the thickness of the lamella is found to be the same as the wall thickness of the vesicles in same picture. This is not surprising because both vesicles and lamellae are bilayer aggregates.

Although it has been known for a long time that some small molecule surfactants form vesicles, the formation of block copolymer vesicles was suggested only rarely and on the basis of indirect evidence. In one case, it was reported[20] that when poly(styrene-*b*-isoprene), PS-*b*-PI, block copolymers were dissolved in aniline, the PI blocks associated to form aggregates. In an analysis of the small angle X-ray scattering experimental results using different models, it was found that the vesicle model described the experimental system much better than the spherical micelle model for the block copolymer with relatively short PS block length. Very recently, static and dynamic light scattering has

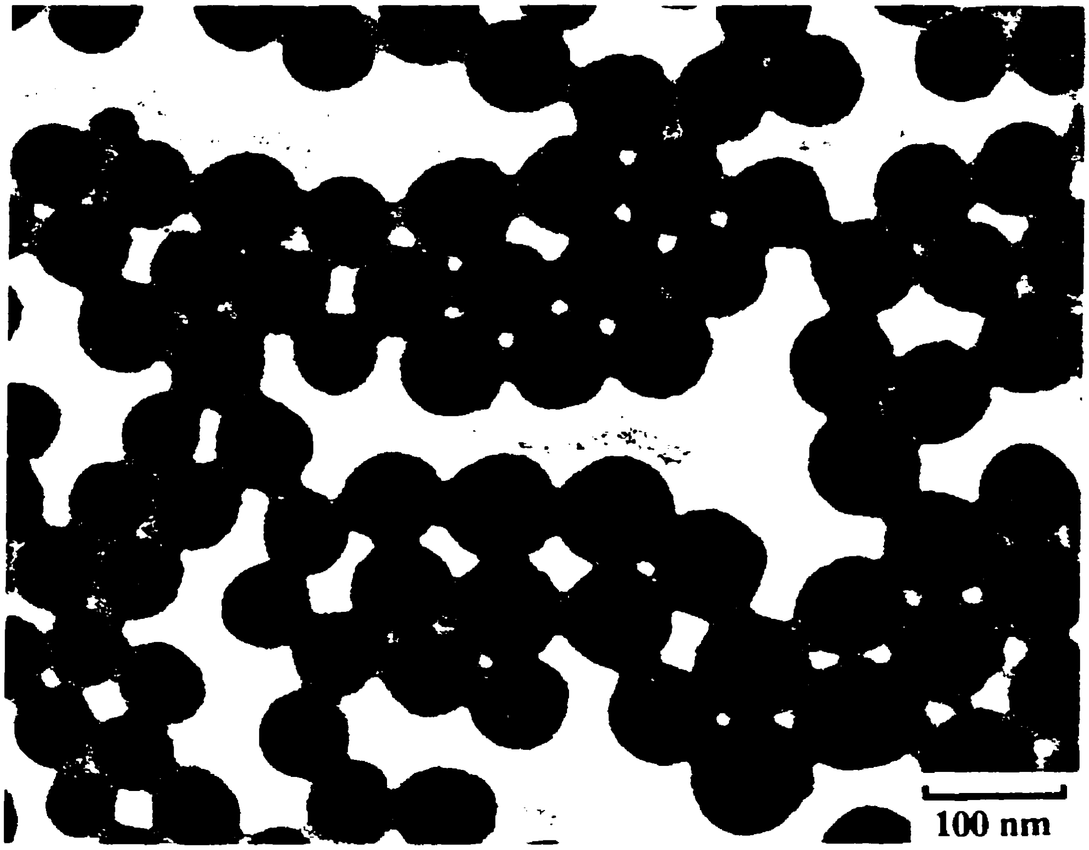

Figure 5.3. TEM picture of the vesicles from the block copolymer 410-*b*-20.

been used to study the system of poly(α-methystyrene)-*b*-poly(vinyl-p-phenethyl alcohol) (PαMS-*b*-PVPA) in mixed selective solvents[14]. The block copolymer had a composition of [PαMS]/[PVPA] = 90/10 in molar mass. When the solvent is selectively good for the short block (PVPA), the copolymer formed crew-cut micellar aggregates. Because the measured radius of gyration of the core part was much larger than expected, several possible structures of the aggregates were suggested, including vesicles. However, the authors pointed out that the vesicle structure, while possible, was most unlikely for a number of reasons. By contrast to the above reports, the copolymer vesicles in the present study are observed directly and clearly by TEM. Thus, it is believed that this is the first direct observation of the existence of glassy block copolymer vesicles prepared in solution.

5.3.1.4. Compound Micelles. When the PAA block length becomes very short, it is found that the solutions are extremely turbid. Figure 5.4 shows the morphology of the micelle-like aggregates (*mlas*) made from the block copolymer with the shortest PAA block length (200-*b*-4). These *mlas* are solid, highly polydisperse spheres. Because of the very large size of some of these micelles, they are subject to settling due to gravity.

In order to study the internal morphology of these compound micelles, thin sections of about 60 nm were prepared by microtomy at room temperature of specimens embedded in epoxy resin. To increase the contrast between the PAA and the PS regions, the sections were stained with CsOH(aq), and washed with deionized water to remove excess CsOH. A micrograph of a section of the spheres along with a schematic picture (Figure 5.5) shows that the spheres have a structure similar to that of the block copolymers cast from a solution in a good solvent for the PS blocks, in which the blocks form reverse *mlas* with the polar cores on the inside and the styrene in the corona. The difference in the degrees of darkness of some of the ionic aggregates (reverse micelle cores) is probably related to difference in the degree of neutralization as consequence of differences in the distances of the aggregates from the surface of the cut. It is likely that the carboxylate groups near the surface (close to the neutralization solution) may be more completely neutralized than those in the interior. The outer surface of these large compound micelles is hydrophilic because of the presence of the short PAA chains. This gives the micelles considerable stability, and allows even those which have settled to the bottom of the container to be resuspended. The micelles do not coalesce at room temperature. We believe that this micellar morphology has not been reported before.

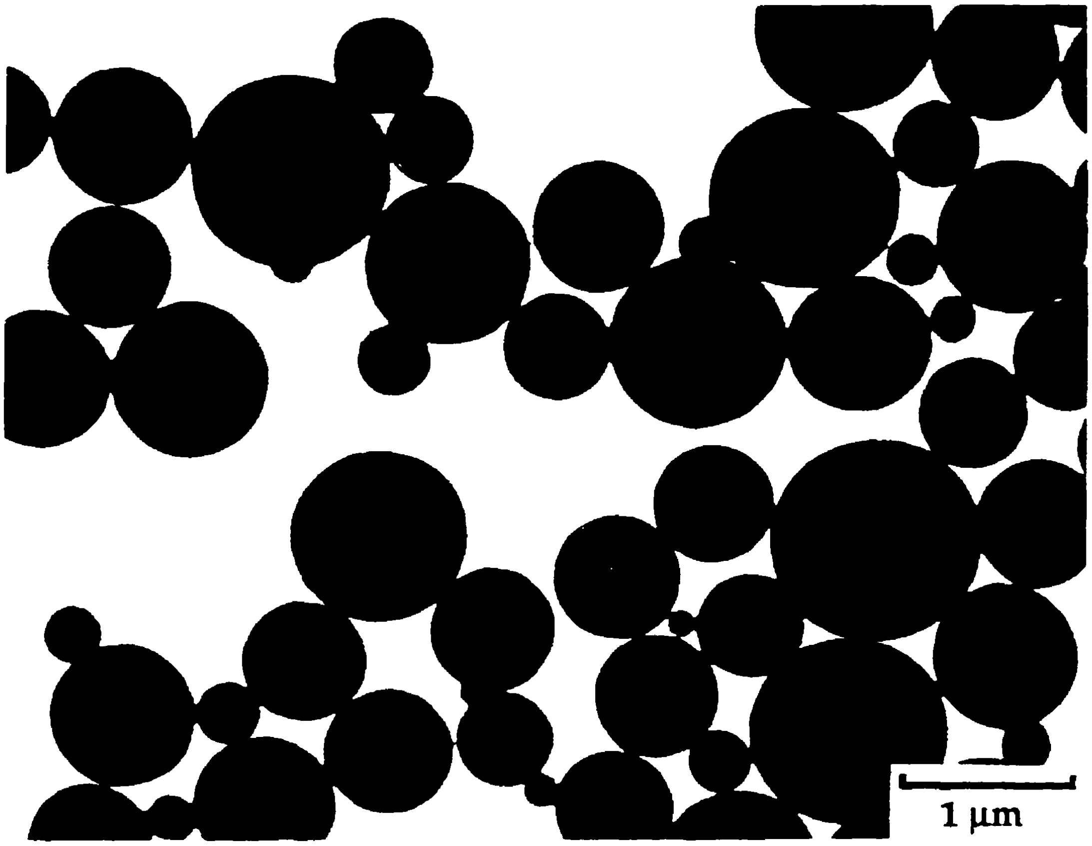

Figure 5.4. TEM picture of the compound micelles from the block copolymer 200-*b*-4.

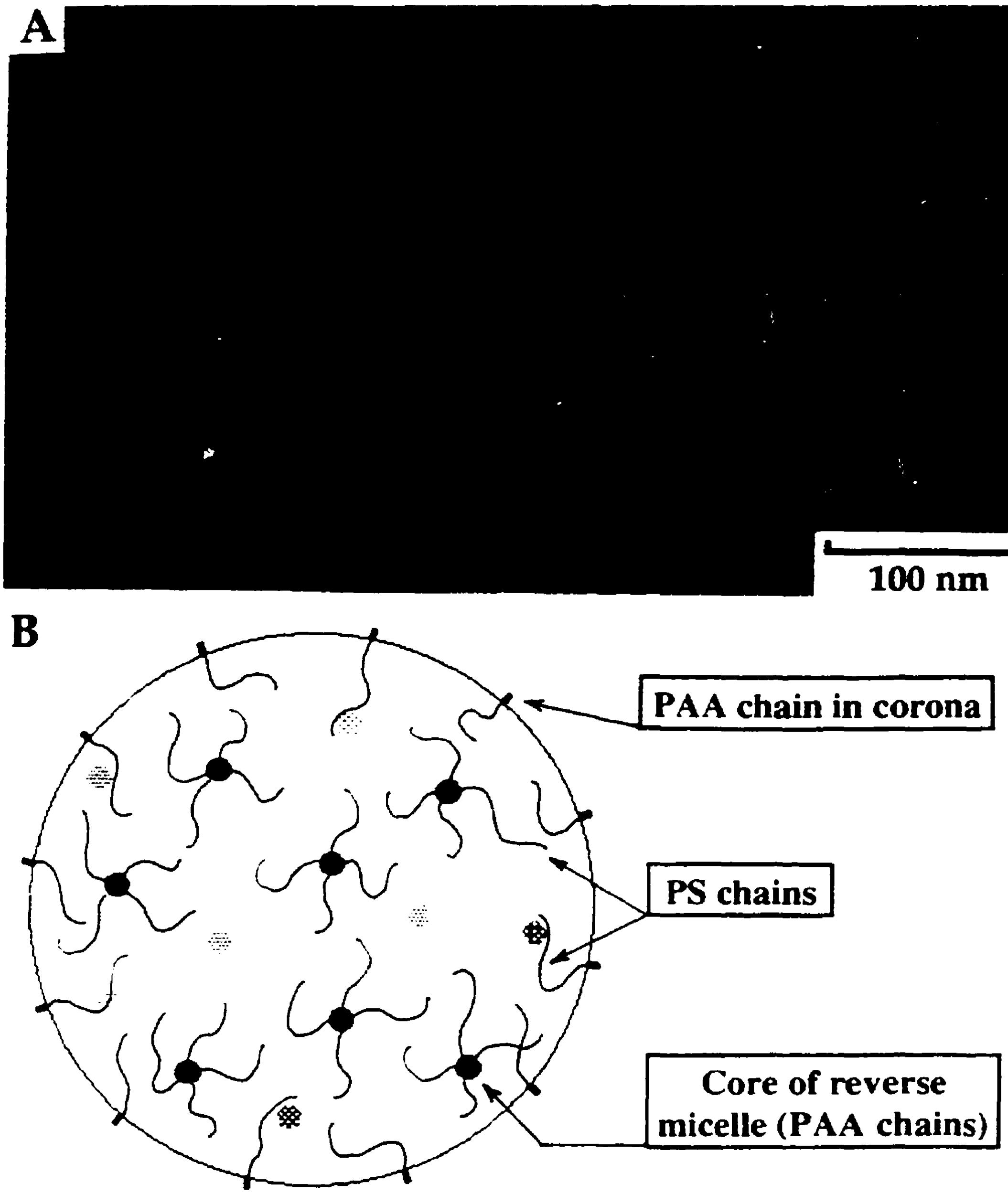

Figure 5.5. (A): The internal morphology of the large compound micelles in Figure 5.4. The elongation of the particle shape in one direction is probably caused by the strong shear forces during microtoming; (B): A schematic structure of the large compound micelle filled with bulk reverse micelles. The different degree of darkness of the PAA cores of the reverse micelles represents differences in the degrees of neutralization for different distances from the neutralizing solution.

5.3.2. PS Chain Extension in the Aggregates.

5.3.2.1. Spherical micelles. For a compact micelle core, some of the core-forming blocks must span the distance from the core/corona interface to the core center. Therefore, it is of interest to see to what extent the PS chains in the spherical core are stretched in the radial direction compared with their dimensions in the unperturbed state. Because stretching results in a decrease of the entropy of the PS chains, this feature is believed to be important during the formation of the aggregates since it most likely influences the final morphologies.

Table 5.2 gives the values of the degree of stretching, which is expressed as the ratio of the micelle core radius to the PS chain end-to-end distance in the unperturbed state. Clearly, not all chains are stretched to the same extent, but some must be. Because the end-to-end distance of a polymer chain in the unperturbed state is proportional to square root of the degree of polymerization, $N_{PS}^{1/2}$, the degree of stretching, S_c, can be given by

$$S_c \propto R_{core} N_{PS}^{-0.5} \tag{5.2}$$

It is easy to obtain the dependence of S_c on the composition of the copolymers by inserting equation 5.1 into 5.2 as

$$S_c \propto N_{PS}^{-0.1} N_{PAA}^{-0.15} \tag{5.3}$$

It is clear that the degree of stretching decreases as the PS and/or the PAA block lengths increase. Equation 5.3 has been used to fit the data of S_c in Table 5.2. A linear relation is, indeed, found between S_c and $N_{PS}^{-0.1}N_{PAA}^{-0.15}$, with a linear correlation coefficient of 0.96.

The above considerations apply to micelles in aqueous solution. However, it has to be pointed out that, at the moment of the formation of the micelles, the cores are expected to be swollen by the DMF rich solvent mixture. The degrees of stretching of the

PS blocks at the onset of micellization are therefore higher than the corresponding values given in Table 5.2. Since the micelle cores are totally deswelled in aqueous solutions, the degrees of stretching of the PS blocks are decreased. These arguments may explain why some values of the degree of stretching in Table 5.2 are less than unity.

The degree of stretching is proportional to the dimension of the core region, which, in turn, is determined by the aggregation number (N_{agg}). It has been found that N_{agg} depends on the solvent quality for the blocks of the copolymers.[23] Thus, it is expected that the degree of the stretching should be related to the solvent quality during micellization. At this point, it is useful to introduce the concept of the critical water content (*cwc*), i.e. the water content at which micelles start to form. At the *cwc*, PS blocks of the copolymers begin to associate reversibly to form micelles. A study of the phase behavior of polymer/DMF/water systems has shown that the critical water content decreases with increasing PS block length.[44] This means that the copolymers with longer PS blocks form aggregates at a lower water content than those with shorter blocks. From a thermodynamic point of view, the micelles form at values of the χ parameter which decrease with increasing PS block length, since water is non-solvent for the PS blocks.

When the value of χ parameter is relatively low, the core, at the onset of micellization, would be expected to be swollen to a higher degree, which implies a lower volume fraction of the PS blocks in the swollen core region. Given the PS block volume fraction in the swollen core region, f_{PS}, and the radius of the swollen core, R'_{core}, the radius of the unswelled core in the aqueous solutions, R_{core}, can be given as

$$R_{core} = f_{PS}{}^{1/3} . R'_{core} \qquad (5.4)$$

Equation 5.4 shows that a lower volume fraction of the PS blocks will give a smaller core size after the core becomes deswelled in aqueous solution. For the copolymer with shorter PS chain length, the micellization occurs at a higher water content. The core is expected to be less swollen compared to that of the copolymers with longer PS chain lengths. A higher polymer fraction in the swollen core will give a larger compact micelle core after the micelles are isolated into aqueous solutions. This may explain, in part, why the degree of stretching of the PS block decreases with increasing PS block length.

5.3.2.2 Aggregates with Other morphologies. While the degree of PS chain stretching in the spherical micelle cores is dependent on the composition of the copolymers, it is found that the degree of stretching decreases as the morphology changes from sphere to cylinder, and to vesicle. For example, the block copolymers 200-*b*-21, 200-*b*-15 and 200-*b*-8 have the same PS block, and yield, respectively, spherical micelles, cylindrical micelles and vesicles. The degrees of stretching of PS chains are 1.41, 1.26 and 0.99. If the last two copolymers were to form spherical micelles, the stretching would be expected to increase as PAA block length decreases. According to equation 5.3, the values of S_c would be 1.47 and 1.62, respectively (rather than 1.26 and 0.99). Thus, the decrease of the degree of stretching accompanying the morphological transitions must be related to the geometric shapes of the aggregates.

The discussion of the effect of aggregate geometry on stretching can start from a consideration of the balance between two relevant contributions to the free energy of micellization, i.e. the surface tension between the core and the solvent, and the stretching force of the PS blocks in the core. From a thermodynamic point of view, an increase of the aggregation number is favored because it decreases the interface area between the solvent and the aggregating blocks. For the case of spherical micelles, the core radius R_{core} has to increase in order to increase the aggregation number. As a result, the degree of stretching of the PS chains has to increase correspondingly, which is thermodynamically unfavorable. For the cylinder, however, the additional degree of freedom along the axis allows many chains to be incorporated into the structure without significant changes in their conformation. The same applies to vesicles and lamallar micelles. Another factor which affects the degree of the PS block stretching may be the interaction between the corona chains, i.e. the repulsion between the corona chains on the surface of the core. This will be discussed in section 5.3.3.2.

5.3.3. Area Per Corona Chain at the Core/corona Interface.

It has been suggested that the area per corona chain on the core surface is an important factor among those controlling the aggregation number and the structure of the micelles.[9,23] Obviously, a small surface area per corona chain means a lower interfacial energy between the core and the solvent, but a stronger steric repulsion among the corona chains. Thus, it is useful to know the relation between the density of the corona chains on the surface of the core, the polymer composition, and the dimension of the PS core region.

5.3.3.1. Spherical Micelles. For spherical micelles in the present system, the well defined micelle core sizes determined by TEM allow the calculation of the average surface area per corona chain, A_c. Assuming that the micelle core is a compact sphere and that the density of the polystyrene blocks in the core is homogeneous, A_c is given by

$$A_c = 4\pi R_{core}^2/N_{agg} \tag{5.5}$$

N_{agg}, in turn, can be calculated as

$$N_{agg} = (4/3)\pi R_{core}^3/V_s N_{PS} \tag{5.6}$$

where V_s is the volume per polystyrene repeat unit (0.167 nm^3). A combination of equations 5.5 and 5.6 yields the relationship between A_c and the core radius as

$$A_c = 3V_s N_{PS}/R_{core} \tag{5.7}$$

The calculated values of A_c are given in Table 5.2. For the present system, because $R_{core} \propto N_{PS}^{0.4} N_{PAA}^{-0.15}$, it can be shown that

$$A_c \propto N_{PS}^{0.6} N_{PAA}^{0.15} \tag{5.8}$$

One can see that A_c increases with PS block length, and that for a constant PS block length, the area also increases as PAA block length increases, although not as strongly. Figure 5.6 shows a plot of the area per corona chain against the compositions of the copolymers according to equation 5.8. The linear relationship is clear; the correlation coefficient is 0.98.

For copolymers with a PS block of a constant length, equation 5.7 implies that the larger the micelle core, the smaller the surface area per corona chain. Obviously, a small A_c can decrease the total surface energy of the micelle core. However, this will be opposed by an increase of the deformation energy of the PS blocks in the core and the repulsive energy between the corona chains. Thus, the final value of A_c will be determined by the force balance among these factors. In the following sections, the effects of the corona-forming and core-forming blocks on A_c will be discussed.

5.3.3.1.1. Effect of the Core-forming Block on A_c. In the micelle system of polystyrene-*b*-poly(methacrylic acid) block copolymers in a mixed solvent of dioxane and water, it was found that the values of the surface area per corona chain fall in a narrow range, which was ascribed to the possible existence of an approximately constant optimum value of that parameter.[9] Furthermore, it was suggested that in micelle formation, the interfacial tension between the core and the solvent and the osmotic force acting on the micelle-forming chains balance in a way that maintains a constant interface area per chain.[23] This is clearly not observed in the present crew-cut micelle system. Equation 5.8 shows how the surface area per corona chain is dependent on the PS chain length in this case. The dependence of A_c on the core-forming block can vary from system to system. However, whatever the dependence of A_c on the insoluble block length, equation 5.7 must hold. Three cases can be distinguished by considering different degrees of stretching of the PS chains in the core.

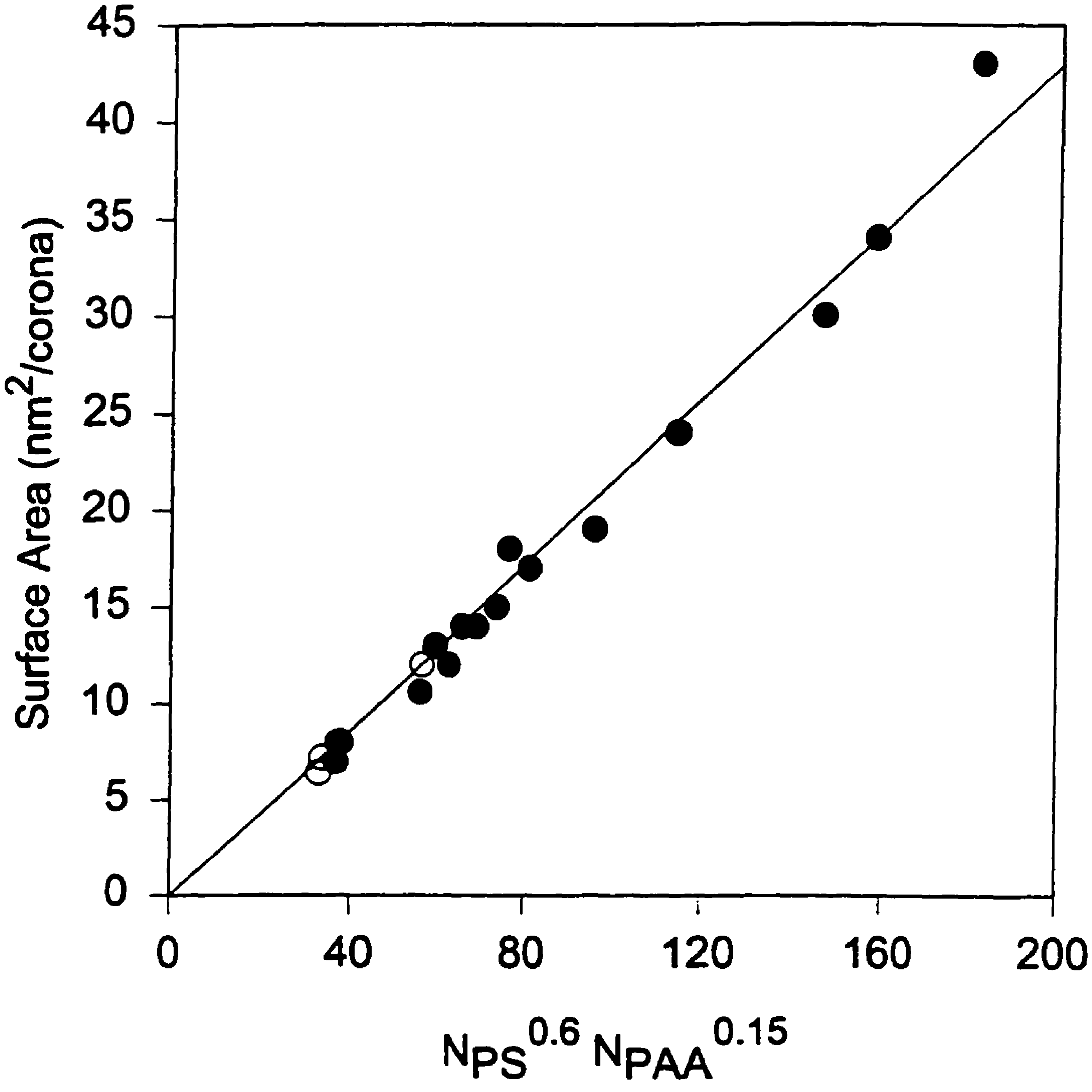

Figure 5.6. A plot of the surface area per corona chain at the interface of the core/corona shell versus $N_{PS}^{0.6}\ N_{PAA}^{0.15}$, where N_{PS} and N_{PAA} are the degrees of polymerization of the PS and the PAA blocks, respectively. Open circles represent data from the spherical micelles with added homopolystyrene (*cf.* section 5.3.4.3.)

First, when the core forming chain is fully extended, equation 5.7 predicts that the value of A_c will become independent of the length of core forming chain. An example may be the spherical micelles of small molecule surfactants. In those systems, the surface area per head group is mainly determined by the balance between the surface tension of the micelle core and the repulsion between head groups. Because of the very strong surface tension of the core, the radius of the micelle core is almost equal to the length of hydrophobic chain in the fully extended state, which means that

$$R_{core} \propto N_c \tag{5.9}$$

where N_c is the number of carbon atoms in the hydrophobic chain. In practice, it has been shown that the surface area per head-group depends mainly on the nature of head-group, and is almost independent on the hydrophobic chain length. Second, when the degree of stretching of the core forming block is high, but the chains are not fully extended, equation 5.7 predicts that a weak dependence exists between A_c and the PS block length. This was, indeed, found to be the case for some star type micelle systems, where the corona-forming blocks are much longer than the core-forming blocks, and the core-forming blocks are highly stretched.[23,45] Last, when the R_{core} is related to N_{PS} by an exponent which is much less than one, the value of A_c will become strongly dependent on the PS block length. This is the case in the present system.

5.3.3.1.2. Effect of the Corona-forming Block on A_c. According to equation 5.8, the surface area per corona chain is also dependent on the soluble block length (N_{PAA}). One possible origin of this dependence may be the steric repulsion between the corona chains, i.e. in cases where the structure of the micelles is mainly determined by the cooperation of the repulsion between the corona chains, the surface tension of the micelle core and the deformation (stretching) of the PS blocks in the core. Obviously, the strength of the steric repulsion between the corona chains is related to the chain density on the surface of the micelle core. Thus, it is essential to know the density of the corona chains. In the studies of polymers adsorbed on solid surfaces,[46,47] a dimensionless parameter, σ, has been used to describe the chain density on the surface. Since similarities exist between grafted polymer chains on a solid surface and corona chains on the surface of a micelle core, it is of interest to use this parameter to explore the density of the corona chains on the surface of the micelle core in relation to various molecular parameters.

σ is defined as the number of terminally grafted chains (corona chains in the present system) per unit area times a^2, where a is the length of the repeat unit (~ 0.25 nm for styrene). Thus, its value can be calculated from the equation

$$\sigma = a^2/A_c \tag{5.10}$$

When the surface density of the corona chains is low, i.e. the coil domains of the corona chains do not overlap, each chain occupies roughly a hemisphere of radius R_g (the radius of gyration of the corona chain).[46] The low σ region can then be defined by

$$\sigma < a^2/R_g^2 \tag{5.11}$$

or

$$\sigma a^{-2} R_g^2 < 1 \tag{5.12}$$

Since in a good solvent

$$R_g \approx a N_A^{3/5} \tag{5.13}$$

where N_A is the degree of polymerization of the corona block, the condition for low surface density of the corona chains can be obtained by inserting equation 5.13 into equation 5.12. This yields

$$\sigma N_A^{6/5} < 1 \tag{5.14}$$

Equation 5.14 implies that as $\sigma N_A^{6/5}$ becomes greater than 1, corona chains have to adopt conformations which are extended in the direction perpendicular to the surface due to steric repulsion between the corona chains.

It is interest to calculate the values of $\sigma N_A^{6/5}$ for the spherical micelles of the present system. The results are given in Table 5.4. For comparison, the values of $\sigma N_A^{6/5}$ for some other systems reported in literature are also calculated and given in Table 5.4. It is found that the value of $\sigma N_A^{6/5}$ depends on the composition of the copolymers, and generally increases in proportion to the content (mol %) of the corona-forming blocks in the copolymers. For the present system, the values of $\sigma N_A^{6/5}$ fall in the range 0.2 to 1.4. They are less than unity for most of the micelles, except for three samples with relatively long PAA blocks, where $\sigma N_A^{6/5}$ is slightly higher than unity. This indicates that the surface density of the corona chains is low. It is noted that the values of $\sigma N_A^{6/5}$ are also low in the crew-cut micelles of polystyrene-*b*-poly(4-vinylpyridinium methyl iodide) copolymers in aqueous solutions,[13] as well as in the micelle system of polystyrene-*b*-poly(methacrylic acid) copolymers in the mixed solvent of dioxane and water.[9] However, the values of $\sigma N_A^{6/5}$ are very high for the micelles with relatively long corona-forming blocks,[23, 45] implying that the densities of the corona chains are very high on the core surface. In those systems with high surface densities of the corona, the chains are expected to be highly expanded from the core because of the strong steric repulsion between the corona chains. In the last two systems in Table 5.4, the core-forming blocks were also found to be highly stretched. As a result, the surface areas per corona chain showed a weak dependence on the lengths of both blocks of the copolymers. For the present system, the steric repulsion between the corona chains is not strong because of the low values of $\sigma N_A^{6/5}$. Thus the value of A_c is mainly determined by the cooperation of two factors, the interfacial tension between the core and the solvent and the force of stretching of the core-forming blocks. As a result, A_c shows a weaker dependence on the length of the corona-forming (PAA) block, but a stronger dependence on the length of the core-forming (PS) block.

Table 5.4. Density of corona chains on the surface of the core in several block copolymer micelle systems.

System	Type of Micelles	Solvent	Range of soluble block content (mol%)	Range of $\sigma N_A^{6/5}$	Ref.
PS-b-PAA	crew-cut	water	4 - 20	0.2 - 1.4	Present
PS-b-P4VP.MeI	crew-cut	water	8 - 13	0.5 - 0.9	13[a]
PS-b-PMAA	intermediate	80 % dioxane/ 20 % water	20 - 53	0.6 - 2	9 [b]
PS-b-P4VP	star	toluene	70 - 85	13 - 20	23 [c]
PS-b-PACs	star	toluene	88 - 99	12 - 200	45[d]

a. Crew-cut micelles made from the polystyrene-*b*-poly(4-vinylpyridinium methyl iodide) copolymers in aqueous solutions.

b. Micelles of polystyrene-*b*-poly(methacrylic acid) copolymers in 80 % dioxane and 20 % water mixture.

c. Micelles of polystyrene-*b*-poly(4-vinylpyridine) copolymers in toluene.

d. Micelles of polystyrene-*b*-poly(cesium acrylate) in toluene.

5.3.2. Non-spherical Aggregates. It was shown above that for spherical micelles, the surface area per corona chain (A_C) depends on the lengths of both the PS and the PAA blocks. In this part, the values of A_C of non-spherical aggregates as well as their relation to the dimensions of the PS regions will be discussed. It is noted that the values of A_C for non-spherical aggregates are lower than those of the spherical micelles (*cf.* section 5.3.4.3.), and that A_C decreases as the morphology changes from spherical to cylindrical, and to vesicular (Tables 5.2 and 5.3). Since morphology changes occur when the length (or content) of the PAA blocks decreases, one of the reasons for the decrease in area can be a shortness of the PAA blocks in the cylindrical micelles and vesicles. However, the geometric shapes of the different morphologies can also play an important role. This is discussed below.

For an aggregate made from copolymers with a constant PS block length, according to equations 5.5 and 5.6, the surface area per corona chain, A_c, is determined by the ratio of surface area to volume of an individual aggregate. An increase in the ratio will increase the surface area per corona chain. For spherical micelles, $A_c = 4\pi R^2/N_{agg}$; since $N_{agg} = (4/3)\pi R^3/V_{chain}$, $A_c \propto 3/R$. Similarly, for cylindrical and lamellar micelles, $A_c \propto 2/R$ and $1/R$, respectively; in the latter case, R is half of the lamellar thickness. Among these different structural aggregates, for a comparable dimension of the PS region (R), the spherical micelle gives the largest value of the surface to the volume ratio. The ratios decrease for different morphologies in the order of sphere, cylinder, vesicle and lamella. This suggests that non-spherical aggregates will show a lower value of the surface area per corona chain than spherical micelles. Certainly, for each morphology, the value of A_C decreases as the dimension of the PS region (R) increases.

On the basis of discussion above, one can speculate on the dependence between the surface area per coronal chain (A_C) and the degree of stretching of the core forming chain (S_C) for the different morphologies. One starts by considering an aggregate with the PS dimension of R. For a spherical micelle, due to a larger surface to volume ratio, and the consequently large exposure of the hydrophobic styrene surface to water, the micelle tends to increase its core size, R_{core}, thus decreasing the value of A_c. The increase of the core size is mainly balanced by an increase of the degree of stretching of the PS blocks. As a result, the PS blocks in the core will be more stretched. However, for non-spherical aggregates, because of a lower surface to volume ratio, the steric repulsion between the corona chains is increased. The increased steric repulsion will push the corona chains away from each other, which is, in turn, mainly balanced by an increase of the surface tension of the core. As a result, the aggregate will decrease the dimension of the PS block region, for example the wall thickness of the vesicles; the PS chains become more relaxed, and their degree of stretching is decreased. This explains why the PS chains in the spherical micelles are more stretched than that in the cylindrical micelles and the bilayer aggregates (*cf* section 5.3.2.2.).

5.3.4. Effects of Added Homopolystyrene on the Morphologies.

It was shown above that the core radius of the spherical micelles depends on the lengths of both the insoluble and the soluble blocks; moreover, as the content of soluble block of the copolymers decreases, the morphology of the copolymer aggregates changes from spheres to cylinders, to bilayers, and eventually to compound micelles. Since the morphology changes as the PS block content in the copolymers increases, it is of interest also to study of the effects of added homopolystyrene on the morphologies.

5.3.4.1. Relevant Published Studies. In order to understand the effect of added homopolystyrene, it is useful review briefly some of the literature relevant to this topic. Whitmore and Smith[48] in a combined theoretical and experimental study, reported recently on ternary mixtures of homo-polystyrene/polystyrene-*b*-poly(ethylene oxide)/homo-poly(ethylene oxide), PS/PS-b-PEO/PEO. In that system, the major component is the PS homopolymer, which forms the matrix, while the PEO blocks of the copolymers form spherical micelle cores which are swollen by the PEO homopolymer.

That system is of interest because of its similarities to the present system. The authors showed that the number of micelles per unit volume is controlled primarily by the copolymer content. An increase of copolymer content in the mixture increases the number density of micelles per unit volume. PEO homopolymer is solubilized essentially uniformly in the micelle cores up to the solubility limit, which is directly proportional to the existing volume fraction of the PEO blocks of the copolymer in the blends. In contrast to the effect of increasing the copolymer content, the addition of PEO homopolymer only swells the existing micelle cores but does not change their number density or their aggregation numbers. Within the limit of solubilization, all of the added PEO homopolymer is solubilized. Therefore, the following relationship between the core radii before (R_0) and after (R) the addition of PEO homopolymer can be expected:

$$R \cong (1 + \phi_{hPEO}/\phi_{cPEO})^{1/3} R_0 \qquad (5.15)$$

where ϕ_{hPEO} and ϕ_{cPEO} are the volume fractions of PEO homopolymer and PEO blocks of the copolymers in the micelle core, respectively.

It is believed [48]that the solubilization of homopolymer into micelle core is due to the entropy associated with the low homopolymer concentration localized within the micelle core rather than the smaller volume associated with a separate homopolymer phase in the core. The solubilization entropy is opposed by an increase in the stretching of the core forming block as well as the increase in the interfacial energy of the swollen micelles. It was argued that if this were not the case, i.e. if the copolymer relaxed to a less stretched conformation with the homopolymer accumulating towards the centers, the free energy would be minimized by the formation of few very large domains. This would then be a macrophase-separated system, with the surface decorated by copolymer acting as an emulsifier.[48] Characteristically for this case, the particles would be highly polydisperse.

The study of Whitmore and Smith[48] is confined to aggregates with cores of spherical shape. In our case, we are dealing not only with spherical cores, but also with cores of other shapes, i.e. cylinders and vesicles. Therefore, it would be very useful for the present study to benefit from an investigation of a parallel system to ours, i.e. a system analogous to that of Whitmore and Smith, but involving non-spherical aggregates. Unfortunately, we are not aware of the existence of such a study. However, for binary mixtures of block copolymers (A-*b*-B) and homopolymers (homo-A), or ternary mixtures of A-*b*-B, homo-A and homo-B where the block copolymer is the major component, there are a number of experimental[49-53] and theoretical[54,55] studies, for example, the swelling polystyrene-*b*-polyisoprene (PS-*b*-PI) block copolymers by PS homopolymer. When the PS-b-PI copolymers form an alternating lamellar microdomain structure, two possible extreme structures of the mixture can be encountered.[50] In the first case, the PS homopolymer (homo-PS) is located in the PS microdomains of the copolymer. However, the homo-PS chains are not uniformly distributed among the PS blocks, and tend to aggregate in the central regions of PS domains. In this case, the average distance between the chemical junctions of PS-PI blocks is not affected at all by the solubilization of homopolymer; the interfaces, on the other hand, move further apart. The other possible extreme is represented by the case in which homo-PS is uniformly distributed among the PS blocks. The uniform solubilization will lead to a conformational change of both the PS and PI blocks. The PS block will tend to expand along the direction normal to the interface. Also, the average distance between the chemical junctions of PS-PI blocks will increase because of the incorporation of homo-PS chains into PS block microdomain. In order to maintain a constant density within the PI microdomain, the dimension of PI microdomain will contract.

Experimentally,[49-52] it was found that when the homo-PS content in the mixture is relatively low, it is essentially distributed throughout the corresponding domains. Although the conformational entropy decreases as a result of chain stretching due to the solubilization of the homopolymer, this entropic penalty can be compensated by the entropy gained from the mixing of the homo-PS and PS block chains. As the homopolymer content in the mixture increases, the lateral expansion of the PS blocks will reach its limit. Beyond that point, the addition of homopolymer induces asymmetric swelling, i.e. the homo-PS chains start to accumulate near the center of PS block microdomain. Thus, the homopolymer concentration profile has a maximum in the center of the PS layer. If the homopolymer content in the mixture increases further, swelling the block copolymers by homopolymers may induce a morphology change of the microdomains, even leading to the formation of an inverted phase. Morphology changes or formation of inverted morphologies are mainly a result of the swelling of the minor block of the copolymer to such an extent that its effective volume per chain is larger than that of the unswollen major block of the copolymer.[53]

5.3.4.2. Spherical Crew-cut Micelles. On the basis of information above, one can explore the behavior of added homopolystyrene in the present system. To incorporate homopolystyrene into the spherical micelle cores, homo-PS was dissolved in the copolymer/DMF solutions before the addition of water. During micellization of the copolymers, the homo-PS solubilized into the micelle core. It was found that the solubilization depends on a number of factors. Most importantly, the homo-PS should have a higher value of the critical water content for precipitation than that of the block copolymer. Otherwise, the homo-PS chains will precipitate first from the solution as the water content increases, without becoming incorporated into the PS core of the copolymer micelle.[44]

Upon addition of homopolystyrene, the block copolymers which form spherical micelles without homo-PS, still yield spherical micelles. Some characteristics of the swollen spherical micelles are given in Table 5.5. Taking the system of PS(500)-*b*-PAA(58)/PS(180) as an example, one can see that when the weight ratio of homopolystyrene to copolymer is low (< 10:90), the micelles are generally monodisperse (standard deviation in the core radius: 6%). The core radius increases only slightly with the addition of homopolystyrene. As the ratio increases to 20:80, the increase of the core radius becomes more pronounced, and the core size becomes more polydisperse (standard deviation 11 %). When the ratio exceeds 30:70, the sizes of the micelles become even more polydisperse and very large particles start to form in solutions (standard deviation 26 %). No morphological transitions are induced by the addition of homopolystyrene.

Table 5.5. Some characteristics of the spherical micelles with and without added homopolystyrene.

Polymers PS-*b*-PAA & PS	Composition a	Experimental Diameter b (nm)	*s.d.* (± nm)	Calculated diameter c (nm)	A_c (nm^2/per chain)	N_{agg}
500-*b*-58	100 : 0	30	2.4	30	17	160
500-*b*-58 & 180	95 : 5	30	2.3	30	18	152
500-*b*-58 & 180	90 : 10	31	2.2	31	19	164
500-*b*-58 & 180	80 : 20	36	3.8	32	17	231
500-*b*-58 & 180	70 : 30	37	9.7	33	16	271
1140-*b*-165	100 : 0	40	2.2	40	29	180
1140-*b*-165 & 500	90 : 10	42	3.2	41	30	180

a. Weight ratio of the block copolymer to the homopolystyrene in the samples.

b. Measured micelle core size from TEM.

c. Calculated micelle core size (equation 5.15).

It is of interest to compare the experimentally determined core radii with those calculated from equation 5.15. One can see from Table 5.5 that when the weight ratio of the homo-PS to the diblock copolymer is less than 10/90, the core radii from TEM are in good agreement with the calculated values. The aggregation numbers remain almost constant. These suggest that most of the solubilized homo-PS chains are distributed essentially uniformly in the micelle cores. As the ratio of the homo-PS to the copolymer is increased to 20/80, the experimental core size is appreciably larger than that expected from equation 5.15. The aggregation number is also increased. This implies that progressively more homo-PS chains accumulate in the core center as the added homopolymer content is increased. The stretching entropy penalty for the PS blocks is reduced as the homo-PS goes to the center. Finally, as the ratio of the homo-PS to the copolymer is increased further to 30/70, very large particles are seen. The very large particles are, very probably, aggregates of homo-PS chains with the surface decorated by the copolymers.

5.3.4.3. Non-spherical Crew-cut Aggregates. For the non-spherical aggregates, it was found that the addition of homopolystyrene does change the morphologies, in contrast to the behavior of the spherical micelles. Figure 5.7 shows that the morphology changes from vesicles to spheres upon the addition of 5 wt.% PS(38) homopolystyrene to the 200-*b*-8 diblock. The morphology also changes from cylinders to spheres by the addition of 5 wt.% PS(38) homopolystyrene to the 180-*b*-14 diblock. The characteristics of the aggregates before and after the addition of homo-PS are summarized in Table 5.6. With the addition of homopolystyrene, the core dimensions of the resulting spherical micelles increase considerably relative to the diameters or thicknesses of the aggregates without added homopolystyrene; however, the polydispersity of the micelles is still low. Because of the low content of homopolystyrene and the low polydispersity of the core sizes of the resulting spherical micelles, it is thought that most of the homo-PS chains are distributed essentially uniformly throughout the cores. Indeed, after the effect of

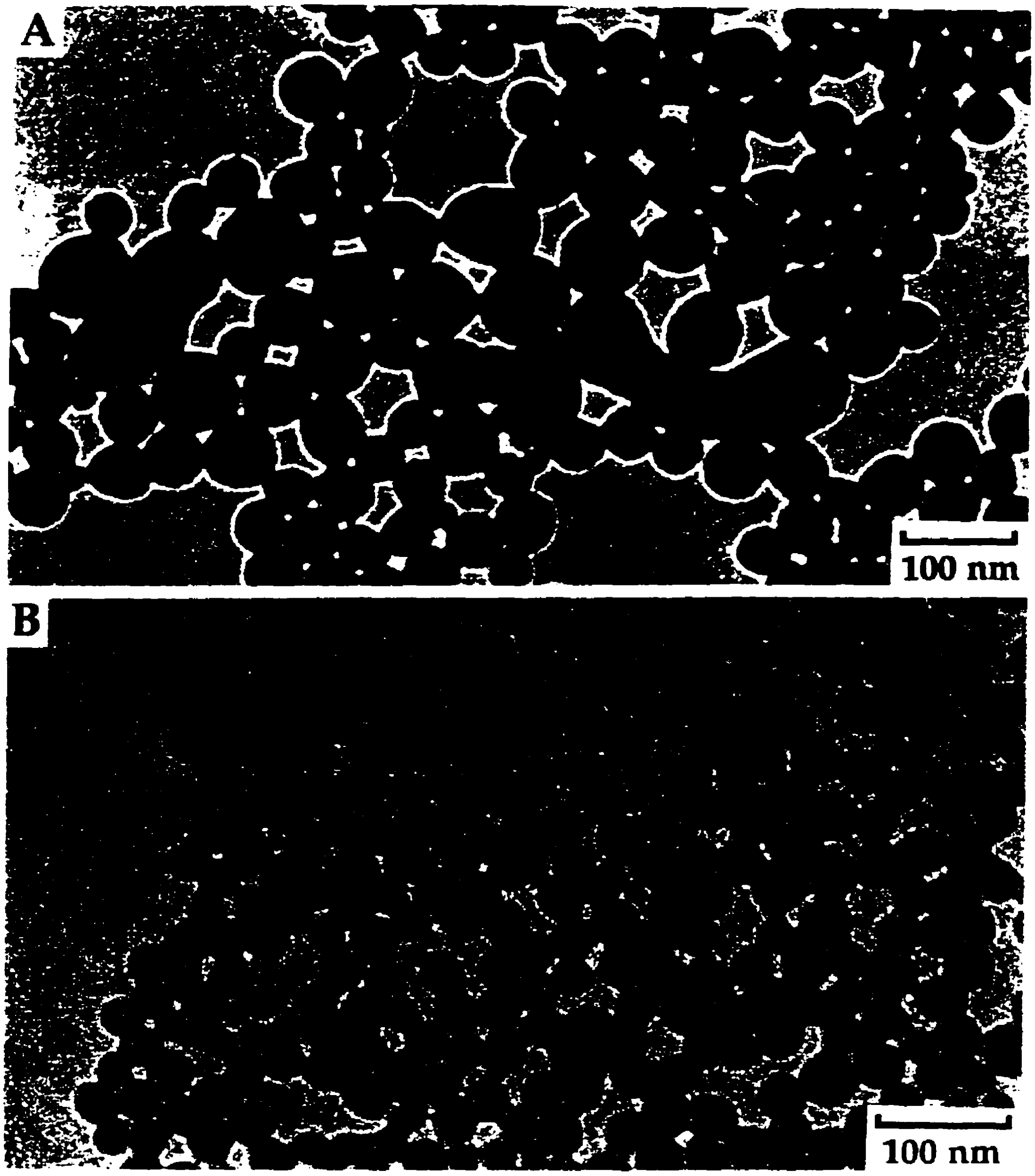

Figure 5.7. The Morphologies of the aggregates formed by the block copolymer 200-*b*-8, (A) without added homopolymer; (B) with 5 wt.% of added homopolystyrene PS(38).

Table 5.6. Some characteristics of originally non-spherical copolymer aggregates with and without added homopolystyrene.

Polymers PS-b-PAA & PS	Composition[a]	Morphology	Diameter or wall thickness from TEM(nm)[b]	*s.d.* (± nm)	Calculated diameter (nm)[c]	S_c[d]	A_c[c] (nm^2)
180-*b*-14	100	Rod	23	--	--	1.32	5.2
180-*b*-14 & 38	95 : 5	Sphere	27	1.7	27	1.53	7.2
200-*b*-8	100	Vesicle	18	--	--	0.99	4.2
200-*b*-8 & 38	95 : 5	Sphere	33	2.8	31	1.79	6.4
410-*b*-16	100	Vesicle	22	--	--	0.84	6.6
410-*b*-16 & 180	90 : 10	Sphere	37	2.4	37	1.42	12

a. Weight ratio of block copolymer to homopolystyrene.

b. Diameter of cylindrical micelles or wall thickness of vesicles.

c. Core diameter calculated from the scaling relation $R_{core} \propto N_{PS}^{0.4}N_{PAA}^{-0.15}$. The effect of the added homopolystyrene on the core size has been corrected by equation 5.15; the table gives R_0.

d. Degree of stretching of the PS blocks. Definitions are given in Tables 5.2 and 5.3.

added homopolymer on the core radius is corrected according to equation 5.15. it is found that the corrected core radii, R_0, of the spherical micelles are in good agreement with the values calculated by the scaling relation found for the present system, $R_{core} \propto N_{PS}^{0.4}N_{PAA}^{-0.15}$ (equation 5.1). It should be noted that after the morphologies change from non-spherical to spherical, the surface area per corona chain increases considerably, implying that the surface area is mostly dependent on the conformation of the PS blocks and the geometric shape of the aggregates, and not primarily on the length of the PAA block itself. The surface area data for these spherical micelles are included in Figure 5.6 (open circles). It is clear that there is a linear relationship between the surface area and $N_{PS}^{0.6}N_{PAA}^{0.15}$, as suggested in equation 5.8.

After the morphology changes from non-spherical to spherical, the increased dimensions of the PS regions suggest that the degree of stretching of PS chain may be increased. However, it is possible that the stretching of the PS blocks is not directly related to the dimensions of these partly filled spheres because of the possible slight accumulation of some of the homopolystyrene chains in the core center. A small amount of accumulated homopolystyrene can have a major effect on the deformation of the PS blocks in the core region. This argument can be supported by considering, for example, the mixture of 90 wt% 410-b-16 diblocks and 10 wt% PS(180) homopolystyrene. The resulting spherical micelles have an average radius of 37 nm (Table 5.6). If all the added homopolystyrene chains were distributed homogeneously in the core, some of PS blocks of the copolymers would need to span the space from the surface to the center of the core. The calculated degree of stretching of the PS block would be about 1.42. However, if only 10% of the added homopolymer were to accumulate in the core center and the rest to distribute homogeneously throughout the entire core region, the degree of the PS block stretching would be reduced to 1.10. The detailed distribution in any particular case would thus involve a balance of the entropic contributions of homopolymer distribution vs. chain stretching.

One can speculate about the origin of the dependence of the morphological transitions on the block copolymer composition. Without added homopolymer, as the content of insoluble (PS) blocks in the copolymers decreases, the degree of stretching of the PS block increases (*cf.* equations 5.3); the change in morphology from spherical to non-spherical can reduce the thermodynamic stretching penalty. With the addition of homopolymer, the morphology change from non-spherical to spherical may be ascribed to two possible aspects. One is the decreased degree of stretching of the PS blocks due to the accumulation of a small amount of homopolystyrene in the center; another is the entropy gained from mixing the homopolystyrene with the PS blocks in the cores.

5.3.5. Comparison of Multiple Morphologies to Those in Other Systems.

The main purpose of this section is to compare the present system to other systems exhibiting multiple morphologies. As mentioned briefly in the introduction, many examples of multiple morphologies have been observed in micro-phase separated systems.[27-41] The copolymer/homopolymer blends and small molecule surfactants are of particular interest here because of a range of similarities to the present system; most importantly, both involve a low concentration of aggregating material in a solvent or homopolymer matrix.

5.3.5.1. Comparison with copolymer/homopolymer blends. For the block copolymer/homopolymer blends, it was reported by Kinning et al[33] that blending poly(styrene-butadiene) diblocks with a large amount of homopolystyrene results in the formation of a micellar phase consisting of spherical domains of the butadiene blocks. However, the morphology of the butadiene domains can change from spherical to cylindrical and eventually to vesicular, by increasing the butadiene block content in the block copolymers or the homopolystyrene molecular weight, or the volume fraction of the block copolymer in the blends. The major difference between the blend systems and micelle solutions of the present study is the size of the solvent molecules. By extrapolating the reported trends for the styrene homopolymer to the low molecular weight (i.e. solvent) region, multiple morphologies of block copolymer micelles can be expected only if the block copolymer has a very short soluble block length, with the long block remaining insoluble. This is consistent with the present results, since the morphologically interesting regions occur only for small fractions of soluble blocks in the copolymers. For a typical series of the block copolymers, e.g. 200-*b*-y, as the length of the PAA (soluble) block decreases, the morphology of the formed aggregates changes in the order of sphere (200-*b*-21), cylinder (200-*b*-15), bilayers (vesicle and lamella) (200-*b*-8), and the compound micelle (200-*b*-4).

While the morphology changes as the PAA block contents in the copolymers decrease, it has been observed that the spherical micelles exist in almost all solutions, as evidenced from their presence on a number of micrographs in which other morphologies are dominant. This phenomenon was also found in the copolymer/homopolymer blends.[33] For the present system, the presence of spherical micelles can be explained by one of two possibilities. One may be that in the process of the addition of water to the polymer/DMF solution, boundaries of stabilities of various morphologies are being crossed, depending on where exactly the region in the phase diagram for a particular morphology was located for a specific run. The phase diagram in the present case is obviously complicated by the multiplicity of factors, i.e. the lengths of both the PS and the PAA blocks, the water content in the DMF, and the total polymer concentration. All of these factors influence the observed morphology. Thus, as water is added, some of the micelles are precipitated, and the polymer concentration changes so that, at some point, a morphological boundary may be crossed.[44] In addition to the above, it should be borne in mind that styrene homopolymer is usually present in the copolymer, because with the addition of *tert*-butyl-acrylate monomer during synthesis, some of homopolystyrene chains may have been killed. The presence of homopolymer is known to affect the morphology, as was shown in section 5.3.4. Thus, since the partitioning of homopolymer into copolymer may be dependent on the total polymer concentration and the water content in DMF, it is entirely possible that the micelles that precipitated first in a particular run have a different homopolystyrene content than those prepared in the late stages of the same run. Thus, it is conceivable that the spherical morphology due to the presence of homopolymer may be favored either in the early or later stages of the micellization run, depending on the relative solubility of the homopolymer in the block copolymer as a function of the relevant parameters.

5.3.5.2. Comparison with small molecule surfactants. It has been known for many years that aggregates with different morphologies can form in small molecule surfactants systems.[41] The formation of various morphologies is explained in terms of a dimensionless packing parameter, v/a_0l_c, where a_0 is the optimal surface area of the polar head, and v and l_c are the volume and the critical length of the hydrophobic part of the surfactant molecule. The value of the parameter v/a_0l_c determines the geometry of the aggregates. For example, if $v/a_0l_c \leq 1/3$, spherical structures are formed. As the value of v/a_0l_c increases, the morphology of the aggregates can change from spherical to cylindrical, to vesicular and planar, and eventually to inverted spherical.[41] The critical values of v/a_0l_c for different morphological transitions can easily be obtained by using, for example, the micelle core radius, R_{core}, instead of l_c in v/a_0l_c.[41] Because a_0 is found experimentally to be dependent of the nature of the head group and almost independent on the hydrophobic chain length, and l_c can be estimated from semi-empirical equations, the parameter v/a_0l_c has been used to predict the morphologies of the aggregates successfully. For example, most single-chain surfactants form spherical micelles, while most double-chain surfactants form bilayers because of a higher value of v/l_c.

For the present system, the morphology changes as the length of the corona-forming block decreases. Certainly, as the PAA block length decreases, the surface area per corona chain also decreases. As a result, the value of v/a_0l_c will increase correspondingly. However, this may not be the primary reason for the morphological changes from spherical to non-spherical as can be seen by considering the balance among a number of forces.

For the micelles of small molecule surfactants, strong repulsion exists between head groups. The surface area per head group is mainly determined by the balance of forces between head group repulsion and hydrophobic attraction of the core surface. Changes in the stretching force of the hydrophobic chains is less important because the chains are stretched already.

For the copolymer crew-cut micelles, the surface area per corona chain is largely dependent on the conformation of the insoluble block (PS) and the geometric shape of the aggregates, not the length of PAA block itself. The repulsion between the corona chains is relatively less important because the blocks are short and acidic. For example, the vesicles formed by the block copolymer 410-*b*-16 have an average surface area of 6.6 nm^2/corona chain. However, with the addition of 10 % PS(180), the resulting spherical micelles show an average surface area 12 nm^2/corona chain (Table 5.6). It can be argued that if the repulsion between corona chains were the primary factor which determines the value of the surface area, one would not see such a big change in the surface area per chain in going from one morphology to another. Concerning the core regions, the insoluble blocks are essentially random coils, and are only stretched to a small extent relative to the end-to-end distance in their unperturbed state. The degree of PS block stretching is a function of the length of PAA blocks. Thus, it is believed that the geometric structures of the aggregates are mainly controlled by the balance of forces between hydrophobic attraction (surface tension) and the stretching of chains in the core-forming block.

5.3.6. Additional Considerations of the Formation of the Aggregates.

5.3.6.1. Theoretical studies of spherical micelles in the literature. Theoretical treatments of spherical block copolymer micelles, pioneered by de Gennes,[17] have been reported extensively in the literature.[56-62] The main goals of these studies were to find relations between structural parameters of the micelles and the molecular characteristics of the constituent block copolymers using a free energy minimization approach with respect to micellar structure parameters (i.e. the aggregation number or the micelle radius), and then to compare the results of the calculations with the available experimental results.

de Gennes[17] analyzed the formation of diblock copolymer micelles in selective solvent by minimizing the free energy per molecule of an isolated micelle with respect to the aggregation number. Within the framework of that treatment, the free energies of formation of the micellar core-solvent interface and the free energy of stretching of the core-forming blocks control the micellization behavior. On this basis, the treatment predicts that the micelle core radius R_{core} is related the molecular size N_B of the core-forming block as $R_{core} \propto N_B^{2/3}$, when the interfacial energy is large, and as $R_{core} \propto N_B^{1/2}$ when the interfacial energy between the core surface and the solvent is low.

For the formation of diblock copolymer micelles in a homopolymer solvent resulting from the minimization the total free energy of the whole system rather than the free energy of an isolated micelle,[56] Leibler et al found that for blocks that show weak incompatibility, $R_{core} \propto N_B^{0.53}$. The solvent compatible block was considered to have no influence on the micellar characteristics. Later, a relationship between the core radius and the copolymer composition, $R_{core} \propto N_B^{\alpha} N_A^{-\gamma}$, was obtained by Whitmore and Noolandi[58], where N_B and N_A represent the degrees of polymerization of the insoluble and soluble blocks, respectively. In their study, qualitative agreement between experiment and theory was obtained for the system of polystyrene-*b*-polybutadiene copolymer micelles in polybutadiene homopolymers. Theoretical values for the exponents lay in the range $0.67 \leq \alpha \leq 0.76$ and $0 \leq \gamma \leq 0.1$, showing that the soluble block had a relatively weak influence on the size of the micelle core.

Nagarajan and Ganesh[61] formulated their theory of micellization of diblock copolymer A-*b*-B in a solvent selective for A, on the basis of multicomponent solution approach similar to that Leibler et al.[56] The Gibbs energy change in terms of standard chemical potential was expressed on the basis of considerations of all relevant physicochemical changes accompanying the transfer of a copolymer molecule from the unimer state to a micelle. They predicted that the soluble block can exert a large influence on the structure of the micelle, particularly in the case of copolymer molecules in which the soluble block is in a good solvent. It was found that the core radius depended on the copolymer composition in the manner $R_{core} \propto N_B^{\alpha} N_A^{-\gamma}$. The values of the exponents, α and γ, depended on the copolymer/solvent system. For polystyrene-*b*-polybutadiene block copolymers in heptane, they found $R_{core} \sim N_B^{0.70} N_A^{-0.08}$; for poly(oxyethylene)-*b*-poly(oxypropylene) copolymers in water they found $R_{core} \sim N_B^{0.73} N_A^{-0.17}$. The larger dependence of R_{core} on N_A in the latter system was attributed to the fact that water is a good solvent for poly(oxyethylene) under the conditions of the measurement.

5.3.6.2. Spherical Micelles. The present experimental data suggest that the dependence of the core radius on the length of the insoluble block is weaker than that predicted by the theories.[57-61] The difference might be attributable to the conditions under which the micelles form. Generally, the theoretical predictions for the core radius are obtained for a constant value of χ , the interaction parameter of the insoluble block and solvent. However, in the present system, the micelles form and the structures "freeze" at values of χ which decrease with increasing core-forming block length (*cf.* section 5.3.2.1.).[44] Since the aggregation number should also decrease with decreasing χ, the radius of the core should scale more weakly with the core-forming block length than it does at a fixed χ.

Another reason which may explain the weaker dependence of the core size on the length of the insoluble block can be the value of the surface tension of the core during micellization. Originally, when the block copolymer, PS-*b*-PAA, is dissolved in DMF, the polymer disperses molecularly in the solvent. As water addition progresses, the solvent becomes progressively worse for the PS blocks, until micellization starts at some critical water content. The originally formed micelle cores are probably highly swollen by a DMF rich solvent. The interfacial energy between the core surface and the solvent must be quite low. The low interfacial energy, which is associated with the process of the micellization, is thought to be a very important parameter in the present system. A high interfacial energy will force the micelle to increase its size in order to decrease the surface area per corona chain, the increase in size being balanced by a higher degree of stretching of the core forming block. Accordingly, a low interfacial energy system will result in a weaker dependence of the core radius of the formed micelles on the length of the core-forming block, as predicated by the theoretical study of de Gennes.[17] Finally, the stronger dependence of the micelle core size on the corona-forming block may be ascribed to the stronger interaction (compatibility) between the PAA block and the solvents, with the influence of PAA block becoming relatively more prominent in the system of low interfacial energy.

5.3.6.3. Non-spherical Micelles. While most of the theoretical studies on block copolymer micellization focus on spherical micelle structures, some papers[62-64] explored theoretically the formation of nonspherical micelles as well as the transition between two different morphologies, e.g. from spherical to rod-like, in terms of changes of the molecular parameters of the polymers, such as the degrees of polymerization of the component blocks of the copolymer and the size of the solvent molecules. Munch and Gast[62] considered the formation of lamellar micelles of block copolymer in solution. It was found that the block copolymer will form lamellar domains in the composition region where the core-forming block is much longer than the corona-forming block. Thus, the lamellar micelles form at copolymer concentrations below the critical micellization concentration found for spherical micelles. Studies also show a significant effect of the size of the solvent molecules on the boundary for the formations of the lamellar and the spherical micelles. Specifically, when the blocks of the copolymers are equal in length, lamellar micelles are favored as the solvent size increases. Mayes and de la Cruz[63] studied cylindrical versus spherical micelle formation in block copolymer/homopolymer blends. A trend toward cylinder formation was observed with increasing core-forming block fraction of the copolymers and increasing homopolymer (solvent) molecular weight. By minimizing the total free energy of a system of micelles, it was found that spherical micelles are precluded because of the higher critical micellization concentration compared to that for cylindrical micelles. Nagarajan[64] studied the shape transitions of block copolymer aggregates. On the basis of model of an uniform deformation for the copolymer blocks, changes in morphology progressively from sphere to cylinder, and to bilayer can be predicated as the insoluble block content increases. While the core dimension of the preferred geometry increases with increasing insoluble block content in the copolymer, the core dimension is predicted to decrease discontinuously in parallel with the morphology changes. This is qualitatively in agreement with the trend of morphological changes as a function of the block copolymer composition found in the present study.

The major contributions to the thermodynamics of the block copolymer micellization are considered to originate mainly from three sources, i.e. micelle core, the interaction between the corona and the solvent, and the core/corona interface. For the crew-cut micelle system, the contribution of the micellar core and the interfacial tension becomes more important, considering the very short corona block lengths. Thermodynamically, large aggregates are limited for the spherical micelles by the deformation energy of the core-forming blocks. Energy is needed to stretch the copolymer chains from their unperturbed dimensions by confining them to a characteristic micelle geometry. Cylindrical and bilayer aggregates, however, allow more chains to be incorporated into the structure without significant changes in chain configuration. Because of the low interfacial energy between the core and the solvent, the stretching contribution to the free energy appears largely responsible for the transition from spherical to non-spherical micelles. The present experimental results show that the degree of stretching of the PS blocks decreases progressively in parallel with changes of the morphologies from sphere to cylinder and to vesicle.

Because the morphological transitions occur in the composition regions of very low fraction of soluble blocks in the copolymers, it seems likely that, for these very short block lengths, the maintenance of differential solubility may be the crucial factor leading to the formation of the various morphologies. In the present system, it is possible to maintain differential solubility, even for the short blocks, because of the large difference in solubility between the hydrophilic and the hydrophobic segments. Once formed, the aggregates in their various morphologies can be deswelled in water, which makes them very stable because of the strong interactions between the acidic or ionic aqueous corona-forming PAA blocks and water. Also, at room temperature, the deswelled cores are well below the glass transition temperature of bulk polystyrene. The latter feature is certainly helpful, but not essential for stability.

5.4. CONCLUSIONS

Transmission electron microscopy was used to study crew-cut micelle-like aggregates of polystyrene-*b*-poly(acrylic acid) (PS-*b*-PAA) block copolymers in low molecular weight solvents. The aggregates were formed under conditions of near thermodynamic equilibrium, and then isolated into water. Because of the large weight-fraction of the PS blocks in the copolymers (from 80 to 98%), the aggregates are readily observable by TEM and their dimensions are measurable from the prints directly.

For spherical micelles, it was found that the micelle cores are generally monodisperse. A comparison between star and crew-cut micelles shows that the latter structures are distinguished by a low density of corona chains on the core surface, and a low degree of stretching of the PS chains in the cores. The core radius (R_{core}), the surface area per corona chain (A_c) and the degree of stretching of the PS blocks in the core (S_c) depend on the copolymer compositions, and scale according to the following relations:

$$R_{core} \propto N_{PS}^{0.4} N_{PAA}^{-0.15}$$

$$A_c \propto N_{PS}^{0.6} N_{PAA}^{0.15}$$

$$S_c \propto N_{PS}^{-0.1} N_{PAA}^{-0.15}$$

These characteristics of the crew-cut micelles result mainly from effects of a low interfacial energy between the core region and the solvent during micellization, as well as the procedures used for the preparation of micelles, as a result of which the values of χ decrease with increasing length of the core-forming block.

As the content of the soluble block (PAA) in the block copolymer decreases, the morphology of the micelles (or aggregates) changes progressively from spheres to cylinders, to bilayers (both vesicles and lamellae), and eventually to compound (inverted) micelles with a hydrophilic surface. The compound micelle is believed to be a new morphology formed by block copolymers in solution. The morphological transitions are believed to be mainly due to changes of the degree of stretching of the PS blocks in the core regions as the block copolymer composition changes.

Homopolystyrene can be solubilized in the core during micellization. The homopolymer chains are generally distributed throughout the core when their content is relatively low. As the content of added homopolystyrene increases, a trend of the homopolymer accumulation in micelle core center can be inferred. The addition of homopolystyrene changes the morphologies of the aggregates from bilayers or cylinders to spheres. The change in morphology is ascribed mainly due to the reduced degree of stretching of the PS blocks and possibly the mixing entropy, both of which are associated with the solubilization of the homopolystyrene into the micelle cores.

While various morphologies of the micelles or aggregates of copolymers have been observed in many other systems, it is believed that the present system provides the first instance in which all these multiple aggregate morphologies, i.e. spheres, cylinders, vesicles or lamellae, and large compound micelles, have been observed directly in block copolymers in a low molecular weight solvent with changing copolymer composition. It is also believed that this is the only way so far to prepare glassy vesicles of block copolymers, which form spontaneously and which can be stabilized and isolated in water.

5.5. ACKNOWLEDGMENTS.

We would like to thank The Natural Sciences and Engineering Research Council of Canada(NSERC) for continuing support of this research.

5.6. REFERENCES.

1. Price, C. In *Developments in block copolymers*; Goodman, I. Ed.; Applied science publishers: London, 1982; Vol. 1, p 39.
2. Selb, J.; Gallot, Y. In *Developments in block copolymers*; Goodman, I. Ed.; Applied science publishers: London, 1985; Vol. 2, p 27.
3. Tuzar, Z.; Kratochvil, P. In *Surface and Colloid Science*; Matijevic, E. Ed.; Plenum Press: New York, 1993; Vol. 15, p 1.
4. Xu, R.; Winnik, M. A. *Macromolecules* **1991**, *24*, 87.
5. Wilhelm, M.; Zhao, C-L.; Wang, Y.; Xu, R.; Winnik, M. A. *Macromolecules* **1991**, *24*, 1033.
6. Prochazka, K.; Kiserow, D.; Ramireddy, C.; Tuzar, Z.; Munk, P.; Webber, S. E. *Macromolecules* **1992**, *25*, 454.
7. Tuzar, Z.; Kratochvil, P.; Prochazka, K.; Munk, P. *Collect. Czech. Chem. Commun.* **1993**, *58*, 2362.
8. Astafieva, I.; Zhong, X. F.; Eisenberg, A. *Macromolecules* **1993**, *26*, 7339.
9. Qin, A.; Tian, M.; Ramireddy, C.; Webber, S. E.; Munk, P. *Macromolecules* **1994**, *27*, 120.
10. Desjardins, A.; Eisenberg, A *Macromolecules* **1991**, *24*, 5779.
11. Desjardins, A.; van de Ven, T. G. M.; Eisenberg, A. *Macromolecules* **1992**, *25*, 2412.
12. Gao, Z.; Desjardins, A.; Eisenberg, A. *Macromolecules* **1992**, *25*, 1300.
13. Gao, Z.; Varshney, S. K.; Wong, S.; Eisenberg, A. *Macromolecules* **1994**, *27*, 7923.
14. Honda, C.; Sakaki, K.; Nose, T. *Polymer* **1994**, *35*, 5309.
15. Zhang, L.; Barlow, R. J.; Eisenberg, A. *Macromolecules* **1995**, *28*, 6055 (chapter 3 of this thesis).

16. Halperin, A.; Tirrell, M.; Lodge, T. P. *Adv. Polym. Sci.* **1992**, *100*, 31.

17. de Gennes, P. G. In *Solid State Physics*, Liebert, L. Ed.; Academic press, New York, 1978; supplement 14, p. 1.

18. Utiyama, H.; Takenaka, K.; Mizumori, M.; Fukuda, M.; Tsunashima, Y.; Kurata, M. *Macromolecules* **1974**, *7*, 515.

19. Price, C. *Pure and Appl. Chem.* **1983**, *55*, 1563.

20. Zhou, Z.; Chu, B. *Macromolecules* **1988**, *21*, 2548.

21. Hilfiker, R.; Wu, D. Q.; Chu, B. *J. Colloid Interface Sci.* **1990**, *135*, 573.

22. Gast, A. P.; Vinson, P. K.; Cogan-Farinas, K. A. *Macromolecules* **1993**, *26*, 1774.

23. Antonietti, M.; Heinz, S.; Schmidt, M.; Rosenauer, C. *Macromolecules* **1994**, *27*, 3276.

24. Zhao, J. Q.; Pearce, E. M.; Kwei, T. K.; Jeon, H. S.; Kesani, P. K.; Balsara, N. P. *Macromolecules* **1995**, *28*, 1972.

25. Schillén, K.; Brown, W.; Johnsen, R. M. *Macromolecules* **1994**, *27*, 4825.

26. Glatter, O.; Scherf, G.; Schillén, K.; Brown, W. *Macromolecules* **1994**, *27*, 6046.

27. Meier, D. J. In *Thermoplastic Elastomers*; Legge, N. G., Holden, G., Schroeder, H. E., Eds., Hanser: New York, 1987, Chapter 11.

28. Brown, R. A.; Masters, A. J.; Price, C.; Yuan, X. F. In *Comprehensive Polymer Science: Polymer Properties* Allen, S. G., Bevington, J. C., Booth, C., Price, C. Eds.; Pergamon press: Oxford, 1989; Vol. 2, p 155.

29. Thomas, E. L.; Alward, D. B.; Kinning, D. J.; Martin, D. C.; Handlin, D. L., Jr.; Fetters, L. J. *Macromolecules* **1986**, *19*, 2197.

30. Hasegawa, H.; Tanaka, H.; Yamasaki, K.; Hashimoto, T. *Macromolecules* **1987**, *20*, 1651.

31. Thomas, E. L.; Anderson, D. M.; Henkee, C. S.; Hoffman, D. *Nature* **1988**, *334*, 598.

32. (a) Förster, S.; Khandpur, A. K.; Zhao, J.; Bates, F. S.; Hamley, I. W.; Ryan, A.

J.; Bras,W. *Macromolecules* **1994**, *27*, 6922. (b) Hajduk, D. A.; Harper, P. E.; Gruner, S. M.; Honeker, C. C.; Kim, G.; Thomas, E. L.; Fetters, L. J. *Macromolecules* **1994**, *27*, 4063.

33. Kinning, D. J.; Winey, K. I .; Thomas, E. L. *Macromolecules* **1988**, *21*, 3502.
34. Bates, F. S.; Kumar, A.; Schulz, M. F. *J. Polym. Sci., Polym. Phys. Ed.* **1995**, *33*, 1423.
35. (a): Zhu, J.; Eisenberg, A.; Lennox, R. B. *J. Am. Chem. Soc.* **1991**, *113*, 5583. (b): Zhu, J., Lennox, R. B.; Eisenberg, A. *J. Phys. Chem.* **1992**, *96*, 4727. (c): Zhu, J.; Eisenberg, A.; Lennox, R. B. *Macromolecules* **1992**, *25*, 6547.
36. Meszaros, M.; Eisenberg, A.; Lennox, R. B. *Faraday Discuss.* **1994**, *98*, 283.
37. van Hest, J. C. M.; Delnoye, D. A. P.; Baars, M. W. P. L.; van Genderen, M. H. P.; Meijer, E. W. *Science* **1995**, *268*, 1592.
38. Tanford, C. *The Hydrophobic Effect*, 2nd ed., Wiley: New York, 1980.
39. Gruen, D. W. R. *J. Phys. Chem.* **1985**, *89*, 146.
40. Kaler, E. W.; Murthy, A. K.; Rodriguez, B.; Zasadzinski, J. A. N. *Science* **1989**, *245*, 1371.
41. Israelachvili, J. N. *Intermolecular and surface forces*, 2nd edition, Academic press: London, 1992.
42. Zhang, L.; Eisenberg, A. *Science* **1995**, *268*, 1728 (chapter 4 of this thesis).
43. Zhong, X. F.; Varshney, S. K.; Eisenberg, A. *Macromolecules* **1992**, *25*, 7160.
44. Zhang, L.; Shen, H.; Eisenberg, A. *Macromolecules* **1997**, *30*, in press (chapter 8 of this thesis).
45. Nguyen, D.; Williams, C.; Eisenberg, A. *Macromolecules* **1994**, *27*, 5090.
46. de Gennes, P. G. *Macromolecules* **1980**, *13*, 1069.
47. Hadziioannou, G.; Patel. S.; Granick, S.; Tirrell, M. *J. Am. Chem. Soc.* **1986**, *108*, 2869.
48. Whitmore, M. D.; Smith, T. W. *Macromolecules* **1994**, *27*, 4673.

49. Hashimoto, T.; Tanaka, T.; Hasegawa, H. *Macromolecules* **1990**, *23*, 4378.
50. Tanaka, T.; Hasegawa, H.; Hashimoto, T. *Macromolecules* **1991**, *24*, 240.
51. Tanaka, T.; Hashimoto, T. *Macromolecules* **1991**, *24*, 5713.
52. Winey, K. I.; Thomas, E. L.; Fetters, L. J. *Macromolecules* **1991**, *24*, 6182.
53. Winey, K. I.; Thomas, E. L.; Fetters, L. J. *Macromolecules* **1992**, *25*, 2645.
54. Shull, K.; Winey, K. I. *Macromolecules* **1992**, *25*, 2673.
55. Banaszak, M.; Whitmore, M. D. *Macromolecules* **1992**, *25*, 2757.
56. Leibler, L.; Orland, H.; Wheeler, J. C. *J. Chem. Phys.* **1983**, *79*, 3550.
57. Noolandi, J.; Hong, K. M. *Macromolecules* **1983**, *16*, 1443.
58. Whitmore, M. D.; Noolandi, J. *Macromolecules* **1985**, *18*, 657.
59. Zhulina, E. B.; Birshtein, T. M. *Vysokomol. Soedin.* **1985**, *27*, 511.
60. Halperin, A. *Macromolecules* **1987**, *20*, 2943.
61. Nagarajan, R.; Ganesh, K. *J. Chem. Phys.* **1989**, *90*, 5843.
62. Munch, M. R.; Gast, A. P. *Macromolecul* **1988**, *21*, 1360.
63. Mayes, A. M.; de la Cruz, M. O. *Macromolecules* **1988**, *21*, 2543.
64. Nagarajan, R. in *Solvents and Self-organization of Polymers*, NATO ASI Series E, Webber, S. E.; Munk, P.; Tuzar, Z. Eds.; Kluwer Academic Publishing: 1996,, vol. 327, p 121.

Chapter 6

Ion-Induced Morphological Changes in “Crew-Cut” Aggregates of Amphiphilic Block Copolymers

ABSTRACT

The addition of ions in micromolar ($CaCl_2$ or HCl) or millimolar (NaCl) concentrations can change the morphology of crew-cut aggregates of amphiphilic block copolymers in dilute solutions. In addition to spherical, rodlike, and univesicular or lamellar aggregates, an unusual large compound vesicle (LCV) morphology can be obtained from a single block copolymer. Some features of the spontaneously formed LCVs may make them especially useful as drug delivering vehicles, and as models of biological cells. Gelation of a dilute spherical micelle solution can also be induced by ions due to the formation of a cross-linked "pearl necklace" morphology.

6.1. INTRODUCTION

Most aggregates formed by the self-assembly of amphiphilic block copolymers in selective solvents are spherical and consist of a core and a coronal shell. The core is composed of the insoluble blocks, while the corona contains the soluble blocks which are highly swollen by the solvent. Such structures have been explored in detail. [1] We have described the formation of aggregates of multiple morphologies of one family of highly asymmetric polystyrene-*b*-poly(acrylic acid), PS-*b*-PAA in dilute solution, [2] in which the length of the insoluble PS blocks was much longer than that of the soluble PAA blocks. They were therefore described as "crew-cut" aggregates. As the length of the PAA block decreased, the morphology changed from spherical to rodlike, to lamellar or vesicular, and finally to large compound micelles (LCMs) consisting of an assembly of inverted spherical micelles surrounded by a hydrophilic surface. A more detailed description of the multiple morphologies and the characteristics of the crew cut micelle-like aggregates is available. [3] More recently, it was shown that PS-*b*-PEO diblocks [PEO, poly(ethylene oxide)], in dilute solution, can also form aggregates with various morphologies from block copolymers of different compositions. [4]

Morphological changes can also be induced in an identical block copolymer by the addition of ions in micromolar ($CaCl_2$ or HCl) or millimolar (NaCl) concentrations. The morphologies are the same as those produced by changes in the copolymer composition in the absence of added ions, which suggests that the morphological changes are probably induced by decreased repulsion (both steric and electrostatic) among the hydrophilic segments due to protonation of PAA (by HCl), or ion-binding or bridging (by Ca^{2+}). In addition, aggregates of a new morphology, consisting of large compound vesicles, have been prepared and are described. The large compound vesicles may be useful as possible drug delivering vehicles, and as models of stable microstructured biomaterials. Finally, ion-induced gelation can occur in which spherical micelles in aqueous solution form a cross-linked "pearl necklace" structure in the presence of 20 mM HCl. These results suggest that the versatility of the crewcut aggregates is much greater than originally suspected.

6.2. RESULTS AND DISCUSSION

The PS-*b*-PAA or PS-*b*-PEO diblocks were dissolved in N,N-dimethylformamide (DMF) to give a stock solution of 1 weight %. Deionized water was then added to the copolymer solutions with stirring; micellization took place between about 4 to 6 weight % of water. However, the addition of water was continued until 25 weight % of water had been added, in order to make sure that the structure of the formed aggregates is kinetically frozen. The aggregates were isolated into water by dialyzing the resulting solutions against distilled water to remove the DMF. A dynamic equilibrium between aggregates and unimers undoubtedly exists in the early stages of water addition during micellization. At some point, however, as the DMF is forced out of the core, the equilibrium is frozen because of the glassy nature of the PS chains.

A set of transmission electron microscopy (TEM) images [5] of the aggregates prepared from the same diblock copolymer [PS(410)-*b*-PAA(25); the numbers in brackets indicate the degree of polymerization of the blocks] at different concentrations of added HCl is shown in Figure 6.1. Without added acid, the aggregates are small spheres of low polydispersity with an average diameter of 29 nm. When the HCl concentration is 190 μM (or a molar ratio, R, of added HCl to acrylic acid repeat units of 0.035), the aggregates are still spherical (Figure 6.1-A), but with an average diameter of 38 nm. However, for 210 μM HCl (R = 0.040), spherical, rodlike, vesicular, and lamellar aggregates coexist in the solution (Figure 6.1-B), the predominant morphology being rodlike. For 240 μM HCl (R = 0.045), most of the aggregates become vesicular, with rodlike aggregates still observed occasionally (Figure 6.1-C), and for 270 μM HCl (R = 0.050), the aggregates become large compound vesicles (LCVs) (Figure 6.1-D). The same morphology was observed for 530 μM HCl (R = 0.10); no further morphological change was observed. Addition of salt can also induce morphological changes of the aggregates. The effect of divalent ions, such as Ca^{2+}, is much stronger than that of univalent ions, such as Na^{+} (Table 6.1).

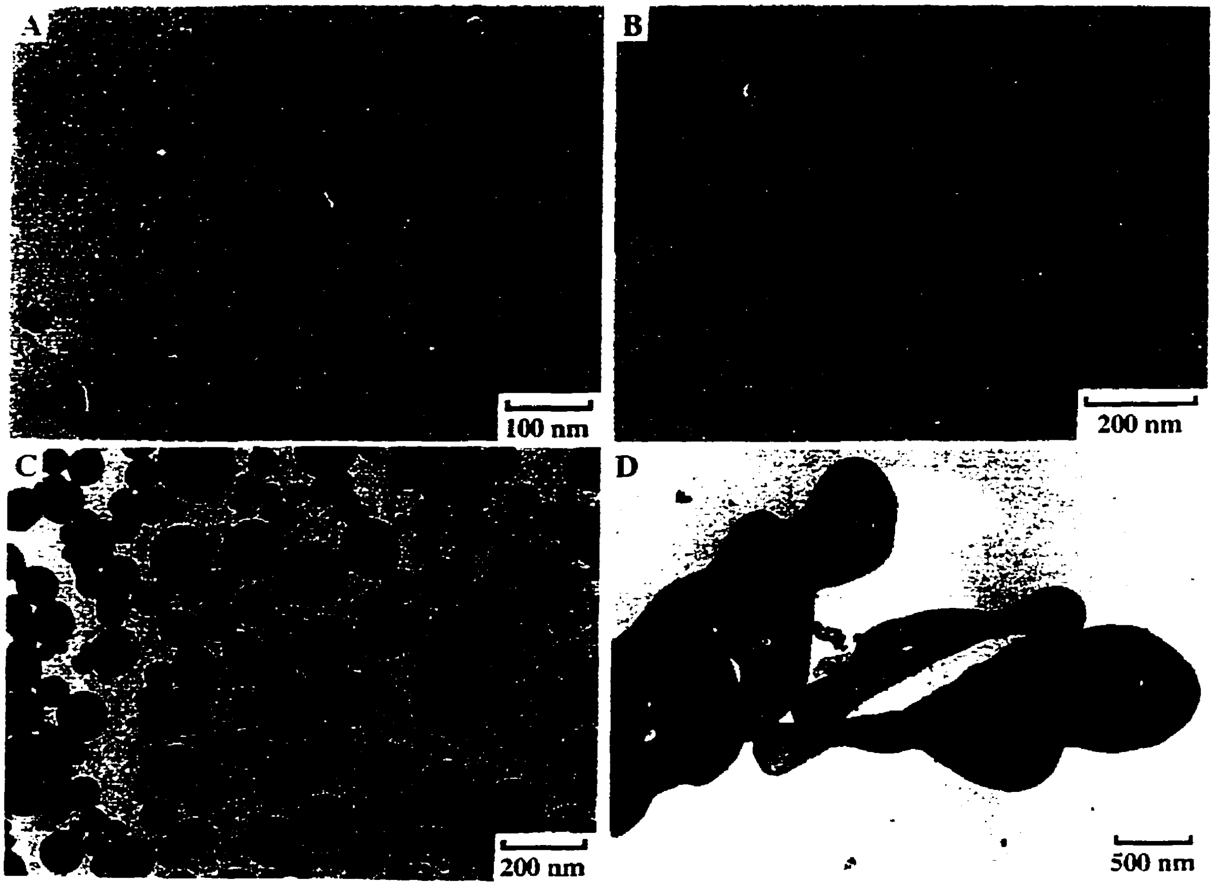

Figure 6.1. Aggregates of various morphologies made from PS(410)-*b*-PAA(25) by the addition of HCl to different final concentrations: (A) 190 μM (R = 0.035), (B) 210 μM (R = 0.040), (C) 240 μM (R = 0.045), and (D) 270 μM (R = 0.050). R represents the molar ratio of added salt or acid to acrylic acid repeat units.

Table 6.1. Summary of the effect of added acid or salt concentration (mole/litre) on aggregate morphology of PS(410)-*b*-PAA(25) diblock copolymer. In the table, numbers in brackets represent the molar ratio of added salt or acid to acrylic acid repeat units.

Additive	Dominant morphology			
	Spheres	Rods	Vesicles	LCV's
HCl	1.9 x 10^{-4}	2.1 x 10^{-4}	2.4 x 10^{-4}	2.7 x 10^{-4}
	(0.035)	(0.040)	(0.045)	(0.050)
NaCl	2.1 x 10^{-3}	3.2 x 10^{-3}	1.1 x 10^{-2}	2.1 x 10^{-2}
	(0.40)	(0.60)	(2.0)	(4.0)
$CaCl_2$	1.2 x 10^{-4} M		1.4 x 10^{-4}	2.8 x 10^{-4}
	(0.023)		(0.026)	(0.053)

The usefulness of ions in controlling block copolymer morphology is also demonstrated when HCl is added to spherical micelles of PS(500)-*b*-PAA(60) in pure water, in which the PS cores are below their glass transition temperature. When HCl is added to a 1 weight % aqueous solution of the spherical copolymer aggregates to an acid content ~20 mM (R = 2), the solution gels over a very narrow acid content range. Electron microscopy shows that a "pearl necklace" morphology is formed, with occasional multifunctional "beads" maintaining the gelled network, as shown in Figure 6.2 for a sonicated solution of the gel. The "pearl necklace" morphology is, most likely, a result of the acid driving the spheres to form rods. However, the glassy nature of the PS cores of the beads makes it impossible to complete the transformation. The "pearl necklace" thus represents an intermediate step between the sphere and the rod.

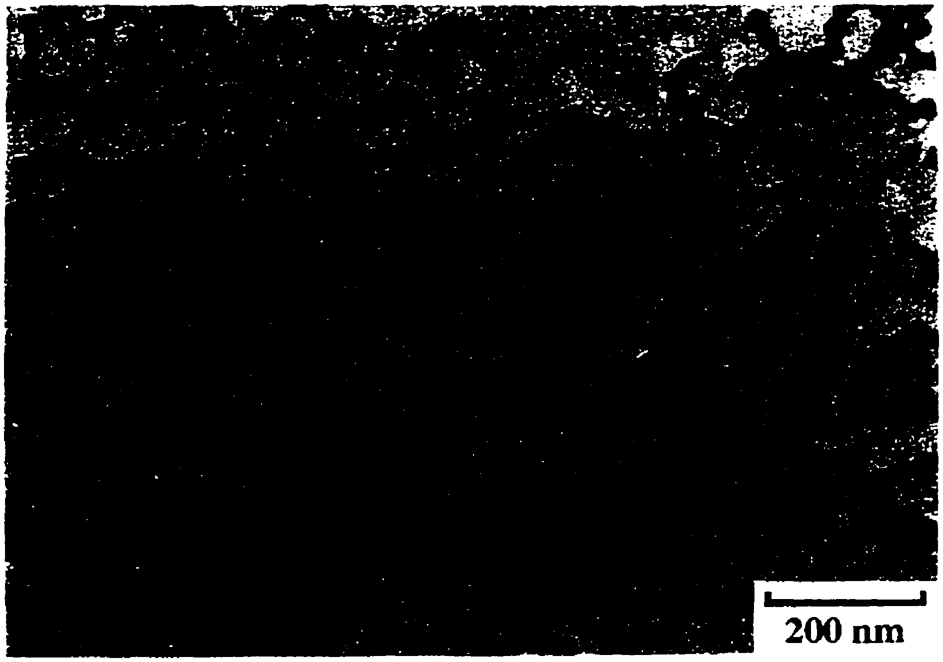

Figure 6.2. "Pearl necklace" morphology of the aggregates in the gelled aqueous solution of spherical micelles of PS(500)-*b*-PAA(60), induced by the addition of HCl (~ 20 mM). Sonication was used to break down the gel network structure for TEM sample preparation.

Ion-induced morphological changes were also found in the PS-*b*-PEO. For example, PS(240)-*b*-PEO(80) gives rods in the absence of salt but gives lamellae and vesicles in the presence of 1.3 mM LiCl (R = 0.10). Preliminary results suggest that the PS-*b*-P4VP.MeI [P4VP.MeI, poly(4-vinylpyridinium methyl iodide)] also yields multiple morphologies in the presence of salt. [6] The P4VP.MeI is ionic, the PAA is ionizable, and the PEO is non-ionic. Thus, the control of aggregate morphology of amphiphilic block copolymers by micromolar concentrations of ions seems to be general.

The LCVs appear to be a new morphology. They were also observed for PS(410)-*b*-PAA(13) with 255 μM HCl (R = 0.09) (Figure 6.3-A), for PS(240)-*b*-PEO(15) without any added salt (Figure 6.3-B) and for PS(240)-*b*-PEO(45) with 1.6 mM KF (R = 0.10). In the PS-*b*-PAA system, the thicknesses of both the inside and outside walls of the aggregates are uniform and equal. Their structure bears some resemblance to that of aggregated soap bubbles, and their outer surface must be hydrophilic because of the presence of the short PAA chains. The LCVs are irregular in shape in Figure 6.1-D but are more nearly spherical in Figure 6.3. These differences may be due to the polydispersity of the primary vesicles, the softness of the wall, as well as the surface energy and the shear conditions under which the LCVs were formed. The LCVs are subject to settling due to gravity, but they are very stable, and do not coalesce at room temperature. They can also be resuspended after settling. This aggregation process may provide an easy way to trap chemicals or drugs, and then separate them from the rest of the solution.

The self-assembly of vesicles has become a topic of current interest. [7] In that case, chemical species, that is, bis-phospholipids, were incorporated into the vesicle walls, to aid their aggregation into higher order (multivesicular) structures. As is shown here, the LCVs can be formed spontaneously under a range of conditions. They are thus a "normal" aggregate morphology. These higher order structures might be of interest in leading to new methods for processing artificial tissue-like composites and soft biomaterials. [7] In addition, controlled drug delivery appears as a distinct possibility since the multiple concentric layers might provide a convenient timing mechanism.

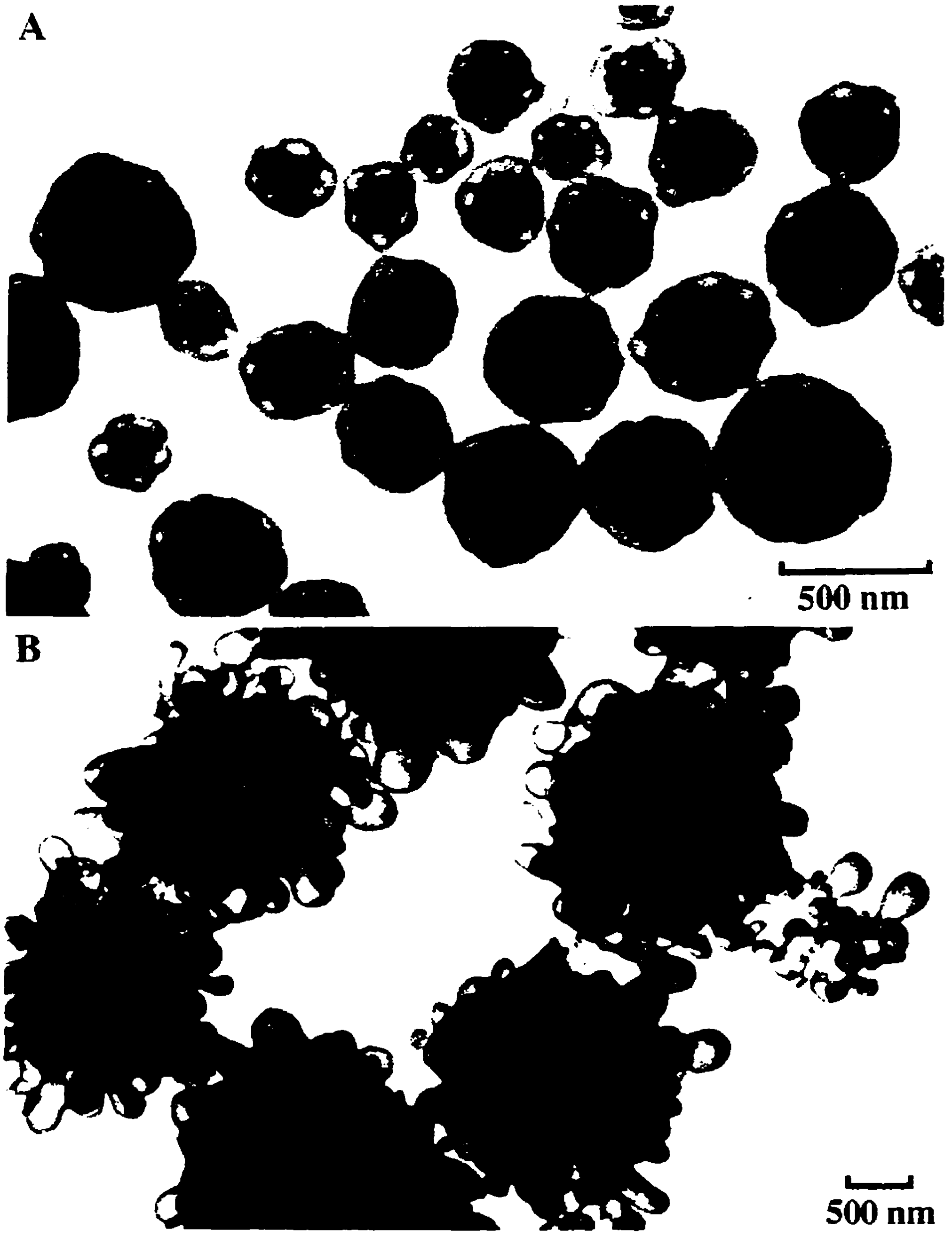

Figure 6.3. Large compound vesicles made from (A) PS(410)-*b*-PAA(13) in the presence of 255 μM HCl (R = 0.09) and (B) PS(240)-*b*-PEO(15) in the absence of salt.

The aggregate morphology of small molecule amphiphiles can be changed by added salt [8] but much higher salt concentrations are needed (usually $\geq 10^{-1}$ M) compared to that for the present system (10^{-4} M for $CaCl_2$ or 10^{-2} M for NaCl).

Changing the salt or acid content has a parallel effect on the morphology as changing the copolymer composition. [2,3] Thus, the morphological changes appear to be a result of a gradual decrease in repulsion among the corona chains as the concentration of added ions increases. Both steric and electrostatic repulsions are involved among the partially ionized PAA chains. [9] The addition of the strong acid, HCl, protonates the ionized carboxylic acid groups, and shifts the PAA to a lower degree of ionization; as a result, the overall repulsion among the PAA chains is decreased.

For $CaCl_2$, at the onset of the morphological transition from spheres to vesicles for PS(410)-*b*-PAA(25), the $CaCl_2$ concentration is equivalent to 2.3 Ca^{2+} per hundred acrylic acid repeat units; thus, two PAA blocks share one Ca^{2+} if all the added Ca^{2+} ions are near the PAA chains. When the aggregates are LCVs, the number of Ca^{2+} per PAA block is about 1.5. Thus, the morphogenic effect is believed to be due to Ca^{2+} binding to the carboxylic acid of the PAA. Both inter- and intra-molecular bridging appears possible. As a result, the effective distance between the PAA blocks is greatly reduced, which has the same effect on the morphology as a decrease in the block length. The relatively weaker morphogenic effect of added NaCl can be ascribed to both weak Na^{+} binding and a screened electrostatic field of the charged PAA segments. The morphological changes in PS-*b*-PEO are, very possibly, also caused by ion-binding to the PEO blocks.

6.3. ACKNOWLEDGMENT.

We thank H. Shen for his consent to report results of preliminary experiments of PS-*b*-P4VP.MeI system, and C. J. Clarke, M. Moffitt, and L. Cuccia for useful discussions. We also thank The Natural Sciences and Engineering Research Council of Canada(NSERC) for continuing support of this research.

6.4. REFERENCES AND NOTES

1. C. Price, in *Developments in Block Copolymers*, I. Goodman, Ed. (Applied Science, London, 1982), vol. 1, pp. 39-80; J. Selb, and Y. Gallot, *ibid.*, I. Goodman, Ed. (Applied Science, London, 1985), vol. 2, pp. 27-96; Z. Tuzar, and P. Kratochvil, in *Surface and Colloid Science*, E. Matijevic, Ed. (Plenum, New York, 1993), vol. 15, pp. 1-83; M. D. Whitmore and J. Noolandi, *Macromolecules* **18**, 657 (1985); A. Halperin, *ibid.* **20**, 2943 (1987); R. Nagarajan and K. Ganesh, *J. Chem. Phys.* **90**, 5843 (1989); R. Hilfiker, D. Q. Wu, B. Chu, *J. Colloid Interface Sci.* **135**, 573 (1990); A. P. Gast, P. K. Vinson, K. A. Cogan-Farinas, *Macromolecules* **26**, 1774 (1993); I. Astafieva, X. F. Zhong, A. Eisenberg, *ibid.* **26**, 7339 (1993); A. Qin, M. Tian, C. Ramireddy, S. E. Webber, P. Munk, *ibid.* **27**, 120 (1994); M. Antonietti, S. Heinz, M. Schmidt, C. Rosenauer, *ibid.* **27**, 3276 (1994); O. Glatter, G. Scherf, K. Schillén, W. Brown, *ibid.* **27**, 6046 (1994); L. Zhang, R. J. Barlow, A. Eisenberg, *ibid.* 28, 6055 (1995) (chapter 3 of this thesis).
2. L. Zhang and A. Eisenberg, *Science* **268**, 1728(1995) (chapter 4 of this thesis).
3. L. Zhang and A. Eisenberg, *J. Am. Chem. Soc.* **118**, 3168(1996) (chapter 5 of this thesis).
4. K. Yu and A. Eisenberg, *Macromolecules* **1996**, *29*, 6359.
5. A Phillips EM410 microscope was used for the TEM studies. Samples were deposited from aqueous solutions onto copper EM grids, which had been pre-coated with a thin film of Formvar and then coated with carbon; then, the grids were shadowed with palladium/platinum alloy. A detailed description of the experimental conditions can be found elsewhere.[3]
6. H. Shen and A. Eisenberg, unpublished results.
7. S. Chiruvolu *et al.*, *Science* **264**, 1753(1994).
8. S. Ozeki, S. Ikeda, *J. Colloid Interface Sci.* **87**, 424(1982); Y. Talmon, D. F. Evans, B. W. Ninham, *Science* **221**, 1047(1983); D. D. Miller, D. F. Evans, G. G.

Warr, J. R. Belare, B. W. Ninham, *J. Colloid Interface Sci.* **116**, 598(1987); F. J. Schepers, W. K. Toet, J. C. van de Pas, *Langmuir* **9**, 956(1993); B. J. Ravoo, J. B. F. N. Engberts, *ibid.* **10**, 1735(1994); A. Sein, J. B. F. N. Engberts, *ibid.* **11**, 455(1995); S. Miyagishi, H. Kurimoto, T. Asakawa, *ibid.* **11**, 2951(1995); L. L. Brasher, K. L. Herrington, E. W. Kaler, *ibid.* **11**, 4267(1995).

9. L. Zhang, H. Shen and A. Eisenberg, *Macromolecules* **1997**, *30*, in press (chapter 8 of this thesis).

Chapter 7

Morphogenic Effect of Added Ions on Crew-Cut Aggregates of Polystyrene-*b*-Poly(acrylic acid) Block Copolymers in Solutions

ABSTRACT

The morphology of crew-cut aggregates of amphiphilic block copolymers in dilute solutions can be controlled by the addition of ions in micro-molar (HCl, NaOH, $CaCl_2$, $Ca(Ac)_2$) or milli-molar (NaCl) concentrations. The copolymers are highly asymmetric polystyrene-*b*-poly(acrylic acid) diblocks, PS-*b*-PAA, in which the lengths of the insoluble PS blocks are much longer than those of the soluble PAA blocks. In addition to spherical, rod-like and uni-vesicular or lamellar aggregates, large compound vesicles (LCVs), a new morphology, can be obtained from a single block copolymer. The morphogenic effect of different added ions on the crew-cut aggregates can be ascribed to the changed repulsive interactions among the hydrophilic PAA segments, due to neutralization by NaOH, protonation by HCl, ion-binding or bridging by Ca^{2+}, and electrostatic screening by NaCl, respectively. The formation of the LCVs may involve a secondary aggregation of individual vesicles and a subsequent fusion process. Some features of the spontaneously formed LCVs may make them especially useful as drug delivering vehicles, and as models of biological cells.

7.1. INTRODUCTION

The self-assembly of highly asymmetric amphiphilic block copolymers in solutions has been receiving much attention in this laboratory [1-5] and in others. [6,7] The aggregates are "crew-cut" because their cores are made from long core-forming blocks, attached to much shorter corona-shell forming blocks. [8] For polystyrene (PS) based copolymers, [1-5] aggregates of this type were prepared by dissolving copolymers in a common solvent for both of the blocks, then adding water to induce the aggregation of the PS blocks. The aggregates were isolated into water by dialyzing the resulting solution. Due to the large fraction of the insoluble PS blocks in the copolymers and the resulting extremely low critical micellization concentration (cmc) as well as the glassy nature of the PS cores at room temperature, the structures of the aggregates are kinetically frozen and observable directly by electron microscopy. For polystyrene-*b*-poly(acrylic acid), PS-*b*-PAA, diblocks, it was found that in dilute solution aggregates of various morphologies can be made depending on the copolymer composition.[3] Specifically, as the length of the PAA block decreased, the aggregate morphology changed from spherical to rod-like, to lamellar or vesicular, and finally to large compound micelles (LCMs) consisting of an assembly of inverted spherical micelles surrounded by a hydrophilic surface. The morphology of the aggregates is undoubtedly a result of the interplay of several different factors during the formation of the aggregates. Most importantly is the force balance involving three factors, i.e. the deformation (stretching) of the PS blocks in the core, the surface tension between the core and the solvent, and the interactions among the corona chains. It was also shown that polystyrene-*b*-poly(ethylene oxide) diblocks, PS-*b*-PEO, in dilute solution, can also form aggregates of different morphologies from block copolymers of different compositions.[5]

Very recently, in a short report,[4] we described the phenomenon of added-ion-induced morphological changes in crew-cut aggregates of amphiphilic block copolymers. It was shown that the morphology of the aggregates made from an identical block copolymer can be controlled by the addition of ions in micro-molar ($CaCl_2$ or HCl) or milli-molar (NaCl) concentrations to the original solutions. Morphological changes at such low added ion contents are significant The morphologies are the same as those produced by changing in the copolymer composition in the absence of added ions. For PS-*b*-PAA copolymers, the morphogenic effect of added ions on the aggregates is probably a result of decreased repulsion among the PAA segments due to protonation (by HCl), or ion-binding or bridging (by Ca^{2+}). However, the added ion effect seems to be general because it has also been observed in systems of block copolymers in which the hydrophilic blocks are ionic (P4VP.MeI) or non-ionic (PEO). That report also described aggregates of a new morphology, i.e. large compound vesicles. These may be especially useful as possible drug delivery vehicles, and as models of stable microstructured biomaterials. In addition, an ion-induced gelation phenomenon was demonstrated in which spherical micelles in aqueous solution form a crosslinked "pearl necklace" structure in the presence of 20 mM HCl.

In this paper, we present a detailed study of the morphogenic effects of added ions on the crew-cut aggregates of polystyrene-*b*-poly(acrylic acid) diblocks in solutions of low molecular weight solvents.

7.2. EXPERIMENTAL SECTION

The copolymers used in this study are polystyrene-*b*-poly(acrylic acid) diblocks, PS-*b*-PAA. The anionic polymerization method used to synthesize the PS-*b*-PAA copolymers has been described previously in detail.[3] In the text, the copolymer samples are differentiated by the previously developed notation, i.e. PS(410)-*b*-PAA(25) represents a copolymer containing 410 styrene units and 25 acrylic acid units. All copolymers had a relatively narrow distribution of molecular weights, with a polydispersity index (M_w/M_n), estimated by gel permeation chromatography (GPC), in the range of 1.04 - 1.06.

To prepare aqueous solution of the crew-cut aggregates, the copolymers were first dissolved in N,N-dimethylformamide (DMF), a common solvent for both PS and PAA blocks, to give a stock solution. The stock solution was divided into several portions. Different amounts of salt, acid or base were added (as aqueous solutions) to each of the containers. Subsequently, deionized water was added dropwise to the copolymer solutions, with stirring. The increment of water content by each step of the water addition was 0.3 wt. % per 10 seconds. As the addition of water progressed, the quality of the solvent for the PS block decreased gradually. Micellization took place in the range of ca. 4 ~ 6 wt. % water in solution, as indicated by the appearance of turbidity. However, the addition of water was continued until 25 wt. % of water had been added, i.e. well after the aggregation occurred in order to make sure that the structure of the formed aggregates is kinetically frozen.[9] The aggregates were isolated into water by dialyzing the resulting solutions to remove the DMF. In the present studies, the initial polymer concentration in DMF (before the addition of water) was 1 wt. % for most of studies unless specified otherwise.

Transmission electron microscopy (TEM) was performed on a Phillips EM410 microscope operating at an acceleration voltage of 80 kV. To prepare TEM samples for the study of the size and the morphology of the aggregates, a drop of the dilute aqueous solution (about 1 mg/ml) was deposited onto a copper EM grid, which had been pre-coated with a thin film of Formvar and then coated with carbon. Two minutes after the deposition, the aqueous solution was blotted away with a strip of filter paper. Finally, the grids were shadowed with a palladium/platinum alloy.

Proton NMR spectra in solution were recorded on a Varian XL-200 spectrometer. Deuterated N,N-dimethylformamide (DMF-d_7, 99.5 % D; from Aldrich) was used as the solvent. Water was added directly to the polymer/DMF solutions in the NMR sample tubes with a microsyringe. Vigorous shaking homogenized the solution. All the experiments were performed at 18 ±0.2 °C. Tetramethylsilane served as the internal reference for the zero point of chemical shift, and the residual proton resonance of the solvent served as another internal reference, its chemical shift being set to 8.01 ppm. The chemical shift of the water protons was an average over the different types of water protons because of the fast exchange.

7.3. RESULTS

7.3.1. Effect of added acid on the aggregate morphology.

Figure 7.1 presents a set of TEM pictures which show aggregates of various morphologies prepared from the same diblock copolymer but with different amounts of added HCl. The copolymer is PS(410)-*b*-PAA(13) at an initial concentration 1 wt. % in DMF. Without the added acid, this polymer yielded small spherical micelles of low polydispersity with an average diameter of 31 nm (Figure 7.1-A). When the added HCl concentration was 113 μM (or a molar ratio, R, of added HCl to acrylic acid repeat units of 0.04), the aggregates were still spherical (Figure 7.1-B), but with an average diameter of 37 nm. However, as the HCl concentration was increased to 141 μM (R = 0.05), vesicular aggregates started to form; most of the aggregates were still spherical (Figure 7.1-C). As the added acid concentration was increased further to 155 μM (R = 0.055), most of the aggregates became vesicular (Figure 7.1-D). When the HCl concentration reached 170 μM (R = 0.06), the aggregates were still vesicular, but the average size increased (Figure 7.1-E). When the HCl concentration was 200 μM (R = 0.07), most of the aggregates became tubular or elongated vesicles (Figure 7.1-F), with many small vesicles seen in the background. At an HCl concentration of 225 μM (R = 0.08), large compound vesicles (LCVs) were formed (Figure 7.1-G). The same morphology was observed at an HCl content of 253 μM (R = 0.09), but the aggregates became more spherical, the average size decreased, and the structure became more dense. A schematic cross-section of these multi-vesicular aggregates is shown in Figure 7.1-I.

When acetic acid was used instead of HCl as the additive for this block copolymer solution, it was found that even an acetic acid concentration up to 4 mM (R=0.8) showed no effect on the morphology. The aggregates were still spherical.

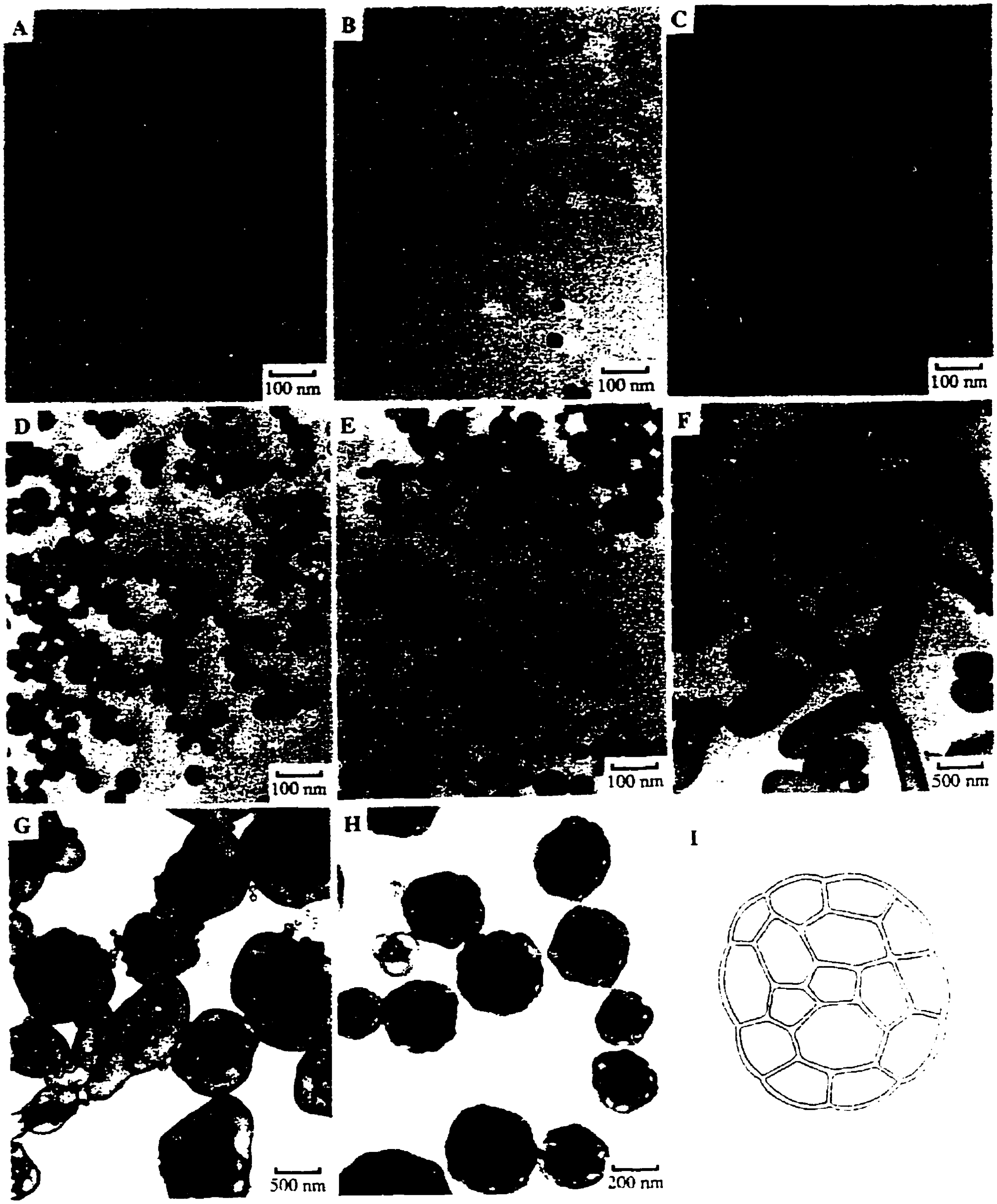

Figure 7.1. Aggregates from PS(410)-*b*-PAA(13) without any additive (A), and with added HCl to different final concentrations: (B) 113 μM (R = 0.04), (C) 141 μM (R = 0.05), (D) 155 μM (R = 0.055), (E) 170 μM (R = 0.06), (F) 200 μM (R = 0.07), (G) 225 μM (R = 0.08), (H) 253 μM (R = 0.09), and (I) a schematic picture of the cross-section of an LCV in (H).

7.3.2. Effect of added NaOH on the aggregate morphology.

Addition of NaOH can also induce morphological changes. Figure 7.2 shows the TEM pictures of the aggregates prepared without and with the addition of different amounts of NaOH. The copolymer is still PS(410)-*b*-PAA(13), but at a 2 wt. % concentration in DMF. As shown in Figure 7.2-A, at that concentration and without any added NaOH, the copolymer yielded vesicular aggregates. However, when the NaOH concentration was 28 μM (R = 0.005), Figure 7.2-B shows that most of the aggregates became spherical with an average diameter 38 nm, while vesicles were only observed occasionally. As the NaOH concentration was increased to 56 μM (R = 0.01), the aggregates were spherical with an average diameter 35 nm (Figure 7.2-C). At a NaOH concentration of 115 μM (R = 0.02), the average diameter decreased further to 33 nm.

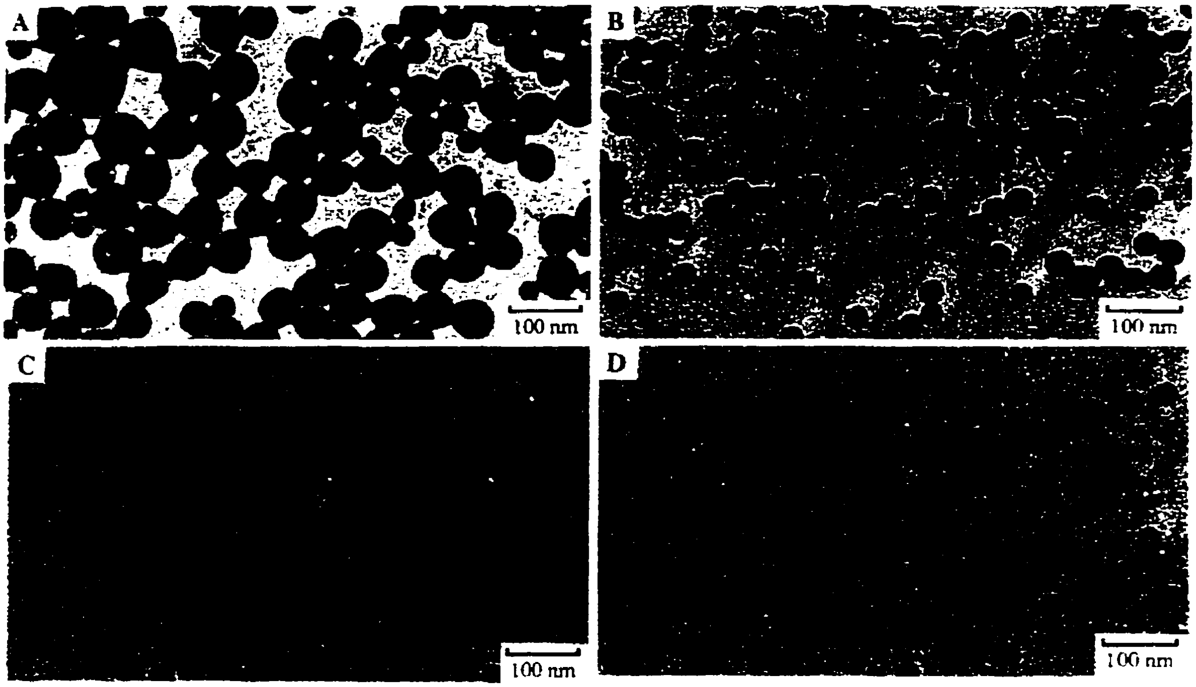

Figure 7.2. Aggregates from PS(410)-*b*-PAA(13) without any additive (A), and with added NaOH to different final concentrations: (B) 28 μM (R = 0.005), (C) 56 μM (R = 0.01), (D) 115 μM (R = 0.02).

7.3.3. Effect of added salt on the aggregate morphology.

The aggregate morphology can also be changed by the addition of salt. It was found that the effect of di-valent ions, e.g. Ca^{2+}, is much stronger than that of univalent ions, e.g. Na^+. Figure 7.3 shows that the morphology changes progressively as a function of added NaCl concentration. The copolymer is PS(410)-*b*-PAA(25) with an initial concentration of 1 wt. % in DMF. Specifically, without added salt, the copolymer formed spherical aggregates with an average diameter 29 nm (Figure 7.3-A). When the concentration of added NaCl was 1.1 mM (R = 0.2), the aggregates were spherical with an average diameter 33 nm (Figure 7.3-B). At a NaCl concentration of 2.1 mM (R=0.40), the average diameter of the aggregates increased further to 37 nm (Figure 7.3-C). When the NaCl concentration was increased to 3.2 mM (R = 0.6), the aggregates became cylindrical (Figure 7.3-D). In the concentration range of 4.0 to 10.6 mM NaCl (R = 0.8 to 2.0), cylindrical and vesicular aggregates coexisted. However, as the NaCl concentration was increased, the majority of the aggregates shifted from cylindrical to vesicular and the overall size of the vesicles increased progressively (Figure 7.3-E to G). When the NaCl concentration was increased to 16 mM (R = 3.0), the aggregates became large vesicles with diameters up to 400 nm, while rod-like aggregates were observed only rarely (Figure 7.3-H). Finally, LCVs were formed when the NaCl concentration was above 21 mM (R = 4.0) (Figure 7.3-I). Table 7.1 summarizes the given dominant morphologies of the aggregates made from different copolymers vs. the added NaCl concentration.

When $CaCl_2$ was added instead of NaCl, it was found that much lower concentrations of the added salt were needed to induce morphological transitions. Figure 7.4 shows the morphologies as a function of added $CaCl_2$ concentration. The copolymer is PS(410)-*b*-PAA(13). As mentioned earlier, without added ions, the aggregates were spherical with an average diameter of 31 nm (*cf.* Figure 7.1-A). When the added $CaCl_2$ concentration was 71 μM (R=0.025), the micelles were still filled spheres, but their average size increased to 39 nm (Figure 7.4-A). When the $CaCl_2$ concentration was 85 μM (R=0.03), the copolymers started to form vesicles, while most of the aggregates were still spherical (Figure 7.4-B).

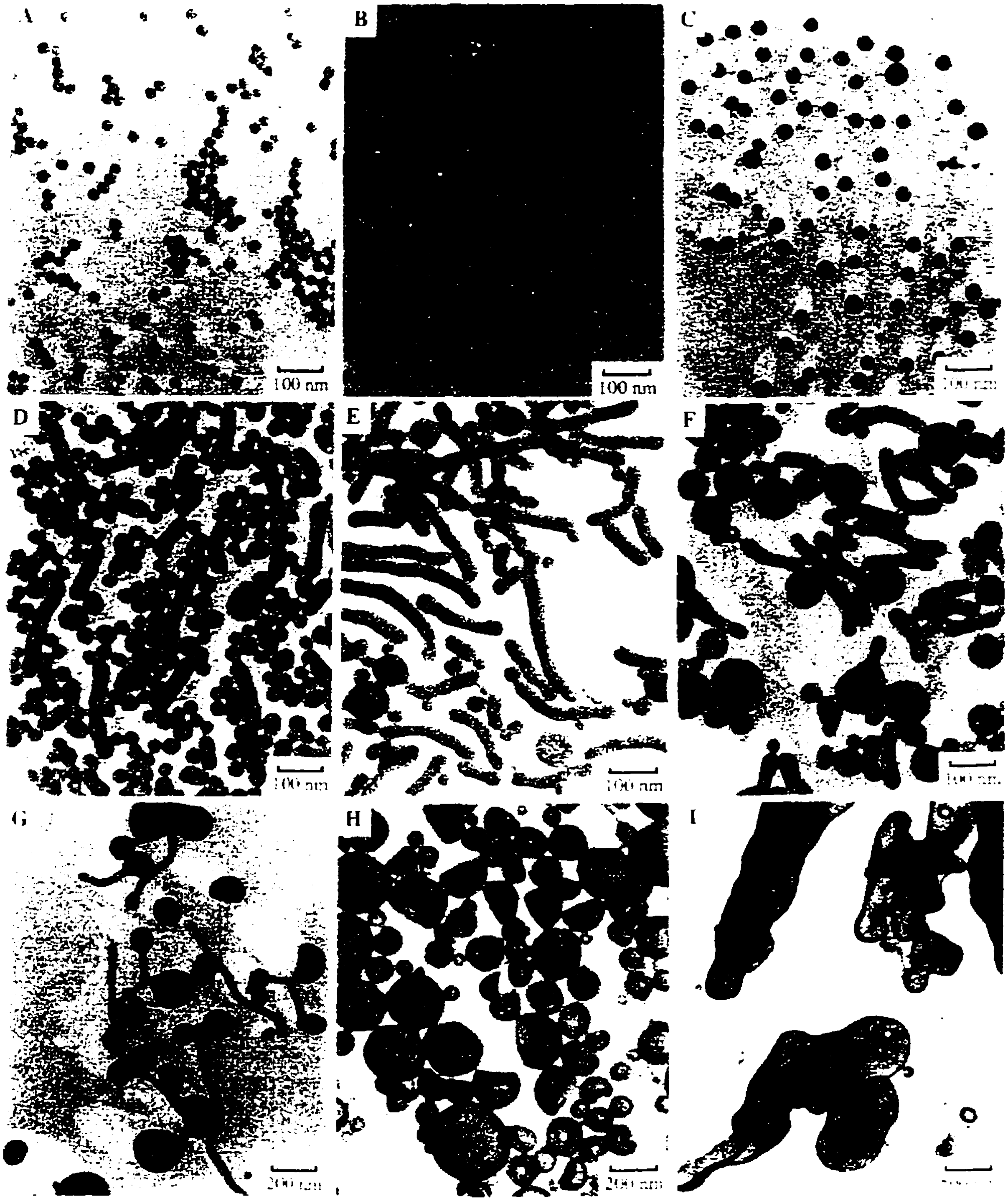

Figure 7.3. Aggregates from PS(410)-*b*-PAA(25) without any additive (A), and with added NaCl to different final concentrations: (B) 1.1 mM (R = 0.20), (C) 2.1 mM (R = 0.40), (D) 3.2 mM (R = 0.60), (E) 4.3 mM (R = 0.80), (F) 5.3 mM (R = 1.0), (G) 10.6 mM (R = 2.0), (H) 16.0 mM (R = 3.0), and (I) 21 mM (R = 4.0).

Table 7.1. Summary of the effect of added NaCl (mole/litre) on the aggregate morphology. The initial copolymer concentration in DMF is 1 wt. %. The numbers in parentheses represent the molar ratio of added NaCl to acrylic acid.

Copolymer	Dominant Morphology			
PS-*b*-PAA	Spheres	Rods	Vesicles	LCVs
410-*b*-13	$< 2.3 \times 10^{-3}$ (0.80)		$2.8 \sim 4.2 \times 10^{-3}$ (1.0 ~ 1.5)	5.6×10^{-3} (2.0)
410-*b*-25	$< 2.1 \times 10^{-3}$ (< 0.40)	$3.2 \sim 5.3 \times 10^{-3}$ (0.60 ~ 1.0)	$5.3 \sim 16 \times 10^{-3}$ (1.0 ~ 3.0)	2.1×10^{-2} (4.0)
660-*b*-24	$< 4.8 \times 10^{-3}$ (< 1.7)	5.7×10^{-3} (2.0)*	$5.7 \sim 8.5 \times 10^{-3}$ (2.0* ~ 3.0)	1.1×10^{-2} (4.0)

* At this NaCl concentration, rod-like micelles and vesicles coexist almost evenly.

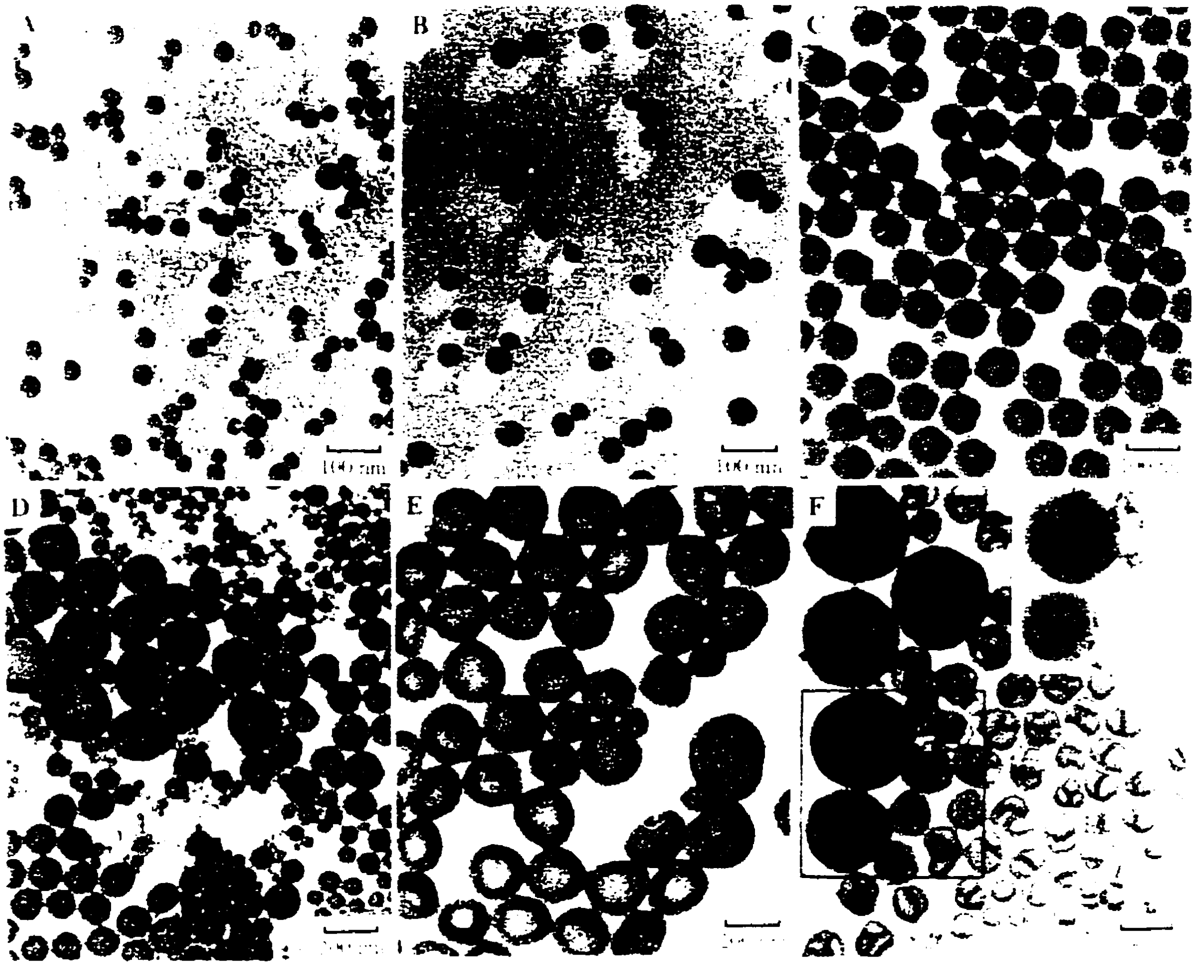

Figure 7.4. Aggregates from PS(410)-*b*-PAA(13) with added $CaCl_2$ to different final concentrations: (A) 71 μM (R = 0.025), (B) 85 μM (R = 0.03), (C) 90 μM (R = 0.032), (D) 99 μM (R = 0.035), (E) 115 μM (R = 0.04), and (F) 130 μM (R = 0.045).

When the $CaCl_2$ concentration was between 90 and 115 μM (R=0.032 and 0.04), the copolymer yielded vesicles (Figure 7.4-C to E); however, with increasing the $CaCl_2$ concentration, the average size of the vesicles increased rapidly, e.g. with outer diameters up to 300 nm in Figure 7.4-E. Finally, spherical LCVs were formed when the $CaCl_2$ concentration was between 130 and 170 μM (R = 0.045 and 0.06). One example is given in Figure 7.4-F, which also shows a range of aggregates, the structures of which are intermediate between uni-vesicular and LCV. For the different copolymers, the observed dominant morphologies of the aggregates at various concentrations of added $CaCl_2$ are summarized in Table 7.2.

Table 7.2. Summary of the effect of added $CaCl_2$ and $Ca(Ac)_2$ (mole/litre) on the aggregate morphology. The initial copolymer concentration in DMF is 1 wt. %. The numbers in parentheses represent the molar ratio of added $CaCl_2$ or $Ca(Ac)_2$ to acrylic acid.

Copolymer PS-*b*-PAA	Additive	Dominant Morphology			
		Spheres	Vesicles	LCVs	LCMs
410-*b*-13	$CaCl_2$	$< 8.5 \times 10^{-5}$ (< 0.03)	$9.0 \sim 11 \times 10^{-5}$ ($0.032 \sim 0.04$)	$1.3 \sim 1.7 \times 10^{-4}$ ($0.045 \sim 0.06$)	
	$Ca(Ac)_2$	$<2.8 \times 10^{-4}$ (< 0.10)			4.0×10^{-4} (0.14)
410-*b*-25	$CaCl_2$	$< 1.2 \times 10^{-4}$ (< 0.023)	$1.4 \sim 2.0 \times 10^{-4}$ ($0.026 \sim 0.038$)	$2.4 \sim 4.8 \times 10^{-4}$ ($0.045 \sim 0.09$)	
	$Ca(Ac)_2$	6.5×10^{-4} (< 0.12)			8.1×10^{-4} (0.15)

The effect of added $Ca(Ac)_2$ on the aggregate morphology was also explored. For the case of PS(410)-*b*-PAA(25) copolymers, it was found that when the concentration of added $Ca(Ac)_2$ was 650 μM (R=0.12), the aggregates were still spherical with a slightly increased average diameter 30 nm (compared to an average diameter 29 nm of the micelles prepared without added ions). However, when $Ca(Ac)_2$ concentration was 810 μM (R=0.15), the aggregates became much more polydisperse and contained many particles with the diameters over 100 nm. As the added $Ca(Ac)_2$ concentration was increased further, the aggregates became highly polydisperse, and spheres of several hundred nm in diameter were formed. These large spheres cannot possible be primary spherical micelles. They appear to be large compound micelles (LCM) consisting of many inverted spherical micelles surrounded by a hydrophilic surface. The results of added $Ca(Ac)_2$ are also summarized in Table 7.2 for different copolymers.

7.3.4. Solution NMR study. Figure 7.5 shows three typical NMR spectra of PS(180)-*b*-PAA(28)/DMF solutions. Spectrum A was recorded before the addition of water. All three proton peaks originate from the residual protons in the DMF. From the relative intensities of these peaks, the doublet peaks between 2.5 and 3 ppm can be ascribed to the methyl protons in DMF. The single peak at 8 ppm is due to the single proton bonded to the carbon atom. Spectrum B was recorded when the added water concentration was about 0.6 wt. %. Obviously, the new peak at ca. 3.8 ppm is due to the water protons. Spectrum C was obtained from the same solution, but with an added water content of 6 wt. %. Compared to spectrum B, the peak of the water protons narrowed and its position shifted from 3.8 to 4.0 ppm. Furthermore, splitting of the lines was observed although the side peaks are very weak relative to the major peak.

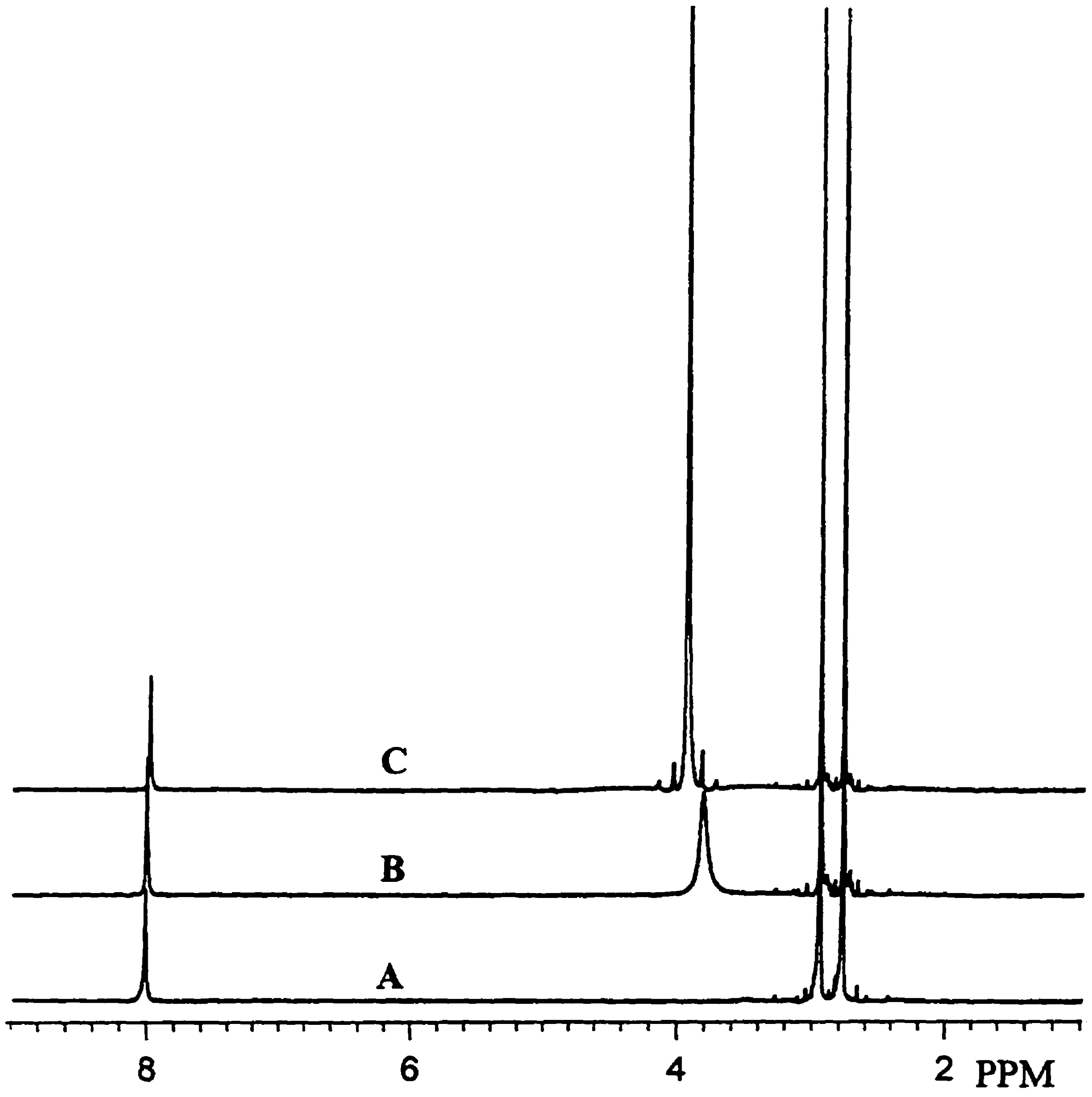

Figure 7.5. Three typical proton NMR spectra from PS(180)-*b*-PAA(28)/DMF solution before the addition of water (A), and after the addition of water to 0.6 wt. % (B) and 6 wt. % (C). The copolymer concentration in DMF is 0.1 wt. %.

7.4. DISCUSSION

7.4.1. Comparison of the morphogenic effect of added ions in amphiphilic diblocks to those in small molecule surfactants.

It is known that one can change the morphologies of aggregates of small molecule surfactants by adding electrolytes.[10,11] In ionic[12-14] and nonionic[15,16] surfactants, it was reported that the addition of salt, e.g. alkali metal chloride, can change the aggregate morphology from spheres to rods, or from rods to vesicles, etc. The changes of aggregate morphology are a result of reduced electrostatic repulsion among charged headgroups due to counterion binding. In those surfactant systems, the added mono-valent salt concentration is usually in the range of 10^{-1} moles to several moles per liter. The effect of added electrolytes also depends on the structure of the surfactant head group, the length of the hydrophobic chain, etc. Usually, the strength of the added salt effect increases as the valence of the salt ions increases, but decreases with increasing length of hydrophobic chain.[17-19] The importance of electrostatic interactions among head groups on the phase behavior of surfactant system has been demonstrated in studies of the aggregate structures made from mixtures of anionic and cationionic surfactants.[20,21]

Similarly, changing the pH of the solution can also affect the aggregation behavior. In the monoalkyl disodium phosphates,[22] thermally stable unilamellar vesicles with diameters between 25 and 60 nm were formed at room temperature. Lowering the pH leads to partial protonation of the phosphate headgroup and to decrease of the electrostatic repulsion among the headgroups. This results in large vesicle diameters (50 to 100 nm). The effect of added $CaCl_2$ was also described. [22] It was found that a large increase in the tendency of the vesicles to aggregate was induced when the added $CaCl_2$ concentration was > 0.5 mM.

To our knowledge, ion-induced morphological changes have not been reported before in solutions of block copolymer aggregates. For the present system, it has been shown that the addition of electrolytes can change the aggregate morphology progressively from spheres to rods, to vesicles, and to large compound vesicles. The added electrolyte concentrations at the onset of the morphological transitions are only of the order of 10^{-4} moles for $CaCl_2$, NaOH and HCl, and 10^{-3} moles for NaCl. It should be recalled that once the aggregates are formed, the copolymer chains are no longer uniformly distributed in the solution. Thus, the acrylic acid units are confined to spherical corona shells around the micelle cores in the spherical micelles; similar considerations also apply to the other geometries. In the corona shell, the concentration of acrylic acid repeat units are estimated to be ~ 1 M. Under these circumstances, if the microions are distributed evenly in the whole solution, the acrylic acid concentration in the corona shell is about two orders of magnitude higher than that of the NaCl, and about three orders of magnitude higher than that of the $CaCl_2$. Ion-induced morphological changes in the block copolymer aggregates at such low ion contents are significant. As will be shown in the following section, water preferentially accumulates to some extent around the PAA segments during the formation of the aggregates, i.e. the water content in the PAA corona shell is higher than that in the rest regions of the solution. Therefore, there may be some enrichment of the added ions in the corona shell as well, considering that the ions are most likely more soluble in the water rich regions than in the water depleted regions. The degree of enrichment of the added ions around the PAA segments is difficult to estimate. However, even if all the added ions were to accumulate around the PAA segments, the effect is still very strong, especially in view of the fact that a concentration change by less than 20 μM of $CaCl_2$ or HCl can induce morphological changes, e.g. from spheres to vesicles for the aggregates of PS(410)-*b*-PAA(13) copolymer. In the following section, we will discuss the possible causes of the effect of the addition of different electrolytes on the morphology of the block copolymer aggregates.

7.4.2. Cause of the added ion effect on the aggregate morphology.

The detailed causes of the effect of added ions on the aggregate morphology probably differ for different additives. However, in general, the effect must be related to the influence of the added ions on the force balance during the formation of the aggregates. Although many factors undoubtedly enter into the force balance, the aggregate morphology is mainly controlled by three factors, i.e. the extension (stretching) of the PS blocks in the core, the surface tension between the core and the solvent, and the repulsion among the corona chains.[3] Specifically, when the inter-chain repulsive interactions become weaker, the aggregate sizes can increase in order to decrease the interfacial energy between the core and the solvent. However, the increase of the core size is restricted by an entropic penalty resulting from the stretching of the PS blocks. At some point, as the strength of the repulsive interactions among corona chains decreases and the stretching of the PS chains increases, the aggregates change their morphology from spherical to rod-like, and from rod-like to bilayer in order to reduce entropic penalty due to PS chain stretching. Therefore, the repulsion among the PAA corona chains, especially if they are partially ionized, plays a considerable role in determining the final morphology of the aggregates. Certainly, the added ions may also affect the surface tension between the core and the solvent in the course of aggregate formation. However, the strength and direction of this effect is not clear.

7.4.2.1. Micro-environments of the PAA chains during micellization. Before we discuss the influence of the added ions on the repulsion among the corona chains, it is very helpful to explore qualitatively the change in the micro-environment of the PAA segments in the course of water addition. The information about the distribution of added water in the solutions can be obtained by analyzing the line widths of the water proton NMR spectra. The study is based on the difference in mobility between the water molecules and the polymer chains in solution. Usually, small molecules show a very narrow resonance peak because of their high mobility, while polymer chains give relatively broad NMR peaks because of their high molecular weight and low mobility. Thus, if the added water molecules bond to (or interact with) polymer chains, their mobility is decreased, and the NMR peak will be broadened as a result of this interaction. If, on the other hand, added water molecules distribute themselves evenly in the solution, their mobility should not be affected at all because the major component of the solution, DMF, is also a small molecule. Figure 7.6 shows a plot of the full-width at half-height (FWHH) of the water proton NMR peak against the added water content in solutions. For both the DMF solvent and the homopolystyrene/DMF solution, as the water content increased, the FWHH of the water proton peak did not change very much, indicating that the water molecules were generally distributed evenly in the solutions. There was evidently no strong interaction between water molecules and homopolystyrene chains. However, for the block copolymer/DMF solution, it was found that the FWHH of the water proton peak was very large at low water contents, and then decreased as the water content increased. The broadened peak of water protons in this case must be a reflection of the interaction between water molecules and the PAA segments as a result of which the mobility of water molecules is reduced. This suggests that, to some extent, the added water accumulated preferentially near the PAA blocks. Therefore, although the micellization usually started at a water content around 5 wt. %, the local water concentration around the PAA blocks could actually be higher than the overall water concentration in the solution. On the basis of the above fact, we now address the question of how the added ions affect the repulsion among the PAA blocks (corona chains).

7.4.2.2. Effect of added acid or base on inter-corona-chain repulsion. Since the water is preferentially distributed around the PAA segments, the PAA blocks probably behave in a manner similar to that in aqueous solutions, i.e. they are partially ionized. If the acrylic acid were distributed uniformly in the solution, then the concentration of acrylic acid units in a 1 wt. % copolymer solution would be about 3 to 5 mM, depending on the copolymer composition. The degree of the ionization is about 10 ~ 13 % as calculated from a pKa of 4.25 for propionic acid in water. However, we are dealing not with pure water, but a DMF/water mixture. Also, the PAA blocks are confined to the coronal shells.

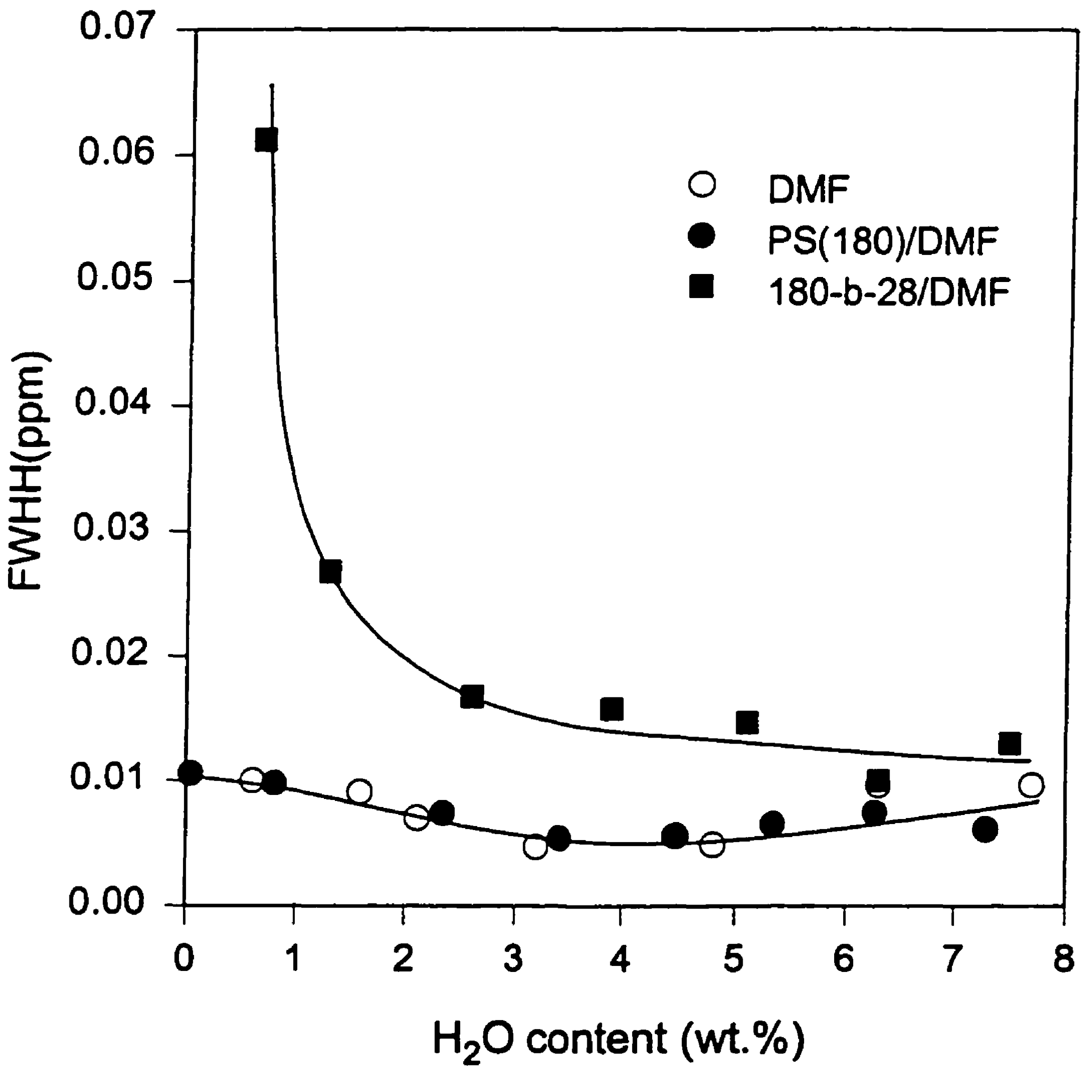

Figure 7.6. A plot of the full width at half height (FWHH) of the water proton NMR peak against the added water content in (○) DMF solvent, and in solutions of (●) 1.0x10^{-3} (g/g) PS(180) in DMF and (■) 1.0x10^{-3} (g/g) PS(180)-*b*-PAA(28) in DMF. The lines are shown as a guide for the eye.

Thus, the dissociation of the PAA may be different, and is most likely lower. In any case, because HCl is a strong acid and the acrylic acid is a weak acid, the addition of HCl protonates the ionized carboxylic acidic units of the PAA blocks, leading to a still lower degree of ionization. As a result, the charge density of the PAA blocks decreases, and the overall (both electrostatic and steric) repulsion among the corona chains decreases as well. When acetic acid was added instead of HCl, it showed only a very weak morphogenic effect on the aggregates. For PS(410)-*b*-PAA(25) copolymer, an addition of 210 μM HCl (R=0.04) changed the aggregate morphology from spherical to rod-like. However, when acetic acid was added, the aggregates were still spherical even when the concentration of added acetic acid was increased to 4 mM (R=0.8). This may be due to the fact that acetic acid is a weak acid (pKa = 4.74), and its effect on the ionization of the PAA blocks is very weak.

When NaOH was used as an additive, the morphology was found to change in an opposite direction i.e. from vesicles to spheres, and then to smaller spheres with increasing NaOH concentration. This effect is not surprising, since the added NaOH neutralizes the PAA segments. As a result, the degree of ionization and the coil dimension of the PAA blocks and the repulsion among the PAA corona chains are increased.

The effect of added HCl on the aggregate morphology was further explored by using PS(410)-*b*-PAA(25) copolymers in which the PAA segments had been pre-neutralized to a degree of 5 % by using NaOH. To neutralize the PAA blocks, the copolymers were dissolved in tetrahydrofuran (THF), and a NaOH/methanol solution was added. The copolymers were then precipitated into methanol and dried under vacuum at 60 °C. The dominant morphologies of the aggregates for various added HCl concentrations are summarized in Table 7.3. Because neutralization increases the degree of ionization of the PAA segments, a higher concentration of added HCl was needed. One can see that the pre-neutralization of the PAA blocks by NaOH only shifts the morphological transitions to a higher HCl contents, but that the overall amount of HCl needed to change the morphology from spheres to LCVs remains practically the same.

Table 7.3. Summary of the effect of added HCl (mole/litre) on the aggregate morphology of a PS(410)-*b*-PAA(25) diblock copolymer with and without pre-neutralization. In the table, numbers in parentheses represent the molar ratio of added HCl to acrylic acid.

$\frac{M_{NaOH}}{M_{PAA}}$	Dominant Morphology			
	Spheres	Rods	Vesicles	LCVs
0	1.9×10^{-4} (0.035)	2.1×10^{-4} (0.040)	2.4×10^{-4} (0.045)	2.7×10^{-4} (0.050)
0.05	4.5×10^{-4} (0.085)	4.9×10^{-4} (0.092)	5.1×10^{-4} (0.095)	5.6×10^{-4} (0.105)

7.4.2.3. Effect of added salt on inter-corona-chain repulsion. The effect of added $CaCl_2$ on the aggregate morphology is remarkably strong. From Table 7.2 and 7.3, one can see that changes in the aggregate morphology can be achieved with much lower concentrations of $CaCl_2$ than of NaCl. At the onset of the morphological transition from spheres to vesicles for PS(410)-*b*-PAA(25), the total amount of $CaCl_2$ in the solution was equal to 2.3 calcium cations per hundred acrylic acid repeat units. In that case, even if all the added Ca^{2+} ions were to interact with the hydrophilic chains, on average two PAA blocks would be sharing one Ca^{2+}. When the aggregates are LCVs, the number of Ca^{2+} ions per PAA block is about 1.5. The morphogenic effect appears to be caused by strong Ca^{2+} binding and bridging to the carboxylate groups of the PAA segments. Because of this ion binding or bridging, a simultaneous HCl effect may also be involved. This speculation is based on the following consideration: Ca^{2+} binding is essentially a reaction of the Ca^{2+} with carboxylic acid groups of the PAA chains to form calcium acrylate. In the process, protons are released. Because the counter anions are Cl^- (rather than carboxylate), the released protons will suppress the dissociation of the PAA segments, an effect similar to that of added HCl. Therefore, it is very possible that the strong morphogenic effect of added $CaCl_2$ on the aggregates is a combined result of calcium ion binding and protonation.

For $Ca(Ac)_2$, strong calcium ion binding and bridging are still operative. However, the protons produced as a result of the ion binding and bridging can combine with the acetate anions to yield acetic acid molecules, the morphogenic effect of which is very weak. From another point of view, the addition of $Ca(Ac)_2$ does not affect the ionization (or charge density) of the PAA segments appreciably because acetic acid is a weak acid. Therefore, the effect of added $Ca(Ac)_2$ on the aggregate morphology is mainly a result of the Ca^{2+} binding and bridging to the PAA segments. As was shown in Section 3.3., when the added $Ca(Ac)_2$ concentration was 650 μM (R=0.12), the aggregates were still spherical and the average core diameter changed only very little. As the concentration was increased further, for example, to 810 μM (R=0.15), the morphology changed directly from small primary spherical micelles to large compound spherical micelles (LCMs). No intermediate morphologies, i.e. rod-like or vesicular, were observed.

The formation of LCMs can be related to the phase separation behavior of the copolymer/DMF solution as the aqueous $Ca(Ac)_2$ is added. Light scattering studies [8] showed that when the added $Ca(Ac)_2$ concentration in a 1 wt.% PS(410)-*b*-PAA(25) solution was below 650 μM (R=0.12), the copolymers were still dispersed as single chains at a water content of 3 wt. %. Subsequent addition of more water (at constant $Ca(Ac)_2$ concentration) induced PS block aggregation. However, when the added $Ca(Ac)_2$ concentration was increased to 810 μM (R=0.15) (at a water content of 3 wt. %), the PAA blocks of the copolymer started to self assemble to form reverse micelle-like aggregates; adding more water at that point induced PS block aggregation also, which produced the large compound micelles (LCMs). The degree of reverse micelle-like aggregation increased further as the added $Ca(Ac)_2$ concentration was increased, which resulted in the formation of LCMs of increased size. The formation of reverse micelle-like aggregates is thus most likely due to the interactions of the added $Ca(Ac)_2$ with acrylic acid units, i.e. binding and bridging, leading to the formation of calcium acrylate. As the fraction of calcium acrylate in the PAA segments increases, the PAA blocks become less soluble, and finally aggregate. Therefore, in view of the relationship between the aggregate morphology and the added $Ca(Ac)_2$ concentration, the formation of LCMs can be ascribed to the presence of reverse micelle-like aggregation, not an increased degree of stretching of the PS blocks in the core. This possibility can also be deduced from changes of the average core diameter of the spherical micelles before the morphological transition occurs, which will be discussed in section 4.3.1. It is worth mentioning here that the phase separation behavior of copolymer/DMF solutions accompanying the addition of aqueous solutions of NaCl, or NaOH, or $CaCl_2$ was also examined. [9] It was found that in the additive concentration range employed in the present study, the addition of NaCl, $CaCl_2$, or NaOH does not induce reverse micelle-like aggregation of the copolymers.

When compared to $CaCl_2$ and $Ca(Ac)_2$, the effect of NaCl is much weaker. The weaker effect on the morphology can be ascribed to a weak Na^+ binding to the PAA segments given that sodium acrylate is a strong electrolyte. The effect is possibly a screened electrostatic field of the partially charged PAA segments in the presence of NaCl.

7.4.3. Stability and characteristics of the various aggregates.

In this section, we discuss the regions of stability of the aggregates of different morphologies in DMF/water mixtures as well as some of their characteristics in water.

7.4.3.1. Spherical micelles. In the absence of added ions, it was reported in previous papers [2,3] that the average core radii of spherical micelles vary with copolymer composition according to

$$R_{core} \sim N_A^{0.4} N_B^{-0.15}$$

where N_A and N_B are the degrees of polymerization of the PS and PAA blocks, respectively. For copolymers with a PS block of constant length, equation 1 implies that the shorter the PAA block, the larger the spherical micelle core. In the present system, for a single block copolymer, the core sizes of the spherical micelles depend on the concentration of added ions. Thus, changing the added ion concentration has a parallel effect on the aggregate morphology as changing the copolymer composition. Figure 7.7 shows a plot of the average core diameters of the spherical micelles as a function of the concentrations of the different additives.[23] Clearly, the changes of micelle core sizes are not a linear function of the additive concentration. For HCl or NaCl, as the additive concentration increases, the core size increases at first relatively slowly, then more rapidly and finally the morphology of the aggregates changes. For NaOH, the average diameter of the micelles decreases as the added NaOH concentration increases at first rapidly, and then more slowly. The changes in the PS core dimensions are a result of the fact that the addition of NaOH increases the repulsive interactions among the corona chains, while added HCl or NaCl decreases the inter-chain repulsion. The rapid change of the micelle core sizes just before or after the morphological transition suggests that the thermodynamic penalty from the PS block stretching is largely responsible for the morphological transition.

In the case of added $Ca(Ac)_2$, the core sizes of the small spherical micelles change only slightly as the concentration of added $Ca(Ac)_2$ increases (Figure 7.7-B). Before the morphological transition from small spherical micelles to LCMs, the average core diameter is only around 30 nm, while for the other additives, i.e. HCl, NaOH or NaCl, the values are around 38 nm. This implies that the penalty from the PS block stretching in the cores is not crucial at this core dimension. Therefore, the morphological transition from spherical micelles directly to LCMs by addition of $Ca(Ac)_2$, as discussed in section 4.2.3, appears to be due to the formation of reverse micelle-like aggregates, rather than an increased degree of PS block stretching.

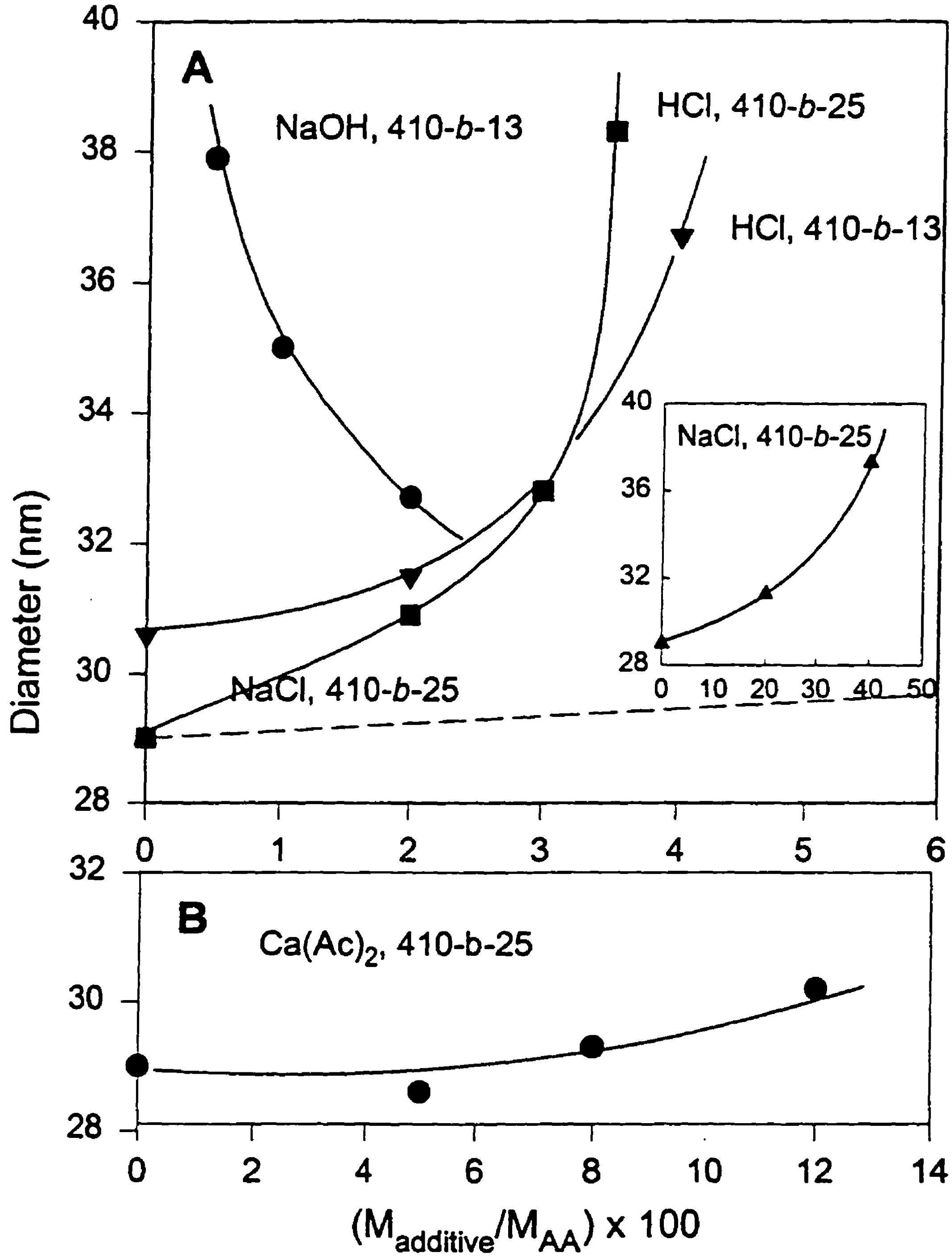

Figure 7.7. Plot of the average core diameter (D/nm) versus molar ratio of the different additives to acrylic acid repeat units ($M_{additive}/M_{AA}$) for spherical micelles from different block copolymers. The type of the additive and the copolymer are indicated near each curve. For the NaOH effect, the initial copolymer concentration in DMF was 2 wt. %. For the others, the initial concentration was 1 wt. %. The lines are shown as a guide for the eye.

7.4.3.2. Aggregates of other morphologies. As the concentration of added acid or salts increases, the core diameter of the spherical micelles increases. At some point, the aggregates change their morphology progressively from spheres to rods, to vesicles, and eventually to LCVs, in order to reduce the entropic penalty due to the stretching of the PS chains in the micelle core. Therefore, along with the morphological changes, the dimensions of PS cores change also. The addition of NaCl to PS(410)-*b*-PAA(25) copolymer solution (*cf.* Figure 7.3) provides a typical example. When added NaCl concentration is 2.1 mM (R=0.4), the core diameter of the spherical micelles increases to 37 nm. As the added NaCl concentration is increased to 3.2 mM (R=0.6), the PS core diameter of the rod-like micelles decreases to 34 nm. When vesicles form, the thickness of the PS wall decreases again to 25 nm. The decrease of PS core dimension accompanying the morphological transitions is also related to an effect of different geometries of the aggregates on the force balance during micellization. A more detailed discussion can be found elsewhere.[3]

Changing the additive concentration has a similar effect on the aggregate morphology as changing the copolymer composition; however, it is more easily controlled if one wishes to obtain a desired morphology. It has been shown that the range of stability of various morphological aggregates is a function of the copolymer composition and molecular weight.[3] However, when the PS block of the copolymers gets longer, the preparation of rod-like micelles and vesicles becomes more difficult because the composition range for these aggregates becomes very narrow. Specifically, when the PS block length of the copolymers exceeds 600 repeat units, it has not been possible to prepare rod-like micelles or vesicles by changing copolymer composition alone without added ions. However, aggregates of various morphologies from PS(660)-*b*-PAA(24) copolymer are obtained easily by adding NaCl to different final concentrations.

The addition of NaCl to PS(410)-*b*-PAA(25) changes the morphology gradually from spheres to rod-like micelles, to vesicles and to large compound vesicles (LCVs);

however, rod-like micelles are missing among the aggregates made from PS(410)-*b*-PAA(13). Even for PS(410)-*b*-PAA(25), when $CaCl_2$ is used as the additive, rod-like micelles have not been observed. A possible reason for the absence of rod-like micelles may be the delicacy of the force balance involved in the formation of different morphologies. The control of the repulsive interactions among the corona chains by the addition of NaCl is relatively easy because of the relatively weak morphogenic effect of NaCl on the aggregates. Therefore, relatively large quantities have to be added to achieve changes in morphology, and the rod-like micelle region can be located even if it is narrow. By contrast, when $CaCl_2$ is used, much smaller quantities of $CaCl_2$ are needed to achieve changes in morphology because of its strong morphogenic effect on the aggregates. Therefore, the region of rod-like micelles is more difficult to locate, in view of the fact that the change of added $CaCl_2$ concentration is only about 20 μM for the morphological transition from spheres to vesicles for PS(410)-*b*-PAA(25) aggregates, and only 5 μM for PS(410)-*b*-PAA(13) aggregates (*cf.* Table 2). Another possibility is that the region of stability of the rod-like micelles is narrow, and depends not only on the PS block length, but also on the PAA block length. As the PAA block length decreases, the originally narrow region for the rod-like micelles becomes even more narrow, and more difficult to locate, as it is for PS(410)-*b*-PAA(13).

7.4.3.3. Large compound vesicles. The LCVs appear to be a new morphology for block copolymer aggregates in solution.[5] Their structure bears some resemblance to that of aggregated soap bubbles, and their outer and inner surfaces must be hydrophilic because of the presence of the short PAA chains. The LCVs are irregular in shape when they are made from the copolymers with relatively long PAA segments, for example, PS(410)-*b*-PAA(25) (Figure 7.3-I) or PS(660)-*b*-PAA(21). However, those made from the copolymers with relatively short PAA segments are generally spherical, for example PS(410)-*b*-PAA(13) (Figure 7.4-F). Furthermore, as the added ion concentration increases, the LCVs become more spherical and their sizes shrink because of smaller primary cell dimensions (Figure 7.1-G and H). The differences in the geometric shapes of the LCVs may be related to differences in the PAA block length, the dimension of the primary vesicles, the softness of the wall, as well as the surface energy and the shear conditions under which the LCVs are formed. In the present study, we do not see a further morphological transition from the LCVs to large compound micelles (LCMs), probably because the PAA blocks are not short enough. However, in view of the characteristics of LCVs made from the copolymers with different PAA block length and different added salt or acid concentrations, the structure of LCMs has a superficial resemblance to that of LCVs when the inner-diameter of the vesicular cell of the LCVs becomes very small so that it looks like a core of reverse micelle-like aggregate. Finally, it should be pointed out that LCVs are subject to settling due to gravity. However, they are very stable, and do not coalesce at room temperature since they can be resuspended after settling.

While the spherical micelles, rod-like micelles and individual vesicles resemble morphologies formed mainly under thermodynamic control, the LCVs probably result from kinetic control. Because the thicknesses of both inside and outside walls of these aggregates are uniform and equal, their formation may involve a secondary aggregation of individual vesicles and a subsequent fusion process. For small molecule surfactants, vesicle fusion is believed to occur very rapidly, and is usually over within 0.1 - 1 ms.[24] However, the fusion process of the vesicles made from the copolymers may be much slower because of the lower mobility of these high molecular weight molecules. Therefore, as the added ion concentration increases, the rate of effective collisions of the colloid particles increases. The captured vesicles fuse with each other to form large, less curved, vesicles, as shown in Figure 7.1, 7.3 and 7.4. When the rate of effective collisions of vesicular aggregates becomes faster than the subsequent fusion process as the added ion concentration increases further, the LCVs may result. In Figure 7.4-F, a range of aggregates, the structures of which are intermediate between uni-vesicular and LCV, can be seen. This may be taken as an evidence of kinetic control.

The self-assembly of vesicles has become a topic of current interest. In one case,[24] chemical species such as bis-phospholipids, were incorporated into the vesicle walls, to aid their aggregation into higher order (multivesicular) structures. As is shown here, the LCVs can be formed spontaneously under a range of conditions. They are thus a "normal" aggregate morphology. It has been suggested [25] that these higher order structures might be of interest in leading to new methods for processing artificial tissue-like composites, and soft biomaterials. In addition, controlled drug delivery appears a distinct possibility since multiple concentric layers might provide a convenient timing mechanism.

7.5. CONCLUSIONS

The morphology of the block copolymer aggregates formed from a single block copolymer can be controlled via the addition of micro-molar $CaCl_2$, $Ca(Ac)_2$, NaOH or HCl, or milli-molar NaCl. Ion-induced morphological changes in dilute solutions of block copolymer aggregates at such low ion contents are novel and significant. The effect of added ions on the aggregate morphology is parallel to a change in the soluble block length, but it is more easy to control. Although the morphogenic effect of added ions may differ for different additives, it can be ascribed to a changed repulsion among the coronal chains, due to protonation by HCl, ionization by NaOH, ion-binding and bridging by Ca^{2+}, and a screened electrostatic field of charged PAA segments by NaCl. In addition to the various aggregates, i.e. spherical micelles, rod-like micelles, vesicles and large compound micelles, which had been described before, [3] large compound vesicles, a new morphology, are obtained. The formation of the LCVs may be a result of kinetic control involving collisions of vesicular aggregates and a subsequent fusion process. A number of novel features of the LCVs may make them especially useful as drug delivery vehicles. Furthermore, the spontaneous formation of the LCVs might provide a practical method for making stable artificial tissue-like composites and soft biomaterials with tunable properties. Thus, the versatility of crew-cut micelles is much greater than was originally suspected. From a fundamental point of view, the discovery of the strong effect of added ions on the morphology of polymeric amphiphilies in dilute solution may lead to an improved understanding of the nature of interactions in these systems, and their consequences for the structure of macromolecular assemblies.

7.6. ACKNOWLEDGMENTS. We would like to thank The Natural Sciences and Engineering Research Council of Canada(NSERC) for continuing support of this research.

7.7. REFERENCES AND NOTES

1. Gao, Z.; Varshney, S. K.; Wong, S.; Eisenberg, A. *Macromolecules* **1994**, *27*, 7923.
2. Zhang, L.; Barlow, R. J.; Eisenberg, A. *Macromolecules.* **1995**, *28*, 6055 (chapter 3 of this thesis).
3. Zhang, L.; Eisenberg, A. *Science* **1995**, *268*, 1728 (chapter 4 of this thesis); *J. Am. Chem. Soc.* **1996**, *118*, 3168 (chapter 5 of this thesis).
4. Zhang, L.; Yu, K.; Eisenberg, A. *Science* **1996**, *272*, 1777 (chapter 6 of this thesis).
5. Yu, K.; Eisenberg, A. *Macromolecules* **1996**, *29*, 6539.
6. Honda, C.; Sakaki, K.; Nose, T. *Polymer* **1994**, *35*, 5309.
7. Guo, A.; Liu, G.; Tao, J. *Macromolecules* **1996**, *29*, 2487.
8. de Gennes, P. G. In *Solid State Physics*, Liebert, L. Ed.; Academic press, New York, 1978; supplement 14, p. 1; Halperin, A.; Tirrell, M.; Lodge, T. P. *Adv. Polym. Sci.* **1992**, *100*, 31.
9. Zhang, L.; Shen, H.; Eisenberg, A. *Macromolecules* **1997**, *30*, in press (chapter 8 of this thesis).
10. Israelachvili, J. N.; Mitchell, D. J.; Ninham, B. W.; *J. Chem. Soc., Faraday Trans.* II, **1976**, *72*, 1525.
11. Mitchell, D. J.; Ninham, B. W. *J. Chem. Soc., Faraday Trans.* II, **1981**, *77*, 601.
12. Ozeki, S.; Ikeda, S. *J. Colloid Interface Sci.* **1982**, *87*, 424.
13. Sein, A.; Engberts, J. B. F. N. *Langmuir* **1995**, *11*, 455.
14. Miyagishi, S.; Kurimoto, H.; Asakawa, T. *Langmuir* **1995**, *11*, 2951.
15. Schepers, F. J.; Toet, W. K.; van de Pas, J. C. *Langmuir* **1993**, *9*, 956.
16. Sein, A.; Engberts, J. B. F. N.; van der Linden, E.; van de Pas, J. C. *Langmuir* **1993**, *9*, 1714.
17. Talmon, Y.; Evans, D. F.; Ninham, B. W. *Science* **1983**, *221*, 1047.
18. Lei, X.-G.; Zhao, G.-H.; Liu, Y.-C.; Turro, N. J. *Langmuir* **1992**, *8*, 475.
19. Fonteijn, T. A. A.; Hoekstra, D.; Engberts, J. B. F. N. *Langmuir* **1992**, *8*, 2437.

20. Kaler, E. W.; Murthy, A. K.; Rodriguez, B. E. Zasadzinski, J. A. N. *Science* **1989**, *245*, 1371.
21. Brasher, L. L.; Herrington, K. L.; Kaler, E. W. *Langmuir* **1995**, *11*, 4267.
22. Ravoo, B. J.; Engberts, J. B. F. N. *Langmuir* **1994**, *10*, 1735.
23. It should be pointed out that in the early stages of the copolymer micellization, the micelle cores are swollen with DMF. After the micelles have been isolated in water, the cores as observed by TEM are totally deswelled and their sizes are reduced. Therefore, the degrees of stretching of the PS blocks in the swollen core and in the deswelled core are different, but related each other. This was discussed in Ref. 3.
24. Israelachvili, J. N. *Intermolecular and surface forces*, 2nd edition, Academic press: London, San Diego, 1992.
25. Chiruvolu, S.; Walker, S.; Israelachvili, J. N.; Schmitt, F.-J.; Leckband, D.; Zasadzinski, J. A. *Science* **1994**, *264*, 1753.

Chapter 8

Phase Separation Behavior and Crew-Cut Micelle Formation of Polystyrene-*b*-Poly(acrylic acid) Copolymers in Solutions

ABSTRACT

Static light scattering was used to study the phase separation behavior of homopolystyrene and polystyrene-*b*-poly(acrylic acid) (PS-*b*-PAA) in DMF as a function of added water content. It was found that the critical water content, *cwc*, at which phase separation starts, depends on both the polymer concentration and the molecular weight. The higher the polymer concentration and the molecular weight, the lower the *cwc*. For PS homopolymer, phase separation involves the precipitation of the polymer chains. In the copolymer solution, phase separation results in the formation of regular crew-cut micelles consisting of a PS core and a PAA corona shell. The change of the micelle fraction as a function of water addition can be estimated from the relationship between the *cwc* and the initial copolymer concentration. The influence of added electrolytes, i.e. NaOH, HCl, NaCl, $CaCl_2$, or $Ca(Ac)_2$, on the self-assembly process of the copolymers in DMF was also explored.

Since the micelle cores are highly swollen by DMF in the early stages of their formation, the structures are labile. As the added water content increases, the cores become gradually less swollen and the mobility of the polymer chains in the cores decreases. A preliminary study of polymer chain exchange among the micelles was performed by mixing two solutions of micelles of different sizes at different water contents and studying the micelle core size distribution by transmission electron microscopy. It is shown that the copolymer chain exchange within a one day period is significant at a water content of 6 wt. %, but becomes negligible when the water content is increased to ~ 11 wt. %.

8.1. INTRODUCTION

Amphiphilic block copolymers undergo self-assembly in a selective solvent to form aggregates of a core-shell structure.[1] Aggregates are frequently referred to as star micelles when the corona forming blocks are much longer than the core forming blocks. Aggregates of another kind, namely crew-cut micelles, [2] have been receiving attention recently in this laboratory [3-9] and in others. [10,11] In contrast to star micelles, crew-cut micelles are made from copolymers in which the insoluble blocks are much longer than the soluble blocks. Therefore, they have a rather large core and a relatively short corona; thus, their structure is, in some ways, similar to that of polymer nanospheres, [11] polymer latex particles prepared by emulsion polymerization, [12] as well as that of polymer chains grafted onto a solid surface. [13] Since the micelles are prepared from well defined block copolymers, the core size and the corona shell dimension can be controlled by varying the block lengths of the copolymers. Furthermore, because the blocks of the copolymer are linked chemically, the density of the corona chains is better defined than that of polymers grafted onto a solid surface or of stabilizer layers on the surface of latex particles. The crew-cut micelles may thus serve as the model systems for the studies of polymer grafting, latex surfaces and brushes.

To make the crew-cut micelle solution, [3-9] the block copolymers, e.g. polystyrene-*b*-poly(acrylic acid), are first dissolved in N,N-dimethylformamide (DMF), a common solvent for both of the blocks. Then, a precipitant for the polystyrene block, i.e. water or methanol, is added to induce the formation of micelles. Finally, the DMF is removed from the micelle solution by dialyzing the resulting solutions against water. [3-6] The structure of the micelles in water is stable because the fraction of the insoluble PS block is high and the core is glassy at room temperature. This makes it possible to study the morphologies by transmission electron microscopy (TEM), and to measure the core sizes directly from the prints.

For polystyrene-*b*-poly(acrylic acid) (PS-*b*-PAA) diblock copolymers, aggregates with various morphologies have been prepared from copolymers of different compositions. [4,6] When the PAA block content is relatively high, the copolymer chains aggregate to form spherical micelles of low polydispersity. Compared to star micelles, the crew-cut micelles have a low density of coronal chains on the core surface (i.e. a large surface area per corona chain), and a low degree of stretching of the PS chains in the core. As the content of the soluble block (PAA) in block copolymer decreases, the morphology of the aggregates changes progressively from spheres to cylinders, to bilayers (both vesicles and lamellae), and eventually to large compound micelles. The morphology of the crew-cut aggregates is mainly controlled by three factors, i.e. the stretching (deformation) of the PS chains in the core, the surface tension between the PS core and the solvent, and the inter-corona-chain interactions.

The solubilization of homopolystyrene in the micelle cores has also been studied.[6] It was found that the homopolystyrene chains are generally distributed throughout the cores when the homopolystyrene content is relatively low. As the content of added homopolystyrene increases, homopolymer accumulation in the center of the micelle core can be deduced. The addition of homopolystyrene changes the morphologies of the aggregates from either bilayers or cylinders to spheres; this is ascribed mainly to the reduced degree of stretching of the PS blocks in the cores and possibly the effect of mixing entropy, both of which are associated with the solubilization of the homopolystyrene into the micelle cores.

More recently, it was found that the morphological changes can also be induced by the addition of micro- or milli-molar NaCl, $CaCl_2$, $Ca(Ac)_2$, HCl, or NaOH to the DMF solution. [7,8] The effect of added ions on the aggregate morphology is similar to that of changing block copolymer composition. In general, the effects can be ascribed to a change of the repulsive interactions among the corona chains accompanying the addition of ions. In addition to the morphologies which can be produced by varying the copolymer composition in the absence of added ions, i.e. spheres, rods, bilayers and large compound micelles, aggregates of a new morphology, large compound vesicles (LCVs), are also obtained. The formation of LCVs appears to be a result of kinetic control involving a secondary aggregation of many individual vesicles and a subsequent PS wall fusion process. The morphogenic effects of copolymer composition and added ions on the aggregate morphology is also found in the self-assembly system of polystyrene-*b*-poly(ethylene oxide) copolymers.[7,9]

The study of crew-cut aggregates is still in the early phases and many of the fundamental aspects related to their formation as well as the different morphologies still remain unexplored. Because the crew-cut micelles are prepared by adding a precipitant to a homogeneous copolymer solution, a phase separation process is involved in the course of micellization. Although it has been used to prepare star micelles of copolymers, [14] the addition of a precipitant is not a classical method, and thus it has not been explored before in detail. It has been shown in previous chapters [3-9] that this method yields essentially monodisperse micelles and various other morphologies. Therefore, the study of the phase separation behavior of block copolymers in DMF/water mixtures becomes essential for an understanding of the micellization process. In this chapter, we first investigate the phase separation behavior of PS-*b*-PAA block copolymer solutions as a function of the copolymer concentrations and compositions, as well as the presence of added electrolytes. Then, a preliminary study of the relationship between the lability of the micelle structure and the added water content is presented, to verify the conditions under which the formed micelles become structurally frozen aggregates. A parallel study of the thermodynamics of the micelle formation has been conducted, and will be described in a forthcoming paper.[15] Static light scattering and transmission electron microscopy (TEM) techniques are used.

8.2. EXPERIMENTAL SECTION

8.2.1. Polymer Samples. Polystyrene-*b*-poly(acrylic acid) diblock copolymers, PS-*b*-PAA, were synthesized by sequential anionic polymerization of styrene monomer followed by *tert*-butyl-acrylate monomer. The polymerization process was carried out in tetrahydrofuran (THF) at -78°C under nitrogen gas. Before the addition of *tert*-butyl-acrylate monomer, an aliquot of the reaction medium was withdrawn to obtain homopolystyrene (PS), which thus had an identical polystyrene chain length as that in the diblock copolymer which was to be synthesized subsequently. A more detailed description of the procedures can be found elsewhere. [16]

The degree of polymerization and the polydispersity of the polymers were measured by size exclusion chromatography (SEC). All the homopolystyrenes and their diblock copolymers in the form of *tert*-butyl-acrylate gave one narrow SEC peak. The composition of the block copolymer was determined from FTIR measurements, from which the degree of polymerization of the poly(*tert*-butyl-acrylate) was calculated. The as synthesized block copolymers were hydrolyzed to the acid form (PS-*b*-PAA) in toluene at 110 °C by refluxing overnight in the presence of *p*-toluene sulfonic acid as the catalyst (5 mol% relative to the polyacrylate content). FTIR studies showed that the hydrolysis was essentially complete. The basic characteristics of the polymers are listed in Table 8.1. The polymer samples are differentiated by the notation developed previously, e.g. the PS(500)-*b*-PAA(60) denotes a copolymer containing 500 styrene units and 60 acrylic acid units. PS(180) refers to homopolystyrene with 180 units in the chains.

8.2.2. Static Light Scattering. Light scattering experiments were performed on a DAWN-F multiangle laser photometer (Wyatt Technology, Santa Barbara, CA) equipped with a He-Ne laser (632.8 nm). The polymer solutions were prepared by dissolving polymers into N,N-dimethylformamide (DMF). The DMF (Aldrich) was used as received without any further purification. According to the manufacturer, the water content is less than 0.02%. The solutions with different concentrations were obtained by stepwise dilution of a more concentrated solution. The solutions were filtered through a membrane filter with nominal pore size of 0.45 μm. Deionized water (Milli Q) was added to the polymer/DMF solutions with a microsyringe. The experiments were performed at room temperature. The scattered light intensity was recorded 15 min after the addition of water and mixing of the solution.

8.2.3. Transmission Electron Microscopy (TEM). A Phillips EM410 microscope was used for the studies. To prepare TEM samples, a drop of dilute aqueous solutions (about 1 mg/ml) was deposited onto copper EM grids, which had been pre-coated with a thin film of Formvar (polyvinyl formaldehyde plastic) and then coated with carbon. The aqueous solution was allowed to stay about two minutes on the copper grid, and then was blotted away with a strip of filter paper. Finally, the samples were shadowed with palladium/platinum alloy at a angle ~ 35°.

Table 8.1. Molecular characteristics of homopolystyrene and of polystyrene-*b*-poly(acrylic acid) diblock copolymers

polystyrene (PS)	Mw/Mn	copolymer (PS-*b*-PAA)	Mw/Mn
PS(86)	1.09	170-*b*-33	1.08
PS(170)	1.07	410-*b*-25	1.05
PS(390)	1.05	390-*b*-41	1.06
PS(500)	1.04	500-*b*-60	1.04
PS(1140)	1.05	1140-*b*-165	1.06

8.3. RESULTS AND DISCUSSION

8.3.1. Phase Separation of Polymer/DMF/Water Solutions.

DMF is a common solvent for both blocks of the polystyrene-*b*-poly(acrylic acid) copolymers. The dissolution of the copolymers in DMF as single chains has been confirmed by static light scattering measurement of the molecular weight. Because water is a good solvent for poly(acrylic acid), but a precipitant for polystyrene, as water is added to the copolymer/DMF solution, the solvent becomes progressively worse for the polystyrene block. Eventually, the copolymer solution undergoes phase separation and the polystyrene chains aggregate, which is reflected in a sudden change in the scattered light intensity.

8.3.1.1. Addition of Water to Homopolystyrene/DMF Solutions. Before exploring the phase separation behavior of the copolymer/DMF solutions resulting from the addition of water, it is useful to study the homopolystyrene (homo-PS) solutions because the major component of the PS-*b*-PAA copolymers is polystyrene. Figure 8.1 presents experimental curves of the scattered light intensity from the PS(170) homopolymer solutions as a function of added water content. For each solution, as long as the water content is relatively low, the scattered light intensity changes only very little, implying that the polymer chain dimensions do not change appreciably. However, when the water content reaches some critical value, the scattered light intensity increases rapidly. The drastic increase in the scattered light intensity indicates that a phase separation has occurred. For the more concentrated solutions, the solutions turns cloudy at that point; a PS rich phase is observed on the bottom of the light scattering vials after the solutions are allowed to stand for a few hours. Figure 8.1 also shows that the onset of phase separation shifts to higher water contents as the initial polymer concentration in DMF decreases, indicating that the polymer chains in more dilute solution remain soluble to a higher water content; as might be expected, the solubility of homo-PS decreases as the water content increases.

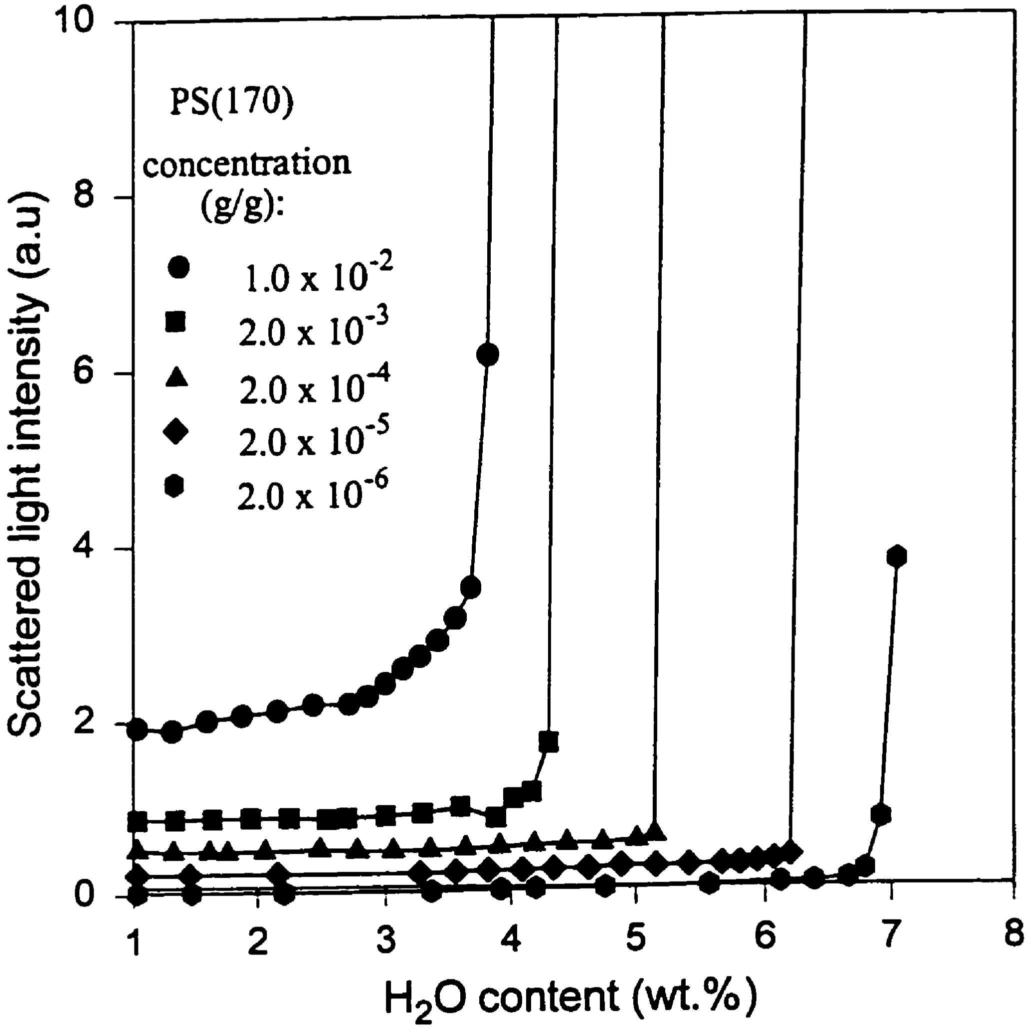

Figure 8.1. Scattered light intensity as a function of added water content in PS(170)/DMF solutions of different concentrations.

For each solution, a critical water content, *cwc*, can be defined as the water content at which phase separation starts; it is obtained from the intercept of the nearly horizontal and vertical straight line segments of the light scattering curve. A plot of the *cwc* as a function of polymer concentration for different PS homopolymers is given in Figure 8.2. A linear relationship is found between the *cwc* and the logarithm of the polymer concentration, which has been seen in other polymer-solvent-precipitant systems.[17] The *cwc* decreases as the polymer concentration increases. For a specific polymer concentration, the *cwc* decreases as the polymer molecular weight increases. It is well known that the solubility of a polymer is related to its chain length. This is the case here also, as can be seen by going horizontally across the plot for any water content. Figure 8.2 also shows that the relationship between the *cwc* and the polymer concentration changes with the molecular weight of the polymers. The higher the molecular weight, the larger the slope *d[log C]/d[cwc]* of the lines. This means that the higher the molecular weight, the stronger the effect of water on solubility. Finally, it is noteworthy that all the straight lines intersect at a polymer concentration of ~1 g/g (which corresponds to the density of the bulk phase), at a water content about 2 wt. %. This may indicate that even if the molecular weight and the concentration of polystyrene become very high, the polymer will not phase separate from a DMF/water mixture for a water content less than 2 wt. %. Obviously, the solution behavior of polystyrene/DMF/water mixtures is complex but quite interesting. However, since the primary object of present paper is the study of micellization of block copolymers, the topic of solubility of homopolystyrene in this mixed solvent will not be pursued further here.

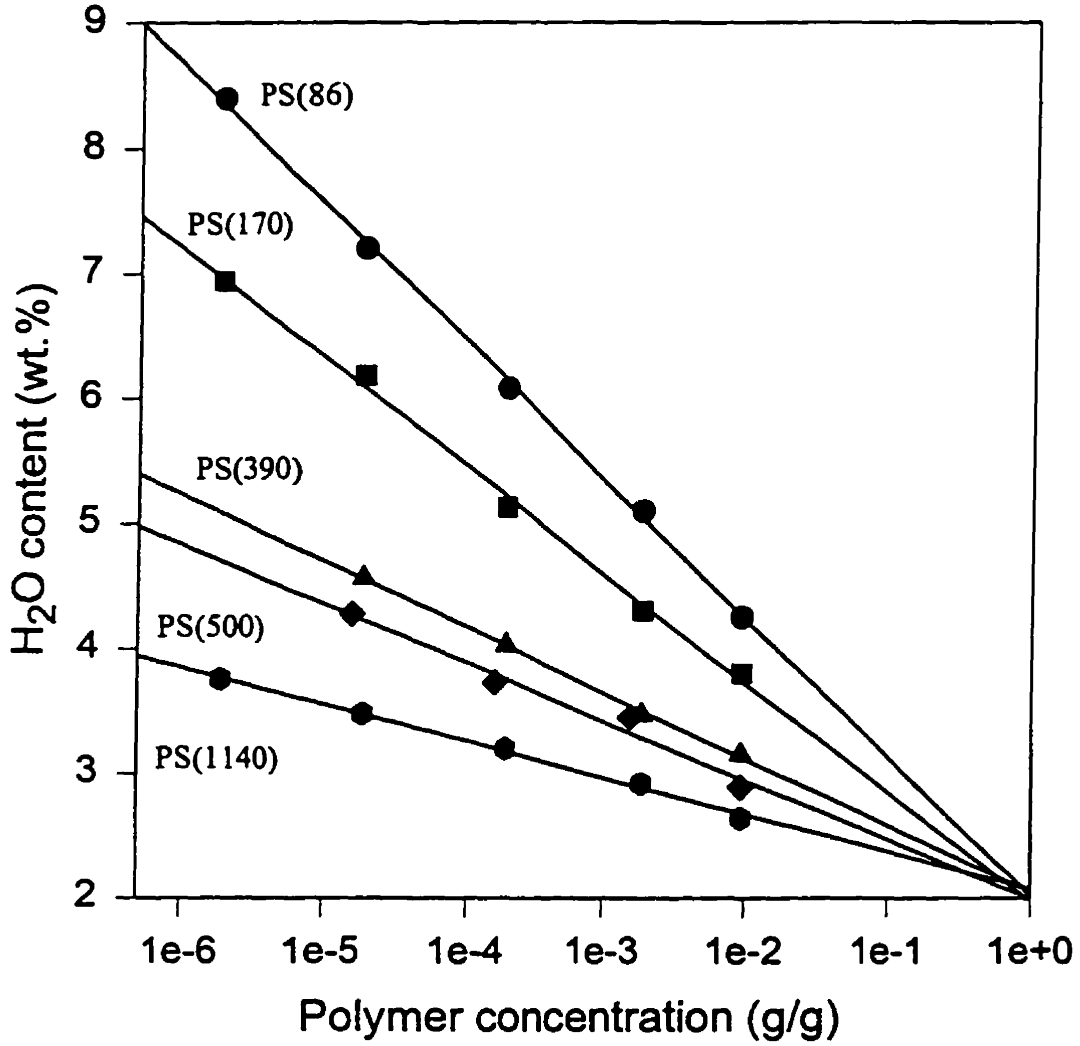

Figure 8.2. A plot of the critical water content versus polymer concentration for solutions of homopolystyrene of different molecular weights.

8.3.1.2. Addition of Water to PS-*b*-PAA/DMF Solutions. For PS homopolymer solution at any reasonable polymer concentration, phase separation occurs when the added water content reaches a certain level. For the block copolymers, the phenomena show some similarity to the case of homo-PS. As can be seen in Figure 8.3, when water content is relatively low for all of the solutions, the intensity of scattered light changes only little. At some critical value, the increase of the intensity becomes very steep for all polymer concentrations. The drastic change in the intensity indicates that phase separation has occurred. In contrast to homo-PS solutions where the polymer chains collapsed and precipitated out, the solutions of diblock copolymers were found to be very stable after microphase separation. This occurs because phase separation of the copolymer solution results in the formation of micelles, with the polystyrene blocks of the copolymers aggregating to form the micelle core, and the PAA blocks to form the corona shell. Because both DMF and water are good solvents for acrylic acid, the hydrophilic interaction between the PAA segments and the solvents prevents the particles from precipitating through secondary aggregation. Figure 8.3 also shows that as the initial copolymer concentration decreases, the phase separation shifts to a higher water content, which means that the copolymer solubility in DMF/water mixture decreases as the water content increases.

As in the case of homo-PS solutions, the *cwc* can be obtained from the light scattering curves in Figure 8.3 for copolymer solutions of different concentrations. Figure 8.4 shows a plot of the *cwc* against the logarithm of the polymer concentration for copolymers of different molecular weight. For convenience, the data for some of the homopolystyrene solutions are also shown in this plot. It is found that here also a linear relationship exists between the *cwc* and the logarithm of the block copolymer concentrations. One can see that the onset of phase separation of the corresponding diblock copolymer solutions (with the same polystyrene segment length and concentration as that of the homopolymer) always occurs at a higher water content. Because both water and DMF are good solvents for PAA blocks, it is reasonable to believe that the interaction between the solvent and the acrylic acid units prevents the collapse of the copolymer molecules from the solution until a higher water content is reached. The linear relationship has only a slightly different slope (smaller *d[log C]/d[cwc]*) compared to that of the corresponding homo-PS solutions, probably due to the large weight-fraction of polystyrene in the block copolymers. Furthermore, for a specific polymer concentration, the *cwc* decreases with an increase of the PS block length. This implies that the copolymers with longer PS blocks start to form micelles at a lower water content than shorter blocks do. Because the solvent-PS (Flory-Huggins) interaction parameter, χ, increases as the water content increases, from a thermodynamic point of view, the micelles form at χ values which decrease with increasing the PS block length and/or polymer concentration.

8.3.1.3. Addition of Water to Polymer Mixtures in DMF Solutions. In a previous paper,[6] it was reported that PS homopolymer can be solubilized into the micelle cores during micellization of the copolymers, by dissolving the homopolymer in the copolymer/DMF solutions before the addition of water. Therefore, it is of interest to study the phase separation of the solutions composed of two different polymers in DMF as the addition of water progresses. For this purpose, four different polymer mixtures were prepared from PS(500)-*b*-PAA(60) and PS(170), PS(500)-*b*-PAA(60) and PS(1140), PS(1140)-*b*-PAA(165) and PS(180), and PS(1140)-*b*-PAA(165) and PS(170)-*b*-PAA(33), respectively. The weight ratio of the two selected polymers in the mixtures was one to one. We chose the above polymer combinations because of the large differences in their critical water contents.

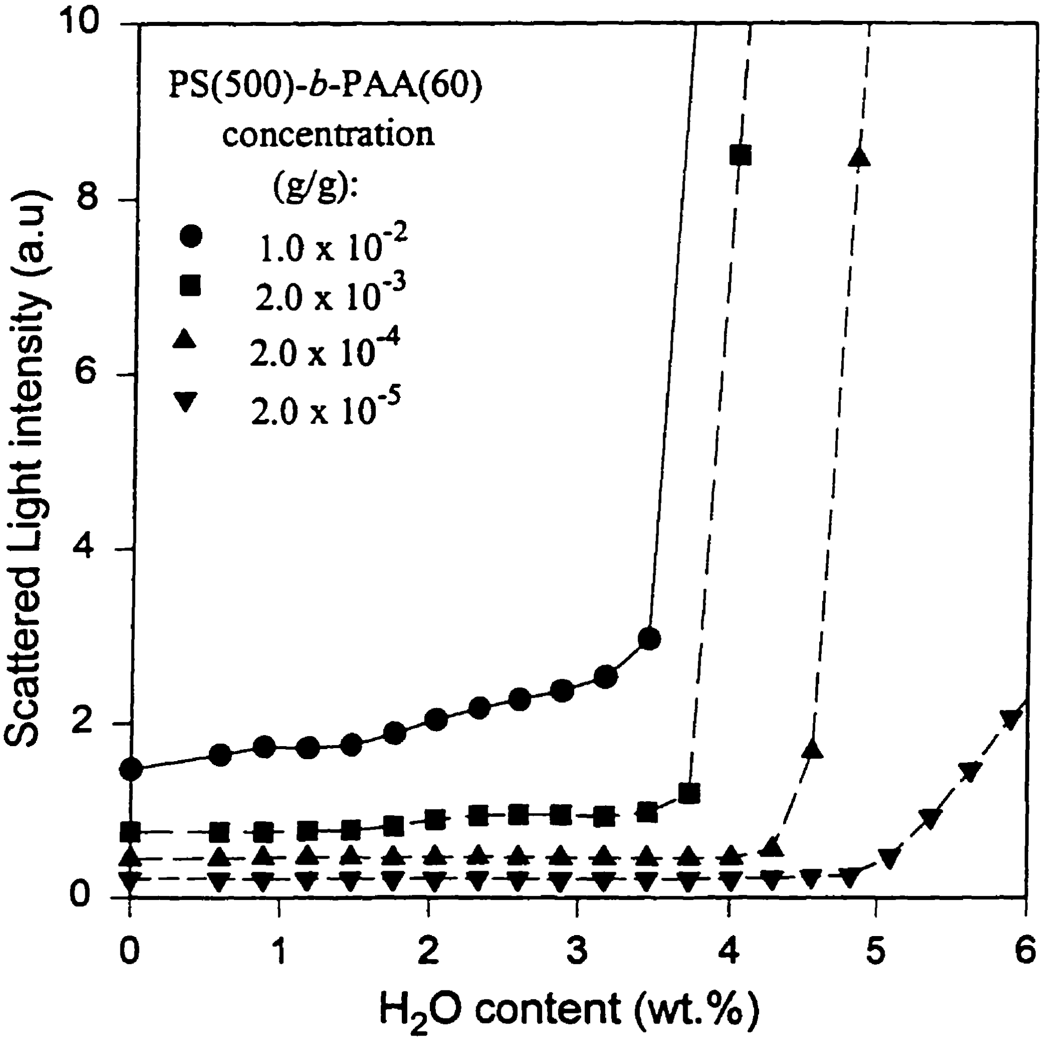

Figure 8.3. Scattered light intensity as a function of added water content in PS(500)-*b*-PAA(60)/DMF solutions of different concentrations.

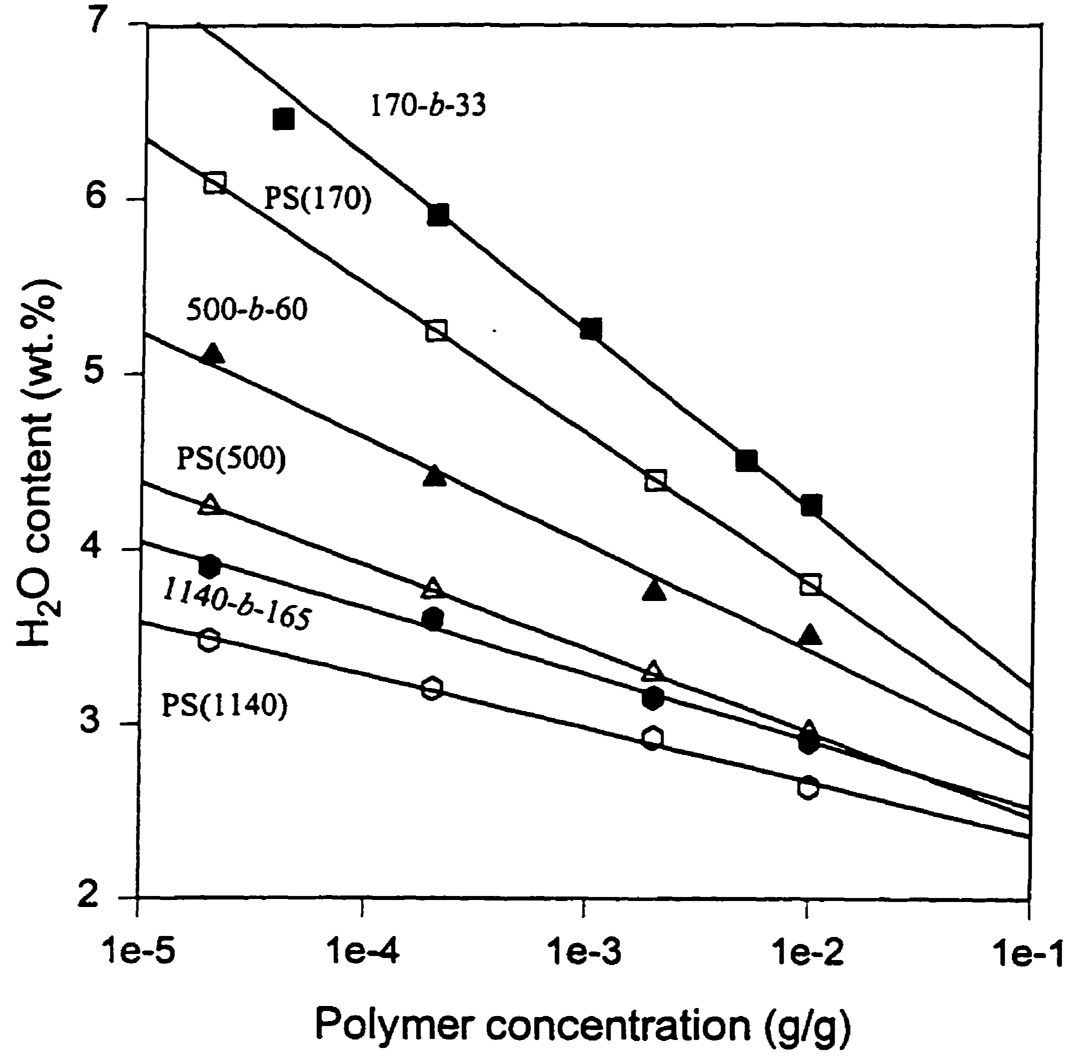

Figure 8.4. A plot of the critical water content versus polymer concentration for solutions of homopolystyrenes and of PS-*b*-PAA block copolymers of different molecular weights.

It was found that all solutions gave curves of the scattered light intensity versus the added water content which are very similar to those shown previously in Figures 8.1 and 8.3. Figure 8.5 shows a plot of the *cwc* from the solutions of polymer mixtures as a function of the logarithm of the total polymer concentration. One can see that the *cwc* decreases as the total polymer concentration increases. Again a linear relationship is found. The *cwc* of the solution of a mixed polymers depends mainly on the component polymer which has the lower critical water content alone. For example, for comparable concentrations, the solution of the mixture of PS(500)-*b*-PAA(60) and PS(170) has a *cwc* which is only slightly higher than that of the solution of PS(500)-*b*-PAA(60) alone. The solution of PS(500)-*b*-PAA(60) and PS(1140) mixture has a *cwc* which is only slightly higher than that of PS(1140) alone, but much lower than that of PS(500)-*b*-PAA(60) alone. Furthermore, if one considers that the *cwc* is plotted against the total polymer concentration in Figure 8.5, and that each polymer component in the mixtures accounts for 50% of the total concentration, the *cwc* of the solution of the mixed polymers is almost identical to that of the solution of the component polymer having the lower *cwc* alone.

On the basis of the above results, one can deduce that if one wishes to incorporate homopolystyrene into the copolymer micelle cores, the homo-PS should have a higher *cwc* than that of the block copolymer. Otherwise, the homo-PS chains will precipitate first from the solution as the water content increases, without becoming incorporated into the PS core of the copolymer micelle. The *cwc* can be increased by decreasing the polymer concentration and/or molecular weight.

8.3.1.4. Dependence of the Degree of Micellization on the Water Content. It is clear from the above that for a copolymer solution of a certain initial concentration, when the water content is below a critical value, the copolymer chains are unassociated; at the critical water content, the copolymers start to associate; as the addition of water progresses further, more and more copolymer chains associate to form micelles and the concentration of the copolymers in single chain form decreases. Thus, it is of interest to

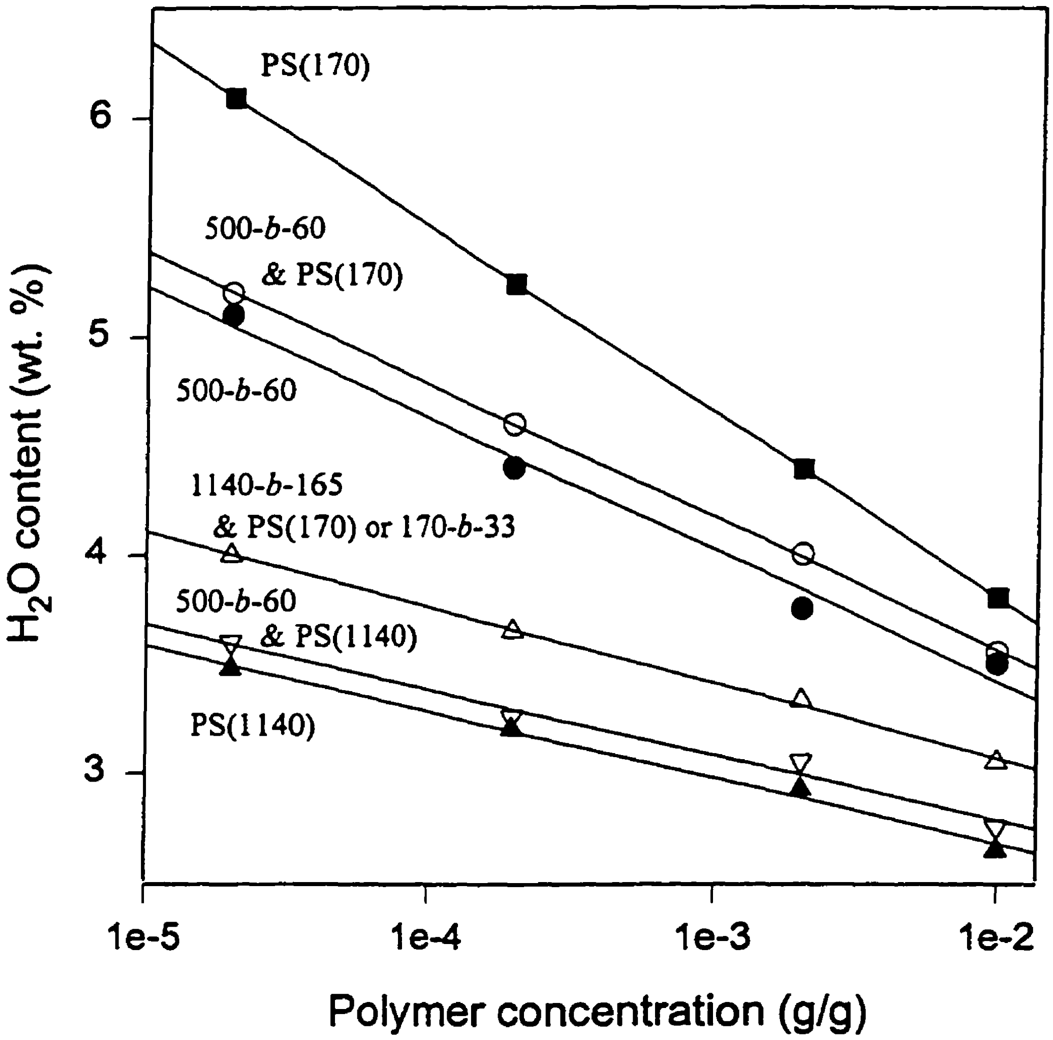

Figure 8.5. A plot of the critical water content versus total polymer concentration in solutions of polymer mixtures.

see how the micelle fraction of the copolymers depends on the change of water content beyond the critical value.

According to the plots in Figure 8.4, the relationship between the *cwc* and the initial copolymer concentration, C_0, can be expressed as

$$\mathrm{cwc} = -A \cdot \log C_0 + B \qquad (8.1)$$

or

$$C_0 = \exp[2.303(B-\mathrm{cwc})/A] \qquad (8.2)$$

where A and B are constant for a specific copolymer. At the critical water content, the copolymer concentration represents actually the critical micellization concentration (CMC), which depends on the polymer molecular weight and the water content. As the added water content increases further, more and more copolymer chains form micelles. However, the concentration of the unassociated polymer chains, CMC, still obeys the relationship of equation (1). Thus, we have

$$\mathrm{CMC} = \exp[2.303(B-H_2O\%)/A] \qquad (8.3)$$

where $H_2O\%$ represents the water content in the solution. it is worthy of note that the molecular weight distribution of the block copolymer should also have an effect on the micellization behavior or the critical micellization concentration (CMC) as shown in an earlier study.[18] However, in the present simplified treatment, we do not consider the polydispersity in the copolymer molecular weight.

The micelle fraction can be defined as a ratio of the associated polymer to the total polymer, $(C_0 - \mathrm{CMC})/C_0$. A combination of equations (2) and (3) yields the following relationship

$$\begin{aligned}(C_0 - \mathrm{CMC})/C_0 &= 1 - \exp[2.303(\mathrm{cwc}-H_2O\%)/A] \\ &= 1 - \exp(-2.303\Delta_{H_2O}/A) \qquad (8.4)\end{aligned}$$

where Δ_{H_2O} represents the increment of the water content since the copolymers started to associate. When the value of Δ_{H_2O} is zero (or less), the ratio of $(C_0 - CMC)/C_0$ equals zero, because all the copolymer chains are unassociated in the solution when the water content is below the *cwc*. Figure 8.6 shows a plot of the micelle fraction against the increment of the water content for different block copolymers. It is clear that the micelle fraction depends on the copolymer molecular weight and the water content. For copolymers with longer PS chains, the micellization is completed within a narrower range of the water increments. However, the copolymers with shorter PS block length show a broader water increment range needed for a complete micellization. Since the value of the solvent-PS interaction, the χ parameter, is a function of the water content, this means that, even for an individual copolymer solution, the micelles may be formed at a value of the χ parameter which is slightly different from micelle to micelle. However, as will be seen later on in section 3.3., at this water content range, the structure of the micelles is not frozen. A dynamic equilibrium between the micelles and copolymer unimers exists. Therefore, the structural parameters of the micelles can still change in response to the slightly changed solvent environment. As a result, the slight increase of the value of the χ parameter during micellization may not affect the core size distribution appreciably since it has been found that the formed micelles are generally monodisperse.

8.3.2. Phase Separation of Polymer/DMF/Water Solutions Containing Electrolytes.

Recently, it has been found that small amounts of added electrolytes, e.g. HCl, $CaCl_2$ or NaCl, can have a very strong effect on aggregate morphologies. [7,8] Electrolytes in aqueous solution are added to the copolymer/DMF solutions before adding more deionized water to induce the PS block aggregation. As a typical example, for a 1 wt. % PS(410)-*b*-PAA(25) solution, without any added HCl, the aggregates are spherical micelles; when the added HCl concentrations are 210, 240 and 270 μM, the aggregates are rod-like micelles, vesicles and large compound vesicles, respectively.[7] In this section,

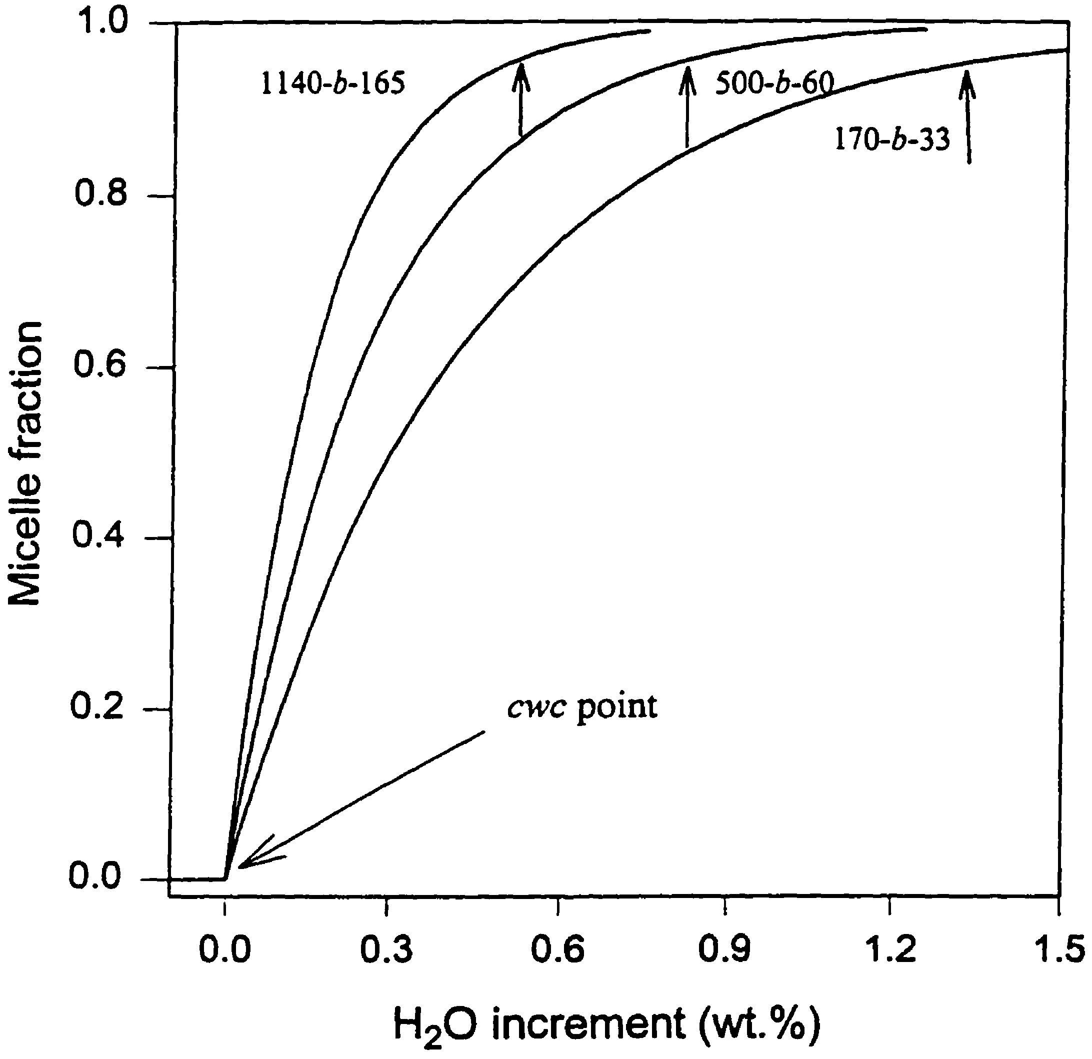

Figure 8.6. A plot of the micelle fraction as a function of the water increment beyond the critical water content. Arrows indicate 95% micellization.

we discuss the influence of the added electrolytes on the phase separation behavior of the copolymer solutions. In particular, we emphasize the state of the copolymers upon dissolution in the presence of added electrolytes and some water, but not enough to induce PS block aggregation. In order to connect the present study with the morphogenic effect of added electrolytes on the aggregates,[8] the experimental conditions and the concentration range of the added electrolytes are designed specifically to be similar to those under which the aggregates of different morphologies are formed.

8.3.2.1. Addition of NaOH (aq) to Polymer/DMF Solutions. It was found that the phase separation behavior of PS(170) homopolymer solution did not change at all when 0.010 M NaOH(aq) was added instead of pure water. This is not surprising, because polystyrene is non-ionic, so the effect of the added electrolyte on polymer chain dimension should be very limited. However, for the block copolymers, the phase separation behavior becomes more complicated. Figure 8.7 shows a plot of the scattered light intensity against the water content for the addition of 0.030 M NaOH(aq) to PS(170)-*b*-PAA(33) copolymer/DMF solutions of different polymer concentrations. For the 1 wt. % copolymer solution, the scattered light intensity increases rapidly when the water content reaches 4.2 wt. %, which is similar to the behavior when adding deionized water. However, for more dilute solutions, the scattered light intensity starts to increase rapidly at much lower water contents than those observed when deionized water is added.

Considering the fact that NaOH has almost no effect on the phase separation of the homopolystyrene solutions, the different phase separation behavior of the copolymer solution should be related to the neutralization of the acrylic acid units (to sodium acrylate) by the NaOH. It is known that PS-*b*-PANa diblock copolymers in DMF form reverse micelles, which have a PANa block core and a PS corona shell. [19] The degree of reverse micellization depends on the degree of neutralization of the PAA blocks. [20] In the present system, as the addition of NaOH (aq) progresses, more and more acrylic acid units become neutralized; in addition, the water content also increases. For NaOH

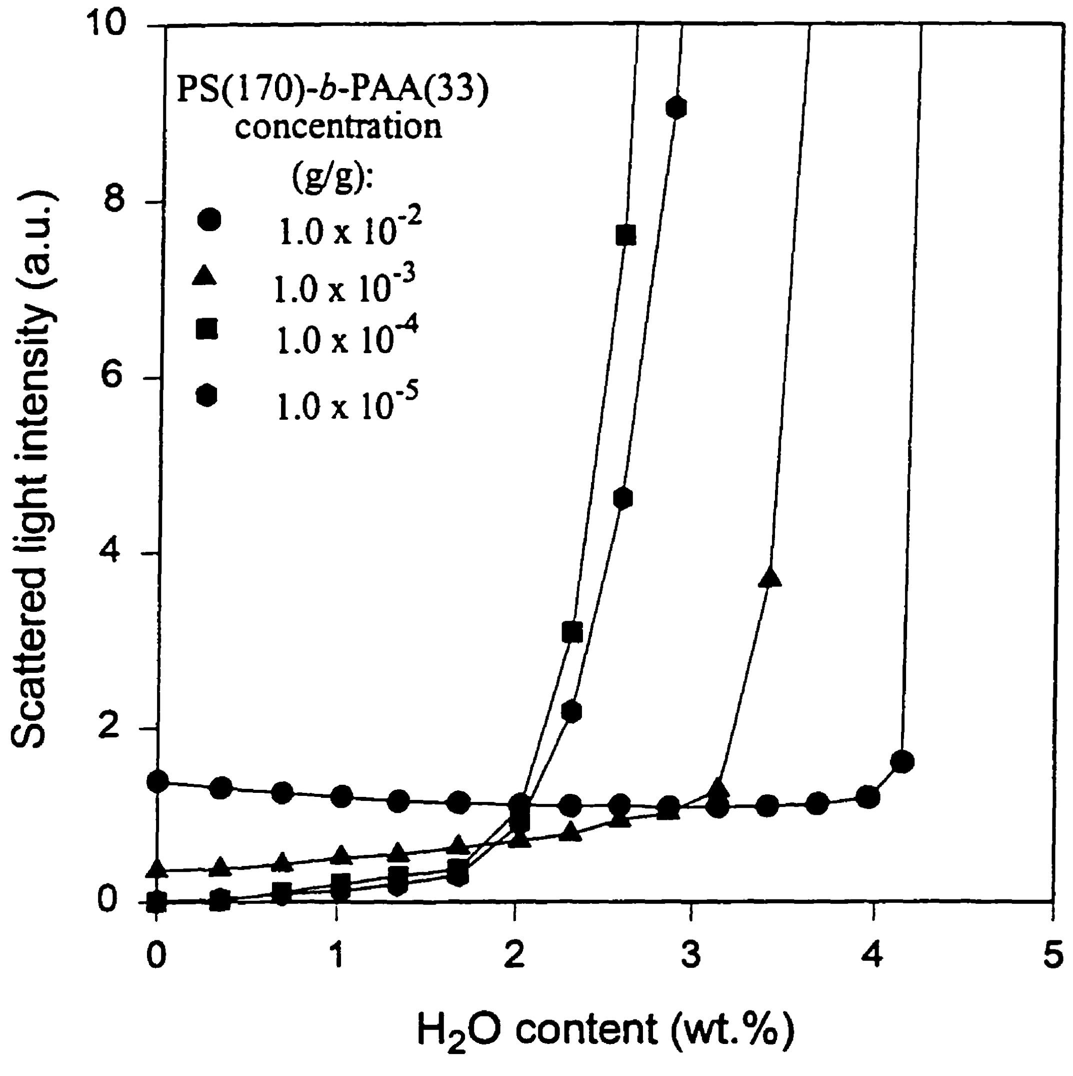

Figure 8.7. Scattered light intensity, from PS(170)-*b*-PAA(33)/DMF solutions of different concentrations, as a function of added water content introduced by adding 0.030 M NaOH aqueous solution.

solutions of the same concentration, the degree of neutralization of the PAA blocks increases much faster for the more dilute polymer solutions than that the more concentrated solutions. Therefore, in the more concentrated copolymer solutions, when the water content reaches some critical point for the PS block precipitation, the neutralization degree of the PAA blocks could be still low. A low degree of neutralization of the PAA blocks does not lead to the formation of reverse micelle-like aggregates. [19] As a result, the phase separation resulting from the addition of NaOH (aq) is similar to that resulting from the addition of deionized water. However, for a more dilute copolymer solution, before the water content reaches the critical point for the PS block precipitation, the degree of neutralization of the PAA blocks could already be very high. A high degree of neutralization of the PAA blocks leads the formation of reverse micelles. Naturally, both mechanisms of aggregation lead to increase in the scattered light intensity.

It is of interest to study the relationship between reverse micellization and the degree of neutralization of the PAA blocks. Because reverse micellization also increases the scattered light intensity, it is difficult to determine the position of *cwc* for the PS block aggregation from the curves in Figure 8.7. However, although the formation of reverse micelles increases the scattered light intensity, the appearance of the solutions is almost clear because of the small core sizes of the reverse micelles. By contrast, the onset of the PS block aggregation can be observed by a turbid appearance of the solutions. Because the solubility of the PS blocks is very sensitive to the water content, as a good approximation, the water content at which the solution starts to become turbid represents the critical point for the PS block aggregation. For this experiment, the initial copolymer concentration in DMF was 1 wt. %. NaOH (aq) in different amounts was first added to the copolymer solutions in different vials. Then, deionized water was added right until the solutions became cloudy. This study is based on the fact that the *cwc* is a function of the molecular weight of the PS block (*cf.* Figure 8.2). At a constant polymer concentration, the higher the molecular weight, the lower the *cwc*. If the polymers are unassociated, the *cwc* is determined by the molecular weight of the polymer single chains. When the copolymer chains become associated to form star type reverse micelles, the *cwc* is then determined by the molecular weight of the reverse micelles rather than of the polymer single chains. The only difference is that the copolymer chains are linear before aggregation, but become a star type after the formation of reverse micelles. The much higher apparent molecular weight of the reverse micelles leads the phase separation to occur at a lower water content.

Figure 8.8 shows a plot of the *cwc* (or water content at the cloud point) versus the molar ratio of the added NaOH molecules to the acrylic acid units (or the degree of neutralization of the PAA blocks). As can be seen, for both of PS(170)-*b*-PAA(33) and PS(410)-*b*-PAA(25) copolymers, when the neutralization degree is relatively low, e.g. less than 10 %, the *cwc* does not change very much, indicating that the copolymers before the onset of phase separation were still dispersed as single chains. As the degree of neutralization of the PAA blocks increases, the *cwc* decreases, implying the formation of reverse micelle-like aggregates and also showing that the extent of the aggregation (or the aggregation number) increases. For different copolymers, the detailed shapes of the curve of *cwc* versus the neutralization degree are somewhat different, which may be related to the copolymer composition, the block lengths of both the PS and the PAA, etc.

8.3.2.2. Addition of Other Electrolytes to the Copolymer/DMF Solutions. In this section, we explore the effect of other added electrolytes on the phase separation behavior of the copolymer solutions. The electrolytes used for this study are HCl, NaCl, $CaCl_2$ and $Ca(Ac)_2$ because they show a strong morphogenic effect on the crew-cut aggregates. [7,8] The aqueous electrolyte solutions were added to the copolymer/DMF solutions. The scattered light intensity was monitored after each addition. After the concentration of added electrolytes in the copolymer solution reached a predetermined level, deionized water was added until phase separation occurred.

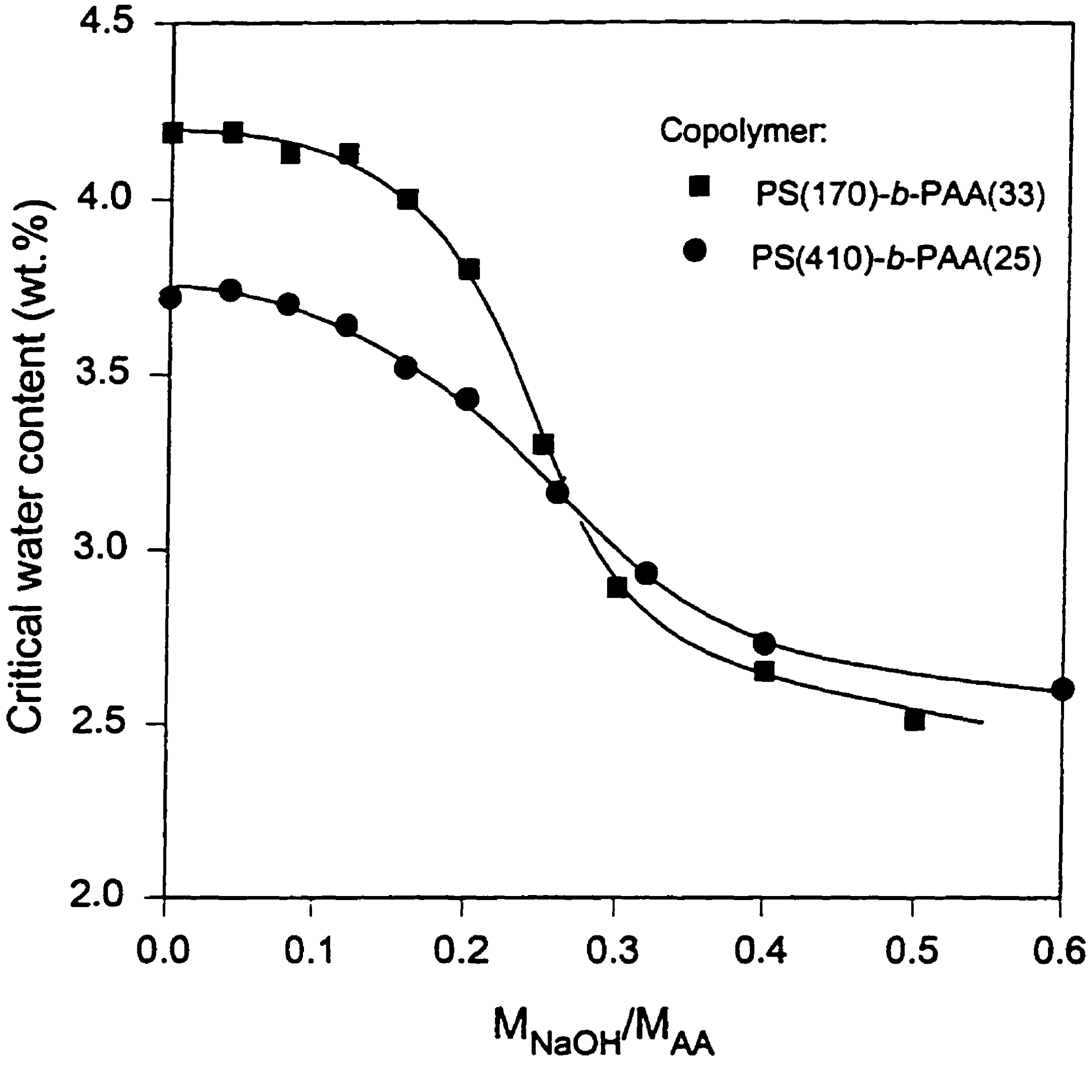

Figure 8.8. A plot of the critical water content as a function of molar ratio of the added NaOH molecules to the acrylic acid units (AA) of the PS(170)-*b*-PAA(33) and PS(410)-*b*-PAA(25) copolymers, M_{NaOH}/M_{AA}. The initial copolymer concentration is 1 wt. %.

Figure 8.9 shows a plot of the scattered light intensity versus the water content from a 1 wt. % copolymer solutions during the addition of different electrolyte solutions. The copolymer is PS(410)-*b*-PAA(25). The arrows indicate the positions after which only deionized water was added instead of the electrolyte solutions. The concentrations of added electrolytes at the indicated points were 0.54 mM (R=0.1) for HCl, 21 mM (R=4.0) for NaCl, 0.54 mM (R=0.1) for $CaCl_2$, and 1.4 mM (R=0.25) for $Ca(Ac)_2$. R is the molar ratio of added electrolyte equivalents to acrylic acid units from the copolymers. Generally, when HCl, $CaCl_2$ or NaCl was used, the curves of the scattered light intensity vs. the water content are similar to that obtained by adding only deionized water. When only deionized water is added, the *cwc* of this solution is 3.7 wt. %. For the addition of HCl, the same *cwc* is obtained as for the addition of deionized water. For the case of $CaCl_2$ or NaCl addition, the phase separation occurs at a water content which is only slightly lower than that when HCl or deionized water is used. Therefore, one can conclude that, at least for the present concentration levels of added electrolytes, no reverse micelle-like aggregation occurs prior to the normal micellization resulting from the water addition.

When $Ca(Ac)_2$ solution is added, the phase separation behavior is more complicated. As shown in Figure 8.9, the curve of the scattered light intensity as a function of the water content can be divided into different regions. First, when the water content was below 0.8 wt.% (corresponding to a $Ca(Ac)_2$ concentration of 0.7 mM or R=0.13), the intensity does not change very much during the addition of the $Ca(Ac)_2$ solution. Second, in the range of the water content from 0.8 to 1.6 wt.% (or a concentration of $Ca(Ac)_2$ from 0.7 to 1.4 mM, corresponding to R=0.13 to 0.25), the intensity increases continuously. The third region extends from a water content of 1.6 to 3 wt. %, the region in which deionized water is added instead of the $Ca(Ac)_2$ solution. The scattered light intensity first increases slowly and then more rapidly at a water content around 3 wt.%. At that point, the solution turns turbid, indicating that the PS chains are collapsing.

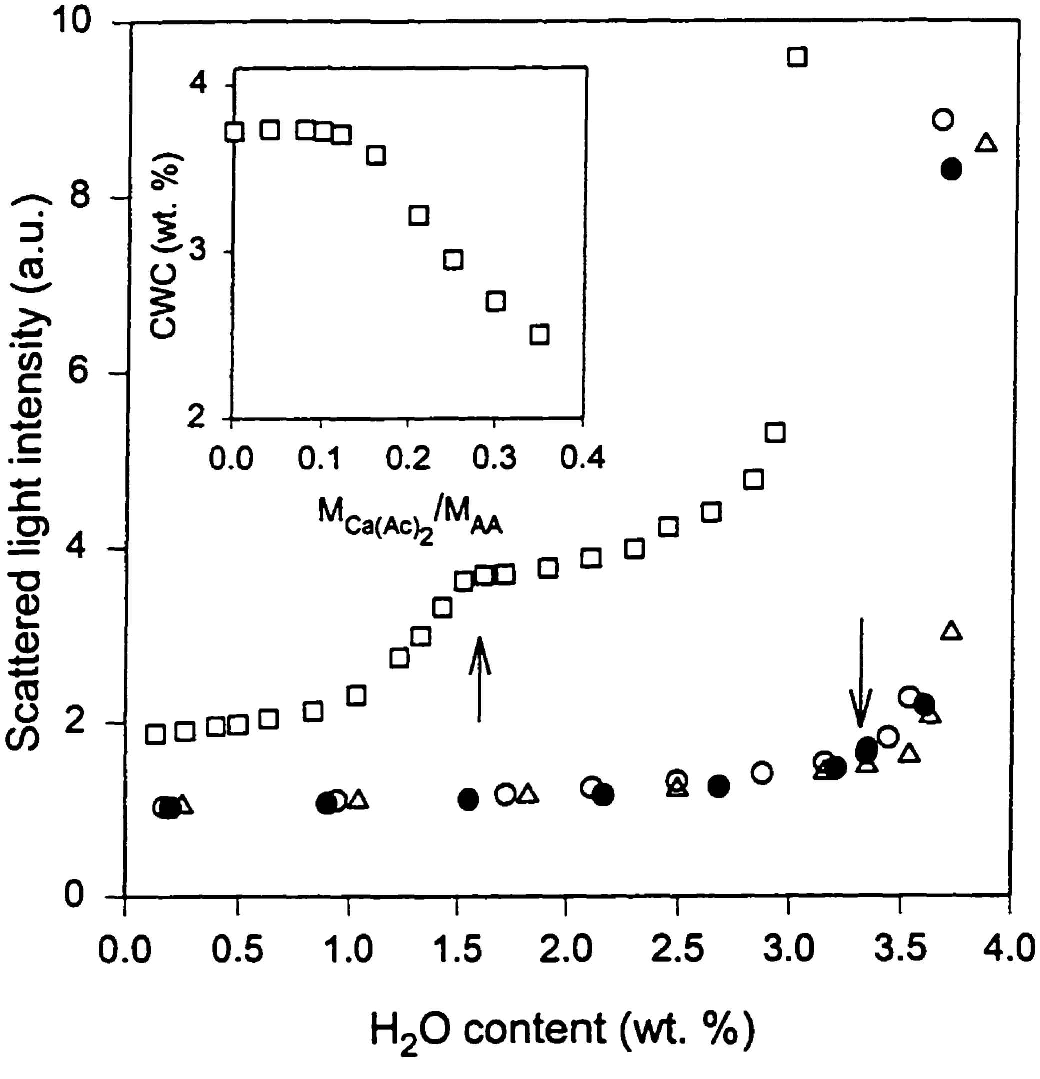

Figure 8.9. Scattered light intensity as a function of added water content from 1 wt. % PS(410)-*b*-PAA(25)/DMF solutions. The arrows indicate the positions after which deionized water was added instead of the aqueous electrolyte solutions. The concentrations of added electrolytes at the points indicated by the arrows were 0.54 mM (R=0.1) for HCl (△), 21 mM (R=4.0) for NaCl (●), 0.54 mM (R=0.1) for $CaCl_2$ (○), and 1.4 mM (R=0.25) for $Ca(Ac)_2$ (□), respectively. The insert is a plot of the critical water content as a function of the molar ratio of added $Ca(Ac)_2$ to the acrylic acid (AA) units from the copolymers, $M_{Ca(Ac)_2}/M_{AA}$.

The *cwc* is apparently lower than those for the other electrolytes, which suggests that reverse micellization of the copolymers has taken place to some extent before the PS chains collapse. Therefore, the increase of the scattered light intensity in the second region (ca, 0.8 to 1.6 wt. % water) reflects the formation of reverse micelle-like aggregates.

In order to understand at what concentration of added $Ca(Ac)_2$ the copolymers start to form the reverse micelles, it is of interest to examine how the *cwc* for PS block aggregation changes as a function of the added $Ca(Ac)_2$ concentration. The insert in Figure 8.9 shows a plot of the relationship between the *cwc* and the molar ratio R of added $Ca(Ac)_2$ to the acrylic acid (AA) units in the solution. Below $R = 0.12$ (i.e. below a molar concentration of $Ca(Ac)_2$ of 0.65 mM), the *cwc* does not change appreciably with R. However, when R exceeds 0.12, the *cwc* starts to decrease as the concentration of added $Ca(Ac)_2$ increases, indicating that the copolymers starts to form reverse micelle-like aggregates when the concentration of the added $Ca(Ac)_2$ is about 0.65 mM ($R=0.12$).

The formation of reverse micelle-like aggregates is most likely related to the interaction of the added $Ca(Ac)_2$ with acrylic acid units, leading to the formation of calcium acrylate. As the added $Ca(Ac)_2$ concentration increases, the fraction of calcium acrylate in the PAA segments increases. As a result, the PAA blocks become less soluble, and finally aggregate to form reverse micelles. It is worth recalling that the addition of $CaCl_2$ did not cause the formation of reverse micelle-like aggregates (Figure 8.9). One possible reason is that the highest concentration of added $CaCl_2$ in this study was 0.54 mM, i.e. below the critical concentration for the reverse micelle formation.

8.3.3. Preliminary studies of polymer chain exchange kinetics between micelles.

So far, we have explored the phase separation behavior of the polymer/DMF/water solution with and without added electrolytes. For the PS-*b*-PAA copolymer solution, the phase separation corresponds to the formation of the block copolymer micelles with PS cores. It has been suggested in previous papers [4-6] that in the early stages of micellization, the micelle cores are swollen with DMF. When DMF concentration in the cores is high, the micelle structures could be quite labile. As the water concentration increases, the DMF concentration in the micelle cores decreases as does also the mobility of the polymer chains. At some point during the water addition, the micelles become frozen on the time scale of the experiment, and retain their structural integrity in the process of further water addition and subsequent dialysis. In this section, we explore the lability of the micelle structure as a function of the water content, i.e. a process controlled by kinetics of polymer chain exchange.

The copolymers, PS(1140)-*b*-PAA(165) and PS(170)-*b*-PAA(33), are used in this part of the study. On the basis of the results of light scattering studies, these two polymers form micelles at different water contents. As shown in Figures. 8.4 to 8.6, for a 1 wt. % copolymer solution, PS(1140)-*b*-PAA(165) copolymers start to form micelles at a water content of ~3 wt. %, and when water content reaches about 3.5 wt. %, more than 95 % of the copolymer chains are present as micelles. However, PS(170)-*b*-PAA(33) copolymers start to form micelles only at a water content of ~ 4.3 wt. %, and only when water content reaches about 5.5 wt. %, are more than 95 % of the copolymer chains aggregated. Furthermore, as shown in Figure 8.5, for the solutions of these two copolymer mixtures, the *cwc* is mainly determined by the fraction of the PS(1140)-*b*-PAA(165) copolymer. Therefore, as water is added to a solution of these two copolymers, the PS(1140)-*b*-PAA(165) copolymer starts to form micelles at a lower water content, and PS(170)-*b*-PAA(33) starts to form micelles at a higher water content. Some of the latter polymer would be expected to be solubilized into the micelles of the former; this will be discussed below.

Figure 8.10 shows a TEM picture of the aggregates made from a mixture of PS(1140)-*b*-PAA(165) and PS(170)-*b*-PAA(33). The total initial copolymer concentration was 2 wt.% with an equal weight of each of the two copolymers. The aggregates were prepared by the addition of water at a rate of 0.4 wt. % per 10 seconds until 25 wt. % water had been added. The resulting solution was then dialyzed against water to remove the DMF. A bimodal distribution of micelle sizes is seen. The larger particles have an average diameter of 48 nm, while the smaller particles have an average diameter of 24 nm. For each copolymer alone, the average spherical micelle core diameters are 38 nm and 25 nm for PS(1140)-*b*-PAA(165) and PS(170)-*b*-PAA(33), respectively.[4,5] Therefore, the particles with smaller sizes are most likely formed from PS(170)-*b*-PAA(33), while the micelles with the larger diameters are formed from both PS(1140)-*b*-PAA(165) and PS(170)-*b*-PAA(33). In the early stages, one can expect that as the addition of water progresses, PS(1140)-*b*-PAA(165) copolymers start to form micelles first. Once these micelles are formed, PS(170)-*b*-PAA(33) copolymer chains can partition between the swollen micelles of PS(1140)-*b*-PAA(165) and the solvent, because the previously formed large PS micelle cores provide a better environment for the PS segments of the PS(170)-*b*-PAA(33) chains. Therefore, the formation of the larger particles is a result of the incorporation of PS(170)-*b*-PAA(33) chains into the micelle cores of the PS(1140)-*b*-PAA(165).

The bimodal distribution of the micelle sizes in Figure 8.10 appears also to be a result of kinetically controlled process of polymer chain exchange. As was mentioned above, once the micelles of PS(1140)-*b*-PAA(165) copolymers are formed, PS(170)-*b*-PAA(33) copolymer chains partition between the PS micelle cores of PS(1140)-*b*-PAA(165) and the solvent. When the added water content exceeds some value, single chains of PS(170)-*b*-PAA(33) copolymers can also aggregate to form micelles (with smaller core sizes). However, the copolymer chain exchange among the micelles driven by the mixing entropy should homogenize the micelle sizes. The final state of the system

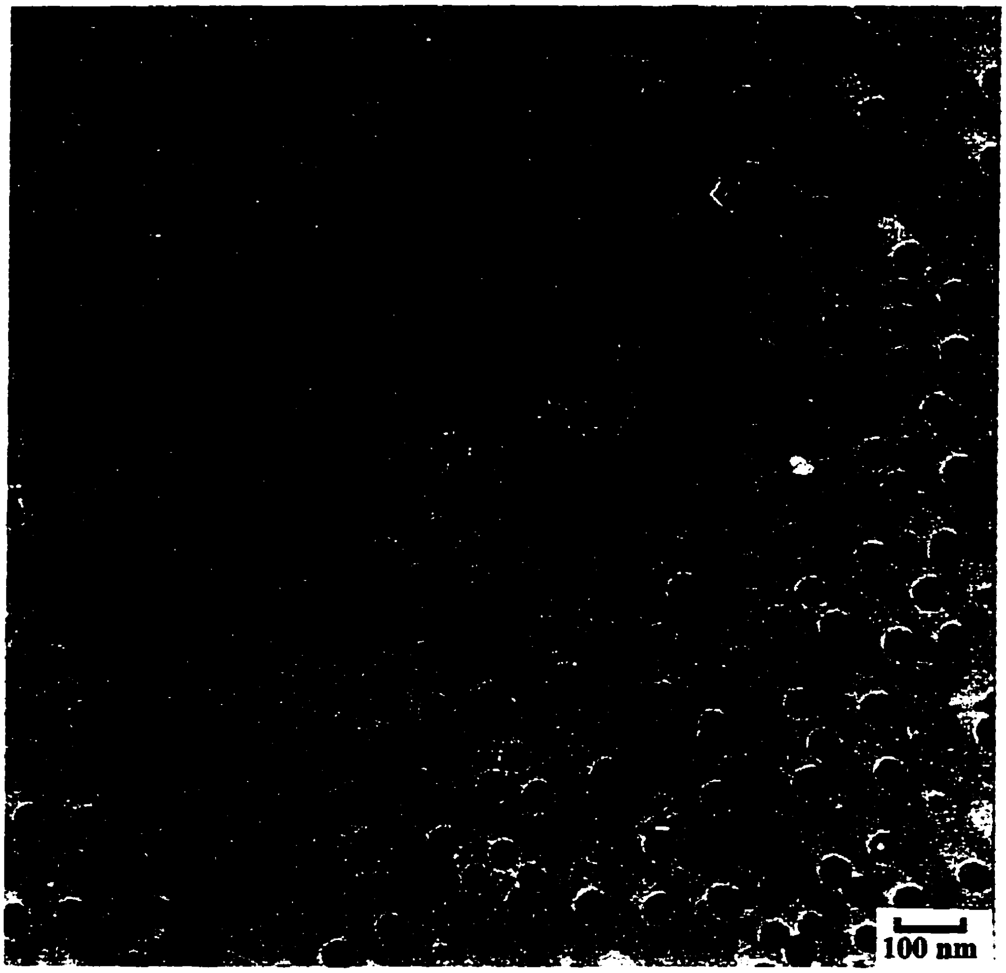

Figure 8.10. TEM picture of the spherical micelles from mixed copolymers of PS(1140)-*b*-PAA(165) and PS(170)-*b*-PAA(33), resulting from an uninterrupted water addition at a rate of 0.4 wt. % per 10 seconds until 25 wt. % water in the solution.

depends on the rate of water addition. If water is added slowly, the rate of the polymer chain exchange remains relatively high for longer periods. As a result, the size distribution of aggregates can become mono-modal instead of bimodal. On the other hand, if the water addition is fast, before an equilibrium resulting from polymer chain exchange can be established, the micelle cores are already frozen due to the decrease of the mobility of polymer chains in the cores as the water content increases. Therefore, micelles with two populations of the sizes are obtained.

In order to verify that chain exchange kinetics are operative in the above experiment, aggregates were also prepared in a different way. The same solution was used as for the aggregates in Figure 8.10, but after 5 wt. % water had been added, the addition of water was stopped for one day, and then continued until 25 wt. % water was added. A TEM picture of the aggregates is shown in Figure 8.11. The distribution of the aggregates is monomodal with an average diameter of 41 nm. It is noteworthy that the average diameter of the micelle cores is larger than those made from either PS(1140)-*b*-PAA(165) or PS(170)-*b*-PAA(33) alone; this increase in size is probably caused by an increased polydispersity of the PS segments in the mixture of the two copolymers.[21]

That the rate of copolymer chain exchange depends on the water content provides a way to study the conditions under which the micelles become structurally frozen. The experiment is based on mixing two solutions of micelles of different sizes (which had been prepared separately from different copolymers) at different water contents. If the mobility of polymer chains is significant at a particular water content, chain exchange between different micelles will change the sizes of the micelles over the time scale of the experiment. If, on the other hand, the mobility of the polymer chains is low, the chain exchange process is very slow so that the micelles will retain their structural integrity. For this experiment, two stock copolymer/DMF solutions were prepared, which contained either 2 wt. % PS(1140)-*b*-PAA(165) or 2 wt. % PS(170)-*b*-PAA(33) copolymers. After the addition of water to the separate solutions reached different predetermined values,

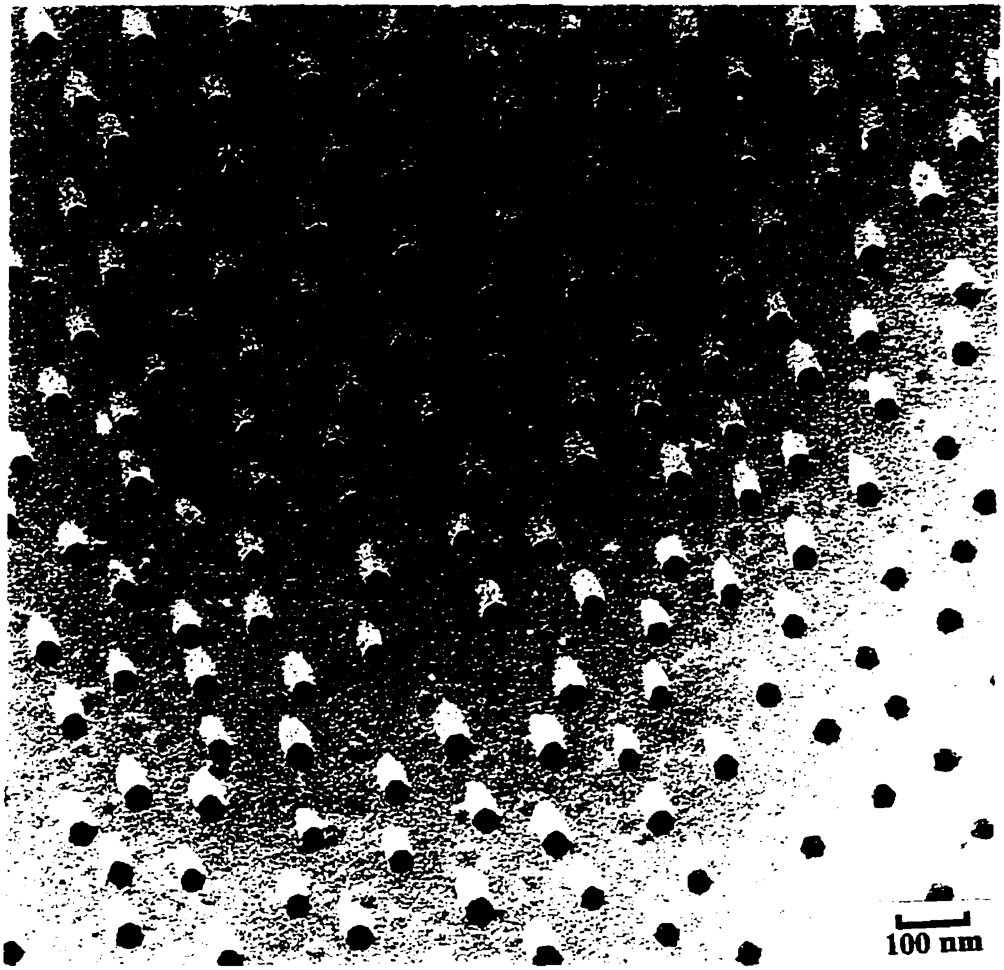

Figure 8.11. TEM picture of the spherical micelles from the same mixed copolymers as for the micelles in Figure 8.10, with the water addition interrupted for one day at 5 wt. %.

aliquots of each of the two solutions were withdrawn and mixed. The mixed solutions at those specific water contents were stirred for one day to allow polymer chain exchange and partition over that time scale. Then, the addition of water was continued until the water concentration in the solution was 25 wt. %. Finally, the aggregates were isolated into water by dialyzing the resulting solutions against water to remove the DMF. The micelle sizes were analyzed by TEM.

Figure 8.12-A and B show the size distributions of the spherical micelles from separate solutions of PS(1140)-*b*-PAA(165) and PS(170)-*b*-PAA(33). Each of the samples shows a single size distribution. The average diameters are 37 nm and 25 nm for the micelles of the two copolymers, respectively. Because of the relatively narrow size distribution, the regions of the micelle sizes are separated reasonably well. The size distributions of the micelles made by mixing the above two different copolymer micelle solutions at different water contents are shown in Figure 8.12-C to G. When the micelle solutions are mixed at 5 wt. % water content (Figure 8.12-C), the micelle size distribution is mono-modal with an average core diameter of 41 nm. When the water content at mixing was 6 wt. % (Figure 8.12-D), the size distribution of micelles is similar to that of micelles made by mixing solutions at 5 wt. % water (Figure 8.12-C); some apparently smaller micelles are seen only very rarely. When the two solutions are mixed at higher water contents, i.e. 7 and 9 wt. % (Figure 8.12-E and F), more and more smaller micelles can be seen in the micrographs. Bimodal distributions of the micelle core sizes are clear, indicating that the rate of polymer chain exchange among the micelles of different sizes has slowed down significantly. Finally, when the two micelle solutions are mixed at an added water content of 11 wt. % (Figure 8.12-G), the micelles have two populations, the size distribution of which is similar to the sum of the size distributions in Figure 8.12-A and B. Although the two micelle solutions are mixed with each other and allowed to interact for one day, the micelles retain their structural integrity. Chain exchange over the time scale of one day is therefore negligible, and the structures of the micelles are kinetically frozen.

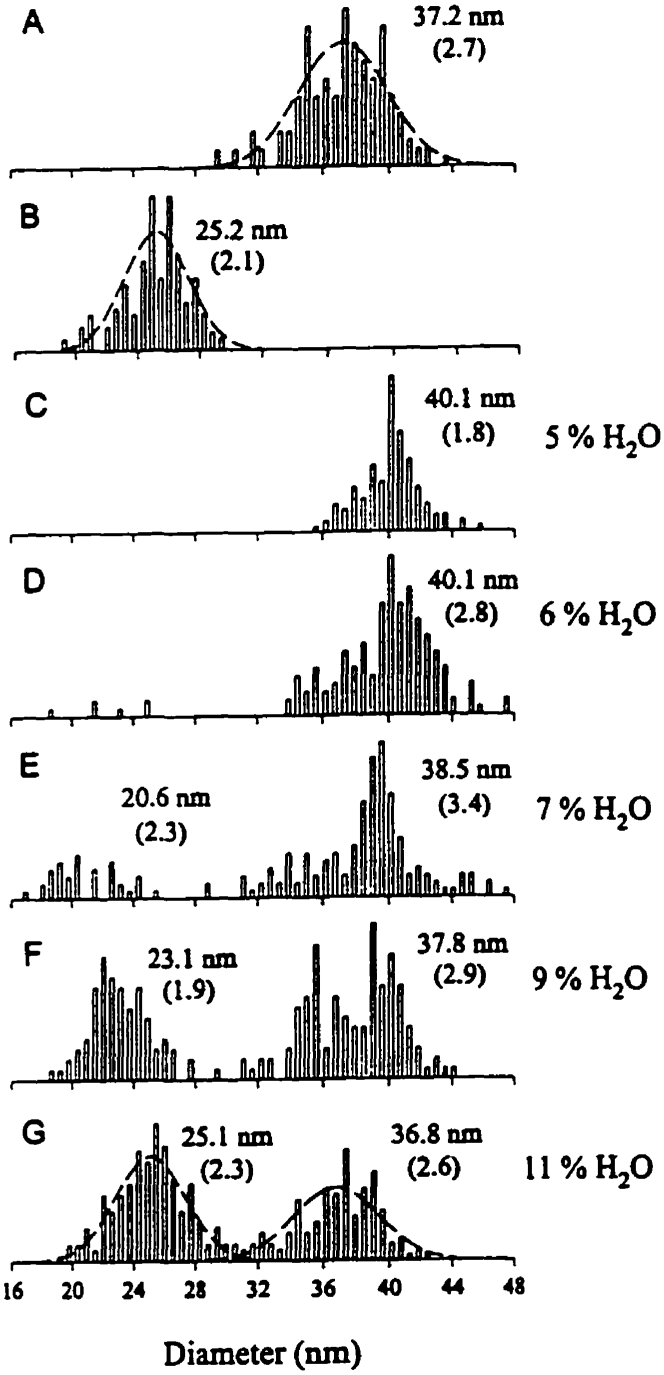

Figure 8.12. Size distribution of the spherical micelles made from PS(1140)-*b*-PAA(165) (A) and PS(170)-*b*-PAA(33) (B), and made by mixing the above two different copolymer micelle solutions when the added water contents are 5 (C), 6 (D), 7 (E), 9 (F) and 11 wt. % (G), respectively. The numbers are the average core diameters with the standard deviations in parentheses for each size distribution. The dotted line represents a Gaussian fit.

8.4. SUMMARY

Phase separation behavior of homopolystyrene and of polystyrene-*b*-poly(acrylic acid) copolymers in DMF solution as a function of the added water content has been explored by light scattering. Starting as a homogeneous solution in DMF, the polymers phase separate when the added water content reaches some critical point. The critical water content, *cwc*, at which the phase separation starts depends on both the polymer concentration and the molecular weight. The higher the polymer concentration and molecular weight, the lower the *cwc*. The relationship between the *cwc* and the logarithm of the polymer concentration is linear. Compared to homopolystyrene solutions, the corresponding PS-*b*-PAA diblock copolymer solutions (of the same polystyrene segment length and concentration as that of the homopolymer) always phase separate at a higher water content. For solutions of mixed polymers, the *cwc* is largely determined by the component which alone has the lower *cwc*.

For homopolystyrene/DMF solutions, phase separation involves the precipitation of the polymer chains. For PS-*b*-PAA diblock copolymer solutions, phase separation results in the formation of micelles, with the PS blocks forming the micelle core and the PAA blocks forming the corona shell. The change of the micelle fraction as the water is added can be estimated from the relationship between the *cwc* and the initial copolymer concentration. For the three block copolymers used, the ΔH_2O values for 95 % micellization are ~ 0.5 % for PS(1140)-*b*-PAA(165), ~ 0.8 % for PS(500)-*b*-PAA(60) and 1.3 % for PS(170)-*b*-PAA(33).

The influence of added electrolytes on the phase separation is related to the interaction between the additives and the PAA segments of the copolymers. When NaOH is added, the PAA segments are neutralized and the copolymers start to form reverse micelle-like aggregates when they are ~ 10 % neutralized. Because the reverse micelle-like aggregates have a much higher apparent molecular weight than the single copolymer chains, they start to separate from the solution at a lower water content than do the single copolymer chains. When $Ca(Ac)_2$ is added, the copolymer chains start to form reverse micelle-like aggregates when the added $Ca(Ac)_2$ concentration is around 0.7 mM, or at a molar ratio R of added $Ca(Ac)_2$ to acrylic acid units of 0.13. The reverse micellization is due to the formation of calcium acrylate, which decreases the solubility of the PAA segments. Within the concentration levels used in this study for the other electrolytes, i.e. 0.54 mM (R=0.1) for HCl or $CaCl_2$, 21 mM (R=4.0) for NaCl, the copolymers do not form reverse micelle-like aggregates in DMF.

In the early stages of the copolymer micellization, the micelles are highly swollen by DMF, and their structures are labile. As the added water content increases, the micelle cores become gradually less swollen and the mobility of polymer chains in the cores decreases. A preliminary study of the copolymer chain exchange among the micelles has been performed by mixing two micelle solutions of different sizes at different water contents. It is found that when the micelles are formed at a water content of ~ 4 wt. %, the copolymer chain exchange within a one day period is still significant when the water content in the solution is increased to 6 wt. %, but is negligible at a water content of ~ 11 wt. %,.

8.5. ACKNOWLEDGMENTS

We thank the Natural Sciences and Engineering research Council of Canada (NSERC) for supporting this work. We also thank Dr. X.-F. Zhong for useful discussions.

8.6. REFERENCES

1. Price, C. In *Developments in block copolymers*; Goodman, I. Ed.; Applied science publishers: London, 1982; Vol. 1, p 39; Selb, J.; Gallot, Y. In *Developments in block copolymers*; Goodman, I. Ed.; Applied science publishers: London, 1985; Vol. 2, p 27; Tuzar, Z.; Kratochvil, P. In *Surface and Colloid Science*; Matijevic, E. Ed.; Plenum Press: New York, 1993; Vol. 15, p 1; Xu, R.; Winnik, M. A. *Macromolecules* **1991**, *24*, 87; Desjardins, A.; Eisenberg, A *Macromolecules* **1991**, *24*, 5779; Prochazka, K.; Kiserow, D.; Ramireddy, C.; Tuzar, Z.; Munk, P.; Webber, S. E. *Macromolecules* **1992**, *25*, 454; Tuzar, Z.; Kratochvil, P.; Prochazka, K.; Munk, P. *Collect. Czech. Chem. Commun.* **1993**, *58*, 2362; Astafieva, I.; Zhong, X. F.; Eisenberg, A. *Macromolecules* **1993**, *26*, 7339; Qin, A.; Tian, M.; Ramireddy, C.; Webber, S. E.; Munk, P.; Tuzar, Z. *Macromolecules* **1994**, *27*, 120; Khougaz, K.; Astafieva, I.; Eisenberg, A. *Macromolecules* **1995**, *28*, 7135.
2. de Gennes, P. G. In *Solid State Physics*, Liebert, L. Ed., Academic, New York, 1978, suppliement 14, p. 1; Halperin, A.; Tirrell, M.; Lodge, T. P. *Adv. Polym. Sci.* 1992, **100**, 31.
3. Gao, Z.; Varshney, S. K.; Wong, S.; Eisenberg, A. *Macromolecules* **1994**, *27*, 7923.
4. Zhang, L.; Eisenberg, A. *Science* **1995**, *268*, 1728 (chapter 4 of this thesis).
5. Zhang, L.; Barlow, R. J.; Eisenberg, A. *Macromolecules* **1995**, *28*, 6055 (chapter 3 of this thesis).
6. Zhang, L.; Eisenberg, A. *J. Am. Chem. Soc.* **1996**, *118*, 3168 (chapter 5 of this thesis).
7. Zhang, L.; Yu, K.; Eisenberg, A. *Science* **1996**, *272*, 1777 (chapter 6 of this thesis).
8. Zhang, L.; Eisenberg, A. *Macromolecules* **1996**, *29*, in press (chapter 7 of this thesis).
9. Yu, K.; Eisenberg, A. *Macromolecules* **1996**, *29*, 6539.

10. Honda, C.; Sakaki, K.; Nose, T. *Polymer* **1994**, *35*, 5309.
11. Guo, A.; Liu, G.; Tao, J. *Macromolecules* **1996**, *29*, 2487.
12. Fitch, R. M. (Ed.) *Polymer Colloids*, Plenum: New York, 1971.
13. Alexander, S. *J. Phys. (paris)* 1977, **38**, 977; de Gennes, P. G. *Macromolecules* **1980**, *13*, 1069; Hadziioannou, G.; Patel. S.; Granick, S.; Tirrell, M. *J. Am. Chem. Soc.* **1986**, *108*, 2869; Pincus, P. *Macromolecules* 1991, **24**, 2912.
14. Wilhelm, M.; Zhao, C-L.; Wang, Y.; Xu, R.; Winnik, M. A. *Macromolecules* **1991**, *24*, 1033; Wu, G.; Zhou, Z.; Chu, B. *Macromolecules* **1993**, *26*, 2117.
15. Shen, H.; Zhang, L.; Eisenberg, A. manuscript submitted to *J. Phys. Chem.*.
16. Zhong, X. F.; Varshney, S. K.; Eisenberg, A. *Macromolecules* **1992**, *25*, 7160.
17. In *Fractionation of Synthetic Polymers: Principles and Practices* Tung, L. H. ed.; Marcel Dekker, Inc., New York, 1976.
18. Gao, Z.; Eisenberg, A. *Macromolecules* **1993**, *26*, 7353.
19. Gao, Z.; Desjardins, A.; Eisenberg, A. *Macromolecules* **1992**, *25*, 1300.
20. Khougaz, K.; Nguyen, D.; Williams, C. E.; Eisenberg, A. *Can. J. Chem.* **1995**, *73*, 2086.
21. Nguyen, D.; Zhong, X-F.; Williams, C.E.; Eisenberg, A. *Macromolecules* **1994**, *27*, 5173.

Chapter 9

Conclusions, Contributions to Original Knowledge, and Suggestions for Future Work

9.1. CONCLUSIONS AND CONTRIBUTIONS TO ORIGINAL KNOWLEDGE

This section describes the main conclusions and the contributions to original knowledge for this thesis. The section is divided into four parts summarizing, respectively, the results for scaling relations and corona dimensions of the spherical micelles in aqueous solutions (chapter 3 and 5), the various morphologies and characteristics of the crew-cut micelle-like aggregates in aqueous solutions (chapters 2, 4 and 5), the added ion-induced morphological changes of crew-cut micelle-like aggregates (chapters 6 and 7) and the results obtained on the phase separation behavior and the formation of micelles in the block copolymer/DMF solutions as a function of the added water content (chapter 8).

9.1.1. Scaling relations and corona dimensions of spherical micelles.

Chapters 3 and 5 described the first systematic study of the dimensions of both the core and the corona shell of block polyelectrolyte crew-cut micelles. The copolymers were polystyrene-*b*-poly(acrylic acid) diblocks, PS-*b*-PAA. The crew-cut micelles were prepared by first dissolving the diblock copolymers in N,N-dimethylformamide (DMF), which is a common solvent for both PS and PAA blocks. Subsequently, water was added slowly to the polymer/DMF solution, as a result of which the quality of the mixed solvent for the PS block decreased gradually. At a certain water content, the aggregation of PS blocks resulted in micelle formation, as indicated by solution turbidity. In the early stages of micelle formation, the micelles cores were swollen with DMF, and a true equilibrium between micelles and the copolymer unimers was operative. As the water content was increased during the later stages of water addition and subsequent dialysis to remove the DMF, the mobility of the PS segments in the cores decreased, and so did the critical micellization concentration. In the final aqueous solution, the micelle cores were essentially frozen, and a dynamic equilibrium between micelles and single chains was no longer possible. This feature makes the structure of these aggregates very stable during characterization, especially when changes in the micelle concentration are involved.

The micelles were characterized by direct TEM observation. The size distributions of the spherical crew-cut micelles were usually very narrow. Because the corona-forming block (PAA) contents in the copolymers were low, the corona layer on the core surface of the dried micelles must be very thin, and its thickness could be calculated from the composition and the density. Thus, the particle sizes determined by TEM represented the core dimensions to a very good approximation. It was found that the number-average core radius (R_{core}) can be fitted empirically to the formula

$$R_{core} \sim N_{PS}^{0.4} N_{PAA}^{-0.15} \qquad (9.1)$$

where N_{PS} and N_{PAA} are the degrees of polymerization of the PS and the PAA blocks of the copolymers. Assuming that the micelle cores are compact and that the density of polystyrene in the cores is homogeneous, one finds that the surface area per corona chain (A_c) at the core/shell interface and the degree of stretching of PS chains in the cores (S_c) depend on the copolymer composition as the follow:

$$A_c \sim N_{PS}^{0.6} N_{PAA}^{0.15} \qquad (9.2)$$

$$S_c \sim N_{PS}^{-0.1} N_{PAA}^{-0.15} \qquad (9.3)$$

One of the important aspects of this work was the finding that the number average micelle core radius, R_{core}, appeared to depend not only on the length of the insoluble PS block, but also on the length of the soluble PAA block. A comparison of our experimental data with those of theoretical studies and of star type micelle systems was made. Our experimental results suggested that the length of the soluble block was an important parameter among those determining the structure of micelles, mainly due to a strong repulsive interactions among the corona chains. Also, the core radius of the spherical crew-cut micelles showed a relatively weaker dependence of the insoluble PS block length than was predicted by theories, mainly due to a low interfacial energy between the core and the solvent during micellization. Furthermore, because of the relatively strong repulsive interactions between corona chains and the low interfacial energy, the crew-cut aggregates had a low degree of stretching of the PS chains in the cores and a low density of corona chains on the core surface, i.e. a large surface area per corona chain.

The hydrodynamic radii (R_h) of spherical crew-cut micelles were determined by dynamic light scattering (DLS), with extrapolation to infinite dilution. From data of the core radius (R_{core}) and the hydrodynamic radius, it was possible to obtain an estimate of the thickness of the corona shell in solution, and to calculate the degree of extension of the corona chains. It was found that when micelles were prepared by dialysis against distilled water and the resulting micelle solutions had a pH of ~ 7, the PAA segments were highly extended (60 ~ 97 % of the contour length). When micelles were prepared by dialysis against deionized water; the resulting micelle solutions had a pH of ~ 4.5. For PAA homopolymer at this pH, it is known that the degree of ionization of the polymer chains is very low, approaching 0%. Under these circumstances, the degree of extension of corona chains was only 25 %. It was also found that the ionized corona chains, in the presence of an inert electrolyte, such as NaCl, were more stretched than the corona chains of the micelles at pH 4.5, but less stretched than those of the micelles at pH 7.

Results obtained here were compared with relevant data from other experimental studies of micelle structures, and a discussion of results in relation to a number of theoretical studies was presented. We considered the high degree of extension of corona chains observed in the present experiments to be due to the charged nature of the PAA blocks, the low degree of curvature of the core surface to which the chains were attached, the relatively low macroscopic concentration of micelles in the DLS experiments, and the polydispersity of the PAA blocks in the copolymers. When inert electrolytes were added or when the pH of the solution was low, the chains adopted a more random coil conformation because the range of electrostatic repulsion of inter-corona chains was reduced.

9.1.2. Various morphologies and their characteristics.

Chapters 2, 4 and 5 describe the formation of crew-cut aggregates of various morphologies and their characteristics. The morphologies included spheres, rods, lamellae, vesicles and large compound micelles which had hydrophilic surfaces and were filled with reverse micelle-like aggregates.

When the corona forming PAA block content in the copolymers was relatively high, spherical micelles were formed. As the PAA content decreased, the morphology of the aggregates changed progressively from spherical to cylindrical, to bilayers (both vesicular and lamellar), and eventually to the large compound micelles. The compound micelle is believed to be a new morphology formed by block copolymers in solution. As a typical example, for the block copolymers at a constant PS block length of 200 styrene units, when the PAA block lengths were 21, 15, 8 and 4 acrylic acid units, the copolymers formed spherical crew-cut micelles, rod-like micelles, bilayer aggregates, and the large compound micelles, respectively.

The morphological transitions are believed to be mainly controlled by the force balance involving three components, i.e. the stretching (deformation) of the PS chains in the core, the surface tension between the PS core and the solvent, and the repulsive interactions among the corona chains. By considering a spherical micelle as an example, when the PAA block length or coil dimension decreases, the inter-corona chain repulsion decreases; the micelle core size increases in order to decrease the interfacial energy. However, the increase of the core size is restricted by entropic penalty resulting from the stretching of the PS blocks. It cannot continue indefinitely as the soluble block (PAA) length decreases. At some point, the system becomes unstable, and the morphology changes first from spherical to rod-like, and then to lamellar or vesicular. Meanwhile, the degree of stretching of the PS blocks was decreases in parallel with the morphological transitions. For example, the block copolymers PS(200)-*b*-PAA(21), PS(200)-*b*-PAA(15) and PS(200)-*b*-PAA(8) have the same PS block, and yield, respectively, spherical micelles, cylindrical micelles and vesicles. The degrees of stretching of the PS chains are 1.41, 1.26 and 0.99, respectively.

The morphology of the aggregates depended not only on the copolymer composition, but also on the initial concentration in DMF. For example, for PS(410)-*b*-PAA(25), when the initial concentration was 2 wt. %, spherical micelles were formed. Rod-like micelles could be made from a 2.6 wt. % copolymer solution. When the copolymer concentration was 3.0 wt. %, vesicles started to form. If 4.0 wt. % solution was used, most of the aggregates were vesicles with highly polydisperse sizes, with outer diameters ranging from 50 to 500 nm.

The effect of added homopolystyrene on the aggregate morphology was also studied. It was found that upon addition of homopolystyrene, the block copolymers which formed spherical micelles without the added homopolymer, still yielded spherical micelles. The homopolymer chains distributed themselves generally throughout the core when their content was relatively low. The resulting spherical micelles still had a low polydispersity but average core radius increased slightly. As the added homopolystyrene content increased, the core sizes became more polydisperse. Homopolymer accumulation in the center of the micelle core can be inferred. The addition of homopolystyrene changed the morphologies of the aggregates from bilayers or cylinders to spheres. For example, vesicles were formed from a 2 wt. % PS(410)-*b*-PAA(16) solution, but spherical micelles were obtained upon the addition of 10 wt. % PS(180) homopolymer to the copolymer. The change in the morphology caused by the addition of homopolystyrene was ascribed mainly due to the reduced degree of stretching of the PS blocks due to the accumulation of even a small amount of the homopolystyrene in the center of the core, and possibly the mixing entropy, both of which are associated with the solubilization of the homopolystyrene into the micelle cores.

Although various morphologies have been observed in many self-assembling systems, e.g. small molecule amphiphiles in solution, block copolymers in bulk, block copolymer/homopolymer blends, and amphiphilic block copolymers on water surfaces, aggregates of multiple morphologies, i.e. spheres, rods, and vesicles or lamellae, have not been prepared before for the same block copolymer family in solutions of low molecular weight solvents. The present study provides the first instance in which a number of the aggregate morphologies has been observed directly in block copolymers in a low molecular weight solvent. This is believed to be the only way so far to prepare glassy vesicles of block copolymers, which form spontaneously and can be stabilized and isolated in water, and studied directly by electron microscopy. The formation and the characteristics of different morphologies provide unprecedented insight into the factors controlling the architecture of the self-assembled aggregates of block copolymers.

In addition, a needle-like solid, which was highly birefringent after soaking in water, was obtained on drying of aqueous solutions of the spherical micelles. The needles might have an ordered structure, possibly similar to that encountered in crystals. An important aspect here is that the repeat unit is a large micelle ball of several tens of nanometers in diameter. Although, both latex particles and block copolymer micelles in solution show a tendency to order into crystal-like structures in certain ranges of temperature and concentration, we are not aware any micelle or latex systems which spontaneously forms macroscopic needles on drying.

9.1.3. Morphological changes induced by added ions.

Chapters 6 and 7 described the morphological changes of the crew-cut aggregates induced by added ions. The morphology of the block copolymer aggregates formed from a single block copolymer sample can be controlled via the addition of micro-molar $CaCl_2$,

$Ca(Ac)_2$, NaOH or HCl, or milli-molar NaCl. In addition to the various aggregates which can be prepared by changing the copolymer composition and concentration, large compound vesicles (LCVs) were obtained. These represent a new morphology. The copolymers used for this study were PS(410)-*b*-PAA(13), PS(410)-*b*-PAA(25), PS(660)-*b*-PAA(24).

As a typical example, from 1 wt. % PS(410)-*b*-PAA(13) solutions, spherical micelles with an average core diameter of 31 nm were formed. When added $CaCl_2$ concentration was 71 μM (R=0.025, where R is the molar ratio of added $CaCl_2$ molecules to acrylic acid repeat units), the micelles were still spherical, but their average core diameter was increased to 39 nm. The copolymers started to form vesicles when the $CaCl_2$ concentration was 85 μM (R=0.03). When the $CaCl_2$ concentration was between 90 and 115 μM (R=0.032 and 0.04), the copolymer yielded vesicles; however, with increasing $CaCl_2$ concentration, the average size of the vesicular aggregates increased rapidly. Finally, when the $CaCl_2$ concentration was between 130 and 170 μM (R = 0.045 and 0.06), large spherical compound vesicles (LCVs) were formed. The structure of the LCVs has some resemblance to that of aggregated soap bubbles. Their formation may be a result of kinetic control involving collisions of individual vesicles and a subsequent PS wall fusion process. A number of novel features of the LCVs may make them especially useful as drug delivery vehicles. Furthermore, the spontaneous formation of the LCVs might provide a practical method for making stable artificial tissue-like composites and soft biomaterials with tunable properties.

It has been known for many years that the aggregate morphology of small molecule amphiphiles can be changed by added salt. However, to our knowledge, ion-induced morphological changes have not been reported before in solutions of block copolymer aggregates. The present system has shown that the addition of electrolytes can change the aggregate morphology progressively from spheres to rods, to vesicles, and to large compound vesicles. The added electrolyte concentrations at the onset of the morphological transitions are only of the order of 10^{-4} moles for $CaCl_2$, NaOH and HCl, and 10^{-3} moles for NaCl. Ion-induced morphological changes in the block copolymer aggregates at such low ion contents are novel and significant. From a fundamental point of view, the discovery of the strong effect of added ions on the aggregate morphology of polymeric amphiphilies in dilute solution may lead to an improved understanding of the nature of interactions in these systems, and their consequences for the structure of macromolecular assemblies.

The effect of added ions on the aggregate morphology is parallel to a change in the soluble block length; however, it is easier to obtain a desired morphology. It was found that when the PS block length of the copolymers increased beyond a certain point, the preparation of rod-like micelles and vesicles became more difficult. In particular, when the PS block length of the copolymers exceeded 600 repeat units, it was not possible to prepare rod-like micelles or vesicles by varying the copolymer composition and concentration. However, aggregates of various morphologies from PS(660)-*b*-PAA(24) copolymer were obtained by adding NaCl to different concentrations.

The change in the micro-environment of the PAA segments during the formation of the micelles was explored by proton NMR. It was found that the added water accumulates preferentially near the PAA blocks to some extent. Although, for a 1 wt. % polymer/DMF solution, the micellization usually starts at a water content around 5 wt. %, the local water concentration around the PAA blocks could be actually much higher than the overall water concentration in the solution. Therefore, the PAA blocks probably behave in a manner similar to that in aqueous solutions, i.e. they are partially ionized. Because of this, both steric and electrostatic repulsive interactions among the corona chains can be operative during the formation of the micelles. Although the cause of the morphogenic effect of added ions appears to be different for different additives, it can be ascribed to the influence of a changed inter-corona chain repulsion in the presence of added ions on the force balance controlling the final aggregate morphology.

In particular, for the case of added HCl, the effect is ascribed to protonation of the PAA blocks. The addition of strong acid like HCl lowers the degree of ionization of PAA, and thus reduces the electrostatic or steric repulsion among the PAA chains. Therefore, the decreased inter-corona chain repulsion has an effect on the aggregate morphology similar to a decrease in the soluble PAA block length. By contrast, the addition of NaOH has an effect on the aggregate morphology similar to an increase in the soluble PAA block length, since the added NaOH neutralizes the PAA segments. As a result, the degree of ionization and the repulsion among the corona chains increases.

Addition of acetic acid shows almost no effect on the aggregate morphology, probably because acetic acid is a weak acid and its effect on the ionization of the PAA blocks is very weak. The strong morphogenic effect of added $CaCl_2$ on the aggregates originates from a strong Ca^{2+} binding to the carboxylic acid groups of the PAA segments. However, a simultaneous morphogenic effect of HCl might also be involved because the formation of calcium acrylate and release of HCl due to the Ca^{2+} binding. Finally, the relatively weaker morphogenic effect of added NaCl is ascribed to a screened electrostatic field of the partially charged PAA segments in the presence of NaCl.

9.1.4. Phase separation behavior and the micelle formation.

Chapter 8 presents a study of some fundamental aspects of the phase separation behavior and the formation of micelles in the PS-*b*-PAA copolymer/DMF solutions as a function of the added water content. The main method used for this study was static light scattering and TEM.

As a baseline for this study, the phase separation behavior of PS homopolymer solutions was explored first. The homopolymer solutions underwent phase separation as the added water content reached some critical point, which is related to the precipitation of polystyrene chains The critical water content, *cwc*, at which the phase separation of a solution starts depends on both the polymer concentration and the molecular weight. The higher the polymer concentration and the molecular weight, the lower the *cwc*. A linear relationship between the *cwc* and the logarithm of the polymer concentration was found.

For PS-*b*-PAA copolymer solutions, the phase separation behavior is generally similar to that of PS homopolymer solutions. However, the phase separation involves the formation of micelles, with the PS blocks forming the core and the PAA blocks forming the corona shell. The *cwc* depends on both the copolymer concentration and the molecular weight. A linear relationship between the *cwc* and the logarithm of the copolymer concentration was also found. Compared to PS homopolymer solutions, the corresponding PS-*b*-PAA copolymer solutions (with the same PS segment length and concentration as that of the homopolymer) always phase separate at a higher water content. It is evident that at the critical water content, the concentration of the copolymer actually represents the critical micellization concentration, therefore, it was possible to estimate the change of the micelle fraction in the solution as a function of the added water content, utilizing the relationship between the *cwc* and the initial copolymer concentration. In general, once the copolymers started to form micelles, the micellization was essentially complete after the addition of a few percent more water.

The phase separation in solutions of mixed polymers was also explored. The mixed polymers were made from either two different block copolymers or one copolymer and one PS homopolymer. It was found that the *cwc* is largely determined by the component polymer which has the lower *cwc*. This result suggests that if one wishes to incorporate homopolystyrene into the copolymer micelle cores, the homopolymer should show a higher *cwc* for precipitation than that of the block copolymer for micellization. Otherwise, the homopolymer chains will precipitate first from the solution as the water content increases, without becoming incorporated into the PS core of the micelles. A higher *cwc* can be achieved by decreasing the polymer concentration and the molecular weight. This is the basis of the study of the effect of added homopolystyrene on the morphology of the copolymer aggregates (*cf.* Chapter 5, section 5.3.4).

The influence of added electrolytes, i.e. HCl, NaOH, NaCl, $CaCl_2$ or $Ca(Ac)_2$, on the phase separation of the copolymer solution was also studied. The effect of added electrolytes on the phase separation is ascribed to the interaction between the additives and the PAA segments of the copolymers. When NaOH was added, the PAA segments were neutralized and the copolymers started to form reverse micelle-like aggregates when they were ~ 10 % neutralized. Because the reverse micelle-like aggregates have a much higher apparent molecular weight than the single copolymer chains, they start to separate from the solution at a lower water content than do the single copolymer chains. When $Ca(Ac)_2$ was added, the copolymer chains started to form reverse micelle-like aggregates when the added $Ca(Ac)_2$ concentration was around 0.7 mM, or a molar ratio R of added $Ca(Ac)_2$ to acrylic acid units of 0.13. The reverse micellization is due to the formation of calcium acrylate, as a result of which the PAA segments become less soluble. Within the concentration levels for other added electrolytes, i.e. 0.54 mM (R=0.1) for HCl or $CaCl_2$, 21 mM (R=4.0) for NaCl, the copolymers appeared to disperse in solution still as single chains, and no reverse micelle-like aggregates were formed. These results are essential to understand the causes of added ion effect on the aggregate morphology of the block copolymers (*cf.* chapters 6 and 7).

It was expected that, in the early stages of the copolymer micellization, the micelles were highly swollen by DMF. A dynamic equilibrium between micelles and the copolymer unimers was operative, and their structures were labile in a response to changing the solvent quality. As the added water content increased, the micelle cores became gradually less swollen; the mobility of polymer chains in the cores decreased; and the micelle structure eventually became locked. A study of the copolymer chain exchange among the micelles was performed by mixing two separately prepared micelle solutions of different sizes at different water contents, and studying the change of the micelle core size distribution by TEM. It was shown that when the micelles were formed in the water content range of ~ 4 wt. %, the copolymer chain exchange within one day period was still significant at a water content of 6 wt. %, but became negligible when the added water content was increased to ~ 10 wt. %.

9.2. SUGGESTIONS FOR FUTURE WORK

Because the PS-*b*-PAA copolymer system in this thesis provides the first instance which shows that aggregates of various morphologies can be prepared from the same family of the block copolymers in low molecular weight solvent, many aspects of the formation of the aggregates of different morphologies remain unexplored.

In chapters 2, 4 and 5, it was shown that the aggregate morphology depends on the initial copolymer concentration in DMF. However, it is very useful to know the boundaries between the different morphologies as a function of the molecular weight and the composition of the copolymers and the initial copolymer concentrations in DMF in detail. From these studies, a phase diagram or a diagram of stability regions of the various morphologies can be obtained.

Aside of the effect of the copolymer composition, polymer concentration and added ions on the aggregate morphology, which was described in this thesis, the effect of several other factors on the aggregate morphology should been examined, e.g. the polydispersity of both the core-forming PS blocks and the corona forming blocks, and the temperature.

In this thesis, the preparation of solutions of the polymer aggregates involves the dissolution of the block copolymers in DMF and the addition of water to induce the formation of the aggregates. It is also of interest to study the aggregation behavior and the morphological characteristics of the block copolymer aggregates by using other solvents, e.g. tetrahydrofuran, dioxane, or/and by using other precipitant to induce the aggregation, e.g. methanol. Instead of the addition of a precipitant to a solution, it is of interest to explore the formation of the aggregates by dissolving the copolymers directly in a mixture of water and DMF. Some preliminary experiments, which have not been included in this thesis, have shown that very long worm like micelles, vesicles and interconnected rod-like aggregates (or a bicontinuous rod-like structure) can be obtained by using this method. These experiments will allow us to compare morphologies of the aggregates formed under different conditions, which will help us to get deeper insight into the mechanism for the formation of the aggregates of various morphologies.

In chapter 5, it has been shown that added homopolystyrene can swell the spherical micelle cores, but no morphological transitions are induced. However, the addition of homopolystyrene can change the aggregate morphology of the block copolymers from vesicles or rod-like micelles to spherical micelles. While the effect of added core-forming homopolymers on the morphologies are ascribed to the decreased degree of stretching of the PS blocks, it is also of interest to study the effect of added small apolar molecules, such as toluene, on the phase behavior since added apolar small molecules will solublize into the hydrophobic core region. In addition, the solubilization of small apolar molecules into the cores will change the glassy core to a soft one by decreasing the glass transition temperature, which may also be an important factor for the formation of stable aggregates of various morphologies.

In the Chapter 4, the formation of a needle-like solid, which formed at the glass-air interface when a solution of the spherical micelles was dried, has been described. After soaking in water, the needles become highly birefringent, which implies that they may have an ordered structure, possibly similar to that encountered in crystals. It is of interest to study their internal structure, for example, by small angle x-ray scattering and TEM.

IMAGE EVALUATION
TEST TARGET (QA-3)

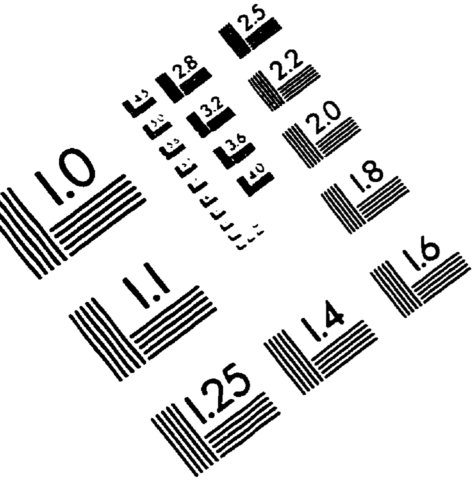

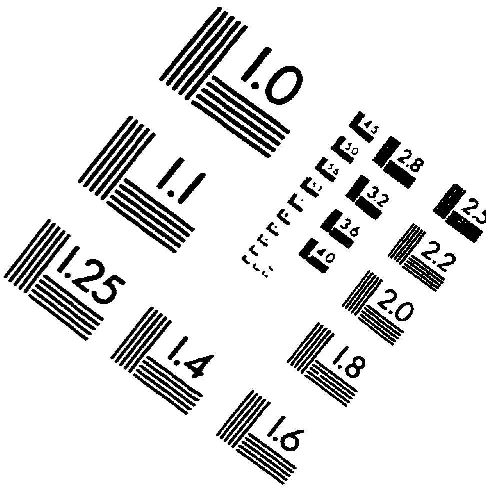

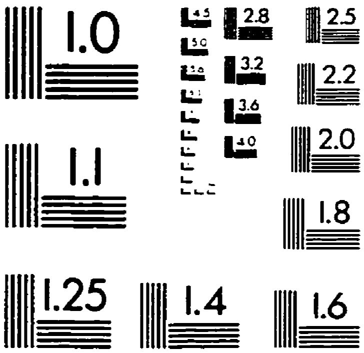

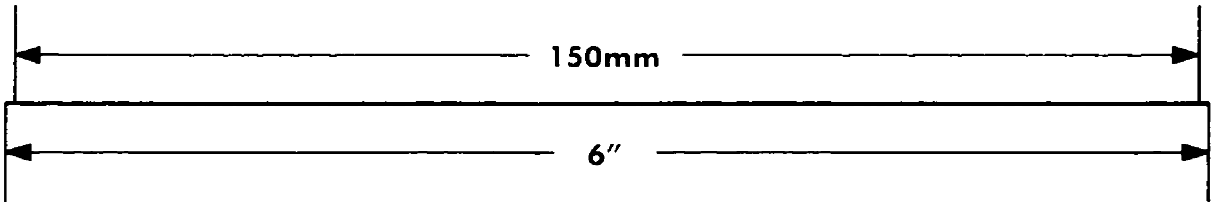

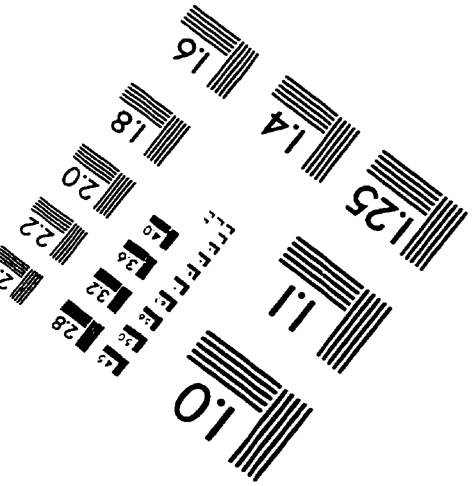

APPLIED IMAGE . Inc
1653 East Main Street
Rochester, NY 14609 USA
Phone: 716/482-0300
Fax: 716/288-5989